

A STATISTICAL AND SYNOPTIC CLIMATOLOGY OF TROPICAL CYCLONE
TORNADO OUTBREAKS

DISSERTATION

Presented to the Graduate Council of
Texas State University-San Marcos
in Partial Fulfillment
of the Requirements

for the Degree

Doctor of PHILOSOPHY

by

Todd W. Moore, B.S., M.S.

San Marcos, Texas
May 2013

A STATISTICAL AND SYNOPTIC CLIMATOLOGY OF TROPICAL CYCLONE
TORNADO OUTBREAKS

Committee Members Approved:

Richard W. Dixon, Chair

Philip W. Suckling

David R. Butler

Barry D. Keim

Approved:

J. Michael Willoughby
Dean of the Graduate College

COPYRIGHT

by

Todd W. Moore

2013

FAIR USE AND AUTHOR'S PERMISSION STATEMENT

Fair Use

This work is protected by the Copyright Laws of the United States (Public Law 94-553, section 107). Consistent with fair use as defined in the Copyright Laws, brief quotations from this material are allowed with proper acknowledgment. Use of this material for financial gain without the author's express written permission is not allowed.

Duplication Permission

As the copyright holder of this work I, Todd W. Moore, authorize duplication of this work, in whole or in part, for educational or scholarly purposes only.

ACKNOWLEDGEMENTS

I would first like to acknowledge my advisor, Dr. Richard W. Dixon, for his guidance, not only with this dissertation project, but throughout graduate school. Second, I would like to thank my committee members, Dr. Philip W. Suckling, Dr. David R. Butler, and Dr. Barry D. Keim, for their guidance and support throughout comprehensive exams and with my dissertation project.

I also would like to acknowledge Roger Edwards of the Storm Prediction Center for his provision, quality control, and maintenance of the Tropical Cyclone Tornado database and the principle investigators on the National Centers for Environmental Prediction-North American Regional Reanalysis project, Fedor Mesinger, Geoff DiMego, and Eugenia Kalnay, along with all of their team members and collaborators.

Lastly, I would like to acknowledge my wife, Siobhan, for her extraordinary patience and understanding throughout this process. Although it may seem so, it has not gone unnoticed and I truly am thankful to have found someone with such qualities.

This manuscript was submitted on 19 December 2012.

TABLE OF CONTENTS

	Page
ACKNOWLEDGEMENTS	v
LIST OF TABLES	ix
LIST OF FIGURES	xi
ABSTRACT.....	xv
CHAPTER	
I. INTRODUCTION	1
1.1 Overview.....	1
1.1.1 Dissertation Organization	2
1.2 Research Motivations.....	3
1.2.1 Tropical Cyclone Tornado Clusters	3
1.2.2 Societal Impacts and Anticipation	4
1.2.3 Geographic Nature	8
1.3 Research Goals, Questions, Objectives, and Assumptions.....	8
1.4 Chapter One Figures	11
II. BACKGROUND AND LITERATURE REVIEW	13
2.1 Introduction and Background	13
2.1.1 Atmospheric Circulation.....	13
2.1.2 Tropical Cyclones	15
2.1.3 Tornadoes.....	17
2.2 Tropical Cyclone Tornadoes.....	19
2.2.1 Definition and Identification.....	19
2.2.2 Climatology.....	22
2.2.2.1 General Frequency	23
2.2.2.2 Temporal Distribution.....	23
2.2.2.3 Spatial Distribution	25
2.2.3 Case Studies	26
2.2.4 Formation, Forecasting, and Detection	27
2.2.5 General Conclusions from the Literature.....	31

2.3 Synoptic Climatology	32
2.3.1 Definition	32
2.3.2 Historical Developments.....	33
2.3.3 Approaches and Methods.....	36
2.4 Synoptic Climatology of Tropical Cyclone Tornadoes	39
2.5 Concluding Remarks.....	43
2.6 Chapter Two Figures.....	46
III. DATA AND METHODS	49
3.1 Data.....	49
3.1.1 Tropical Cyclone Tornado Data.....	49
3.1.2 Synoptic Data.....	50
3.2 Methods.....	55
3.2.1 Tropical Cyclone Tornado Outbreaks: Definition and Identification.....	56
3.2.2 Synoptic Classification Process	59
3.2.2.1 Classification Goals	59
3.2.2.2 Classification Process	60
3.2.2.3 Tropical Cyclone-Westerly Interaction Patterns.....	63
3.2.2.4 No Tropical Cyclone-Westerly Interaction Patterns.....	65
3.2.3 Statistical Analysis.....	65
3.3 Chapter Three Tables.....	73
3.4 Chapter Three Figures.....	78
IV. RESULTS.....	83
4.1 Statistical Description of Tropical Cyclone Tornado Outbreaks	84
4.1.1 Frequency and Severity.....	84
4.1.2 Temporal Characteristics	85
4.1.3 Spatial Characteristics.....	87
4.2 Synoptic Patterns Associated with Tropical Cyclone Tornado Outbreaks	88
4.2.1 Description and Within-Group Analysis of Synoptic Patterns	89
4.2.1.1 Pattern 1 Tropical Cyclone Tornado Outbreaks	89
4.2.1.2 Pattern 2 Tropical Cyclone Tornado Outbreaks	91
4.2.1.3 Pattern 3 Tropical Cyclone Tornado Outbreaks	92
4.2.1.4 Pattern 4 Tropical Cyclone Tornado Outbreaks	94
4.2.1.5 Pattern 5 Tropical Cyclone Tornado Outbreaks	95
4.2.2 Synoptic Pattern Persistence and Variability.....	96
4.2.3 Between-Group Analysis of Synoptic Patterns	97
4.2.3.1 Outbreak Frequency.....	97
4.2.3.2 Outbreak Severity	97
4.2.3.3 Tropical Cyclone Tornado Strength.....	99
4.2.4 Seasonality of Synoptic Patterns.....	99
4.2.5 Tropical Cyclone-Westerly Interaction VS No Tropical Cyclone-Westerly Interaction Outbreaks	101
4.2.5.1 Tropical Cyclone-Westerly Interaction (Patterns 1, 2, and 3)	101

4.2.5.2 No Tropical Cyclone-Westerly Interaction (Patterns 4 and 5)	102
4.2.5.3 Outbreak Severity	103
4.2.5.4 Outbreak Seasonality	104
4.3 Chapter Four Tables.....	105
4.4 Chapter Four Figures	110
V. DISCUSSION OF RESULTS.....	140
5.1 Tropical Cyclone Tornado Outbreaks: Definition Concerns	140
5.2 Tropical Cyclone Tornado Outbreak Climatology	141
5.3 Synoptic Patterns Associated with Tropical Cyclone Tornado Outbreaks: Forcing Mechanisms	144
5.3.1 Importance of the Midlatitude Westerlies.....	148
5.3.2 Seasonality of the Midlatitude Westerlies	151
5.3.3 Comparison of Results with Previous Findings.....	152
5.4 Chapter Five Figures.....	158
VI. CONCLUSION.....	164
6.1 Summary	164
6.2 Future Research	169
6.3 Concluding Statement.....	172
6.4 Chapter Six Tables.....	175
APPENDIX A: LIST OF ACRONYMS.....	176
APPENDIX B: SAFFIR-SIMPSON HURRICANE WIND SCALE AND FUJITA/ENHANCED FUJITA TORNADO DAMAGE SCALE.....	178
APPENDIX C: TC LANDFALLS AND THEIR TCTORS (1995–2010).....	179
APPENDIX D: SYNOPTIC PATTERN PERSISTENCE AND VARIABILITY.....	183
REFERENCES	185

LIST OF TABLES

Table	Page
3.1 List of information provided about TCTORs in the TCTOR dataset (Edwards 2010b)	73
3.2 Selected list of reanalysis projects and their basic temporal and spatial properties ...	74
3.3 List of conceptual and operational variables and sources supporting their link to TCTORs.....	75
3.4 Sample of tornado outbreak definitions.....	76
3.5 Sample of TCTOR outbreak definitions	77
3.6 Primary synoptic hours and six hour windows centered on these synoptic hours used to identify TCTOR outbreaks	77
4.1 Descriptive statistics for TCTOR outbreak severity and the standard area over which TCTOR outbreaks occur for each spatial configuration.....	105
4.2 Description of the five identified synoptic patterns and the frequency at which they occur.....	105
4.3 Descriptive statistics summarizing TCTOR outbreak severity for the five identified synoptic patterns.	106
4.4 Statistics describing the distribution of TCTOR outbreaks about their associated TC landfall, in hours, for each synoptic pattern.....	106
4.5 Result of the Shapiro-Wilk test assessing the normality of TCTOR outbreak severity distributions within each of the five synoptic patterns.	106
4.6 Results of the post hoc Mann-Whitney U test with Bonferroni adjustment to determine which pattern-pairs have significantly different median TCTOR outbreak severity.	107
4.7 TCTOR outbreak frequency cross-tabulated by synoptic pattern and F/EF scale....	107

4.8	TCTOR outbreak frequency cross-tabulated by synoptic pattern and month.....	107
4.9	Descriptive statistics summarizing TCTOR outbreak severity.....	108
4.10	Statistics describing the distribution of TCTOR outbreaks about their associated TC landfall, in hours.....	108
4.11	Result of the Shapiro-Wilk test assessing the normality of TCTOR outbreak severity distributions for TC-westerly interaction and no TC-westerly interaction outbreaks.....	108
4.12	Distribution of TC-westerly (Patterns 1, 2, and 3) and no TC-westerly interaction (Patterns 4 and 5) outbreaks through the early (June and July), middle (August and September), and late (October and November) months of the Atlantic Basin hurricane season.....	109
6.1	Summary of the five synoptic patterns, their verbal description, and their descriptive statistics.	175

LIST OF FIGURES

Figure	Page
1.1 TCTORs associated with TCs Ivan (2004) and Cindy (2005).....	11
1.2 Conceptualization (A) and spatial scaling (B) of atmospheric phenomena involved in a synoptic climatology of TCTORs.....	12
2.1 Simplified model of global atmospheric circulation cells and prevailing winds in the northern hemisphere.....	46
2.2 Illustration of zonal (A) and meridional (B) midlatitude westerly flow patterns	47
2.3 North Atlantic Basin TC tracks, 1995–2010 (TC track shapefiles obtained from NCDC (n.d.)).	48
3.1 Schematic illustrating a TC-relative framework for classifying similar synoptic situations.	78
3.2 Classification tree illustrating the hierarchy of synoptic patterns based on 500 hPa geopotential height and vector wind plots.....	79
3.3 Simplified illustration of an idealized Pattern 1 TCTOR outbreak environment.	80
3.4 Simplified illustration of an idealized Pattern 2 outbreak environment.	80
3.5 Simplified illustration of an idealized Pattern 3 outbreak environment.	81
3.6 Simplified illustration of an idealized Pattern 4 outbreak environment.	81
3.7 Simplified illustration of an idealized Pattern 5 outbreak environment.	82
4.1 Outbreak and isolated TCTORs for TCs Ivan, Rita, and Alberto.....	110
4.2 Scatter plot illustrating the linear association between the total number of TCTORs produced by a TC throughout its life-span and the number of outbreaks that TC produces.....	111

4.3	Bar graph and cumulative percentage graph illustrating the distribution of TCTOR outbreaks, binned by outbreak severity.....	111
4.4	Ten severest TCTOR outbreaks (1995–2010).....	112
4.5	Boxplots illustrating the distribution of TCTOR outbreak severity, stratified by the classification of their parent TC during the outbreak.....	113
4.6	TCTOR outbreak frequency distribution stratified by F/EF Scale rating.....	113
4.7	TCTOR outbreak frequency distribution stratified by month.....	114
4.8	TCTOR outbreak frequency distribution stratified by synoptic hour.....	114
4.9	Scatter plot illustrating the time difference between each TCTOR outbreak synoptic hour and the landfall time of their parent TC, and the number of TCTORs in an outbreak as a function of time from landfall (n = 133) ..	115
4.10	TCTOR outbreak location within the TC environment.....	116
4.11	Illustrative examples of the various spatial configurations in which TCTOR outbreaks occur.....	117
4.12	500 hPa geopotential height (A) and vector wind (B) plots illustrating a synoptic environment characteristic of Pattern 1 (NCEP-NARR plots obtained from NOAA ESRL's Physical Science Division (NOAA (n. d.)).....	118
4.13	Pattern 1 TCTOR frequency distribution stratified by F/EF Scale.....	119
4.14	Pattern 1 TCTOR outbreak frequency distribution stratified by month.....	119
4.15	Pattern 1 TCTOR outbreak frequency distribution stratified by synoptic hour.....	120
4.16	Spatial distribution of TCTORs within Pattern 1 outbreaks.....	120
4.17	500 hPa geopotential height (A) and vector wind (B) plots illustrating a synoptic environment characteristic of Pattern 2 (NCEP-NARR plots obtained from NOAA ESRL's Physical Science Division (NOAA (n. d.)).....	121
4.18	Pattern 2 TCTOR frequency distribution stratified by F/EF Scale.....	122
4.19	Pattern 2 TCTOR outbreak frequency distribution stratified by month.....	122
4.20	Pattern 2 TCTOR outbreak frequency distribution stratified by synoptic hour.....	123
4.21	Spatial distribution of TCTORs within Pattern 2 outbreaks.....	123

4.22	500 hPa geopotential height (A) and vector wind (B) plots illustrating a synoptic environment characteristic of Pattern 3 (NCEP-NARR plots obtained from NOAA ESRL's Physical Science Division (NOAA (n. d.)).....	124
4.23	Pattern 3 TCTOR frequency distribution stratified by F/EF Scale.....	125
4.24	Pattern 3 TCTOR outbreak frequency distribution stratified by month	125
4.25	Pattern 3 TCTOR outbreak frequency distribution stratified by synoptic hour.....	126
4.26	Spatial distribution of TCTORs within Pattern 3 outbreaks.....	126
4.27	500 hPa geopotential height (A) and vector wind (B) plots illustrating a synoptic environment characteristic of Pattern 4 (NCEP-NARR plots obtained from NOAA ESRL's Physical Science Division (NOAA (n. d.)).....	127
4.28	Pattern 4 TCTOR frequency distribution stratified by F/EF Scale.....	128
4.29	Pattern 4 TCTOR outbreak frequency distribution stratified by month	128
4.30	Pattern 4 TCTOR outbreak frequency distribution stratified by synoptic hour.....	129
4.31	Spatial distribution of TCTORs within Pattern 4 outbreaks.....	129
4.32	500 hPa geopotential height (A) and vector wind (B) plots illustrating a synoptic environment characteristic of Pattern 5 (NCEP-NARR plots obtained from NOAA ESRL's Physical Science Division (NOAA (n. d.)).....	130
4.33	Pattern 5 TCTOR frequency distribution stratified by F/EF Scale.....	131
4.34	Pattern 5 TCTOR outbreak frequency distribution stratified by month	131
4.35	Pattern 5 TCTOR outbreak frequency distribution stratified by synoptic hour.....	132
4.36	Spatial distribution of TCTORs within Pattern 5 outbreaks.....	132
4.37	TCTOR outbreak frequency distribution stratified by synoptic pattern	133
4.38	Boxplots illustrating the distribution of TCTOR outbreak severity, stratified by synoptic pattern.....	133
4.39	Relative frequency distribution of June TCTOR outbreaks stratified by synoptic pattern.....	134
4.40	Relative frequency distribution of July TCTOR outbreaks stratified by synoptic pattern.....	134

4.41	Relative frequency distribution of August TCTOR outbreaks stratified by synoptic pattern.....	135
4.42	Relative frequency distribution of September TCTOR outbreaks stratified by synoptic pattern.....	135
4.43	Relative frequency distribution of October TCTOR outbreaks stratified by synoptic pattern.....	136
4.44	TCTOR frequency distribution stratified by F/EF Scale for cases exhibiting TC-westerly interaction (Patterns 1, 2, and 3).....	136
4.45	TCTOR outbreak frequency distribution stratified by month for cases exhibiting TC-westerly interaction (Patterns 1, 2, and 3).....	137
4.46	TCTOR outbreak frequency distribution stratified by synoptic hour for cases exhibiting TC-westerly interaction (Patterns 1, 2, and 3).....	137
4.47	TCTOR frequency distribution stratified by F/EF Scale for cases exhibiting no TC-westerly interaction (Patterns 4 and 5).....	138
4.48	TCTOR outbreak frequency distribution stratified by month for cases exhibiting no TC-westerly interaction (Patterns 4 and 5).....	138
4.49	TCTOR outbreak frequency distribution stratified by synoptic hour for cases exhibiting no TC-westerly interaction (Patterns 4 and 5).....	139
5.1	Map illustrating the distribution of TCTORs that occurred in an outbreak over the period 1995–2010 along with topography and bathymetry.	158
5.2	Schematic of midlatitude westerly meridional flow aloft.....	159
5.3	Schematic of an idealized Pattern 2 outbreak illustrating a potential region of diffluent flow.	160
5.4	Conceptual diagram illustrating the geometry between an ambient wind shear vector (bold red and blue arrows) and a hypothetical TC environment.	161
5.5	500 hPa geopotential height [m] monthly composite plots over the period 1995–2010.....	162
5.6	500 hPa geopotential height [m] plots corresponding to TC Frances' (2004) TCTOR outbreaks in sequential order from the first (top-left) to the last (bottom-right).	163

ABSTRACT

A STATISTICAL AND SYNOPTIC CLIMATOLOGY OF TROPICAL CYCLONE TORNADO OUTBREAKS

by

Todd W. Moore, B.S., M.S.

Texas State University-San Marcos

May 2013

SUPERVISING PROFESSOR: RICHARD W. DIXON

Tropical cyclones are capable of producing tornadoes prior to landfall as their outer rainbands move ashore through several days after landfall as they track inland. These tornadoes do not occur uniformly throughout a tropical cyclones' lifespan but, rather, occur in spatio-temporal clusters. This study sought to identify synoptic patterns associated with these spatio-temporal clusters, or tropical cyclone tornado outbreaks. Tropical cyclone tornado outbreaks are defined as three or more tornadoes in a six hour period centered about a primary synoptic hour and were identified using the Tropical Cyclone Tornado Database produced by Roger Edwards of the Storm Prediction

Center. One-hundred and thirty-three outbreaks were identified over the 1995–2010 period in association with East and Gulf Coast landfalling tropical cyclones. Statistical descriptions of the outbreaks are provided to highlight their typical severity and their temporal and spatial characteristics. Synoptic plots depicting 500 hPa geopotential height contours and 500 hPa wind vectors that temporally correspond to each identified outbreak were obtained from the National Centers for Environmental Prediction-North American Regional Reanalysis project to represent the outbreaks' synoptic environment. Using the synoptic climatology paradigm of pattern recognition, this study categorized 97% of the identified outbreaks into one of five synoptic patterns; the synoptic environments of four outbreaks did not reasonably fit the criteria of any of the five patterns. Outbreaks categorized as Pattern 1, 2, or 3 are produced by tropical cyclones that are beginning to interact with, or are embedded within, the midlatitude westerlies whereas those categorized as Pattern 4 or 5 are produced by tropical cyclones that are isolated from the westerly flow. Various degrees of synoptic scale forcing are likely to be present in Pattern 1–4 outbreaks. The results of this study suggest that tropical cyclone tornadoes can occur in spatio-temporal clusters of relatively high tornadic activity over relatively short time periods and that those tropical cyclones interacting with or located within the midlatitude westerlies are most likely to produce outbreaks.

CHAPTER I

INTRODUCTION

1.1 Overview

Tropical cyclones (TCs) are capable of producing tornadoes (TCTORs) prior to landfall as their outer rainbands move ashore, while they make landfall, and up to several days after landfall as they track inland (see Appendix A for a list of acronyms). Because of their potential to negatively impact both human and economic sectors of society, and because of their intriguing origin within TCs, these phenomena have received substantial attention from the research community (e.g. Pearson and Sadowski 1965; Hill, Malkin, and Schulz 1966; Orton 1970; Novlan and Gray 1974; Gentry 1983; Weiss 1987; McCaul 1991; Spratt et al. 1997; Curtis 2004; McCaul et al. 2004; Schneider and Sharp 2007; Verbout et al. 2007; Edwards 2008 and 2010a; Baker, Parker, and Eastin 2009; Belanger, Curry, and Hoyos 2009; Schultz and Cecil 2009; Cecil and Schultz 2010; Cohen 2010; Edwards et al. 2010; Agee and Hendricks 2011; Moore and Dixon 2011a and 2011b). The overarching goal of this body of research is to better understand TCTORs, with the hope that this understanding will advance our ability to detect, forecast, and warn people who are potentially at risk.

This study aims to complement and contribute to this body of research by identifying and analyzing temporally clustered TCTORs, or TCTOR outbreaks, associated with Gulf Coast and East Coast landfalling TCs in the United States over the

period 1995–2010, and by analyzing the synoptic environments that correspond to the identified outbreaks in search of recurring synoptic patterns. This study defines a TCTOR outbreak as three or more TCTORs in a six hour period centered about a primary synoptic hour (i.e., 0000, 0600, 1200, 1800 Universal Coordinated Time (UTC)). The six hour periods are centered about primary synoptic hours to synchronize the TCTORs in an outbreak and the synoptic plots used to represent the atmosphere during that outbreak. The identified outbreaks and their temporal and spatial characteristics were statistically analyzed. This study employs the synoptic climatology paradigm of pattern recognition to examine the synoptic environments corresponding to each outbreak. The 500 hPa geopotential height and vector wind pots corresponding to each outbreak were manually classified into five discrete synoptic patterns. Because TCs are mobile and dynamic, this study examines the synoptic scale 500 hPa features in a TC-relative framework (i.e., the synoptic scale features are spatially examined relative to the location of their associated TC).

The identification and analysis of TCTOR outbreaks and their corresponding synoptic environments may provide insight into the associations between the synoptic scale environment that a TC is embedded within and the occurrence of TCTOR outbreaks. Further, this insight may contribute to the establishment of analogs to use when assessing the potential for future outbreaks, which may improve our ability to issue outlooks for TCTORs up to a couple of days in advance (Shafer et al. 2009).

1.1.1 Dissertation Organization

The remainder of this chapter discusses the various motivations for the current dissertation and presents research questions and objectives. Chapter two reviews

pertinent background information and literature. Chapter three provides a discussion on data sources, the method used to identify TCTOR outbreaks, the method employed to classify the synoptic environment associated with TCTOR outbreaks, and the statistical methods employed to analyze outbreak characteristics. Chapter four presents the results of the classification and statistical analyses. Chapter five provides a discussion of the results and places them in the context of previous literature. Lastly, chapter six provides a summary of the current dissertation and discusses additional research inspired by this dissertation. All figures and tables in this dissertation are located at the end of their respective chapter unless otherwise noted.

1.2 Research Motivations

This study has been motivated by several issues regarding TCTORs in the United States. These include the tendency for TCTORs to spatially cluster, their potential to negatively impact society, forecasting and warning difficulties, and the geographic nature of a TCTOR synoptic climatology.

1.2.1 Tropical Cyclone Tornado Clusters

During a previous study (Moore and Dixon 2011a) it was observed that the spatial distribution of the TCTORs produced by a TC often exhibits clusters at various scales. This tendency is illustrated by TCs Ivan (2004) and Cindy (2005) and their associated TCTORs (Figure 1.1). Ivan and Cindy produced 118 and 48 TCTORs, respectively, but, rather than producing these TCTORs at an equal rate through time and across space, they produced somewhat discrete groups of relatively high TCTOR activity interspersed with regions of relatively low activity. Several studies have noted the tendency for TCTORs to cluster (e.g., Orton 1970; Curtis 2004; McCaul 1987; McCaul et al. 2004; Baker,

Parker, and Eastin 2009) but none have sought to identify and analyze the occurrence of these clusters in a large sample of TCs.

Why do TCs produce TCTORs at different rates? What are potential causes of this variable TCTOR production? Does the ambient environment in which a TC is located influence TCTOR potential? Research has shown that TCs are not independent of the ambient environment in which they form and track (Gray 1998; Arnott, Evans, and Chiaromonte 2004; Wang and Wu 2004; Molinari et al. 2006; Emanuel 2007; Ritchie and Elsberry 2007; Hendricks et al. 2010; Matyas 2010; Molinari and Vollaro 2010a and 2010b), thus it is plausible to hypothesize that changes in a TC's ambient environment, whether the ambient environment is changing or a TC's relative location within its environment is changing, may be associated with TCTOR variability through time and across space. In an attempt to isolate TCTOR clusters, this study defines, identifies, and analyzes temporally clustered TCTORs (i.e., TCTOR outbreaks). It also will assess possible associations between TCTOR outbreaks and the larger-scale environment surrounding TCs by identifying and analyzing synoptic patterns that correspond to the identified outbreaks.

1.2.2 Societal Impacts and Anticipation

TCTORs have the potential to negatively impact communities along coastlines and far inland. The potential threat is perhaps greatest at distances of 200–500 km from the TC center where TC-related hazards and, therefore, awareness and preparedness, may be low (Weiss 1987; McCaul 1991; Schultz and Cecil 2009). In addition, inland residents located on the periphery of a TC's projected trajectory may be aware of

impending threat, but they may be unprepared because they are not yet expecting TC-related severe weather (Spratt et al. 1997; McCaul et al. 2004).

Previous studies have provided quantitative data that illustrate the potential for impacts. For example, Moore and Dixon (2011b) reported that fourteen of the TCTORs produced by TC Ivan (2004) were responsible for a reported forty-eight casualties and a single TCTOR produced by TC Bonnie (2004) was responsible for thirty-two reported casualties. Other studies (Rappaport 2000; Czajkowski, Simmons, and Sutter 2011) have reported that TCTORs account for 4–5% of TC-related fatalities. In addition to being hazardous to humans, TCTORs also have been shown to be capable of causing a substantial economic loss. Stewart (2006) reported that TCTORs associated with TC Cindy in 2005 caused \$40+ million in economic losses.

Mitigating the economic loss associated with TCTORs may be a difficult task given the surge in economic development to accommodate increasing population in coastal and near-coastal regions, in addition to economic inflation. Human casualties (fatalities and injuries) can, however, be mitigated with improvements to TCTOR outlook, watch, and warning practices. A better physical understanding of TCTORs and the environment in which they occur may help foster such improvements. In addition, knowledge gained through continued study can be communicated to emergency managers and the general public to promote education and raise awareness of TCTORs.

Considerable attention has been given to the forecasting and detection of TCTORs because of their potential to negatively impact society and because of their unique association with TCs. Much of the previous and current research has focused on mesoscale and storm-scale processes such as atmospheric instability and wind shear

parameters, similar to the ingredients-based approach taken with non-TC tornadoes (e.g. McCaul 1991; McCaul and Wiseman 1996; Baker, Parker, and Eastin 2009; Edwards 2010a). Operational forecasting of TCTORs focuses on the juxtaposition of instability and shear parameters in addition to other lifting mechanisms within the TC envelope (Edwards 2008). These forecasting and detection techniques may not be as efficient with TCTORs, however, because the TC environment is vastly different from the environment in which most non-TC tornadoes develop, and because TC supercells are relatively small and shallow (Spratt et al. 1997; Schneider and Sharp 2007). In addition to forecasting and detection problems, relatively short-term watches and warnings may not be effectively communicated to the public because of power outage and the overall chaotic conditions associated with TCs. These factors, along with the relatively small size and short time-span of TCTORs, are likely to exacerbate the already difficult process of issuing tornado warnings and have likely contributed to the disproportionately high number of tornadoes with negative lead time warnings or no warnings in the Gulf Coast and East Coast regions of the United States (Brotzge and Erickson 2009 and 2010), where TCTORs are most common (Schultz and Cecil 2009; Moore and Dixon 2011a).

Root et al. (2007) assert that a synoptic climatology approach, which seeks relationships between the synoptic scale environment and the corresponding smaller-scale surface environment (Yarnal 1993), can provide insight into extreme weather events that may not be recognized by other forecasting and modeling techniques. The pattern recognition paradigm of synoptic climatology is one of the three tornado forecasting approaches employed by the Severe Local Storm (SELS) unit of the National Severe Storms Forecast Center (NSSFC), along with meteorological parameter assessment

(ingredients-based) and climatology (Doswell, Weiss, and Johns 1993). Previous synoptic climatology studies have identified recurring synoptic patterns that are favorable for non-TC tornadoes in certain regions (e.g., Leathers 1993; Davis, Stanmeyer, and Jones 1997) and a more prominent synoptically evident pattern that often is associated with substantial tornado outbreaks in the United States (Miller 1972; Doswell, Weiss, and Johns 1993). Surprisingly few efforts have been directed towards advancing our understanding of the synoptic environment corresponding to TCTOR outbreaks.

Additional study is needed to provide a better understanding of the synoptic environment associated with TCTOR outbreaks. Given its limited application to TCTORS and the need to explore additional methods of anticipating TCTORS, synoptic pattern recognition is a reasonable approach. Cohen (2010) asserts that synoptic pattern recognition can provide a framework for understanding the complex relationship between large-scale synoptic patterns and TCTOR outbreaks and, further, that it should be used by operational forecasters when determining the likelihood of TCTORS. Shafer et al. (2009) have demonstrated the utility of synoptic scale processes in distinguishing tornado outbreak and non-outbreak cases up to three days prior to an event.

If recurring synoptic patterns are found to be associated with TCTOR outbreaks, outlooks could be issued up to several days in advance when similar patterns are emerging. Outlooks are particularly valuable for TCTORS given that shorter-range watches and warnings may not be effectively communicated to the public. Furthermore, because outlooks can foster awareness of potential TCTOR activity days in advance, they might mitigate TCTOR-related casualties through heightened public awareness and emergency preparedness.

1.2.3 Geographic Nature

Synoptic climatology and Geography share several core concepts. Both disciplines have inherent interest of the concepts of space, time, region, and surface environment (Yarnal 1993). Furthermore, synoptic climatology arguably shares interest in the four traditions (i.e., spatial, area studies, man-land, and earth science), or themes, common to geographic inquiry identified by Pattison (1964). Spatial scale is another fundamental geographic concept that is common to the synoptic climatology approach. Because of the discipline's breadth, geographers often are concerned with phenomena at various scales and cross-scale dynamics (Harvey 1969; Abler, Adams, and Gould 1971). Synoptic climatology is likewise concerned with phenomena at multiple scales and cross-scale dynamics (Harman and Winkler 1991; Yarnal 1993). By applying the synoptic climatology framework to TCTORs, this study explores the interconnectedness between planetary and synoptic scale atmospheric circulation patterns, mesoscale or synoptic scale TCs embedded within the larger-scale environment, and small scale or microscale TCTORs embedded within larger-scale TCs (Figure 1.2).

1.3 Research Goals, Questions, Objectives, and Assumptions

The overall goals of this study are (1) to gain a better understanding of TCTOR outbreaks and the environment in which they occur and (2) to identify recurring synoptic patterns associated with TCTOR outbreaks using easily observable and physically meaningful atmospheric variables. Doing so may provide guidance to forecasters when determining the potential for TCTORs. Note, it is not recommended here that forecasters use only synoptic analogs when determining the likelihood of TCTORs but, rather, that this approach be used in conjunction with other approaches.

The following research questions guide this study:

1. What are the statistical characteristics of TCTOR outbreaks?
2. What recurring synoptic patterns are associated with TCTOR outbreaks?
3. How do the identified synoptic patterns vary in terms of the atmospheric variables of which they are composed?
4. What are the statistical characteristics of TCTOR outbreaks within each identified synoptic pattern?
5. Do the statistical characteristics of TCTOR outbreaks differ among the identified synoptic patterns?

To address the above questions, primary objectives of this study are:

1. Define, identify, and statistically analyze TCTOR outbreaks.
2. Identify the synoptic pattern corresponding to each identified TCTOR outbreak.
3. Describe the identified synoptic patterns in terms of the atmospheric variables of which they are composed.
4. Statistically analyze TCTOR outbreaks within each identified synoptic pattern.
5. Compare the statistical characteristics of TCTOR outbreaks among the identified synoptic patterns.

The discipline of synoptic climatology rests upon certain assumptions. Yarnal (1993) provides a list of eight assumptions that are fundamental to all synoptic climatology studies. Below is a list of the assumptions of this study which is adapted from Yarnal's (1993) list.

1. The larger-scale atmospheric circulation is a critical determinant of TCTOR outbreaks.
2. The Bergen school conceptual model of the structure and evolution of midlatitude synoptic scale cyclones is essentially correct.
3. The atmosphere can be categorized into mutually exclusive synoptic patterns.
4. The classification process identifies all important synoptic patterns.
5. The temporal scales of the TCTOR outbreaks and the atmospheric circulation processes involved in the synoptic patterns match.
6. TCTOR outbreak variability within the identified synoptic patterns is not a significant problem.

1.4 Chapter One Figures

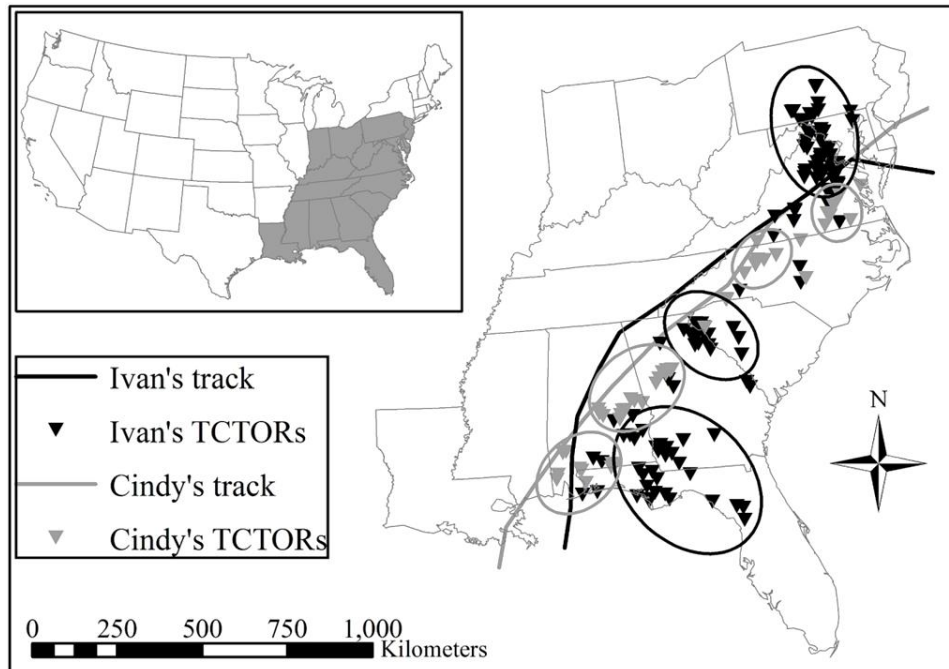


FIGURE 1.1. TCTORs associated with TCs Ivan (2004) and Cindy (2005). Black and gray ellipses illustrate the suggested tendency for TCTORs to cluster. No spatial or temporal parameters were used in the definition or identification of these illustrative examples.

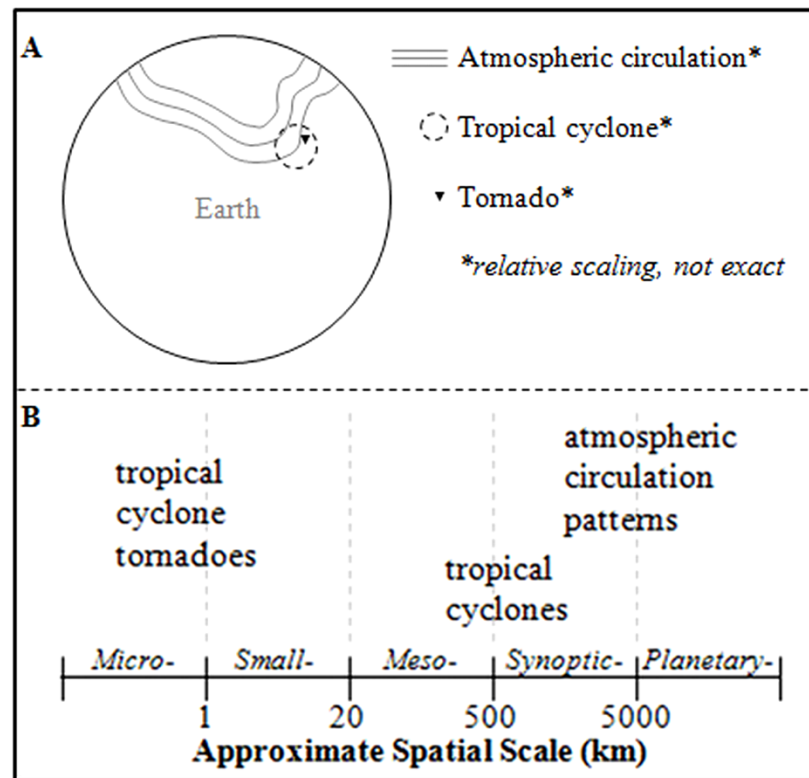


FIGURE 1.2. Conceptualization (A) and spatial scaling (B) of atmospheric phenomena involved in a synoptic climatology of TCTORs. Spatial scale adapted from Barry and Carleton (2001).

CHAPTER II

BACKGROUND AND LITERATURE REVIEW

Big whirls have little whirls that feed on their velocity, and
little whirls have lesser whirls and so on to viscosity
(Richardson 1922, 66).

2.1 Introduction and Background

This study concerns atmospheric vortices and patterns at various spatial scales: atmospheric circulation patterns and other atmospheric fields such as specific humidity at the planetary and synoptic scales, TCs at the synoptic and meso- scales, and tornadoes at the micro-scale (Figure 1.2). The atmosphere is a dynamic fluid in which phenomena acting over different spatial scales interact and influence one another. This cross-scale interaction often results in an energy transfer, or cascade, from larger- to smaller-scale phenomena, as governed by physical laws such as the Law of Conservation of Angular Momentum (Eagleman 1983). The existence of such cross-scale interactions through the atmosphere and their influence on boundary layer conditions is an underlying assumption of synoptic climatology (Yarnal 1993).

2.1.1 Atmospheric Circulation

Latitudinal variations in the receipt of solar radiation induce thermal and pressure gradients that drive the general circulation of the atmosphere (Barry and Carleton 2001;

Lockwood 2005). Once in motion, secondary factors such as Earth's rotational rate and topographic relief influence and shape the global circulation (Barry and Carleton 2001; Lockwood 2005). Myriad other factors influence atmospheric motion on various scales smaller than the planetary scale circulation, but these are beyond the scope of this discussion.

Following a simplified model, the general circulation of the atmosphere displays a tripartite structure of prevailing winds in the northern and southern hemispheres (Lockwood 2005; Figure 2.1). The Hadley Cell is a thermally induced circulation located roughly between the equator and thirty degrees north and south latitude that consists of northeasterly surface winds in the Northern Hemisphere/southeasterly surface winds in the Southern Hemisphere (trade winds), ascending motion near the equator, southwesterly winds aloft in the Northern Hemisphere/northwesterly winds in the Southern Hemisphere (anti-trade winds), and descending motion near thirty degrees north and south latitude (Nieuwolt 1977). From both, the North and South, Poles to approximately sixty degrees north and south latitude are another set of thermally induced cells known as the Polar Cells that consist of easterly surface winds, ascending motion near sixty degrees north and south latitude, westerly winds aloft, and descending motion near the North and South Poles (Lockwood 2005).

Regions of predominately westerly winds known as the westerlies are located within the midlatitudes between the Hadley and Polar Cells of the northern and southern hemispheres (Harman 1991; Barry and Carleton 2001). In the middle and upper altitudes of the midlatitude troposphere, the westerly flow generally creates a circumpolar vortex. This circumpolar vortex is, however, disrupted in the lower portion of the midlatitude

troposphere by baroclinic instability-induced cyclonic vortices, land/sea contrasts, and orographic and frictional effects on atmospheric flow (Barry and Carleton 2001; Lockwood 2005).

The circumpolar vortex in the middle and upper altitudes of the midlatitude troposphere can assume various flow regimes, or patterns, two most general of which are zonal and meridional flow (Figure 2.2). Zonal patterns are dominated by west-to-east flow whereas meridional patterns are dominated by north-to-south or south-to-north flow (National Weather Service (NWS) 2009). The predominant cross-latitude flow of meridional patterns is accomplished through wave trains with superimposed waves of various wavelength and amplitude that progress (west to east movement) or retrograde (east to west movement) through the midlatitude region (Bluestein 1993). Thorough reviews of the various midlatitude flow patterns and their dynamics are provided by Harman (1991), Bluestein (1993), and Barry and Carleton (2001).

2.1.2 Tropical Cyclones

Embedded within the larger-scale atmospheric general circulation are smaller-scale vortices such as TCs. TCs are cyclonic synoptic scale non-frontal systems with a warm core, organized deep convection, and closed wind circulation at the surface that originate over tropical or subtropical waters (NWS 2009). TCs are termed hurricanes when they are located over the Atlantic and Northeast Pacific Oceans, Caribbean Sea, and Gulf of Mexico, typhoons when located over the Northwest Pacific Ocean, and cyclones when located over the Indian Ocean. The Saffir-Simpson Scale can be used to further subdivide TCs based on their maximum one minute sustained wind speed (Appendix B).

TCs are tropical or subtropical-born systems composed of multiple structural elements and meteorological phenomena, and these systems have the potential to impact society within and beyond the Tropics. The general structural model of a TC includes an eye, eye wall, and spiral rainbands. The eye is a relatively calm circular area in the center of a TC with partly cloudy to clear skies whereas the eye wall is an organized band of cumulonimbus clouds encircling the eye (NWS 2009). Beyond the eye wall and region of relatively continuous, dense cloud cover, the convective rain clouds organize into bands that spiral out from the TC center (Elsner and Kara 1999). The eye wall and spiral rainbands consist of various modes of convection including individual convective towers, mesoscale convective systems, quasi linear convective systems, and supercells (Barnes et al. 1983; May 1996; Edwards et al. 2010; Houze 2010). The severe convective storms of which a TC is composed are capable of producing meteorological hazards such as extreme rainfall, extreme straight-line winds, and tornadoes (TCTORs).

The origin of a TC is generally confined to tropical or subtropical water bodies because they require a source of heat and moisture, but they do not develop within approximately eight degrees latitude of the equator as they require a sufficient Coriolis parameter to induce rotation (Gray 1998). The vast majority of Atlantic Basin TCs form and reach hurricane strength between ten and thirty-five degrees north latitude (Elsner and Kara 1999). Over their lifecycle, TCs do not remain immobile over their region of origin but, rather, track over extratropical waters and landmasses (Figure 2.3). In the North Atlantic Basin, the majority of TC tracks assume a general parabolic shape (Elsner and Kara 1999) in which they are initially steered in a westward direction under the influence of the prevailing northeasterly-to-easterly trade winds of the southern portion of

the North Atlantic subtropical anticyclone. While assuming this westward track, TCs also drift northward under the influence of the Coriolis Effect. Eventually, TCs encounter the western portion of the North Atlantic subtropical anticyclone where they assume a more northerly track and are steered more directly towards the midlatitudes. Once located within the midlatitudes, TCs typically are steered northeastward-to-eastward by the predominant westerly flow. Note that not all TC tracks in the North Atlantic Basin assume this general parabolic shape; some assume erratic tracks (Brettschneider 2008).

As TCs are steered through the larger-scale atmospheric circulation, they encounter ambient environments differing in terms of environmental humidity, vorticity, vertical motion, and wind shear, among others, and these environmental parameters influence various TC attributes such as their development, structure, intensity, track, geometric size, and precipitation field (Gray 1998; Arnott, Evans, and Chiaromonte 2004; Wang and Wu 2004; Molinari et al. 2006; Emanuel 2007; Ritchie and Elsberry 2007; Hill and Lackmann 2009; Hendricks et al. 2010; Matyas 2010; Molinari and Vollaro 2010a and 2010b). More exhaustive reviews of the physical attributes and societal impacts of TCs, particularly those of the North Atlantic Basin, are given by Pielke and Pielke (1997), Elsner and Kara (1999), and Keim and Muller (2009).

2.1.3 Tornadoes

Tornadoes are local scale violently rotating, either cyclonically or anticyclonically, columns of air that extend from a severe thunderstorm's cumulonimbus cloud base to Earth's surface (NWS 2009). The severe convective thunderstorms that produce tornadoes range from relatively small scale and isolated cells to convective

systems and supercells embedded within larger-scale midlatitude and tropical cyclonic systems (McCaul 1993; Rasmussen et al. 2000; Davies-Jones, Trapp, and Bluestein 2001; Baker, Parker, and Eastin 2009; Edwards et al. 2010; Grams et al. 2012).

Tornadoes have been documented across the globe, with the exception of Antarctica, but are most common in the United States (Brooks and Doswell 2001; Grazulis 2001; Brooks, Lee, and Craven 2003). The unique combination of geographic features in the United States often leads to the confluence of tornado-favorable ingredients, including instability, moisture, vertical wind shear, and a lifting mechanism (Eagleman 1983; Johns and Doswell 1992). Bates (1962, 242) states that “nowhere else in the world are the controls of the general circulation, geography, orography, and the jet stream more ideally related for the production of the tornado.” In general, the longitudinally oriented Rocky Mountains, Gulf of Mexico, and semi-permanent North Atlantic subtropical anticyclone off of the East Coast lead to a confluence of relatively warm and humid air near the surface transported by southerly winds and relatively cool and dry air aloft transported by westerly-to-northwesterly winds (Eagleman 1983). Incursion of the midlatitude westerly jet stream into this environment provides wind shear and synoptic scale upward vertical motion that can bring about a change from stable to conditionally unstable conditions (Bates 1962).

Within the United States, because of the same geographic reasons previously discussed, tornadoes are not uniformly distributed but are, rather, considered to be most common in a region known as Tornado Alley that spans generally from northwest Texas northeastward through central Minnesota and North Dakota, and from central Colorado and Wyoming eastward to northwest Iowa and east Kansas and Oklahoma (Brooks,

Doswell, and Kay 2003). Tornadoes in this region are predominately associated with severe storms embedded within midlatitude cyclonic systems and other more localized severe convective storms. TCTORs, on the other hand, are most common in another relatively tornado-prone region of the southeast United States known as Dixie Alley (Ashley 2007; Dixon et al. 2011), which is to the south and east of Tornado Alley; i.e., in the Gulf Coast, Appalachian, and East Coastal Plains regions (Novlan and Gray 1974; Shultz and Cecil 2009; Moore and Dixon 2011a).

2.2 Tropical Cyclone Tornadoes

2.2.1 Definition and Identification

Severe convective storms embedded within TCs are capable of producing TCTORs over a several day period spanning from before landfall as their outer rainbands come ashore through several days after landfall as the system tracks over land. Conceptually, TCTORs are simple to define: TCTORs are tornadoes produced by severe convective storms embedded within TCs. Operationally, however, defining and identifying TCTORs becomes more complicated. Spatial and temporal parameters are required to link individual tornadoes with TCs. Otherwise, TCTORs must be manually identified and linked to a TC using sources such as radar, satellite imagery, and synoptic weather maps.

Various spatial buffers and temporal parameters have been used to link tornadoes with their associated TC. Spatial buffers that have been used include 360 km (Cohen 2010), 400 km (Verbout et al. 2007; Moore and Dixon 2011a), 650 km (Belanger, Curry, and Hoyos 2009), 750 km (Schultz and Cecil 2009), and 800 km (McCaul 1991). Cohen (2010) used a 360 km parameter because it best captured the synoptic scale influence of

the TCs in his study. This radius also is approximate to the mean radius (352 km) of the outermost closed isobar of TCs reported by Kimball and Mulekar (2004). The 400 km parameter used by Verbout et al. (2007) and Moore and Dixon (2011a) also is approximate to the 352 km mean radius of the outermost closed isobar and is consistent with the distance at which TCTOR activity begins to decrease (Schultz and Cecil 2009). A radial distance of 360 km or 400 km may, however, result in an undercount of TCTORS, especially with large TCs. Using a larger search radius such as Belanger, Curry, and Hoyos (2009), McCaul (1991), and Schultz and Cecil (2009) reduces the likelihood of underestimating the number of TCTORS, but is likely to introduce tornadoes that are produced by surrounding disturbances rather than the TC. This is especially true for compact TCs.

Temporal parameters that have been used include the day before landfall through the day after landfall (Moore and Dixon 2011a), three days before landfall through three days after landfall (Schultz and Cecil 2009), and two days before landfall through four days after landfall (Verbout et al. 2007). The days prior to landfall account for TCTORS associated with outer rainbands moving ashore prior to landfall. The day of landfall and those following account for TCTORS produced by the system as it moves inland and begins to dissipate or undergo extratropical transition (ET).

According to the above discussion on spatial and temporal parameters, the following sample of operational definitions can be extracted:

- TCTORS are those tornadoes located within 400 km of TC center that occur two days prior to landfall through four days after landfall (Verbout et al. 2007).

- TCTORs are those tornadoes located within 750 km of TC center that occur three days prior to landfall through three days following landfall (Schultz and Cecil 2009).
- TCTORs are those tornadoes located within 400 km of TC center that occur the day before landfall through the day after landfall (Moore and Dixon 2011a).

Other methods, using weather maps, satellite imagery, and radar, have been used to identify TCTORs. For instance, the TCTOR dataset created by Roger Edwards of the Storm Prediction Center (SPC; Edwards 2010b) uses surface maps, upper air maps, and archived satellite imagery to manually verify that TCTORs are located within the cyclonic envelope of their associated TC. Schulz and Cecil (2009) used a similar approach, but only for those TCTORs that met one or more of the following criteria: (1) the TCTOR is located at distances greater than 500 km from their associated TC center, (2) the TCTOR is located at distances greater than 500 km from the coast, and/or (3) the TCTOR occurred more than three days from their associated TC's landfall. Manual verification is more time consuming than using pre-determined temporal and spatial parameters, but it does lead to the development of a more accurate TCTOR dataset that minimizes over- and under-counting. One-time-use datasets that employ different TCTOR identification criteria lead to varying TCTOR counts among studies, as shown by Moore and Dixon (2011a). Because of such inconsistencies, an annually updated and quality controlled dataset such as the TCTOR dataset (Edwards 2010b) should be adopted as the standard for TCTOR analyses. Manual verification also simplifies the definition of a TCTOR to a tornado produced by a severe storm embedded within a TC because it does not rely on spatial and temporal parameters.

2.2.2 *Climatology*

In an attempt to better understand the physical characteristics and occurrence of TCTORs, researchers have aggregated multiple events into large databases, or climatological records. Some of the first TCTOR climatologies appeared in the mid-1960s (e.g., Pearson and Sadowski 1965; Smith 1965; Hill, Malkin, and Schulz 1966). Throughout the years, climatological research has maintained an inductive approach, using TC and tornado observational records to create joint TCTOR databases.

Relatively long periods of record are required to generalize and to capture the inherent variability associated with TCTORs. One of the earliest extensive climatological studies examined twenty-five years (1948–1972) of data (Novlan and Gray 1974). Gentry (1983) followed this study with an examination of the next nine years (1973–1981). More recent studies have benefitted from the availability of a longer period of record, which allows for the examination of more events, and thus the capture of more variability. For example, McCaul (1991) examined the period 1948–1986 and Verbout et al. (2007) examined the period 1954–2004. Two of the most recent studies have examined the longest time periods, 1950–2007 (Schultz and Cecil 2009) and 1950–2005 (Moore and Dixon 2011a). All of the above climatological studies have considered North Atlantic Basin TCs that made landfall along the East Coast or Gulf Coast of the United States with the exception of Moore and Dixon (2011a), who focused specifically on Gulf Coast landfalls. In all, these studies have provided valuable information on TCTOR climatology, including statistics on normal and extreme TCTOR frequency and their temporal and spatial distributions.

2.2.2.1 General Frequency

Continued study throughout the years has shown that TCTORs are fairly common. An early study by Novlan and Gray (1974) reported that only 25% of the TCs in their study period (1948–1972) produced TCTORs. Later, Gentry (1983) reported that 70% of their examined TCs produced TCTORs. Most recently, Moore and Dixon (2011a) reported that 83% of their TCs produced TCTORs. Thus, studies have reported an increasingly large percentage of TCs that produce TCTORs over the years.

The typical number of TCTORs per TC, according to a statistical mean or median, has likewise increased through the years. Novlan and Gray (1974) reported an average of ten TCTORs per TC whereas Moore and Dixon (2011a) reported an average of twenty, and median of thirteen. Similar to that reported by Moore and Dixon (2011a), Belanger, Curry, and Hoyos (2009) reported a median of fifteen TCTORs per TC. These increases, however, do not imply that TCTORs are becoming more common. Rather, the more plausible inference is that advancements in tornado detection technology and increased public awareness have increased the number of reported TCTORs.

Unlike typical TCTOR activity, the variability from TC to TC has been more consistent through time. Studies have consistently reported that TCs have a 100+ range, with some TCs producing no TCTORs while others produce more than 100 (Novlan and Gray 1974; Verbout et al. 2007; Schultz and Cecil 2009; Moore and Dixon 2011a).

2.2.2.2 Temporal Distribution

Various temporal aspects of TCTORs have been examined including seasonality, diurnal distribution, and time of occurrence relative to TC landfall. TCTORs have a distinctly marked seasonal distribution, with the majority occurring in September (Smith

1965; Novlan and Gray 1974; Moore and Dixon 2011a). However, Moore and Dixon (2011a) showed that the median number of TCTORs produced by Gulf Coast landfalling hurricanes does not significantly vary between months. Rather, the seasonality of TCTORs is likely associated with the seasonality of TC landfalls (i.e., more (less) TC landfalls leads to more (less) TCTORs). Moreover, intense TCs, which have been shown to be more likely to produce larger numbers of TCTORs (Smith 1965; Hill, Malkin, and Schulz 1966; Novlan and Gray 1974; McCaul 1991; Verbout et al. 2007; Moore and Dixon 2011a), are more common in August and September.

TCTORs occur most often during afternoon hours (local time). Studies have reported peak activity at varying times in the afternoon including 1700 UTC (Novlan and Gray 1974), 2100–2400 UTC (Gentry 1983; McCaul 1991), 2000–2300 UTC (Schultz and Cecil 2009), and 2000–2200 UTC (Moore and Dixon 2011a). The similarity between these reported trends supports the hypothesis that solar heating and subsequent atmospheric instability increase the likelihood of TCTORs (Edwards 2010a). McCaul (1991), however, reported that values of convective available potential energy (CAPE) at 0000 and 1200 UTC are not significantly different and suggested that a diurnal observation bias may be responsible for the greater number of TCTORs reported during daytime hours. Whether this diurnal tendency is caused by increased solar heating or an observation bias is yet to be conclusively determined.

TCTOR activity is greatest near the time of landfall (Novlan and Gray 1974; Gentry 1983; McCaul 1991; Schultz and Cecil 2009; Moore and Dixon 2011a). In general, TCTOR activity rapidly increases approximately twelve hours before landfall and peaks shortly after landfall where it begins to gradually decrease (McCaul 1991;

Schultz and Cecil 2009; Moore and Dixon 2011a). Elevated TCTOR activity near the time of landfall is likely related to surface friction-induced vertical wind shear (Novlan and Gray 1974; Gentry 1983; McCaul 1991; McCaul and Weisman 1996; Suzuki et al. 2000; McCaul et al. 2004; Verbout et al. 2007). Even though TCTORs are most common near the time of landfall, it is important to note that they have been reported up to seventy-two hours before and after landfall (Schultz and Cecil 2009).

2.2.2.3 Spatial Distribution

TCTORs are spatially dispersed phenomena, although clusters of dense TCTOR activity are apparent when climatological datasets are plotted. These clusters typically are associated with individual TC landfalls. TC Beulah's (1967) TCTORs, for instance, account for a large number of TCTORs that have occurred in south Texas. TCTORs are most prevalent in the Gulf Coast region. According to Novlan and Gray (1974) and Gentry (1983), Gulf Coast-landfalling TCs are more likely than East Coast-landfalling TCs to produce tornadoes, likely because of differences in TC/land orientation. This led Moore and Dixon (2011a) to examine Gulf-Coast landfalling hurricanes exclusively. Their study showed that TC landfalls along the eastern section of the Gulf Coast typically have larger TCTOR outbreaks than landfalls in the central and western section of the Gulf Coast.

The spatial distribution of TCTORs is most dense near the coastline and becomes sparser farther inland (Novlan and Gray 1974; Gentry 1983; Schultz and Cecil 2009; Moore and Dixon 2011a). Moore and Dixon (2011a) reported that approximately 54% (78%) of tornadoes associated with Gulf Coast-landfalling hurricanes were located within 200 km (400 km) of the Gulf Coastline. Likewise, Schultz and Cecil (2009) reported that

approximately 80% of the TCTORs along the East and Gulf coastlines were located within 200 km of the coastline and that 94% were within 400 km. The predominance of near-coastline TCTORs is likely associated with a combination of increased vertical wind shear (Novlan and Gray 1974; Gentry 1983) and increased low-level convergence (Schultz and Cecil 2009), both of which increase as a TC encounters the rougher surface of land.

Research also has examined the spatial distribution of TCTORs within the TC environment. TCTORs have been reported at distances up to 800 km from the TC center (McCaul 1991). TCTORs have, however, been shown to cluster in two regions with respect to distance from TC center: (1) inner core TCTORs located within the eyewall and inner rainbands and (2) outer rainband TCTORs generally located between 200 and 400 km from TC center (Gentry 1983; Weiss 1987; Schultz and Cecil 2009). McCaul (1991) reported an observed maximum in TCTOR frequency at 300 km from TC center. In addition to the favored distance intervals from TC center, TCTORs have been shown to cluster in the right-front quadrant of TCs (Pearson and Sadowski 1965; Smith 1965; Hill, Malkin and Schulz 1966; Orton 1970; Novlan and Gray 1974; Gentry 1983; McCaul 1991; Edwards 2008; Schultz and Cecil 2009; Edwards 2010a). Wind shear (Novlan and Gray 1974; Gentry 1983; McCaul 1991; Bogner, Barnes, and Franklin 2000) and helical flow (McCaul 1991) also are elevated in the right-front quadrant, thus creating a distinct region of TCTOR-favorable conditions.

2.2.3 Case Studies

Detailed accounts of individual TCTOR events have been around for nearly a century (e.g., Gray 1919), and have continued throughout the years (Barbour 1924; Hills

1929; Malkin and Galway 1953; Sadowski 1962; Rudd 1964; Orton 1970; McCaul 1987; Snell and McCaul 1993; Suzuki et al. 2000; Baker, Parker, and Eastin 2009). Many of these case studies have focused on some of the most prolific TCTOR-producing TCs. For instance, Orton (1970) provided an account of the tornado frequency, spatial distribution, and human and economic losses associated with Hurricane Beulah (1967). Baker, Parker, and Eastin (2009) examined Hurricane Ivan (2004) in search of environmental parameters that may support supercell formation, and thus TCTORs, within TC environments. Some of the more recent case studies have proven beneficial to the verification of supercell structures within and near TC environments (Suzuki et al. 2000; Baker, Parker, and Eastin 2009), in turn contributing to our understanding of TCTOR genesis and advancing detection abilities. A primary weakness of these case studies, however, is that they do not facilitate generalization because they do not capture case-to-case variability.

2.2.4 Formation, Forecasting, and Detection

Various meteorological variables, such as moisture, instability, lift, and wind shear, are proposed to be linked to TCTOR formation (Edwards 2008; Edwards et al. 2010). Multiple indices and parameters have been developed to operationalize these variables (Doswell and Schultz 2006). McCaul (1991) provides a summary of specific environmental vertical motion and shear parameters that correlate with TCTOR occurrence. He reported that the bulk Richardson number (BRN), storm relative helicity (SRH), and various measures of vertical wind shear are positively correlated with TCTOR activity and that CAPE is weakly negatively correlated; McCaul et al. (2004) suggested that earlier measurements of CAPE might be biased low, indicating that

convective instability may be more important to TCTOR genesis than previously reported. Of the above parameters, the presence of vertical wind shear is perhaps the oldest and most well supported parameter linked to TCTORS (Novlan and Gray 1974; Gentry 1983; McCaul 1991; McCaul and Weisman 1996; Suzuki et al. 2000; McCaul et al. 2004; Verbout et al. 2007). Gentry (1983) proposed that vertical wind shear is created when surface friction reduces the velocity of low-level winds but not the velocity of higher-level winds. Studies also have shown that mini-supercells often are located within TC rainbands and that these mini-supercells often spawn TCTORS (McCaul 1987; McCaul 1993; McCaul and Weismann 1996; Spratt et al. 1997; Suzuki et al. 2000; McCaul et al. 2004).

Synoptic scale variables have, likewise, been associated with TCTORS. These include dry air intrusion into the TC environment (Novlan and Gray 1974; Vescio, Weiss, and Ostby 1996; Curtis 2004; Cohen 2010), the presence and proximity of a 500 hPa trough in the midlatitude westerlies (Verbout et al. 2007; Baker, Parker, and Eastin 2009), the relative location of a 200 hPa jet (Cohen 2010), and the location of baroclinic (frontal) zones (Edwards and Pietrycha 2006).

Forecasters often utilize many of the meteorological variables and parameters that have been shown to be associated with TCTOR formation when determining the likelihood that a TC will spawn TCTORS. This ingredients-based approach typically concentrates on the concurrent appearance and juxtaposition of instability, lift, and vertical wind shear (Doswell 1987; Johns and Doswell 1992; Doswell, Weiss, and Johns 1993; Edwards 2008; Edwards et al. 2010); moisture is typically not a focus with TCTORS because the TC environment is moisture rich (Edwards and Pietrycha 2006;

Edwards 2008, 2010a, and 2012; Edwards et al. 2010). Schneider and Sharp (2007) provide a list of meteorological parameters and threshold values to distinguish between low and high TCTOR threat.

Other forecasting approaches have been used to assess the likelihood of TCTOR genesis. For instance, Belanger, Curry, and Hoyos (2009) and Cecil and Schultz (2010) employed empirical models to forecast the threat of TCTORs (Belanger, Curry, and Hoyos 2009; Cecil and Schultz 2010). Pattern recognition and analogs also have been proposed as methods of assessing the potential for TCTORs (Cohen 2010). Root et al. (2007) point out that major and extreme weather events may not be recognized in model outputs by even experienced forecasters and, therefore, proposed the use of synoptic pattern recognition and forecast analogs when predicting major and extreme weather events. Similarly, Cohen (2010) recommends the use of synoptic pattern recognition in the forecast process when identifying the likelihood of TCTORs.

The NWS has developed an experimental project known as the Tropical Cyclone Tornado Threat Product to assess and communicate the potential threat of TCTORs (NWS n. d.). Such a product has the potential to advance warning capabilities and increase public awareness of the TCTOR threat. The Tropical Cyclone Tornado Threat Product implements multiple forecasting approaches by considering regional scale environmental conditions and local scale parameters that enhance the potential for TCTORs. Local weather forecast offices (WFOs) issue a threat index ranging from zero (no threat) to five (extreme threat) once a TC watch or warning has been issued for a region. The threat level is based on the likelihood of TCTOR occurrence and the anticipated intensity of the most intense TCTORs.

Despite advances in our understanding of the meteorological variables and parameters that are conducive to TCTORs, forecasting TCTORs, especially those not associated with supercells, remains a difficult and imprecise task (Edwards et al. 2010). Because of forecasting difficulties, TCTOR detection is an important task to the mitigation of TCTOR impacts. Weather radar is the primary tool for operational TCTOR watches and warnings because intense rainfall, low cloud bases, fast translational speeds, and the short-lived nature of TCTORs make visual detection by storm spotters difficult (Edwards 2008). Given its importance, continuous research efforts have been directed towards recognizing and interpreting TCTOR radar signatures (e.g., McCaul 1987; Snell and McCaul 1993; Spratt et al. 1997; McCaul et al. 2004; Schneider and Sharp 2007). This line of research has provided unique insight into the near-TCTOR environment, including their association with mesocyclones and other traditional tornadic radar signatures such as hook echoes.

Weather radar analysis is not without its drawbacks. For instance, the TCTOR-related inflow notches and hook echoes observed by Spratt et al. (1997) were often less apparent than those seen with non-TC tornadoes. In addition, TC supercells, which are responsible for the majority of TCTORs (Edwards et al 2010), are notably different (i.e., smaller and shallower with slower rotational velocity) than non-TC supercells (McCaul 1991). Spratt et al. (1997) argue that, in addition to continued use of advanced weather radar (i.e., weather surveillance radar-88 Doppler (WSR-88D)) technology, model simulations of the structure and evolution of TCTORs and case studies may increase detection and warning capabilities.

2.2.5 General Conclusions from the Literature

The investigation of TCTORs from various perspectives has provided insight into their occurrence. The following bulleted list summarizes general outcomes from the body of TCTOR research that has accrued over the years. This list is not exhaustive and there is no particular ordering.

- TCTORs are most common near the coastline. The clustering of TCTORs near the coastline is most likely associated with the increased vertical wind shear and low-level convergence induced by the differential effect of surface friction.
- TCTORs are most common in the right-front quadrant of TCs, but are possible at any location within the storm environment and within surrounding non-related disturbances.
- A large portion of TCTORs are associated with mini-supercell structures within the deep convection of the eyewall and surrounding rainbands.
- TCTORs have occurred in all months of hurricane season; however, the climatological record indicates maximum activity in September.
- Intense TCs are more likely to produce TCTORs, especially large outbreaks. TCTORs have, however, been reported with tropical systems of all strengths.
- TCTORs are most common near the time of their associated TC's landfall, likely because of the same reason for elevated TC activity near the coastline (see the first bullet).
- A significant diurnal signal is yet to be justified because of potential data bias.
- TCTORs are more common with Gulf Coast landfalls than with East Coast landfalls.

- Elevated levels of SRH, vertical wind shear, and dry air intrusion are indicators of potential TC tornadic activity.
- Various forecasting approaches should be used in conjunction with Doppler radar technology during the detection, forecasting, and warning procedures.

2.3 Synoptic Climatology

2.3.1 Definition

Multiple definitions of synoptic climatology have been given over the years. The bulleted list below provides a sample of these definitions.

- Synoptic climatology relates atmospheric circulation to the surface (Court 1957).
- Synoptic climatology is the study of the relationship between atmospheric circulation and local or regional climate (Barry and Perry 1973).
- Synoptic climatology is the study of the relationship between the atmospheric circulation and the surface environment, where surface environment refers to a particular meteorological phenomenon, the overall weather conditions in the planetary boundary layer, or a non-direct meteorological phenomenon such as air pollution occurring in a region (Yarnal 1993).
- Synoptic climatology studies the relationship of local and regional climate conditions to the atmospheric circulation (Barry and Carleton 2001).

From this sample of definitions it can be concluded that the most distinctive theme of synoptic climatology is its attempt to relate the larger-scale atmospheric circulation to the smaller-scale surface environment. Note that Yarnal (1993) makes the distinction that the surface environment includes meteorological and non-meteorological phenomena. No distinction is made by any of these definitions regarding which

atmospheric variables to use when classifying the atmospheric circulation. However, in a discussion of synoptic and dynamic climatology, Court (1957) commented that synoptic climatology should utilize synoptic scale variables such as pressure patterns, air masses, and map patterns when categorizing atmospheric circulation. A review of the synoptic climatology literature reveals that studies often have utilized the synoptic scale variables suggested by Court (1957) and, furthermore, that they often have utilized variables that are theoretically or empirically linked to the surface environment or phenomenon of interest.

2.3.2 Historical Developments

Humans have long been aware of the link between large scale atmospheric motions and surface weather conditions. Some of the earliest examples of this awareness linked wind direction with typical weather conditions. Barry and Perry (1973), for instance, highlight Biblical references that illustrate knowledge of the link between wind direction and associated surface weather. Another illustration of this awareness is the Tower of the Winds in Athens, Greece, constructed in the second century AD, which associates wind from each cardinal direction with characteristic weather conditions (Karapiperis 1951). Weather lore and adages in many regions of the world provide many more examples that illustrate the awareness of the influence of common large scale atmospheric motions on surface weather (e.g., Inwards 1950; Freier 1992).

In the mid-nineteenth century, the work of William Ferrell and Christophorus Buys-Ballot established the relationship between wind and horizontal pressure gradients. This discovery provided the foundation for synoptic analysis (Leighly 1949) and, as soon as synoptic weather maps were produced in the late nineteenth century, investigators

began manually classifying and analyzing synoptic weather maps, noting commonly recurring synoptic patterns (Barry and Carleton 2001). For instance, Wladimir Köppen studied the influence of pressure patterns and the resultant airflow on weather in St. Petersburg, Russia, using six atmospheric circulation patterns: (1) straight; (2) anticyclonically curved isobars; (3) cyclonically curved isobars; (4) anticyclone center; (5) cyclone center; and (6) intermediate conditions (Barry and Perry 1973). This study has been said to be the beginning of synoptic climatology (Stringer 1972), although the term synoptic climatology was not proposed until the mid-twentieth century. Other influential studies in the early progress of synoptic climatology are those by Ralph Abercromby and Ernest Gold. In the latter half of the nineteenth century, Abercromby analyzed weather conditions over the British Isles in terms of wind vectors using the four cardinal directions (Abercromby 1883 and 1887). Later, in the early twentieth century, Gold classified pressure patterns over England and then related them to local weather conditions (Gold 1920).

The term synoptic climatology was proposed during the Second World War by Woodrow C. Jacobs in the United States and by Charles S. Durst in Great Britain (Hare 1955). Intentions for synoptic climatology at this time were to aid military operations by providing long range weather forecasts (Court 1957; Barry and Perry 1973). Synoptic climatology remained focused on relating synoptic patterns to the corresponding surface weather for the next few decades (Yarnal 1993). Also, prior to the 1980s, many synoptic climatology studies and projects focused on classification methods and schemes (Yarnal et al. 2001). Two highly regarded manually-derived synoptic classifications (Yarnal

1993) were developed in the 1970s: The Lamb Weather Types (Lamb 1972) and The Muller Classification (Muller 1977).

Beginning in the late 1970s, synoptic climatologists expanded their attention from surface weather and began applying the pattern recognition approach to a variety of environmental problems such as air pollution, pollen density, biological stress, crop yields, and water quality and quantity (Kalkstein and Corrigan 1986, Yarnal 1993). Also at this general time, emphasis shifted away from classification methods and schemes and towards their application (Yarnal et al. 2001). To date, the synoptic climatology approach has been applied to various environmental problems and weather phenomena including air pollution (e.g., Comrie and Yarnal 1992; Davis and Gay 1993; Comrie 1994), precipitation (e.g., Keim and Muller 1992; Sweeney and O'Hare 1992; Keim and Faiers 1995; Keim 1996; Konrad 1997), severe winter weather and snowfall (e.g., Leathers and Ellis 1996; Ryan 2009), solar radiation regimes (Suckling and Hay 1978), and non-TC tornadoes, TCTORS, and other severe storms (e.g., Davis and Rogers 1992; Leathers 1993; Davis, Stanmeyer, and Jones 1997; Bentley, Mote, and Byrd 2000; Cohen 2010). A more comprehensive discussion of the application of synoptic climatology to non-TC tornadoes and TCTORS is provided in section 2.4.

The ability of synoptic climatology to simplify a multitude of complex meteorological variables by categorizing them into discrete groups has attracted many researchers focused on a variety of problems (Kalkstein 1979; Perry 1983).

Classification, or the systematic grouping of events into classes based on shared properties or relationships (Abler, Adams, and Gould 1971), is perhaps the most basic procedure by which scientists impose order and coherence upon the large amount of

complex information from the real world; classification reveals patterns that often are obscured in raw data, aids in the formulation of hypotheses, and guides further investigations (Harvey 1969; Abler, Adams, and Gould 1971). Classification is a necessity of scientific endeavor because, as put by Abler, Adams, and Gould (1971, 149), “If every object and event in the world were taken as distinct and unique – a thing in itself unrelated to anything else – our perception of the world would disintegrate into complete meaninglessness.” This is especially true for synoptic climatology, with its attempt to find links between surface phenomena and common modes, or patterns, in the ever-changing atmospheric circulation. Because of the inherent need for synoptic climatologists to simplify the atmospheric circulation, a primary concern of theirs has become to classify the atmosphere into discrete groups (Yarnal 1993).

2.3.3 Approaches and Methods

All synoptic climatology studies share certain steps and characteristics. According to Barry and Perry (1973), all synoptic climatology studies consist of two basic steps: (1) atmospheric circulation classification; and (2) the assessment of the relationship between the atmospheric circulation categories and a given location's or region's weather elements. Later, Yarnal (1993) provided a similar list of commonalities among synoptic climatology studies: (1) they classify the atmospheric circulation; (2) they link two or more scales of analysis: the large-scale atmospheric circulation and the smaller-scale surface environment; (3) they examine the effect of climate variability on the surface environment; and (4) they focus on the spatial unit of region.

Two general methodological approaches exist by which a synoptic climatology study can be designed: (1) circulation-to-environment or (2) environment-to-circulation

(Yarnal 1993). The circulation-to-environment approach proceeds first with the classification of the atmospheric circulation. The surface environment is related to the atmospheric circulation after the classification process. The classification of the atmospheric circulation is, therefore, independent of the corresponding surface environment. For instance, considering TCTOR outbreaks, a circulation-to-environment approach would first proceed with the classification of the atmosphere for a given spatial unit and time period. The classification would identify synoptic patterns that are based on predetermined criteria that favor TCTOR development. After the classification is complete, the surface environment would be categorized as TCTOR outbreak or non-outbreak and then each of the outbreaks and non-outbreaks would be related to its corresponding synoptic pattern.

According to the environment-to-circulation approach, the surface environment controls the classification process. That is, the atmospheric circulation is only classified when a particular surface environment or phenomenon is present. The classification of the atmospheric circulation is, therefore, dependent on the corresponding surface environment. For example, considering TCTOR outbreaks, the initial step would be to identify TCTOR outbreaks. Once the outbreaks are identified, the atmospheric circulation corresponding to each outbreak would be classified.

Multiple classification methods may be used to classify the atmospheric circulation into discrete groups. Yarnal (1993) identified and thoroughly discussed several classification methods including compositing, correlation-based map patterns, eigenvector-based synoptic patterns and map patterns, and manual synoptic patterns, that are commonly used in modern synoptic climatology. Compositing, correlation-based,

and eigenvector-based methods are collectively known as computer-assisted methods (Yarnal 1993). Compositing involves the averaging of synoptic maps that correspond to a specific surface environment. Yarnal (1993) suggests that it is a useful method for taking an initial look at the link between a specific surface environment and the associated atmospheric circulation, but that the averaging of maps induces a false impression of the typical, or normal, synoptic pattern and reduces pattern variability. By reducing pattern variability, an analyst may omit critical, but infrequent, synoptic patterns. Compositing, therefore, should not be used as the sole classification method in an analysis. Correlation-based and eigenvector-based methods utilize algorithms to determine the synoptic map patterns and to sort the data into these patterns (Yarnal 1993). These methods gained popularity in the 1970s and 1980s because they were viewed as being easier to perform and time efficient, and because they were regarded as more objective than manual classification (Barry 1980). Although computer-assisted methods are easier and more time efficient, it is now realized that all methods of classification, including computer-assisted methods, require subjective decisions to be made in the research design process (Yarnal 1993).

Manual synoptic classification involves manually classifying synoptic maps into categories, or synoptic patterns (Yarnal 1993). Manual classification dates back to the development of the synoptic weather map in the late nineteenth century (Barry and Carleton 2001), thus it has withstood the test of time as a viable classification method. Many analysts prefer manual classification techniques because they allow the analyst to become thoroughly aware of, and familiar with, the linkages between the large scale synoptic environment and the surface environment, they allow the analyst to tailor the

classification to their data, and they allow the analyst to completely control the classification process (Yarnal 1993). Computer-assisted methods, on the other hand, have a black-box element regardless of an analyst's knowledge of the method's mathematical foundation and parameters (Yarnal 1993). Barry and Carleton (2001) affirm that persistent examination of synoptic weather maps allows an analyst to gain familiarity with commonly recurring synoptic patterns. Manual classification also ensures that the identified synoptic patterns have meteorological significance (Cannon, Whitfield, and Lord 2002) and its flexibility allows analysts to consider the synoptic patterns occurring several days before and after the surface environment of interest rather than individual days in isolation (Jones, Hulme, and Briffa 1993). Manual classification is, however, not without its limitations. It is a labor and time intensive process and, because of its subjective nature, is difficult to replicate because the classification process will differ between analysts and even with a single analyst (Key and Crane 1986; Yarnal 1993; Barry and Carleton 2001).

2.4 Synoptic Climatology of Tropical Cyclone Tornadoes

In the past, synoptic pattern recognition has been applied to the creation of specialized tornado forecasting techniques (Doswell, Weiss, and Johns 1993). Johns and Doswell (1992) propose that pattern recognition may be valuable to the identification of tornado outbreak potential, but that uncertainty exists concerning the links between synoptic scale processes and tornado outbreaks. In a more recent study, Shafer et al. (2009) demonstrated the utility of synoptic scale variables in distinguishing tornado outbreak and non-outbreak cases up to three days prior to the event and advocate the potential of synoptic scale predictability of tornado outbreaks. Similarly, Mercer et al.

(2012) reported differences in the patterns of 500 hPa and 850 hPa geopotential height composites associated with tornado outbreak and non-outbreak severe weather events.

Synoptic pattern recognition has been extensively applied to non-TC tornadoes in the United States. Certain synoptic patterns, such as those identified by Miller (1972), have successfully described the general environments in which tornado outbreaks tend to occur. Miller's Type B pattern, which is characterized by the concurrence and juxtaposition of a surface midlatitude cyclone, an upper-level trough, a strengthened polar jet stream, and a low-level jet from the south, typifies a "classic" tornado outbreak setting in the United States (Johns and Doswell 1992; Doswell, Weiss, and Johns 1993). Throughout the years, synoptic studies often have reported tornado-favorable patterns similar to Miller's Type B Pattern (e.g., Fujita, Bradbury, and Van Thullenar 1970; Agee et al. 1975; Leathers 1993; Roebber, Schultz, and Romero 2002; Corfidi et al. 2010; Mercer et al. 2012).

Other, often localized, tornado outbreaks are associated with atypical synoptic patterns. Such atypical patterns have led some researchers to focus on synoptic patterns associated with tornado outbreaks in specific geographic regions. Leathers (1993), for example, examined the synoptic conditions associated with tornadoes in the northeastern United States. He reported that the most common synoptic features present during the initiation of tornadic storms were a strong surface cyclone, a mid-tropospheric short wave trough, and a frontal boundary. Davis, Stanmeyer, and Jones (1997) identified five recurring synoptic categories, and a sixth TC category, that are associated with tornadoes in Virginia.

Only a few studies have analyzed synoptic conditions associated with TCTOR outbreaks. Verbout et al. (2007) noted the propensity for recurring TCs to produce TCTOR outbreaks and, thus, examined synoptic conditions in search of recurring patterns in association with TC recurvature. They compared synoptic composites for outbreak and non-outbreak cases associated with TC landfalls in Texas and found that 500 hPa geopotential height and wind shear between the surface and 850 hPa best distinguished between outbreak and non-outbreak landfalls. Outbreak landfalls were associated with a 500 hPa trough in the north-central United States whereas non-outbreak landfalls were associated with a 500 hPa ridge in the north-central United States placing the jet stream farther poleward of the landfalling TC. Further, outbreak landfalls were associated with a relatively high mean low-level wind shear of $4\text{--}8\text{ m s}^{-1}$ whereas the wind shear associated with non-outbreak landfalls was only half as strong. From these results, they hypothesized that the 500 hPa trough situated over the north-central United States enhanced deep-layer shear in recurring TCs, which increased the likelihood of mesocyclogenesis and, therefore, TCTORS.

Cohen (2010) examined the synoptic scale environment associated with TCs, with the intent of distinguishing between TCs that are likely to produce TCTORS and those that are not. He created synoptic composites of 200 hPa flow, 850 hPa flow, mean sea level (MSL) pressure, 500 hPa geopotential height, 200 hPa temperature, and 600 hPa relative humidity for substantially tornadic TCs (four or more tornadoes) and non-substantially tornadic TCs (no more than one tornado). Several of these composites were successful in distinguishing between TCs that produced TCTORS and those that did not. Substantially tornadic TCs were associated with (1) an enhanced 200 hPa jet streak to the

northwest of the TC, (2) an organized, relatively large, and directionally symmetric 850 hPa cyclonic wind field with the strongest flow in the northeast semicircle of the cyclonic envelope, (3) a distinct, organized, and symmetric MSL cyclonic pattern, and (4) a 600 hPa wedge of dry air cyclonically enveloping the TC and intruding into its eastern half.

Belanger, Curry, and Hoyos (2009) examined the usefulness of synoptic scale variables in explaining TCTOR frequency. Rather than using a traditional synoptic classification method such as the compositing technique used by Verbout et al. (2007) and Cohen (2010), they developed two multiple regression models with synoptic scale parameters serving as the independent variables. They hypothesized that TCTOR frequency is dependent upon TC intensity at landfall (maximum one-minute sustained wind speed), TC horizontal size (radius of the outer-most closed isobar), mid-level dry air entrainment (500 hPa specific humidity gradient within 5° from TC center), and TC recurvature (defined as the difference between twelve-hour averaged storm heading at landfall and the twelve-hour averaged storm heading at the time of the last tropical advisory). Their model that included all four predictors, called *Recon*, explained 70% of the variability in observed TCTOR frequency.

Other studies have analyzed or speculated on the importance of synoptic scale variables to TCTOR outbreaks. For instance, multiple studies have noted the importance of the interaction with, and/or entrainment of, a reservoir of mid-tropospheric dry air into the TC environment (Novlan and Gray 1974; McCaul 1987; Curtis 2004). Curtis (2004) examined thirteen TCTOR outbreak cases, eleven of which showed signs of dry air intrusion. He identified two distinct patterns when considering relative humidity at the 500 hPa, 700 hPa, and 850 hPa levels: (1) a region of dry air to the north or northwest of

a TC, which gradually divides into two lobes, one to the northwest and another to the northeast of a TC as it advances; (2) a region of dry air to the east of a TC is entrained into the TC's circulation. Similar to Verbout et al. (2007), Baker, Parker, and Eastin (2009) noted the importance of enhanced vertical wind shear associated with an approaching midlatitude trough to the TCTOR outbreaks produced near the time of TC Ivan's (2004) landfall. Surface baroclinic zones, whether pre-existing boundaries merging with a TC or boundaries developing within the TC environment, also have been linked to TCTORs (Pietrycha and Hannon 2002; McCaul et al. 2004; Edwards and Pietrycha 2006). The origin of these boundaries may be midlatitude frontal cyclones migrating across the United States or, as pointed out by Schultz and Cecil (2009), cloud-free regions produced by mid-tropospheric dry air entrainment can induce differential surface heating and baroclinic boundaries within a TC.

2.5 Concluding Remarks

TCTORs have received substantial attention from the research community to satisfy basic research interests and to address practical issues such as forecasting, warning, and casualty mitigation. Case studies have provided information about TCTORs associated with a single TC landfall. Although these studies do not capture TCTOR variability, in terms of their frequency, intensity, or genesis, they are practical for detailed weather radar studies that provide insight into the mesoscale TCTOR environment. Climatological studies, especially more recent studies, have captured the TCTOR variability missed by case studies and have provided various temporal and spatial generalizations. These studies have essentially provided insight into when and where TCTORs are most prevalent. Other studies have analyzed mesoscale and synoptic

scale environments associated with TCTORs in search of potential variables to distinguish between TCTOR-favorable and non-favorable environments.

The ambient environment in which TCTORs occur is different than that of non-TC tornadoes (McCaul and Weisman 1996). Because of this difference, traditional tornado forecasting and detection procedures, such as the ingredients-based forecasting approach and weather radar detection, may not be as competent with TCTORs. Furthermore, there are inherent difficulties in the dissemination of TCTOR watches and warnings. It therefore seems practical to explore additional approaches that may be useful to the understanding and anticipation of TCTORs. These additional approaches should not replace existing methods but should, rather, be used in conjunction with other methods.

Root et al. (2007) emphasize that major weather events, such as TCTOR outbreaks, often are associated with recurring synoptic patterns, making pattern recognition a practical approach. Also, according to Doswell, Weiss, and Johns (1993), tornado outbreaks are typically associated with certain synoptic patterns, or synoptically evident patterns. More recently, Shafer et al. (2009) demonstrated that synoptic scale variables are capable of distinguishing tornado outbreak and non-outbreak cases up to three days in advance.

A few studies have had success in identifying synoptic patterns associated with TCTOR outbreaks and, therefore, have provided empirical links between multiple synoptic scale variables and TCTORs that provide insight and guidance to future studies. The two previous traditional synoptic studies (Verbout et al. 2007; Cohen 2010) have applied the compositing method, which is a valuable method for taking an initial look at

generalized synoptic patterns (Yarnal 1993). Because of its averaging process, however, a drawback of compositing is that variability is reduced or even lost. It, therefore, seems practical to use another synoptic classification method to investigate synoptic patterns associated with TCTORs. Applying another classification method to TCTORs may verify the previous TCTOR outbreak composites produced by Verbout et al. (2007) and Cohen (2010) and may even provide additional insight overlooked by the compositing process.

Given the limited application of the pattern recognition paradigm to TCTORs, it seems reasonable to manually classify the ambient environment associated with TCTOR outbreaks. Manual classification provides perhaps the most in-depth insight into the relationship between synoptic patterns and the surface environment because of its thorough and iterative process (Yarnal 1993; Barry and Carleton 2001). The identification of synoptic patterns that favor TCTOR outbreaks will provide insight into synoptic scale forcings conducive to TCTORs and may provide forecasters with analogs that can be used to better anticipate TCTORs (Cohen 2010).

2.6 Chapter Two Figures

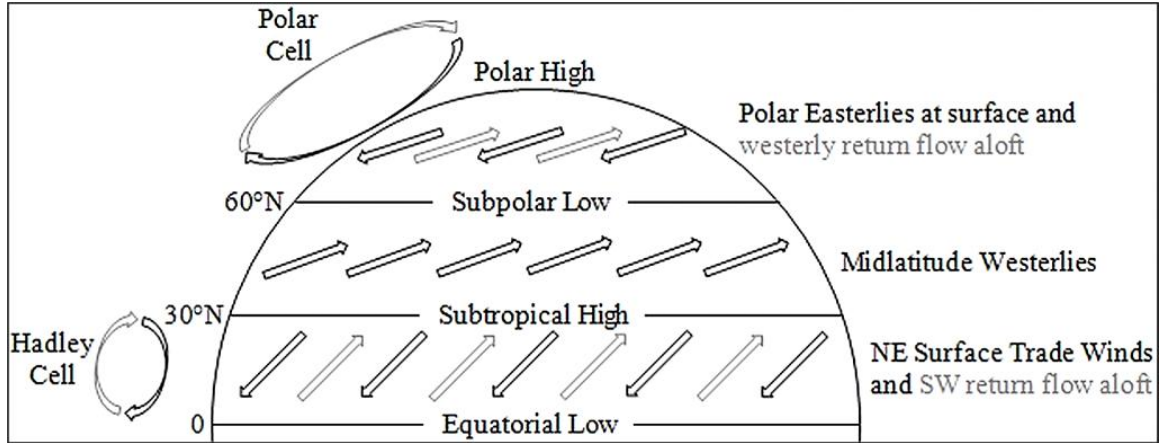


FIGURE 2.1. Simplified model of global atmospheric circulation cells and prevailing winds in the northern hemisphere.

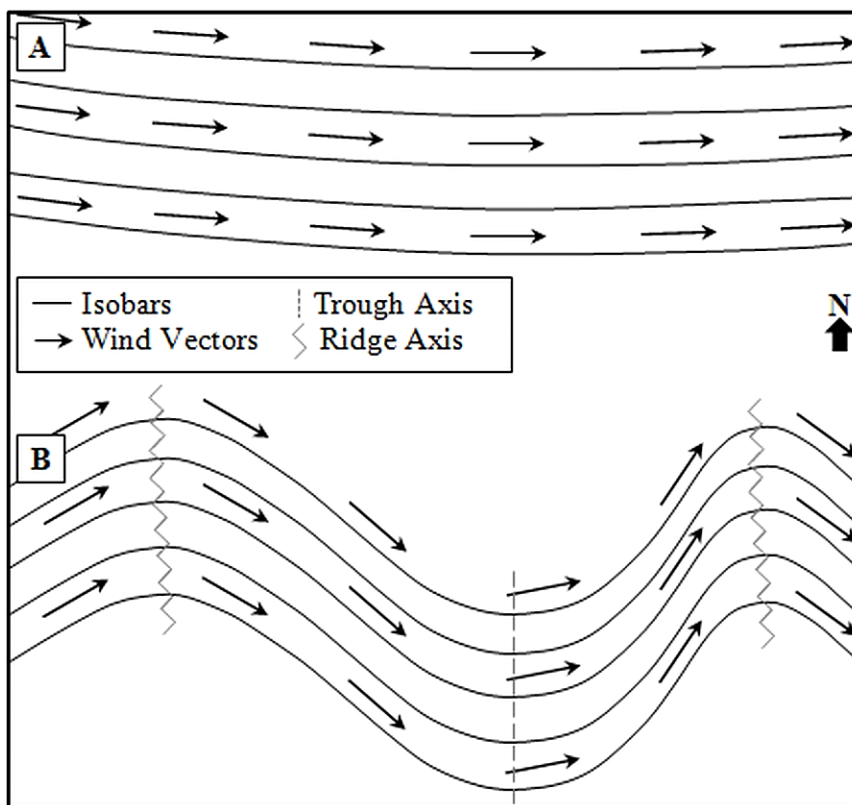


FIGURE 2.2. Illustration of zonal (A) and meridional (B) midlatitude westerly flow patterns.

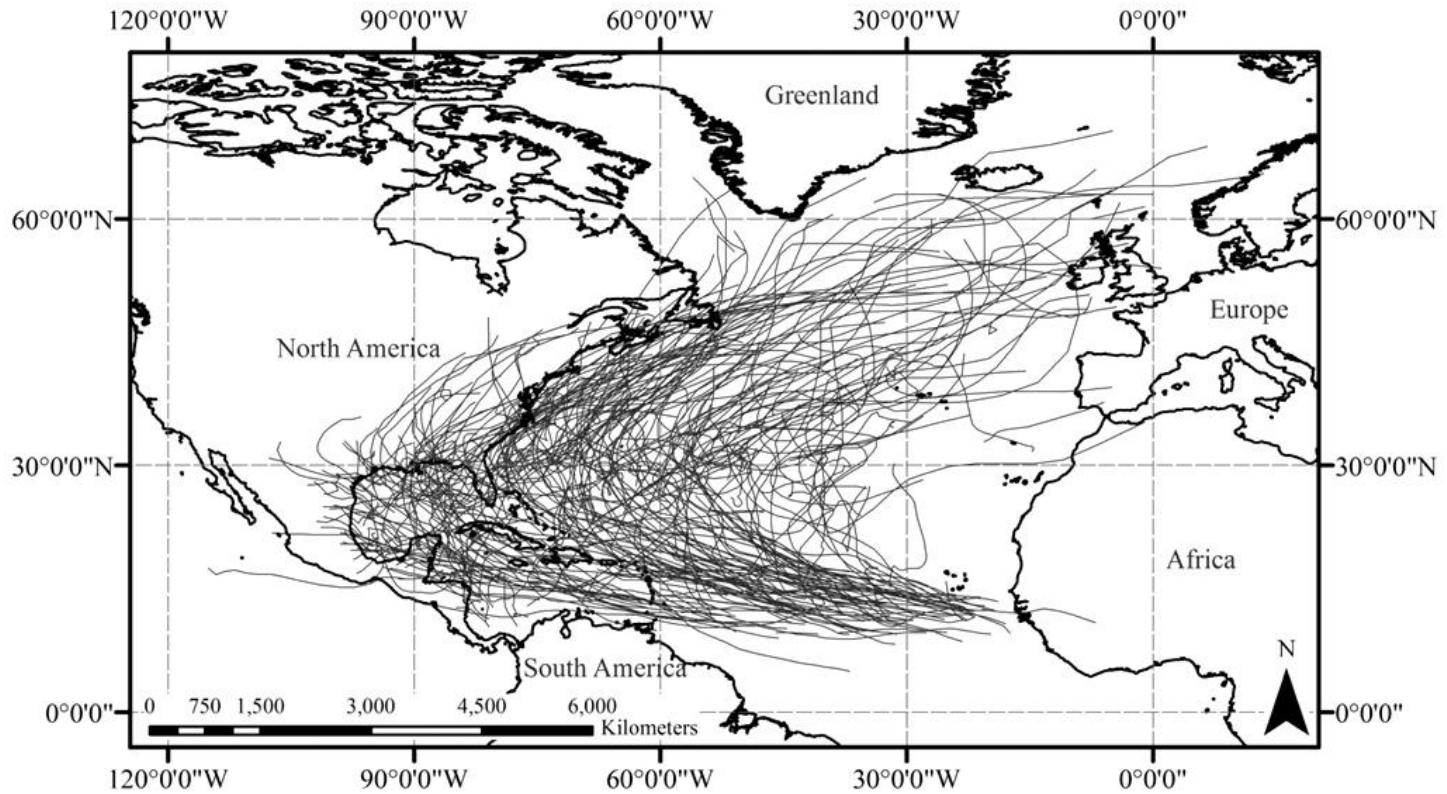


FIGURE 2.3. North Atlantic Basin TC tracks, 1995–2010 (TC track shapefiles obtained from National Climatic Data Center (NCDC) (n.d.)). A few landmasses are labeled for geographic reference. TC tracks are indicated by the dark gray lines. Note the general parabolic shape beginning over tropical and subtropical waters and ending over extratropical landmasses and waters.

CHAPTER III

DATA AND METHODS

3.1 Data

3.1.1 Tropical Cyclone Tornado Data

Tornado data were obtained from the TCTOR dataset developed by Roger Edwards of the SPC in Norman, OK (Edwards 2010b). The TCTOR dataset is compiled from the SPC's ONETOR database and the National Hurricane Center's (NHC's) HURDAT records. The TCTOR dataset provides information about TCTORs produced by TC landfalls along the East Coast and Gulf Coast of the United States over the period 1995–2010. Edwards (2010a) provides a detailed description of the TCTOR dataset, including the criteria used in TCTOR selection, the procedures used to create new variables, and a statistical analysis of the overall dataset.

The TCTOR dataset was chosen for three primary reasons. First, the beginning of its period of record (1995) corresponds with the NWS modernization, specifically the deployment of WSR-88D units, which should minimize data inhomogeneities caused by changes in the warning and verification practices associated with the modernization, while still providing an adequate sample size (Edwards 2010a). In agreement, Agee and Hendricks (2011), in a recent assessment of Florida TCTORs, concluded that the Doppler-era (1996–2010) TCTOR records are more accurate than the pre-Doppler-era (1979–1993) records, which underestimate TCTOR occurrence in Florida. Second,

surface maps, upper air maps, and archived satellite imagery have been used to manually verify that each TCTOR is located within the cyclonic envelope of their respective TC (Edwards 2010a). Third, variables have already been computed that link TCTORs with their associated TC, both temporally and spatially. These include the distance between each TCTOR and their associated TC center and the azimuth of each TCTOR relative to north. Table 3.1 provides a list of the information provided by the TCTOR dataset.

3.1.2 Synoptic Data

The most common data for manual synoptic classification are surface weather and upper-air maps (Yarnal 1993). Reanalysis projects produce retroactive, homogenous records of atmospheric fields (Skaggs 2004; Giles 2005) in the form of raw data and gridded outputs (plots, or maps) and, as a result, have led to significant advancements in the field of synoptic climatology (Sheridan and Cameron 2010). Reanalysis projects, originating in the 1990s, evolved from previous assimilated datasets to address problems associated with their continual progression and with other operational changes such as time of observation (Giles 2005). Multiple reanalysis projects have been developed since the 1990s, with primary differences in their temporal and spatial coverage, temporal and spatial resolution, and vertical layers (Table 3.2).

National Centers for Environmental Prediction-North American Regional Reanalysis (NCEP-NARR) plots (Mesinger et al. 2006) were obtained for the synoptic classification. The NCEP-NARR project is a follow-up to the National Centers for Environmental Prediction-National Center for Atmospheric Research (NCEP-NCAR) Global Reanalysis and is intended to improve upon earlier global reanalysis datasets in resolution and accuracy by providing a long-term, consistent, high-resolution climate

dataset for the North American domain (Mesinger et al. 2006). NCEP-NARR plots are gridded at the highest spatial resolution (32 km) of any of the reanalysis projects and the National Operational Model Archive and Distribution System (NOMADS) provides a built-in grid analysis and display system (GrADS) plotting application that is available for the NCEP-NARR daily dataset (NCDC 2011). Plots also are obtainable through the National Oceanic and Atmospheric Administration's (NOAA's) Earth System Research Laboratory (ESRL) Physical Sciences Division (NOAA n.d.). Given the localized nature of TCTORs, the high spatial resolution of the NCEP-NARR output seems to be the logical choice. NCEP-NARR plots are available every third hour beginning at 0000 UTC. Along with NCEP-NARR plots, daily surface weather maps were obtained from the NOAA's Daily Weather Map series (NOAA 2007) to locate baroclinic zones (Table 3.3).

The synoptic variables and TCTOR outbreaks need to be temporally synchronized to ensure that the identified synoptic patterns are representative of the atmospheric conditions during their corresponding outbreak. The TCTOR outbreak definition used by this study, specifically its requirement that the six hour windows be centered about primary synoptic hours (i.e., 0000, 0600, 1200, and 1800 UTC), was designed to facilitate this synchronization. The NCEP-NARR plots were collected for the primary synoptic hour of their corresponding outbreak. For instance, TC Frances (2004) produced an outbreak on 5 September 2004 during the 1800 UTC period (1500–2059 UTC). The synoptic plots obtained from NCEP-NARR (Table 3.3) were collected for 1800 UTC on 5 September 2004 to represent the atmospheric conditions during this outbreak. NOAA's daily surface weather maps are available once daily at 1200 UTC. For a given outbreak,

therefore, the surface weather map closest to the outbreak's primary synoptic hour was collected. For the previous TC Frances (2004) outbreak, the 5 September 2004 weather map was collected. For those outbreaks with a primary synoptic hour of 0000 UTC, two weather maps were collected, one twelve hours prior to the outbreak and another twelve hours after.

The initial atmospheric plots collected for the synoptic classification process were 200 hPa vector wind, 500 hPa geopotential height and vector wind, 600 hPa specific humidity, 0–180 hPa above surface CAPE, 0–3 km above surface SRH, 900 hPa horizontal convergence, and surface weather analysis maps. These specific plots were chosen because the variables which they represent have either been hypothesized to promote TCTOR genesis or they have been empirically linked to TCTORS (Table 3.3). The classification process is intended to explore these plots and identify physically meaningful synoptic patterns that consist of a single variable or some combination of multiple variables.

The 200 hPa vector wind plots were used to identify the presence and relative location of an upper-tropospheric jet streak. If a TC is located near the favorable right entrance region of a jet streak, it may experience dynamic forcing that enhances TCTOR production. Cohen (2010) created mean composite plots of the 200 hPa vector wind field associated with substantially tornadic (4+ TCTORS) and non-substantially tornadic (≤ 1 TCTOR) TCs and found that substantially tornadic TCs often are located to the southeast of an upper-level jet streak, placing them proximate to the jets streak's favorable right entrance region with positive vorticity advection and upper level divergence. Jet streaks

have likewise been shown to support severe storms and non-TC tornadoes (Beebe and Bates 1955; Rose et al. 2004; Clark et al. 2009).

The 500 hPa geopotential height and vector wind plots were used to identify the general midlatitude westerly trough/ridge pattern. As a TC approaches the midlatitude westerly flow, especially a trough elongated to the south, it begins to encounter increased wind shear (Jones et al. 2003; Molinari and Vollaro 2010). In addition to increased wind shear, a TC located downstream of a trough axis also would experience positive vorticity advection and upper-level divergence (Harman 1991). TCs may also intensify when they begin to interact with the midlatitude westerlies downstream of a trough axis (Hart and Evans 2001; Jones et al. 2003; Ritchie and Elsberry 2007; Molinari and Vollaro 2010). Verbout et al. (2007) and Baker, Parker, and Eastin (2009) reported 500 hPa troughs extending equatorward over the central United States in TCTOR outbreak cases; Verbout et al. (2007) also reported that ridges typically were located over the central United States in non-outbreak cases. Cohen (2010) reported a 500 hPa trough over the western United States and a ridge over the Central Plains region in association with TCTOR outbreaks.

The 600 hPa specific humidity plots were used to identify the general pattern of mid-tropospheric moisture. Mid-tropospheric dry air intrusion may locally increase the environmental lapse rate through evaporative cooling aloft, in turn leading to increased convective instability (McCaul 1987; Vescio, Weiss, and Ostby 1996). The decrease in cloud cover associated with dry air intrusion also may lead to convective instability through enhanced surface heating (Curtis 2004). Curtis (2004) and Cohen (2010) reported mid-level dry air entrainment in association with TCTOR outbreaks and Cohen

(2010), in addition, speculates that dry air intrusion may enhance rear flank downdrafts associated with TC supercells along with potential instability.

CAPE and SRH plots were used to represent potential instability and cyclonic updraft rotation, respectively, in the vicinity of TCTOR outbreaks. Relatively high values of these parameters signify the potential for severe storms and tornadoes (NWS 2009). Previous studies (McCaul 1991; Edwards et al. 2010) have analyzed these parameters in the TC environment surrounding TCTORs and have reported relatively high values of SRH, compared to non-TC tornado environments, but relatively low CAPE values, again compared to non-TC tornado environments. Based on McCaul's (1991) study, Schneider and Sharp (2007) created a table of parameter thresholds, including CAPE and SRH, to distinguish between high and low TCTOR threat. CAPE values greater than 500 J kg^{-1} and SRH values greater than $100 \text{ m}^2 \text{ s}^{-2}$ indicate high TCTOR threat whereas values below these threshold values indicate low threat.

The 900 hPa horizontal convergence plots were used to represent low-level convergence. Gentry (1983) proposed that surface winds slow upon landfall as a result of increased surface friction whereas winds aloft remain relatively unchanged and that this differential friction increases low-level vertical wind shear. Schultz and Cecil (2009), further, proposed that this different friction also may lead to low-level speed convergence near the coastline, in turn creating a TCTOR-favorable environment with upward acceleration, vorticity tilting (from a horizontal to vertical axis), and stretching.

Surface weather maps were used to identify the presence and relative location of baroclinic zones (fronts) near and within the TC environment. Fronts may provide localized forced convection, they may enhance vorticity within the TC environment

(Spratt et al. 1997), and they may aid in the formation and intensification of mesocyclones (Markowski, Rasmussen, and Straka 1998; Rasmussen et al. 2000), all of which can lead to the development and strengthening of TC supercells. Pietrycha and Hannon (2002) reported that nearly all of TC Floyd's (1999) TCTORs developed along a surface warm front and McCaul et al. (2004) reported that many of TC Beryl's (1994) TCTORs that occurred in South Carolina were within proximity to a low-level frontal boundary. Using a larger sample of TCs, Edwards and Pietrycha (2006) also showed that TCTOR potential is heightened when fronts merge with, or develop within, TCs.

3.2 Methods

This study follows the environment-to-circulation approach to synoptic classification. This approach is taken rather than the circulation-to-environment approach because the primary goal of this study is to identify synoptic patterns associated with TCTOR outbreaks rather than the synoptic patterns associated with every six hour time step of a TC. According to the environment-to-circulation approach, TCTOR outbreaks were identified prior to the collection of synoptic plots and the synoptic classification process. Once the outbreaks were identified, synoptic and surface analysis plots corresponding to each outbreak were collected; thus, only synoptic environments corresponding to TCTOR outbreaks were classified and analyzed. The synoptic environments corresponding to each of the outbreaks were manually classified because the process of manual classification is likely to provide in-depth insight into the linkages between the synoptic environment and TCTOR outbreaks that would perhaps be overlooked with a computer-assisted classification (Yarnal 1993; Barry and Carleton 2001).

3.2.1 Tropical Cyclone Tornado Outbreaks: Definition and Identification

Before TCTOR outbreaks can be identified and analyzed, they must be defined. Multiple definitions of a tornado outbreak have been proposed, but a single definition has not yet been adopted (Table 3.4). Galway (1977) points out that the term tornado outbreak can assume various meanings, depending on long-term regional and local tornado activity. One of the earliest definitions proposed by Galway (1975) consists primarily of tornado frequency thresholds (i.e., the number of tornadoes beyond which is considered an outbreak). It is also noted from Galway's (1975) definitions that the tornadoes in an outbreak must be associated with a single weather system but an explicit spatial parameter is not included. Galway's (1977) definition includes a tornado frequency threshold in addition to various spatial scales and configurations over which tornado outbreaks occur. The spatial characteristics reported by Galway (1977), however, were not used to identify tornado outbreaks but were, rather, used to describe the typical spatial characteristics of already-identified outbreaks. The American Meteorological Society (AMS) provides a more general definition by excluding an exact tornado frequency threshold; although they do express that the tornadoes must be associated with a single synoptic scale system (Glickman 2000). Thus, previous tornado outbreak definitions have utilized various tornado frequency thresholds and have not included a spatial parameter for the purpose of tornado outbreak identification. The only similar component within each definition is the requirement that all tornadoes be associated with a single weather system.

Multiple definitions and categorization schemes also have been used to define and analyze TCTOR outbreaks (Table 3.5). All of the definitions of TCTOR outbreak

include a TCTOR frequency threshold of which the values have varied, ranging from a few TCTORS (Cohen 2010) to nearly fifty (Moore and Dixon 2011a). The method by which the frequency threshold value is decided has, likewise, varied. McCaul (1991), for instance, categorized outbreaks by severity and based his threshold values on the frequency distribution of TCs across a range of TCTOR frequencies. Moore and Dixon (2011a) took a similar approach by using the same categorization scheme but, rather than arbitrarily setting the threshold values, they set their threshold values at the 80th and 95th percentiles of the frequency distribution of TCs across a range of TCTOR frequencies (i.e., minor outbreaks are \leq 80th percentile, major outbreak fall between the 80th and 95th percentiles, and severe outbreaks are \geq 95th percentile). Verbout et al. (2007) based their threshold value on the expected annual number of all tornadoes in a given year. Curtis (2004) and Cohen (2010) arbitrarily chose threshold values. The temporal component of these definitions typically spans a several day period, or the lifespan of the TCs analyzed, although none explicitly include a temporal parameter in their definition.

This study defines TCTOR outbreaks as three or more TCTORS in a six hour window centered about a primary synoptic hour (i.e., 0000, 0600, 1200, and 1800 UTC). The TCTOR frequency threshold of three is intended to distinguish between temporally isolated and temporally clustered TCTORS. This threshold is arbitrary but is thought to adequately distinguish between time periods when an isolated one or two TCTORS occur and those when a larger number, or an outbreak, occurs. The threshold value of three is smaller than that used by previous TCTOR outbreak definitions, but this is reasonable given that this study considers TCTORS over a six hour window rather than a several day period. A six hour window is used because a longer period would likely reduce the

variability of observed synoptic environments and a shorter period would reduce the number of identified outbreaks, given that the temporal parameter remains at three. The centering of the six hour windows (Table 3.6) about primary synoptic hours ensures that all TCTORs within a given outbreak occur within three hours of the synoptic snapshot used to represent the environment during that outbreak.

Most outbreak definitions require that tornadoes, or TCTORs, be associated with the same synoptic scale weather system, but strict spatial parameters have rarely been used. The TCTOR outbreak definition used in this study does not include a spatial buffer because measures have already been taken to ensure that the tornadoes included in the TCTOR dataset were produced by the same weather system (i.e., their parent TC).

A benefit of the TCTOR outbreak definition used in this study promotes the use of a systematic and consistent process to identify outbreaks. The identification process consisted first of sorting the TCTOR dataset by date and time. The sorted dataset was then separated into six hour windows, each centered about a primary synoptic hour. The six hour windows with three or more TCTORs were extracted to create a new dataset of TCTOR outbreaks. A limitation of this definition is that it may exclude TCTOR outbreaks that are split between two adjacent six hour windows. For instance, consider the following situation: four TCTORs occur at 1440 UTC, 1455 UTC, 1515 UTC, and 1530 UTC. These four TCTORs occur within six hours of one another, but are split between the 1200 UTC and 1800 UTC windows and, as a result, would not be identified as an outbreak. It could, likewise, partition particularly long-lasting outbreaks into two or more outbreaks. Using a moving temporal window or considering TCTOR outbreaks

over multiple temporal scales would, however, introduce inconsistencies into the synoptic analysis.

3.2.2 Synoptic Classification Process

3.2.2.1 Classification Goals

Synoptic classifications must seek a balance between the number of identified synoptic patterns, the sample size within each pattern, and the variability of individual environments within each pattern (Barry 2005). If numerous patterns are identified, the within-group variability will likely be small, but the sample size of each pattern also will likely be relatively small unless the period of record is suitably long. Conversely, if only a few groups are identified, the sample size within each pattern will be relatively large, but so will the within-group variability. This study sought to optimize the classification scheme by setting goals to minimize within-group variability, to maximize between-group variability, and to ensure adequate sample sizes for statistical analysis. Furthermore, this study sought to identify and define synoptic patterns such that the classification scheme is exhaustive, mutually exclusive, and based on the synoptic environment surrounding a given TC rather than the overall map pattern.

To accomplish the above goals, this study developed a manual classification scheme specifically for TCTOR outbreaks rather than using a generic classification scheme. A TC-relative framework was used in the development of the classification scheme, meaning that emphasis was placed on the general synoptic scale interactions between TCs and their ambient environment, rather than on the overall map pattern.

As an example of the TC-relative framework, consider the 500 hPa geopotential heights associated with two TCTOR outbreaks in which their associated TCs are closed

short wave troughs embedded within a longer-wave trough (Figure 3.1). In one outbreak, the 500 hPa trough, TC, and TCTOR outbreak are located over the south-central United States (Figure 3.1A) whereas they are situated over the east-central United States in the other outbreak (Figure 3.1B). A classification scheme based on the overall map pattern would likely classify these two outbreaks differently because the absolute locations, wavelength, amplitude, and orientation of the synoptic features are different. In a TC-relative framework, however, these two situations are considered to be the same because they represent a similar synoptic situation; i.e., in each situation the TC is a closed short wave trough embedded within a longer-wave 500 hPa trough downstream of the longer-wave trough axis (Figure 3.1C).

3.2.2.2 Classification Process

Manual classification is an iterative process in which an analyst, or group of analysts, become familiar with the range of synoptic situations during a given study period, identify and define recurring synoptic patterns (i.e., if a generic classification scheme is not used), and partition individual cases into the synoptic pattern of which they are most characteristic (Yarnal 1993). The classification process performed in this study was completed in six iterations.

The first iteration involved an examination of all six synoptic variables associated with each TCTOR outbreak (Table 3.3). During this stage, characteristics such as the presence and relative location of a 500 hPa trough, 200 hPa jet streak, 600 hPa dry air entrainment region, and surface fronts were recorded. Also recorded during this stage were the minimum, mid-point, and maximum values of CAPE, SRH, and low-level convergence to capture the range of values present in the outbreak region. At the end of

this stage, it was decided that CAPE, SRH, and low-level convergence are too variable over relatively small spatial areas to be considered in the identification of synoptic patterns. Other studies too have found that thermodynamic and wind shear parameters are highly variable over relatively small spatial areas (e.g. Markowski et al. 1998; French and Parker 2008).

The second iteration re-examined 500 hPa geopotential height and vector wind, 200 hPa vector wind, 600 hPa specific humidity, and surface analysis plots to determine if some combination of these variables could be used to create distinct, physically meaningful synoptic patterns. During this stage it became clear that the use of multiple synoptic variables would create too many synoptic patterns with too few outbreaks within each pattern for statistical analysis. Also during this stage, a marked dichotomy between TCs interacting with the midlatitude westerlies and those not interacting with the midlatitude westerlies was observed in the 500 hPa geopotential height and vector wind plots. This dichotomy is noteworthy and merits further investigation because previous research has documented the role of TC-westerly interaction in altering TC strength and internal structure (Hart and Evans 2001; Arnott, Evans, and Chiaromonte 2004; Jones et al. 2003; Molinari et al. 2006; Molinari and Vollaro 2010a and 2010b), both of which may affect TCTOR potential.

Favorable trough interaction may provide mid- and upper-level dynamic forcing to support TCTOR outbreaks. Previous studies have examined TC-westerly interaction, specifically trough interaction, and reported mixed results. For instance, Verbout et al. (2007) found that TCTOR outbreaks produced by Texas landfalls were associated with a 500 hPa trough situated over the north-central United States and suggested that trough

interaction may enhance vertical wind shear and possibly lead to TC intensification. Alternatively, Cohen (2010) found that substantially tornadic Gulf Coast landfalls are associated with a 500 hPa trough over the western United States and a 500 hPa ridge over the Central Plains, which suggests little TC-trough interaction with the exception of landfalls in the far-western portion of the Gulf Coast region. Because of these somewhat disparate results, the classification developed in this study is based on 500 hPa geopotential height and vector wind plots.

During the third iteration, the TCTOR outbreaks were partitioned into two groups based on whether their associated TC is interacting with the midlatitude westerlies at the 500 hPa level: (1) TC interacting with midlatitude westerlies (TC-westerly interaction); and (2) TC not interacting with midlatitude westerlies (no TC-westerly interaction). While doing so, several subcategories were noted within each of these two primary groups.

The fourth iteration involved recording the various patterns in which the TCs did or did not interact with the westerlies. Five synoptic patterns, three TC-westerly interaction and two no TC-westerly interaction, were extracted from these notes. A classification tree (Figure 3.2), similar to the decision tree method employed by Gamble and Meentemeyer (1997) and Ashley and Ashley (2008), was created to illustrate the hierarchy of synoptic patterns, to aid in the final iterations, and to keep the classification as objective as possible.

The fifth iteration involved partitioning each of the TCTOR outbreaks into one of the five synoptic patterns and the creation of a sixth, other, category for outbreaks that did not reasonably fit the criteria of one of the five patterns. The classification scheme

and its five patterns account for 97% (129 out of 133 outbreaks) of the identified outbreaks. Four outbreaks were classified as other.

The sixth iteration involved a re-partitioning of the 129 previously classified outbreaks; the four outbreaks classified as other were not included in the sixth iteration. The classifications in the fifth and sixth iterations had a 95% match rate (i.e., 123 of the 129 outbreaks were classified the same in both iterations). The remaining 5%, or six outbreaks, that were not identically classified in the fifth and sixth iterations were partitioned into the category of which they were most characteristic.

The five synoptic patterns identified during the classification process could be further subdivided to account for such characteristics as 500 hPa wavelength, wave amplitude, wave tilt, distance between TC center and wave axis, and strength of the flow in which the TC is located. Further refinement would reduce within-group variability, but it also would increase the number of patterns and reduce the sample size of some or all of the patterns. This classification scheme stops after the second subdivision to retain an adequate number of outbreaks in each synoptic pattern.

3.2.2.3 Tropical Cyclone-Westerly Interaction Patterns

Patterns 1, 2, and 3 are subdivisions of the TC-westerly interaction class; i.e., these outbreaks are produced by TCs that are beginning to interact with, or are embedded within, the midlatitude westerlies. Pattern 1 outbreaks are produced by TCs with closed circulation at 500 hPa that are located in the predominately westerly flow of the northern portion of the subtropical ridge (Figure 3.3). A 500 hPa midlatitude trough often is embedded within the westerlies to the north or northwest of the TC.

In the Pattern 1 outbreaks, TCs, the midlatitude westerlies, and the troughs embedded within the westerlies (if existent) are distinct synoptic features. Given the relative positioning of the synoptic features, Pattern 1 show signs of proto-interaction between well-developed TCs and the midlatitude westerlies. The proto-westerly interaction is illustrated by 500 hPa wind vectors from the southern portion of the westerly flow that cyclonically envelop the TC (Figure 3.3).

Pattern 2 outbreaks are produced by TCs that are closed shortwave troughs embedded within the midlatitude westerlies, often downstream of a longer-wave 500 hPa trough axis and upstream of the successive ridge axis (Figure 3.4). Pattern 2 outbreaks are similar to Pattern 1 outbreaks in that both are produced by TCs with closed circulation at the 500 hPa level. The discriminating feature between the two patterns is that Pattern 2 TCs are enveloped by a single, or multiple, circumpolar isoheight(s), giving TCs the appearance of closed shortwave troughs, whereas Pattern 1 TCs are to the south of the southern-most circumpolar isoheight in the westerlies.

Pattern 3 outbreaks are produced by TCs that are open shortwave troughs embedded in the midlatitude westerlies, often downstream of a longer-wave 500 hPa trough axis and upstream of the successive ridge axis (Figure 3.5). Pattern 3 outbreaks are similar to Pattern 2 outbreaks in that they both are produced by TCs that are shortwave troughs embedded within westerlies. The two are different in that Pattern 3 TCs are open shortwave troughs whereas Patterns 2 TCs are closed shortwave troughs.

All outbreaks in Patterns 1–3 meet the criteria of their respective pattern. There is variability, however, in the absolute location of the synoptic features and in the

wavelength, wave amplitude, and wave tilt of any long-wave trough embedded within the westerlies.

3.2.2.4 No Tropical Cyclone-Westerly Interaction Patterns

Patterns 4 and 5 are subdivisions of the no TC-westerly interaction class; i.e., these outbreaks are produced by TCs that are isolated from the midlatitude westerlies. Pattern 4 outbreaks are produced by TCs without closed circulation at the 500 hPa level that are located in the southerly or southwesterly flow of the North Atlantic subtropical anticyclone (Figure 3.6). The location of Pattern 4 TCs relative to the westerlies is similar to the relative location of Pattern 1 TCs. The primary differences are that Pattern 4 TCs do not have closed circulation at the 500 hPa level, whereas Pattern 1 TCs do have closed circulation, and Pattern 4 TCs are dominated by a much more

Pattern 5 outbreaks are produced by TCs with closed circulation at the 500 hPa level that are located in the southern portion of a well-developed subtropical ridge (Figure 3.7). These TCs, therefore, are isolated from the westerlies by a region of relatively high geopotential heights and unorganized 500 hPa flow.

Similar to the first three patterns, all outbreaks in Patterns 4 and 5 meet their respective classification criteria, but they vary in terms of the absolute location of the synoptic features and the 500 hPa midlatitude flow regime.

3.2.3 Statistical Analysis

The TCTOR outbreak dataset was analyzed as a whole and also was re-organized many ways to create different subsets, or samples, for analysis. Various descriptive and inferential statistical techniques were used to analyze the TCTOR dataset and its subsets. For example, the TCTOR outbreak dataset was subdivided into five groups, each

representing one of the five synoptic patterns identified during the synoptic classification process. These five patterns and the TCTOR outbreaks from which they are comprised were treated as individual and independent samples during the statistical analysis. Descriptive statistical metrics were used to summarize the TCTOR outbreaks within each of the synoptic patterns. Inferential techniques were used to test for statistically significant differences across the synoptic patterns. The descriptive metrics and inferential tests were computed using the predictive analytics software PASW Statistics, version 18 by SPSS Inc. (SPSS 2009).

Descriptive statistics are useful metrics for describing the central tendency and variability of a distribution of data. Measures of central tendency describe the average, or typical, value of a given dataset whereas measures of variability describe the spread, or dispersion, of values within a given dataset (Burt, Barber, and Rigby 2009). Descriptive metrics were used to summarize the central tendency and variability of the TCTOR dataset and its subsets. Other descriptive metrics, such as skewness, were used to describe the shape of distributions and to determine whether the majority of values are greater than or less than the mean value (Burt, Barber, and Rigby 2009). These metrics are used to describe data at the interval and ratio scale, such as the number of TCTOR outbreaks per TC, the number of TCTORs per outbreak, and the time difference between each TCTOR outbreak and their respective TC landfall. Frequency and relative frequency counts were used to describe the nominal and ordinal scale data, such as the number of outbreaks per month, per primary synoptic hour, and per synoptic pattern. Frequency counts also were used to analyze the number of TCTORs per F/EF rating.

Spatial statistical metrics were used to summarize spatial characteristics of the TCTOR outbreaks. For instance, azimuth (from north) and range (from their respective TC center) values are provided by the TCTOR dataset that spatially place the TCTORs relative to their respective TC center. The azimuth and range values for each TCTOR within an outbreak were averaged to determine the mean center of that outbreak. The mean center values, therefore, describe the center of their respective TCTOR outbreak relative to their respective TC center and are represented by an azimuth ($^{\circ}$) and a range (km). In addition to mean center, standard distance was computed for each TCTOR outbreak. The standard distance of an outbreak describes the dispersion of TCTORs in that outbreak (Burt, Barber, and Rigby 2009). Standard distance was computed using ArcMap, version ten (ESRI 2010), geographic information software. The standard surface area over which each outbreak was spread also was computed by squaring the standard distance and multiplying by the constant value pi (π) (standard surface area = standard distance² \times π).

Visual examination of the spatial distribution of the outbreaks revealed that they generally conform to one of the following spatial configurations: linear, single-cluster, multi-cluster, or dispersed. The TCTOR outbreaks were manually classified into one of these categories. Descriptive statistical metrics were used to summarize the standard surface area of TCTOR outbreaks for each of the identified spatial configurations. The Euclidean, or straight-line, distance of the dominant linear feature in the linear outbreaks is provided in addition to the standard surface area because it is unlikely that the area of a circle is the best description of a the linear outbreaks. Euclidean distance values were determined with the use of ArcMap, version ten (ESRI 2010).

Inferential statistical tests were used to generalize results obtained from a sample to the larger population (Burt, Barber, and Rigby 2009). They were used to determine whether observed frequency distributions conform to a particular theoretical distribution, such as a uniform distribution. They also were used to determine whether descriptive metrics such as the mean and median significantly differ across two or more samples or whether the observed difference was caused by sample bias (i.e., the observed difference does not indicate a real difference in the distributions but rather indicates that the difference is the result of chance variation between the samples). Unless otherwise noted, all inferential tests were assessed at the 95% confidence level (i.e., $\alpha = 0.05$), meaning that any calculated probability values (p -value) less than or equal to 0.05 led to a rejection of the null hypothesis and an acceptance of the alternate hypothesis. Also note that another interpretation of the calculated p -value is that it is the lowest value at which α may be set and still reject the null hypothesis (Burt, Barber, and Rigby 2009). Thus, the lower the p -value, the more certainty exists in the rejection of the null hypothesis.

The Chi-square (X^2) goodness-of-fit test is useful when comparing an observed distribution to a theoretical distribution of nominal values (Burt, Barber, and Rigby 2009) and was, thus, used to determine whether the TCTOR outbreaks are evenly distributed among the five synoptic patterns. The X^2 test was used because the data for this particular analysis are nominal level. If the TCTOR outbreaks are evenly distributed among the patterns, the frequency distribution should not be significantly different than a uniform distribution. The null hypothesis for this analysis states that the TCTOR outbreaks are uniformly distributed among the five synoptic patterns and the alternate hypothesis is that they are not uniformly distributed among the five synoptic patterns. If

the calculated p -value is less than or equal to 0.05, the null hypothesis is rejected and the conclusion is that TCTOR outbreaks are not uniformly distributed among the synoptic patterns.

Levene's test for homogeneity (equality) of variance is an inferential test that is useful in determining whether multiple groups, or samples, have equal variance (Meyers, Gamst, and Guarino 2006) and was, thus, performed to determine whether the variance of TCTOR outbreak severity (i.e., the number of TCTORS in an outbreak) is equal across the five synoptic patterns. The null hypothesis is that the variance of TCTOR outbreak severity is equal across the synoptic patterns and the alternate hypothesis is that the variance is not equal across the synoptic patterns. If the calculated p -value is less than or equal to 0.05, the null hypothesis is rejected and the conclusion is that the five synoptic patterns have different variance in terms of TCTOR outbreak severity. The coefficient of variation also was compared subjectively across the synoptic patterns to assess the difference in TCTOR outbreak severity variability. The coefficient of variation provides a measure of the relative variability of distributions and is a better indicator than variance or standard deviation when comparing variability across multiple samples with different mean values and sample size; it is defined as the ratio of the standard deviation to the mean (Burt, Barber, and Rigby 2009).

The Shapiro-Wilk test is an inferential test to determine whether an observed distribution significantly departs from normality (Burt, Barber, and Rigby 2009). This test was used to determine whether TCTOR outbreak severity values are normally distributed within each of the five synoptic patterns and within the higher-level groups of TC-westerly interaction and no TC-westerly interaction. Statistical significance for these

tests was assessed at the 0.01 level of significance. These tests employ an α more stringent than 0.05 because normality tests are typically evaluated at the 0.01 or 0.001 significance levels to minimize the likelihood of committing a type I error, which occurs when a true null hypothesis is rejected (Burt, Barber, and Rigby 2009). The null hypothesis for these tests is that TCTOR outbreak severity is normally distributed in the samples and the alternate hypothesis is that TCTOR outbreak severity is not normally distributed in the samples. If the calculated p -value is less than or equal to 0.01, the null hypothesis is rejected and the conclusion is that TCTOR outbreak severity is not normally distributed. These tests are performed because they allow statistically significant conclusions to be stated about the shape of the distributions and, more importantly, knowledge of the underlying distributions is needed for additional inferential tests regarding differences in typical (mean or median) TCTOR outbreak severity across the samples.

The Mann-Whitney U test is useful when determining whether two populations have equal mean ranks; although mean ranks are computed and compared, the hypotheses typically are stated in terms of the median (Burt, Barber, and Rigby 2009). A one-tailed Mann-Whitney test was used to determine whether the median TCTOR outbreak severity for TC-westerly interaction outbreaks is greater than that of the no TC-westerly interaction outbreaks. The null hypothesis is that the median outbreak severity for TC-westerly interaction outbreaks is less than or equal to that of the no TC-westerly interaction outbreaks and the alternate hypothesis is that the median outbreak severity for TC-westerly interaction outbreaks is greater than that of the no TC-westerly interaction outbreaks. If the calculated p -value is less than or equal to 0.05, the null hypothesis is

rejected and the conclusion is that the median outbreak severity for TC-westerly interaction outbreaks is greater than that of the no TC-westerly interaction outbreaks. This nonparametric test was used rather than its parametric counterpart, the two sample t -test, because a Shapiro-Wilk test indicated that TCTOR outbreak severity values are not normally distributed within either of the samples, and because the two samples have different sample size.

The Kruskal-Wallis test is an inferential test used to determine whether multiple populations have equal central locations (Burt, Barber, and Rigby 2009). Similar to the Mann-Whitney U test, the Kruskal-Wallis test compares the mean rank of multiple samples, but the hypotheses presented here are stated in terms of the median. Again, this nonparametric test was used rather than its parametric counterpart, the analysis of variance (ANOVA), because a Shapiro-Wilk test indicated that TCTOR outbreak severity values are not normally distributed within any of the five synoptic patterns and because the sample size of the patterns are different. This study employed the Kruskal-Wallis test to determine whether the five synoptic patterns have equal median TCTOR outbreak severity values. The null hypothesis is that synoptic patterns have equal median outbreak severity and the alternate hypothesis is that the synoptic patterns do not have equal median outbreak severity. If the calculated p-value is less than or equal to 0.05, the null hypothesis is rejected and the conclusion is that median outbreak severity is not equal across the five synoptic patterns.

If the null hypothesis is rejected in a Kruskal-Wallis test, the next task is to determine between which pattern-pairs the significant difference exists. In the case of a rejected null hypothesis, this study employs the Mann-Whitney U test with Bonferroni

adjustment to address this question. The Bonferroni adjustment allows the overall level of significance to remain 0.05 by adjusting the significance level at which each pattern-pair comparison is assessed (Rice 2007). The adjustment requires the overall level of significance (0.05) to be divided by the number of comparisons to be made (10), thus giving a significance level of 0.005 (i.e., $0.05/10=0.005$) for each comparison. If the p -value for any of the pattern-pair comparison is less than or equal to 0.005, the two patterns are deemed to be significantly different.

3.3 Chapter Three Tables

TABLE 3.1. List of information provided about TCTORs in the TCTOR dataset (Edwards 2010b).

TC Information	Tornado Information	Derived Information
<ul style="list-style-type: none"> • TC name and year • Linearly interpolated TC latitude/longitude coordinate • Intensity^a • Maximum wind speed at previous 6-hourly observation • Minimum barometric pressure at previous 6-hourly observation 	<ul style="list-style-type: none"> • Year • Month • Day of month • Time of day • State(s) impacted • Number of states impacted • Estimated intensity^b • Number injured • Number killed • Estimated property loss • Estimated crop loss • Begin latitude/longitude • End latitude/longitude • Path length • Path width 	<ul style="list-style-type: none"> • TCTOR azimuth relative to true north • Distance of TCTOR from TC center

- a. TC intensity is rated by SS Scale; or they are categorized as TSs, TDs, or as post landfall systems (including extratropical, remnant lows, no longer classified, etc.). See Appendix B for wind speed estimates for the SS Scale.
- b. TCTOR intensity is rated by the F or EF Scale, depending on the year of occurrence. The F Scale was used prior to 1 February 2007. See Appendix B for wind speed estimates for each F/EF Scale category.

TABLE 3.2. Selected list of reanalysis projects and their basic temporal and spatial properties.

Reanalysis Projects	Temporal Coverage	Spatial Coverage	Temporal Resolution	Spatial Resolution	Vertical Layers
NCEP-NARR ^a	1979–present	North America	8 per day, every 3 hours	~32 km	45
NCEP-NCAR ^b	1948–present	Global	4 per day, every 6 hours	~200 km	28
NCEP-DOE ^c	1979–present	Global	4 per day, every 6 hours	~200 km	28
NCEP-CFSR ^d	1979–present	Global	4 per day, every 6 hours	~38 km	64

a. NCEP-NARR (Mesinger et al. 2006)

b. NCEP-NCAR (Kalnay et al. 1996)

c. NCEP-Department of Energy (DOE) (Kanamitsu et al. 2002)

d. NCEP-Climate Forecast Reanalysis System (CFSR) (Saha et al. 2010)

TABLE 3.3. List of conceptual and operational variables and sources supporting their link to TCTORs.

Conceptual Variable	Operational Variable	Supporting Literature
Relative location of upper-tropospheric jet streak	*200 hPa vector wind [m s^{-1}]	Cohen (2010)
Relative location of mid-tropospheric trough	*500 hPa geopotential height [m] and *500 hPa vector wind [m s^{-1}]	Verbout et al. (2007); Baker, Parker, and Eastin (2009)
Mid-tropospheric dry air entrainment	*600 hPa specific humidity [kg kg^{-1}]	Curtis (2004); Cohen (2010)
Instability	*0–180 hPa above surface CAPE [J kg^{-1}]	McCaul et al. (2004); Edwards et al. (2010)
Lift	**Surface fronts	Pietrycha and Hannon (2002); McCaul et al. (2004); Edwards and Pietrycha (2006)
Rotation	*0–3 km above surface SRH [$\text{m}^2 \text{s}^{-2}$]	McCaul (1991); Edwards et al. (2010)
Low-level convergence	*900 hPa horizontal convergence [100,000 s^{-1}]	Gentry (1983); Schultz and Cecil (2009)

*source: NCEP-NARR (Mesinger et al. 2006)

**source: NOAA Daily Weather Map Series (NOAA 2007)

TABLE 3.4. Sample of tornado outbreak definitions.

Source	Definitions
Galway (1975)	<ul style="list-style-type: none"> ▪ a small outbreak consists of 6–9 tornadoes that are associated with a weather system on a given day ▪ a moderate outbreak consists of 10–19 tornadoes that are associated with a weather system on a given day ▪ a large outbreak consists of 20+ tornadoes that are associated with a weather system on a given day
Galway (1977)	<ul style="list-style-type: none"> ▪ a local outbreak consists of 10+ tornadoes that typically occur over a temporal period of less than seven hours and are confined to a roughly 10,000 n mi² circular region ▪ a progressive outbreak consists of 10+ tornadoes that occur over a temporal period of approximately nine hours are progressively spread from west to east over a region approximately 54,000 n mi² in area; the distance between the first and last tornado is typically longer than 350 n mi ▪ a line outbreak consists of 10+ tornadoes that occur over a temporal period of approximately eight hours in a line along a north-south oriented axis and cover an area of approximately 59,000 n mi²
Glickman (2000)	<ul style="list-style-type: none"> ▪ tornado outbreaks consist of multiple tornado occurrences associated with a particular synoptic scale system

TABLE 3.5. Sample of TCTOR outbreak definitions.

Source	Definitions
McCaul (1991)	<ul style="list-style-type: none"> ▪ a minor outbreak consists of ≤ 8 TCTORs ▪ a major outbreak consists of 9–24 TCTORs ▪ a severe outbreak consists of > 24 TCTORs
Curtis (2004)	<ul style="list-style-type: none"> ▪ TCTOR outbreaks consist of 20+ TCTORs
Verbout et al. (2007)	<ul style="list-style-type: none"> ▪ a TCTOR outbreak is an event with $> 1.5\%$ of the annual expected tornado frequency for a given year with at least eight F1+ tornadoes
Cohen (2010)	<ul style="list-style-type: none"> ▪ substantially tornadic TCs produce 4+ TCTORs
Moore and Dixon (2011a)	<ul style="list-style-type: none"> ▪ a minor outbreak consists of ≤ 21 TCTORs ▪ a major outbreak consists of 22–48 TCTORs ▪ a severe outbreak consists of 49+ TCTORs

TABLE 3.6. Primary synoptic hours and six hour windows centered on these synoptic hours used to identify TCTOR outbreaks.

Primary Synoptic Hour (UTC)	Six Hour Window (UTC)^a
0000	2100 p. d. – 0259 c. d.
0600	0300 c. d. – 0859 c. d.
1200	0900 c. d. – 1459 c. d.
1800	1500 c. d. – 2059 c. d.

a. p. d. denotes previous day and c. d. denotes current day.

3.4 Chapter Three Figures

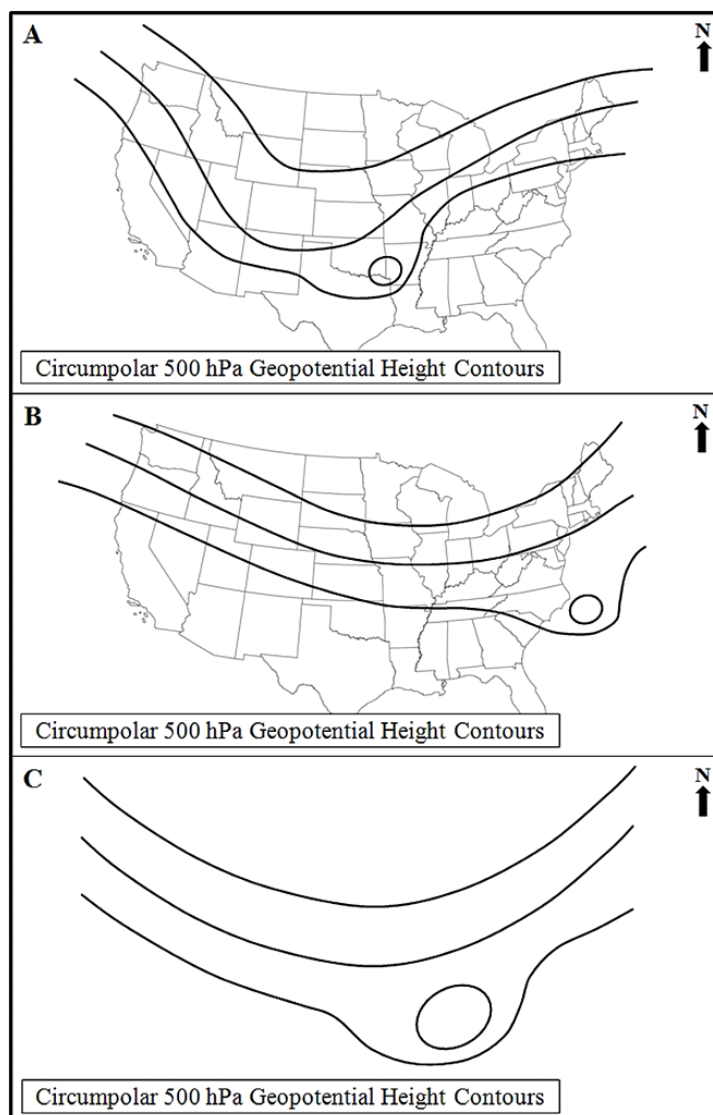


FIGURE 3.1. Schematic illustrating a TC-relative framework for classifying similar synoptic situations. **A** illustrates a TC as a closed shortwave trough embedded within the westerlies over the central United States. **B** illustrates a TC as a closed shortwave trough embedded in the westerlies just off the East Coast of the United States. **C** highlights that both **A** and **B** illustrate similar synoptic environments; i.e., both illustrate a TC as a closed shortwave trough embedded in the westerlies. A basemap of the United States is not illustrated in **C** because the geographic location of the synoptic environment is not considered in the TC-relative framework employed by this study.

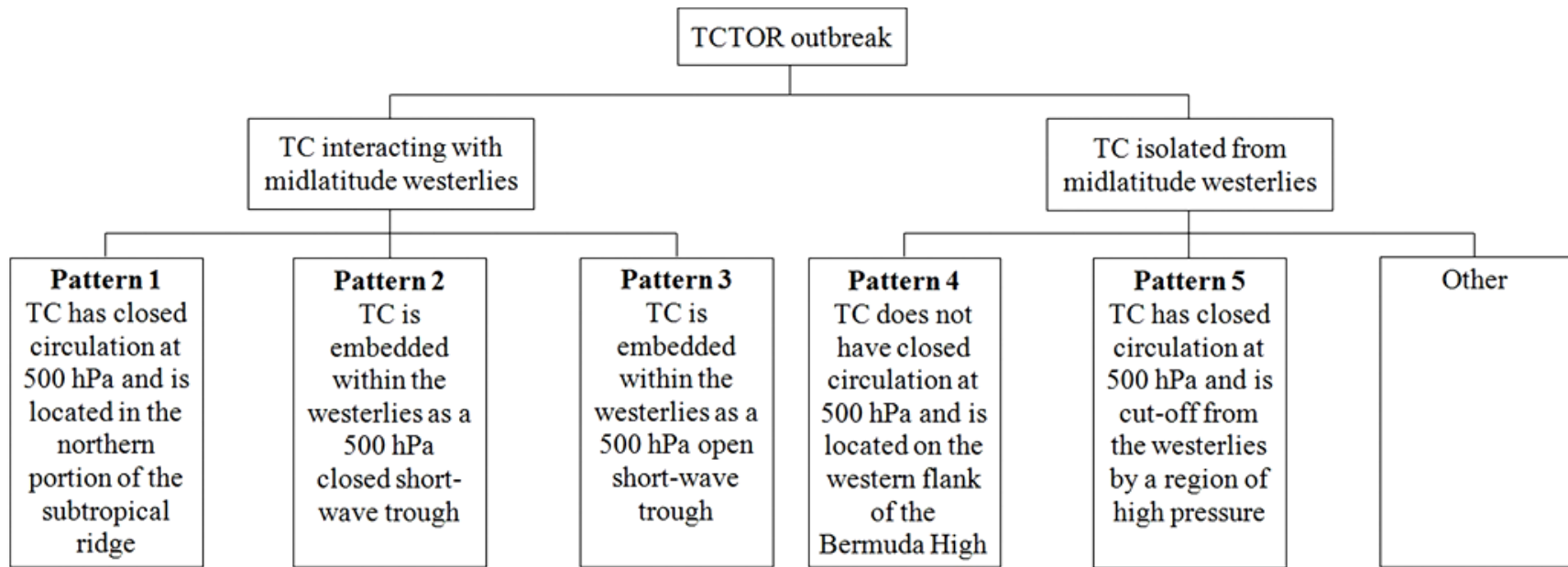


FIGURE 3.2. Classification tree illustrating the hierarchy of synoptic patterns based on 500 hPa geopotential height and vector wind plots.

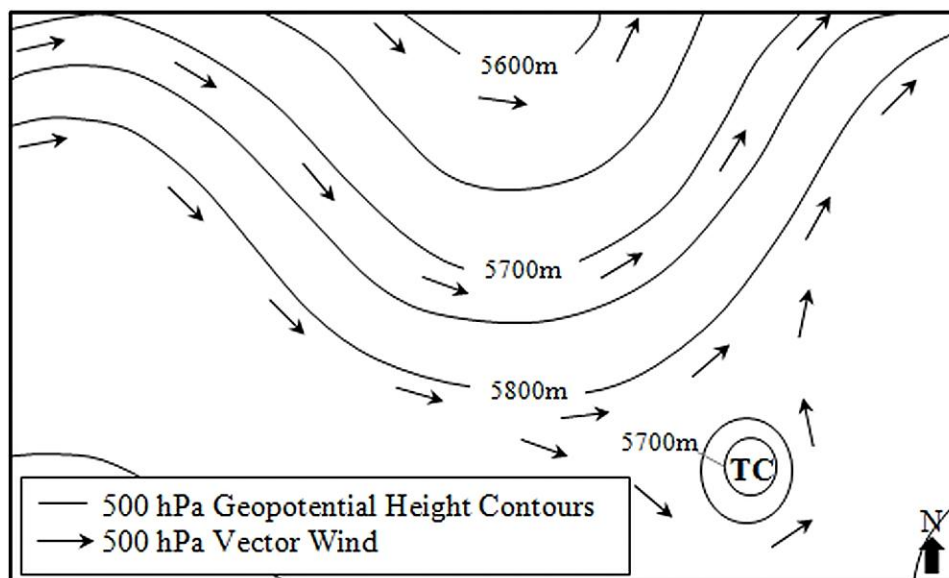


FIGURE 3.3. Simplified illustration of an idealized Pattern 1 TCTOR outbreak environment. Note the closed TC circulation just to the south of the midlatitude westerly flow and the southern-most wind vectors of the westerly flow cyclonically enveloping the TC.

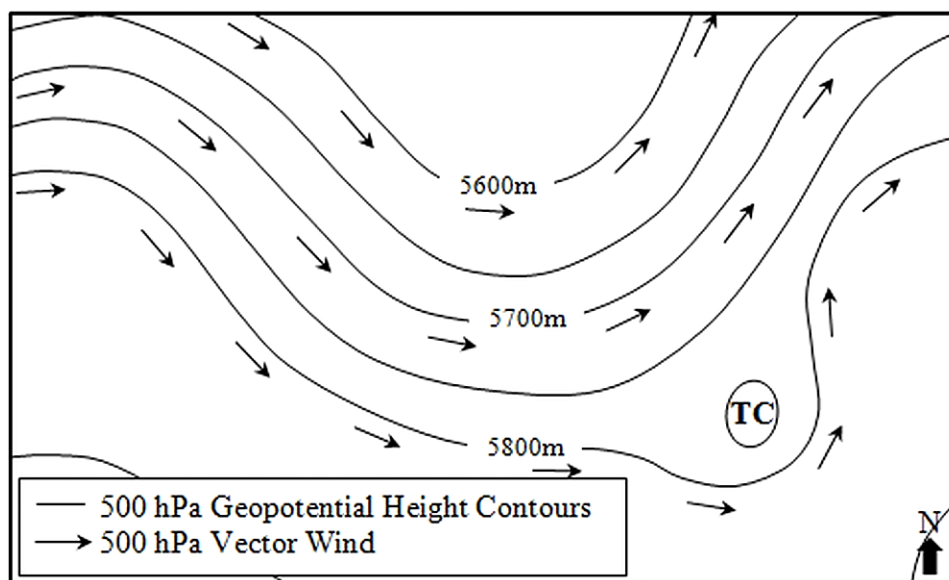


FIGURE 3.4. Simplified illustration of an idealized Pattern 2 outbreak environment. Note the TC embedded within the midlatitude westerly flow as a closed shortwave trough.

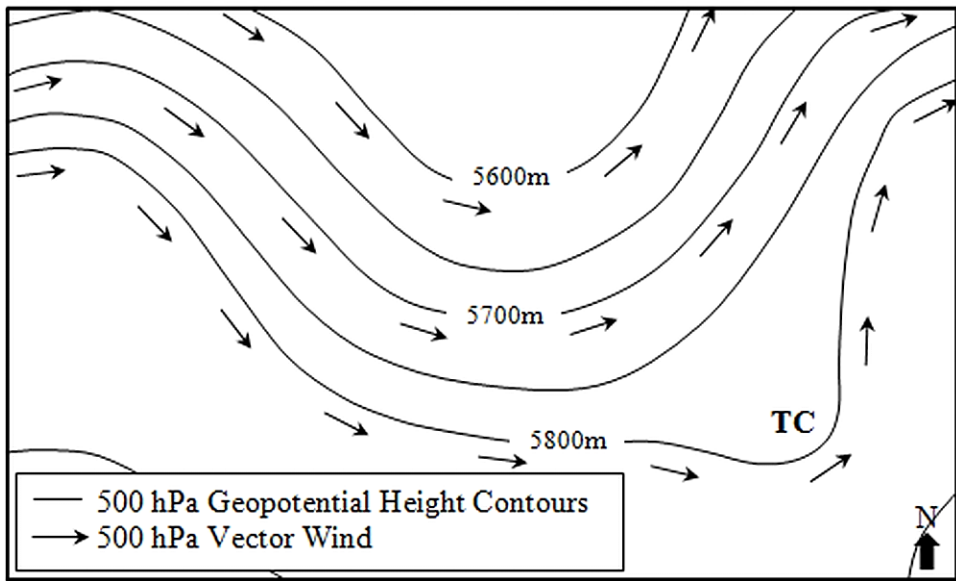


FIGURE 3.5. Simplified illustration of an idealized Pattern 3 outbreak environment. Note the TC embedded within the midlatitude westerly flow as an open short wave trough.

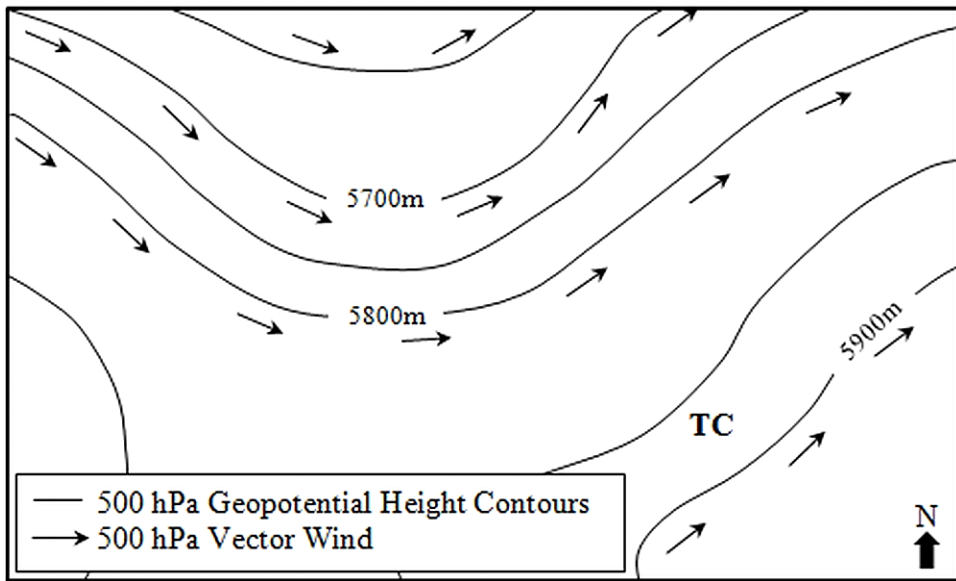


FIGURE 3.6. Simplified illustration of an idealized Pattern 4 outbreak environment. Note the TC without closed circulation embedded within the southwesterly flow of the subtropical ridge.

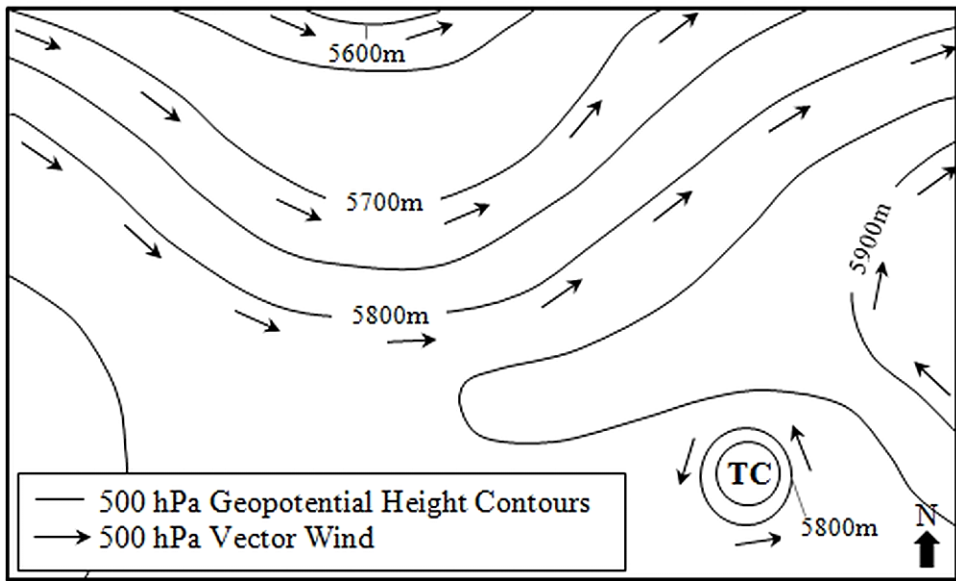


FIGURE 3.7. Simplified illustration of an idealized Pattern 5 outbreak environment. Note the closed TC circulation cut-off from the midlatitude westerly flow to the north by a region of high pressure.

CHAPTER IV

RESULTS

Over the period 1995–2010, sixty-five TCs were responsible for a reported 1163 TCTORs (Appendix C). TCTORs were reported in all years of the record except 2009. Forty-two of the sixty-five TCs (65%) produced one outbreak or more, with a total of 133 outbreaks. The 133 identified outbreaks account for 930 TCTORs, meaning that 80% of all TCTORs over the period 1995–2010 occurred in an outbreak, as defined in this study.

Of the TCs that produced an outbreak, approximately 75%, on average, of their TCTORs occurred in an outbreak (Appendix C). Nearly all of Ivan's (2004) and Rita's (2005) TCTORs were included in outbreaks (Figure 4.1). Ivan (2004) had only three isolated TCTORs, one of which occurred on 17 September 2004 at 1005 UTC approximately twenty-one hours after Ivan's previous TCTOR and approximately five hours prior to the next TCTOR. Ivan's other two isolated TCTORs occurred at 0740 and 0800 UTC on 18 September 2004, which is approximately six hours after the previous TCTOR. Rita (2005) had only a single isolated TCTOR that occurred on 24 September 2005 at 1415 UTC, which is two hours prior to the first TCTOR in Rita's first outbreak. At the other extreme, of Alberto's (2006) TCTORs, only 35% occurred in an outbreak (Figure 4.1). Note that isolated TCTORs are temporally isolated but they often are spatially proximate to other TCTORs.

The remainder of this chapter provides results for the statistical analysis of the TCTOR outbreaks. First, results of the descriptive statistical analysis are discussed for the entire sample of TCTOR outbreaks. Second, results of the descriptive and inferential statistical analyses are discussed for the five synoptic patterns.

4.1 Statistical Description of Tropical Cyclone Tornado Outbreaks

4.1.1 Frequency and Severity

The mean number of outbreaks per TC is 2.06 ± 0.64 (mean \pm 95% confidence interval), but half of the TCs produced no outbreaks or only one. The mean increases to 3.2 when considering only TCs that produced at least one outbreak. Several examples illustrate the capability of TCs to produce a large number of outbreaks. TCs Ivan (2004) and Gustav (2008), for instance, each produced eight outbreaks and TC Frances (2004) produced twelve. Understandably, the number of outbreaks a TC produces is strongly associated with the total number of TCTORs produced (Figure 4.2).

The mean number of TCTORs in an outbreak is 6.99 ± 0.96 (mean \pm 95% confidence interval), but a skewness of +2.4 indicates that most outbreaks consist of fewer TCTORs than this mean value. The median of 5.0 is likely more representative of typical outbreak severity (the number of TCTORs in a given outbreak). The most common outbreak severity is three TCTORs, followed by outbreaks with four then five TCTORs (Figure 4.3). Outbreaks in the middle 50% of the outbreak severity distribution have more than three TCTORs but less than nine. The ten severest outbreaks consisted of more than fifteen TCTORs. These outbreaks were produced by TCs Lili (2002), Frances (2004), Ivan (2004), Katrina (2005), Rita (2005), and Ike (2008) (Figure 4.4). The two most severe outbreaks consisted of thirty-three TCTORs and were produced by TCs Ivan

(2004) and Rita (2005). These outbreaks are particularly notable when considering that the period over which they occur is only six hours; these TCs were producing TCTORs at a rate of 5.5 TCTORs per hour for a six hour period during these outbreaks.

When considering the total number of TCTORs produced by a TC over its life-span, hurricane-strength storms at the time of landfall, specifically major hurricanes (Saffir-Simpson Category 3, 4, and 5), have been shown to produce a relatively large number of TCTORs (Hill, Malkin, and Schulz 1966; Novlan and Gray 1974; McCaul 1991; Verbout et al. 2007; Moore and Dixon 2011a). Few TCTORs, however, occur while their parent TC is at hurricane strength; the majority of TCTORs occur while TCs are weakening after landfall (Novlan and Gray 1974). Only 19% of the outbreaks in this study were produced by hurricane-strength TCs (Figure 4.5). The remaining 81% were produced by TCs that never reached hurricane strength or by those that were hurricane strength but subsequently weakened prior to or during the outbreak.

According to the Fujita (F) and Enhanced Fujita (EF) tornado damage scales (Appendix B), the 930 individual TCTORs that compose the 133 outbreaks range in strength from F/EF0 to F/EF3, but show an overwhelming tendency to be relative weak (Figure 4.6). Approximately 63% of the 930 individual TCTORs are rated F/EF0 and another 30% are rated F/EF1. Only three TCTORs attained F3 rating (all three of these TCTORs are rated by the original F-scale because they occurred prior to 2007).

4.1.2 Temporal Characteristics

The monthly frequency distribution of TCTOR outbreaks is markedly non-uniform, with over half (52%) occurring in September (Figure 4.7). This September peak is consistent with the climatological peak reported by previous studies (Novlan and Gray

1974; Moore and Dixon 2011a). TCs in the North Atlantic Basin also are most common in September (NHC 2012b), which essentially provides more opportunity for TCTOR outbreaks to occur. Also noteworthy is the tendency for more severe outbreaks to occur in mid-hurricane season, particularly September. Eight of the ten most severe outbreaks occurred in September (see Figure 4.4). The TCTOR outbreaks, likewise, did not occur uniformly throughout the day. Rather, they occurred most frequently during mid-day and night hours, local time (1800 UTC and 0000 UTC; Figure 4.8).

Relative to their parent TC's landfall time, the TCTOR outbreaks occurred as early as thirty-two hours prior to, and as late as 141 hours following, landfall, with approximately 75% occurring after landfall (Figure 4.9). Note, landfall time most proximate to a given TCTOR outbreak is used in the case of multiple TC landfalls. The densest cluster, which accounts for 61% of the outbreaks, is located in the forty hour period spanning between twenty hours before and after landfall. The most severe outbreaks tended to occur between landfall and approximately forty hours after landfall.

The outbreaks occurring long before landfall are those produced by outer rainbands coming ashore prior to landfall. Hurricane Dennis' (2005) only outbreak, for example, occurred thirty-two hours before Dennis made landfall along the Florida panhandle and was located approximately 418 km north-northeast of Dennis' center. More outbreaks occurred long after landfall as the TCs tracked inland than long before landfall. Five outbreaks occurred more than 100 hours after landfall. Three of these were produced by TC Katrina [(2005) 127 hours, 121 hours, and 103 hours] as she tracked northward along the East Coast, producing TCTORs as far north as Ohio and

Pennsylvania. TCs Danny (1997) and Fay (2008) also produced TCTOR outbreaks more than 100 hours after landfall (141 hours and 108 hours, respectively).

4.1.3 Spatial Characteristics

The mean center of each outbreak was calculated by determining the mean azimuth and range of all TCTORS in a given outbreak. An overwhelming majority of the outbreak mean centers are located to the east of TC center (Figure 4.10A). Ninety-six percent are located in the northeast (59%) and southeast (37%) quadrants, relative to north (Figure 4.10B). With respect to distance from TC center, the mean centers ranged from 31.35 km to 626.06 km, with half located in the 200–400 km range (Figure 4.10C). The distribution of outbreak mean centers about their TC center is to be expected given that the individual TCTORS that compose these outbreaks have similar spatial distributions (see Edwards 2010a).

Visual observations of the TCTOR outbreaks revealed a particularly intriguing aspect about their spatial distributions. They appear to conform to several general spatial configurations that are similar to Galway's (1977) local, progressive, and line outbreaks. Subjective examination and classification of the outbreak configurations, which is similar to the approach taken by Grams et al. (2012) to classify the convective mode associated with significant tornado events, shows that the outbreaks generally conform to one of the following configurations (Figure 4.11A–D):

- A. Linear: distinct linear feature with at least three TCTORS linearly aligned without a substantial gap; a few isolated TCTORS may accompany the linear feature.

- B. Single-cluster: distinct cluster with at least three TCTORs; a few isolated TCTORs may accompany the single cluster.
- C. Multi-cluster: multiple distinct clusters with at least three TCTORs; a few isolated TCTORs may accompany the clusters.
- D. Dispersed: no distinct linear feature or cluster(s).

Rather than being uniformly distributed amongst these configurations, the outbreaks tended towards the dispersed and single-cluster configurations. Whereas all of the TCTOR outbreaks in this study are equally clustered temporally, per their definition, they are not equally clustered spatially (Table 4.1). The linear and single-cluster configurations have the smallest mean and median standard areas (note, statistics describing the one-dimensional length in kilometers of the dominant linear feature of the linear outbreaks are also provided in Table 4.1). Multi-cluster outbreaks have the largest minimum, mean, and median standard area metrics; dispersed outbreaks have the largest maximum standard area. It is not surprising that multi-cluster outbreaks were dispersed over relatively large surface areas because they typically include a larger number of TCTORs than the other configurations (Table 4.1). The dispersed outbreaks did not have the largest standard surface area metrics, as might have been expected, because they were relatively small outbreaks (i.e., they had the smallest mean and median outbreak severity metrics). The dispersed outbreaks did, however, have the largest maximum standard area metric.

4.2 Synoptic Patterns Associated with Tropical Cyclone Tornado Outbreaks

The hierarchical classification scheme developed in this study is two-tiered (see Figure 3.2). The first partitioning created two classes: (1) TC-westerly interaction and

(2) no TC-westerly interaction. The second partitioning further subdivided these two classes into five synoptic patterns, three of which are TC-westerly interaction patterns and two that are no TC-westerly interaction patterns (Table 4.2). Both tiers of the classification scheme are based on 500 hPa geopotential height and vector wind plots. The two classes, TC-westerly interaction and No TC-westerly interaction, account for all outbreaks. The five synoptic patterns account for 97% of the 133 TCTOR outbreaks. The remaining 3% (four outbreaks) did not reasonably fit the criteria of any of the five synoptic patterns and were, thus, excluded from the statistical analysis. There are, therefore, 129 classified TCTOR outbreaks and a total of 917 individual TCTORs that are discussed in sections 4.2.1–4.2.5.

4.2.1 Description and Within-Group Analysis of Synoptic Patterns

4.2.1.1 Pattern 1 Tropical Cyclone Tornado Outbreaks

Pattern 1 outbreaks are produced by TCs with closed circulation at 500 hPa that are located in the predominately westerly flow to the north of the subtropical ridge, with a 500 hPa midlatitude trough often embedded within the westerlies to the north or northwest of the TCs (Figure 4.12). TCs and midlatitude troughs are distinct synoptic features in Pattern 1 cases. Given the relative positioning of the synoptic features, Pattern 1 cases show signs of proto-interaction between closed circulation TCs and the midlatitude westerlies. The proto-interaction is illustrated by the 500 hPa wind vectors that extend from the southern portion of the westerly flow and cyclonically envelop the TCs. Pattern 1 cases vary in terms of the absolute location of the synoptic features, the distance between the TCs and their corresponding 500 hPa trough, and the wavelength, amplitude, and tilt of the 500 hPa trough/ridge complex.

Twenty-eight percent (thirty-six outbreaks) of the outbreaks were classified as Pattern 1 (Table 4.2). Pattern 1 outbreaks range in severity from three to thirty-three TCTORs per outbreak, but a skewness of +2.1 indicates that they tend towards the lower end of this range (Table 4.3). The outbreaks in Pattern 1 have a mean severity of 7.9 TCTORs per outbreak and a median of 5.0. The standard deviation and coefficient of variation are 6.6 and 0.8, respectively. The middle 50% of Pattern 1 outbreaks have more than four TCTORs but less than eleven. The thirty-six Pattern 1 outbreaks account for 285 individual TCTORs, the majority of which are rated F/EF 0 or F/EF 1 (Figure 4.13).

Pattern 1 outbreaks occurred in all months of the North Atlantic Basin hurricane season except July and November (Figure 4.14). The outbreaks are not, however, uniformly distributed throughout these months. Twenty-six of the thirty-six Pattern 1 outbreaks (72%) occurred in September. The outbreaks also are non-uniformly distributed amongst the primary synoptic hours (Figure 4.15). Twenty-four of the thirty-six Pattern 1 outbreaks (67%) occurred in the 1800 UTC and 0000 UTC windows. Relative to their associated TC landfall, Pattern 1 outbreaks occurred as early as thirteen hours before landfall and as late as 103 hours after landfall, giving them a range of 116 hours about landfall (Table 4.4). The middle 50% of Pattern 1 outbreaks occurred within a twenty-one hour period spanning from forty-five minutes prior to landfall to just over twenty hours after landfall. Spatially, Pattern 1 outbreaks are distributed primarily throughout the southeast United States, in Louisiana, Arkansas, Mississippi, Alabama, Florida, Georgia, and the Carolinas (Figure 4.16).

4.2.1.2 Pattern 2 Tropical Cyclone Tornado Outbreaks

Pattern 2 outbreaks are produced by TCs that are closed shortwave troughs embedded within the midlatitude westerlies, often downstream of a longer-wave 500 hPa trough axis and upstream of the successive ridge axis (Figure 4.17). Pattern 2 cases share many synoptic features with Pattern 1 cases, including closed TC circulation at 500 hPa and proximity between TCs and 500 hPa midlatitude westerlies. The discriminating feature between the two patterns is that TCs in Pattern 2 are north of the subtropical ridge and are encompassed by a single, or multiple, circumpolar isoheight(s), hence their appearance as shortwave troughs. Pattern 2 cases vary in terms of the absolute location of the synoptic features, the distance between the closed shortwave trough and the longer-wave trough axis, and the wavelength, amplitude, and tilt of the longer-wave 500 hPa trough/ridge complex.

Seventeen percent (twenty-two outbreaks) of the outbreaks were classified as Pattern 2 (Table 4.2). Pattern 2 outbreaks range in severity from three to thirty-three TCTORs per outbreak, but a skewness of +1.6 indicates that they tend towards the lower end of this range (Table 4.3). The outbreaks in Pattern 2 have a mean severity of 10.7 TCTORs per outbreak and a median of 9.0. The standard deviation and coefficient of variation are 7.4 and 0.7, respectively. The middle 50% of Pattern 2 outbreaks have more than six TCTORs but less than ten. The twenty-two Pattern 2 outbreaks account for 235 individual TCTORs, the majority of which are rated F/EF 0 or F/EF 1 (Figure 4.18). Two of the three observed F/EF 3 TCTORs occurred in Pattern 2 outbreaks.

Pattern 2 outbreaks occurred in all months of the North Atlantic Basin hurricane season except June and November (Figure 4.19). Similar to Pattern 1 outbreaks, Pattern

2 outbreaks did not occur uniformly throughout these months but, rather, occurred most frequently in September, when sixteen of the twenty-two observed Pattern 2 outbreaks (73%) occurred. Also similar to Pattern 1, rather than being uniformly distributed amongst the primary synoptic hours, Pattern 2 outbreaks were most frequent during the 1800 UTC and 0000 UTC windows when seventeen of the twenty-two outbreaks (77%) occurred (Figure 4.20). Relative to their associated TC landfall, Pattern 2 outbreaks occurred as early as four hours before landfall and as late as fifty-seven hours after landfall, giving them a range of sixty-one hours about landfall (Table 4.4). The middle 50% of Pattern 2 outbreaks occurred within a roughly thirty-one hour period spanning from eleven to nearly forty-two hours after landfall. The spatial distribution of Pattern 2 outbreaks is similar to that of Pattern 1 in that they are both distributed primarily throughout the southeast United States (Figure 4.21). The northern edge of the Pattern 2 distribution, however, extends farther north throughout the Virginias, Maryland, Washington D.C., and Pennsylvania.

4.2.1.3 Pattern 3 Tropical Cyclone Tornado Outbreaks

Pattern 3 cases are similar to pattern 2 cases in that they both are produced by TCs that are north of the subtropical ridge and are shortwave troughs embedded within the midlatitude westerlies, often downstream of a longer-wave 500 hPa trough axis and upstream of the successive ridge axis (Figure 4.22). The difference between the two patterns is that TCs in Pattern 2 cases are closed shortwave troughs whereas those in Pattern 3 are open shortwave troughs. Pattern 3 cases vary in terms of the absolute location of the synoptic features, the distance between the closed shortwave trough and

the longer-wave trough axis, and the wavelength, amplitude, and tilt of the longer-wave 500 hPa trough/ridge complexes.

Thirty-one percent (forty outbreaks) of the outbreaks were classified as Pattern 3, making this the most abundant of the outbreak patterns (Table 4.2). Pattern 3 outbreaks range in severity from three to twenty-four TCTORs per outbreak, but a skewness of +3.0 indicates that they tend towards the lower end of this range (Table 4.3). The outbreaks in Pattern 3 have a mean severity of 5.9 TCTORs per outbreak and a median of 4.5. The standard deviation and coefficient of variation are 3.9 and 0.7, respectively. The middle 50% of Pattern 3 outbreaks have more than four TCTORs but less than eight. The forty Pattern 3 outbreaks account for 235 individual TCTORs, the majority of which are rated F/EF 0 or F/EF 1 (Figure 4.23). One of the three observed F/EF 3 TCTORs occurred in a Pattern 3 outbreak.

Pattern 3 outbreaks occurred in all months of the North Atlantic Basin hurricane season (Figure 4.24). Again, September experienced the most frequent outbreak activity, but rather than having a markedly non-uniform monthly distribution like Pattern 1 and 2, Pattern 3 outbreaks were more evenly distributed throughout hurricane season months. Pattern 3 is the only pattern to have an outbreak in November. Pattern 3 outbreaks are non-uniformly distributed amongst the primary synoptic hours like Patterns 1 and 2 (Figure 4.25). Thirty-one of the forty Pattern 3 outbreaks (78%) occurred in the 1800 UTC and 0000 UTC windows. Relative to their associated TC landfall, Pattern 3 outbreaks occurred as early as fifteen hours before landfall and as late as 141 hours after landfall, giving them a range of 156 hours about landfall (Table 4.4). The middle 50% of Pattern 3 outbreaks occurred within a roughly thirty-eight hour period spanning from

approximately three to forty-one hours after landfall. The spatial distribution of Pattern 3 outbreaks, especially its western edge, is shifted east from that of Patterns 1 and 2 (Figure 4.26). Pattern 3 outbreaks are generally distributed throughout the East Coastal Plains from Florida to Pennsylvania.

4.2.1.4 Pattern 4 Tropical Cyclone Tornado Outbreaks

Pattern 4 outbreaks are produced by TCs without closed circulation at 500 hPa that are located in the southerly or southwesterly flow of the North Atlantic subtropical anticyclone (Figure 4.27). Pattern 4 outbreaks vary in terms of the absolute location of the synoptic features and the 500 hPa midlatitude westerly flow regime.

Ten percent (thirteen outbreaks) of the classified outbreaks are characteristic of Pattern 4, making this the least abundant of the outbreak patterns (Table 4.2). Pattern 4 outbreaks range in severity from three to fourteen TCTORs per outbreak, but a skewness of +1.1 indicates that they tend slightly towards the lower end of this range (Table 4.3). The outbreaks in Pattern 4 have a mean severity of 6.3 TCTORs per outbreak and a median of 4.0. The standard deviation and coefficient of variation are 4.0 and 0.6, respectively. The middle 50% of Pattern 4 outbreaks have more than three TCTORs but less than ten. The thirteen Pattern 4 outbreaks account for eighty-two individual TCTORs, nearly all of which are rated F/EF 0 or F/EF 1 (Figure 4.28).

Pattern 4 outbreaks occurred in all months of the North Atlantic Basin hurricane season except the late months of October and November (Figure 4.29). The majority of Pattern 4 outbreaks (77%) occurred in August and September, with peak activity in August rather than September as seen with Pattern 1–3. The distribution of Pattern 4 outbreaks amongst the primary synoptic hours is non-uniform (Figure 4.30). Ten of the

thirteen Pattern 4 outbreaks (77%) occurred during the 1800 UTC and 0000 UTC windows. Relative to their associated TC landfall, Pattern 4 outbreaks occurred as early as one hour before landfall and as late as eighty-nine hours after landfall, giving them a range of ninety hours about landfall (Table 4.4). The middle 50% of Pattern 4 outbreaks occurred within a fifty-eight hour period spanning from five to sixty-three hours after landfall. Similar to Pattern 3, Pattern 4 outbreaks are primarily distributed throughout the East Coastal Plains region (Figure 4.31). A few of spatial outliers are located in northern Texas and south-central Oklahoma. These two outbreaks were associated with TCs Erin (2007) and Hermine (2010). Both synoptic environments exhibited a well-developed North Atlantic subtropical anticyclone located over the southeast United States and Gulf of Mexico regions, placing their region of southerly or southwesterly flow generally over the south-central United States.

4.2.1.5 Pattern 5 Tropical Cyclone Tornado Outbreaks

Pattern 5 outbreaks are similar to Pattern 1 cases in that both are produced by TCs with closed circulation at 500 hPa. Unlike Pattern 1, however, the Pattern 5 TCs do not exhibit signs of proto-interaction with the midlatitude westerlies because they are located in the southern portion of a distinct subtropical ridge (Figure 4.32). Pattern 5 cases vary in terms of the absolute location of the synoptic features and the 500 hPa midlatitude flow regime.

Fourteen percent (eighteen outbreaks) of the outbreaks were classified as Pattern 5 (Table 4.2). Pattern 5 outbreaks range in severity from three to nine TCTORs per outbreak, but a skewness of +1.3 indicates that they tend slightly towards the lower end of this range (Table 4.3). Note that Pattern 5 has the smallest mean, median, and

maximum outbreak severity metrics. The outbreaks in Pattern 5 have a mean severity of 4.4 TCTORs per outbreak and a median of 3.5. The standard deviation and coefficient of variation are 1.9 and 0.4, respectively. The middle 50% of Pattern 5 outbreaks have more than three TCTORs but less than six. The eighteen Pattern 5 outbreaks account for eighty individual TCTORs, all of which are rated F/EF 0 or F/EF 1 (Figure 4.33).

Pattern 5 outbreaks occurred in the same months as Pattern 4 outbreaks, June through September (Figure 4.34). As with Patterns 1–4, the monthly distribution of Pattern 5 outbreaks is non-uniform, with the frequency at which outbreaks occur increasing from June to a peak September when 55% of the outbreaks occurred. Pattern 5 outbreaks also were most common during the 1800 UTC and 0000 UTC windows when 61% occurred, but the distribution for Pattern 5 outbreaks is not as markedly non-uniform as that of the previous four patterns (Figure 4.35). Relative to their associated TC landfall, Pattern 5 outbreaks occurred as early as thirty-two hours before landfall and as late as thirty-three hours after landfall, giving them a range of sixty-five hours about landfall (Table 4.4). The middle 50% of Pattern 5 outbreaks occurred within a roughly eighteen hour period spanning from nine hours prior to landfall to just over eight hours after landfall. Spatially, Pattern 5 outbreaks are distributed primarily in two near-coast regions in south Texas and in the Florida peninsula (Figure 4.36).

4.2.2 Synoptic Pattern Persistence and Variability

By examining the sequence of synoptic patterns for each TC (Appendix D), it can be determined how many pattern-pairs are persistent (i.e., sequential outbreaks with the same pattern classifications) and how many are variable (i.e., sequential outbreaks with different pattern classifications). Seventy percent of the sequential patterns were

persistent and 30% were variable. Some cases also included more than two persistent sequential patterns. TCs Ivan (2004), Katrina (2005), and Gustav (2008), for example, each had five Pattern 1 outbreaks in sequence; and, these were the first five outbreaks for all three TCs. TC France's (2004) pattern sequence is a unique in that three different patterns showed persistence; Frances produced twelve outbreaks, four Pattern 5's followed by four Pattern 1's then four Pattern 2's.

4.2.3 Between-Group Analysis of Synoptic Patterns

4.2.3.1 Outbreak Frequency

A X^2 goodness-of-fit test for uniformity was used to test whether TCTOR outbreaks are equally common to the five synoptic patterns. If the outbreaks are equally common to the five patterns, the frequency distribution should not significantly differ from a uniform distribution. The results of the test indicate that the frequency distribution does significantly differ from a uniform distribution ($X^2 = 21.12$, $df = 4$, $p < 0.001$; Figure 4.37). The outbreaks occurred most frequently with synoptic Patterns 1 and 3, both of which are TC-westerly interaction patterns. The two synoptic patterns in which TCs are not interacting with the westerlies, Patterns 4 and 5, have the least number of outbreaks.

4.2.3.2 Outbreak Severity

Levene's test for homogeneity of variance was used to test for disparity in terms of the variance of outbreak severity within each of the five patterns. The test indicates that the five patterns do not have equal variance in terms of outbreak severity (Levene's statistic = 5.01, $df1 = 4$, $df2 = 124$, p -value = 0.001). This disparity is clearly displayed by the ranges illustrated in Figure 4.38. Outbreak severity range and variance are greatest

in Patterns 1 and 2. All patterns have the same minimum outbreak severity (3 TCTORs), therefore the range and variance of Pattern 1 and 2 are enlarged by the upper end of their distributions (note the whiskers and extreme values for Patterns 1 and 2). The two most severe outbreaks with thirty-three TCTORs were classified as Pattern 1 and Pattern 2. Whereas the range and variance of outbreak severity differs across the patterns, their coefficients of variation indicate that their relative variability is more consistent across the patterns (Table 4.3).

The positive skewness of the TCTOR outbreak severity distributions implies that none of the synoptic patterns are normally distributed about their mean. The Shapiro-Wilk test of normality verifies that the distribution of outbreak severity does not conform to a normal distribution in any of the five patterns (Table 4.5).

Because TCTOR outbreaks are not normally distributed about their respective mean outbreak severity in any of the patterns, and because the patterns have different sample sizes, the nonparametric Kruskal-Wallis test was used to test for statistically significant differences in median outbreak severity across patterns. The results indicate that median outbreak severity does significantly differ in at least one pair of the patterns ($X^2 = 16.92$, $df = 4$, $p\text{-value} = 0.002$). The nonparametric Mann-Whitney U test with a Bonferroni adjustment to α was used to determine which pattern pairs are significantly different. Statistical significance was assessed at $\alpha = 0.05$ in the Kruskal Wallis test, thus, according to the Bonferroni adjustment, each pattern comparison is assessed at $\alpha = 0.005$. Results indicate that significant differences in median outbreak severity exist between Patterns 2 and 3 and between Patterns 2 and 5 (Table 4.6). It is not surprising that the typical Pattern 2 outbreak was found to be significantly larger than at least one of

the remaining patterns', given that Pattern 2 had the largest median outbreak severity (Figure 4.38; Table 4.3). No significant differences were found between the remaining pattern pairs.

4.2.3.3 Tropical Cyclone Tornado Strength

Weak TCTORs (F/EF 0 and 1) comprise an overwhelming majority of the TCTORs in each of the five synoptic patterns (Table 4.7). Approximately 90% or more of the TCTORs in Pattern 1–4 are rated F/EF 0 or 1 and 100% of Pattern 5 TCTORs are F/EF 0 or 1. Moreover, more than half of the TCTORs in each of the five synoptic patterns are rated F/EF 0. Patterns 4 and 5 (especially 5) are comprised of a disproportionately large number of weak F/EF 0 TCTORs, relative to Patterns 1–3. F/EF 0 TCTORs comprise 71% and 89% of Pattern 4 and 5 TCTORs, respectively, whereas they comprise 65%, 59%, and 52% of Pattern 1, 2, and 3 TCTORs, respectively.

4.2.4 Seasonality of Synoptic Patterns

Each of the five synoptic patterns, except Pattern 4, were most common in September. Pattern 4 was most common in August (Table 4.8). Ninety-five percent of Pattern 1 and 2 outbreaks occurred in August, September, and October. Approximately 90% of Pattern 4 and 5 outbreaks occurred in July, August, and September. Compared to the other synoptic patterns, Pattern 3 outbreaks are much more evenly distributed throughout the North Atlantic Basin hurricane season and, furthermore, Pattern 3 is the only one to be associated with an outbreak in November.

Each month in the North Atlantic Basin hurricane season except August has a dominant synoptic pattern that accounts for a rather distinct peak in TCTOR outbreak activity for that given month (Table 4.8). Pattern 3 accounted for the modal frequency in

all months except September, when Pattern 1 dominated. The below bulleted list discusses the distribution of TCTOR outbreaks by synoptic pattern for each month of the North Atlantic Basin hurricane season.

- June – Seven TCTOR outbreaks occurred in June (Figure 4.39). These outbreaks were associated with Patterns 1, 3, 4, and 5. No Pattern 2 outbreaks occurred in June. Pattern 3 accounts for 57% of all June outbreaks. The remaining 43% (three outbreaks) were evenly distributed across Patterns 1, 4, and 5.
- July – Fifteen TCTOR outbreaks occurred in July (Figure 4.40). These outbreaks were associated with Patterns 2, 3, 4, and 5. No Pattern 1 outbreaks occurred in July. Similar to June, Pattern 3 accounts for over half of all July outbreaks.
- August – Twenty-six TCTOR outbreaks occurred in August (Figure 4.41). Outbreaks from all five synoptic patterns occurred in August and the outbreaks were more evenly distributed across the patterns than seen in June and July. Patterns 1, 3, and 4 each account for 23–31% of all August outbreaks. There is a slight maximum associated with Pattern 3 and distinct minimum with Pattern 2 in August.
- September – Patterns 1, 2, and 5 outbreaks had seasonal peaks in September and Pattern 3 had a slight peak in September (see Figures 4.14, 4.19, 4.24, and 4.34). Consequently, September had the greatest number of TCTOR outbreaks with sixty-seven (Figure 4.42). As in August, outbreaks from all five synoptic patterns occurred in September. Unlike the remaining months, peak activity in September is associated with Pattern 1 rather than Pattern 3.

- October – Thirteen TCTOR outbreaks occurred in October, all of which were associated with Pattern 1, 2, or 3 (Figure 4.43). Similar to June–August, peak October activity is associated with Pattern 3.
- November – One Pattern 3 outbreak occurred in November.

4.2.5 Tropical Cyclone-Westerly Interaction VS No Tropical Cyclone-Westerly Interaction Outbreaks

4.2.5.1 Tropical Cyclone-Westerly Interaction (Patterns 1, 2, and 3)

Seventy-six percent (ninety-eight outbreaks) of the classified outbreaks were produced by TCs that were interacting with, or embedded within, the midlatitude westerlies (Table 4.9). These TC-westerly interaction outbreaks range in severity from three to thirty-three TCTORs per outbreak. A skewness of +2.2 indicates that they tend towards the lower end of this range. The outbreaks associated with TC-westerly interaction cases have a mean severity of 7.7 TCTORs per outbreak and a median of 5.0. The standard deviation and coefficient of variation are 6.1 and 0.8, respectively. The middle 50% of these outbreaks have more than four TCTORs but fewer than ten. The ninety-eight TC-westerly interaction outbreaks account for 755 individual TCTORs, the majority of which are rated F/EF 0 or F/EF 1 (Figure 4.44). Three TC-westerly interaction outbreaks produced the only three F3 TCTORs in the record.

TC-westerly interaction outbreaks occurred in all months of the Atlantic Basin hurricane season (Figure 4.45). The outbreaks are not uniformly distributed throughout hurricane season months. They were most frequent in September, when fifty-three of the ninety-eight TC-westerly interaction outbreaks (55%) occurred. The outbreaks also are non-uniformly distributed amongst the primary synoptic hours (Figure 4.46). Seventy-

two of the ninety-eight TC-westerly interaction outbreaks (73%) occurred in the 1800 UTC and 0000 UTC windows. Relative to their associated TC landfall, TC-westerly interaction outbreaks occurred as early as fifteen hours before landfall and as late as 141 hours after landfall, giving them a range of 156 hours about landfall (Table 4.10). The middle 50% of TC-westerly interaction outbreaks occurred within a roughly thirty-six hour period spanning between three and thirty-nine hours after landfall.

4.2.5.2 No Tropical Cyclone-Westerly Interaction (Patterns 4 and 5)

Twenty-four percent (thirty-one outbreaks) of the classified outbreaks were produced by TCs that were isolated from the midlatitude westerlies (Table 4.9). These no TC-westerly interaction outbreaks range in severity from three to thirteen TCTORs per outbreak. A skewness of +1.6 indicates that they tend slightly towards the lower end of this range. The no-TC-westerly interaction outbreaks have a mean severity of 5.2 TCTORs per outbreak and a median of 4.0. The standard deviation and coefficient of variation are 3.1 and 0.6, respectively. The middle 50% of these outbreaks have more than three TCTORs but less than eight. The thirty-one no TC-westerly interaction outbreaks account for 162 individual TCTORs, the majority of which are rated F/EF 0 or F/EF 1 (Figure 4.47).

Outbreaks without TC-westerly interaction occurred in the early (June and July) and middle (August and September) months of the Atlantic Basin hurricane season, but not in the late months (October and November) (Figure 4.48). The outbreaks are not uniformly distributed throughout the early and middle season months. Rather, they were most common in September, when fourteen of the thirty-one no TC-westerly interaction outbreaks (45%) occurred. The outbreaks also are non-uniformly distributed amongst the

primary synoptic hours (Figure 4.49). Twelve of the thirty-one no TC-westerly interaction outbreaks (39%) occurred during the 1800 UTC window. Moreover, 68% were split between the 1800 UTC and 0000 UTC windows. Relative to their associated TC landfall, no TC-westerly interaction outbreaks have occurred as early as thirty-two hours before landfall and as late as eighty-nine hours after landfall, giving them a range of 121 hours about landfall (Table 4.10). The middle 50% of no TC-westerly interaction outbreaks occurred within a twenty-three hour period spanning from three hours prior to landfall to twenty hours after landfall.

4.2.5.3 Outbreak Severity

Table 4.3 and Figure 4.32 show that mean and median TCTOR outbreak severity differs across the synoptic patterns. A Kruskal-Wallis test verified that the difference in median outbreak severity is statistically significant with at least one pattern pair. In general, especially for median values, the TC-westerly interaction outbreaks (Patterns 1, 2, and 3) have larger central tendency metrics than the no TC-westerly interaction outbreaks (Patterns 4 and 5). A one-tailed Mann-Whitney U test was used to determine whether the median outbreak severity for TC-westerly interaction outbreaks is larger than that of no TC-westerly interaction outbreaks. The nonparametric Mann-Whitney U was used because the sample size of these two groups is vastly different and because a Shapiro-Wilk test indicates that neither of the groups is normally distributed in terms of outbreak severity (Table 4.11). The results indicate that the median outbreak severity for TC-westerly interaction outbreaks is significantly larger than that of no TC-westerly interaction outbreaks (Mann-Whitney $U = 1071.5$, one-tailed p -value = 0.006).

4.2.5.4 Outbreak Seasonality

Because of low monthly frequencies (see Table 4.8), the seasonal distribution is examined with TCTOR outbreaks aggregated into the following groups: early (June and July), middle (August and September), and late (October and November) hurricane season (Table 4.12). Both, TC-westerly interaction and no TC-westerly interaction, outbreaks are most common during the middle season months. By aggregating the data this way, however, it also is shown that TC-westerly interaction outbreaks account for an increasingly large proportion of early, middle, and late season totals as the season progresses, whereas no TC-westerly interaction outbreaks become less common later in the season.

4.3 Chapter Four Tables

TABLE 4.1. Descriptive statistics for TCTOR outbreak severity and the standard area over which TCTOR outbreaks occur for each spatial configuration. Note, bottom italicized row provides statistics describing the length of the dominant linear feature in the linear outbreaks in kilometers. [M=mean, Mdn=median, SD=standard deviation, Min=minimum, Max=maximum, CV=coefficient of variation]

	Outbreak Severity						Standard Area (km ²)					
	M	Mdn	SD	Min	Max	CV	M	Mdn	SD	Min	Max	CV
Linear	8.2	6.0	7.0	3	33	0.8	24,291.8	13,076.2	41,748.5	2,036.2	185,324.9	1.7
Single-cluster	6.8	5.0	4.0	3	24	0.6	23,524.7	10,725.3	35,703.5	532.4	170,235.3	1.5
Multi-cluster	15.1	12.5	6.9	6	33	0.5	60,232.6	46,382.5	49,684.7	20,303.9	225,875.2	0.8
Dispersed	4.2	3.5	2.3	3	15	0.5	31,221.2	21,451.1	43,119.8	2,434.5	264,314.7	1.4
Linear (km)							<i>119.3</i>	<i>96.8</i>	<i>56.9</i>	<i>62.1</i>	<i>259.6</i>	<i>0.5</i>

TABLE 4.2. Description of the five identified synoptic patterns and the frequency at which they occur.

Pattern	Frequency ^a (%)	Descriptive Name
1	36 (28)	TC-westerly interaction: 500 hPa closed TC circulation north of subtropical ridge axis, typically with 500 hPa midlatitude trough to north or northwest of TC
2	22 (17)	TC-westerly interaction: 500 hPa closed shortwave trough embedded within westerlies, typically downstream of a longer-wave 500 hPa trough
3	40 (31)	TC-westerly interaction: 500 hPa open shortwave trough embedded within westerlies, typically downstream of a longer-wave 500 hPa trough
4	13 (10)	No TC-westerly interaction: 500 hPa open TC circulation embedded within southerly or southwesterly flow of the North Atlantic subtropical anticyclone
5	18 (14)	No TC-westerly interaction: 500 hPa closed TC circulation cut-off from midlatitude westerly flow by region of relatively high pressure

a. Four outbreaks did not meet the criteria of the classification scheme and were placed in a sixth other category that is excluded from the statistical analysis of the synoptic patterns.

TABLE 4.3. Descriptive statistics summarizing TCTOR outbreak severity for the five identified synoptic patterns. [N=number of outbreaks, Min=minimum, Max=maximum, Sk=skewness, Mdn=median, M=mean, Q1=first quartile, Q3=third quartile, SD=standard deviation, CV=coefficient of variation]

	N	Min	Max	Sk	Mdn	M	Q1	Q3	SD	CV
Pattern 1	36	3	33	2.1	5.0	7.9	4.0	10.5	6.6	0.8
Pattern 2	22	3	33	1.6	9.0	10.7	5.8	9.0	7.4	0.7
Pattern 3	40	3	24	3.0	4.5	5.9	4.0	7.8	3.9	0.7
Pattern 4	13	3	14	1.1	4.0	6.3	3.0	9.5	4.0	0.6
Pattern 5	18	3	9	1.3	3.5	4.4	3.0	5.3	1.9	0.4

Table 4.4. Statistics describing the distribution of TCTOR outbreaks about their associated TC landfall, in hours, for each synoptic pattern. [M=mean, Mdn=median, SD=standard deviation, CV=coefficient of variation, Min=minimum, Max=maximum, Q1=first quartile, Q3=third quartile]

	M	Mdn	SD	CV	Min	Max	Q1	Q3
Pattern 1	19.0	7.5	33.0	1.7	-13.0	103.0	-0.8	20.3
Pattern 2	26.7	26.0	17.6	0.7	-4.0	57.0	11.0	41.8
Pattern 3	28.7	21.5	38.1	1.3	-15.0	141.0	3.3	41.5
Pattern 4	32.6	18.0	32.5	1.0	-1.0	89.0	5.0	63.0
Pattern 5	0.4	0.0	15.1	37.8	-32.0	33.0	-9.0	8.5

TABLE 4.5. Result of the Shapiro-Wilk test assessing the normality of TCTOR outbreak severity distributions within each of the five synoptic patterns. The null hypothesis is that the distribution of TCTOR outbreak severity is normal. Statistical significance is assessed at $\alpha = 0.01$. Distributions within all patterns are significantly different than normal.

Synoptic Pattern	Shapiro-Wilk Statistic	df	p-value
1	0.73	36	< 0.001
2	0.85	22	0.004
3	0.68	40	< 0.001
4	0.80	13	0.008
5	0.78	18	0.001

TABLE 4.6. Results of the post hoc Mann-Whitney U test with Bonferroni adjustment to determine which pattern-pairs have significantly different median TCTOR outbreak severity. The null hypothesis is that the five patterns have equal median TCTOR outbreak severity scores. Statistical significance was assessed with $\alpha = 0.05$ in the Kruskal-Wallis test thus, according to the Bonferroni adjustment, each individual comparison is assessed at $0.05/10=0.005$. Statistically significant differences are italicized.

Synoptic Pattern Comparison	Mann-Whitney U Statistic	<i>p</i> -value
1 and 2	272	0.046
1 and 3	620	0.289
1 and 4	199	0.415
1 and 5	203	0.023
<i>2 and 3</i>	<i>224</i>	<i>0.001</i>
2 and 4	84	0.043
<i>2 and 5</i>	<i>64</i>	<i>< 0.001</i>
3 and 4	260	0.992
3 and 5	262	0.090
4 and 5	88	0.242

Table 4.7. TCTOR outbreak frequency cross-tabulated by synoptic pattern and F/EF scale.

	F/EF 0	F/EF 1	F/EF 2	F/EF 3	Total
Pattern 1	184	79	22	0	285
Pattern 2	138	80	15	2	235
Pattern 3	122	87	25	1	235
Pattern 4	58	21	3	0	82
Pattern 5	71	9	0	0	80
Total	573	276	65	3	917

TABLE 4.8. TCTOR outbreak frequency cross-tabulated by synoptic pattern and month.

	JUN	JUL	AUG	SEP	OCT	NOV	Total
Pattern 1	1	0	7	26	2	0	36
Pattern 2	0	1	1	16	4	0	22
Pattern 3	4	9	8	11	7	1	40
Pattern 4	1	2	6	4	0	0	13
Pattern 5	1	3	4	10	0	0	18
Total	7	15	26	67	13	1	129

TABLE 4.9. Descriptive statistics summarizing TCTOR outbreak severity. The five synoptic patterns are aggregated into TC-westerly interaction and no TC-westerly interaction groups. [N=number of outbreaks, Min=minimum outbreak severity, Max=maximum outbreak severity, Sk=skewness of the outbreak severity frequency distribution, Mdn=median outbreak severity, M=mean outbreak severity, Q1=first quartile, Q3=third quartile, SD=standard deviation of outbreak severity, CV=coefficient of variation for outbreak severity]

	N	Min	Max	Sk	Mdn	M	Q1	Q3	SD	CV
Westerly interaction*	98	3	33	2.2	5.0	7.7	4.0	9.0	6.1	0.8
No interaction**	31	3	14	1.6	4.0	5.2	3.0	7.0	3.1	0.6

*Patterns 1, 2, and 3

**Patterns 4 and 5

Table 4.10. Statistics describing the distribution of TCTOR outbreaks about their associated TC landfall, in hours. [M=mean, Mdn=median, SD=standard deviation, CV=coefficient of variation, Min=minimum, Max=maximum, Q1=first quartile, Q3=third quartile]

	M	Mdn	SD	CV	Min	Max	Q1	Q3
Westerly interaction*	24.7	15.0	32.6	1.3	-15.0	141.0	3.0	39.3
No interaction**	13.9	6.0	28.5	2.0	-32.0	89.0	-3.0	20.0

*Patterns 1, 2, and 3

**Patterns 4 and 5

TABLE 4.11. Result of the Shapiro-Wilk test assessing the normality of TCTOR outbreak severity distributions for TC-westerly interaction and no TC-westerly interaction outbreaks. The null hypothesis is that the distribution of TCTOR outbreak severity is normal. Statistical significance is assessed at $\alpha = 0.01$. Distributions within both groups are significantly different than normal.

	Shapiro-Wilk Statistic	df	p-value
Westerly interaction	0.74	98	< 0.001
No interaction	0.76	31	< 0.001

TABLE 4.12. Distribution of TC-westerly (Patterns 1, 2, and 3) and no TC-westerly interaction (Patterns 4 and 5) outbreaks through the early (June and July), middle (August and September), and late (October and November) months of the Atlantic Basin hurricane season. Left value is the frequency and the value in parentheses is the relative frequency of early, middle, and late season totals.

	Early	Middle	Late
Westerly interaction	15 (0.68)	69 (0.74)	14 (1.0)
No interaction	7 (0.32)	24 (0.26)	0 (0.0)

4.4 Chapter Four Figures

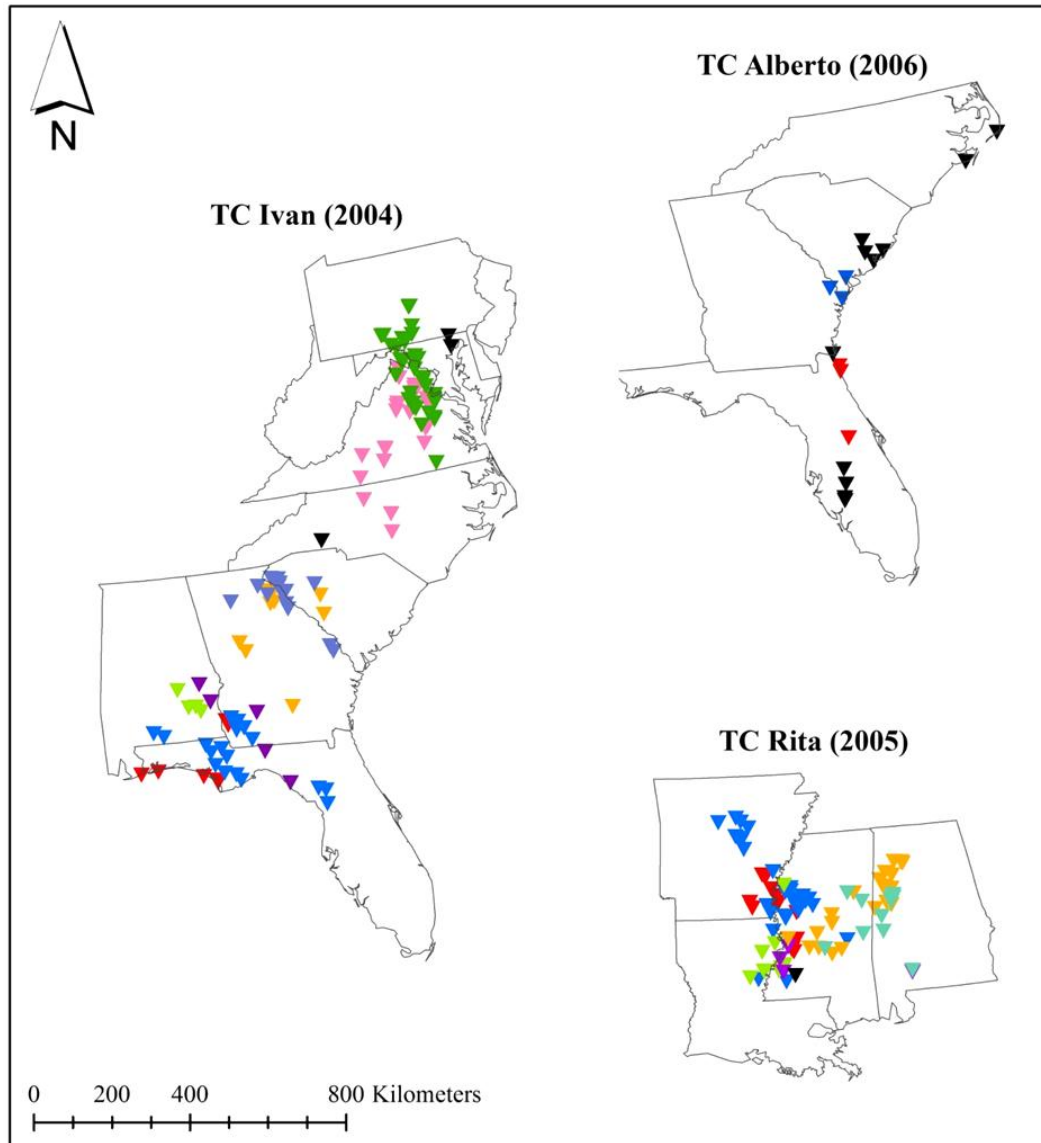


FIGURE 4.1. Outbreak and isolated TCTORs for TCs Ivan, Rita, and Alberto. Individual outbreaks are indicated with separate color triangles and isolated TCTORs are marked with black triangles. Nearly all of Ivan's and Rita's TCTORs were in an outbreak whereas only 35% of Alberto's TCTORs were in an outbreak.

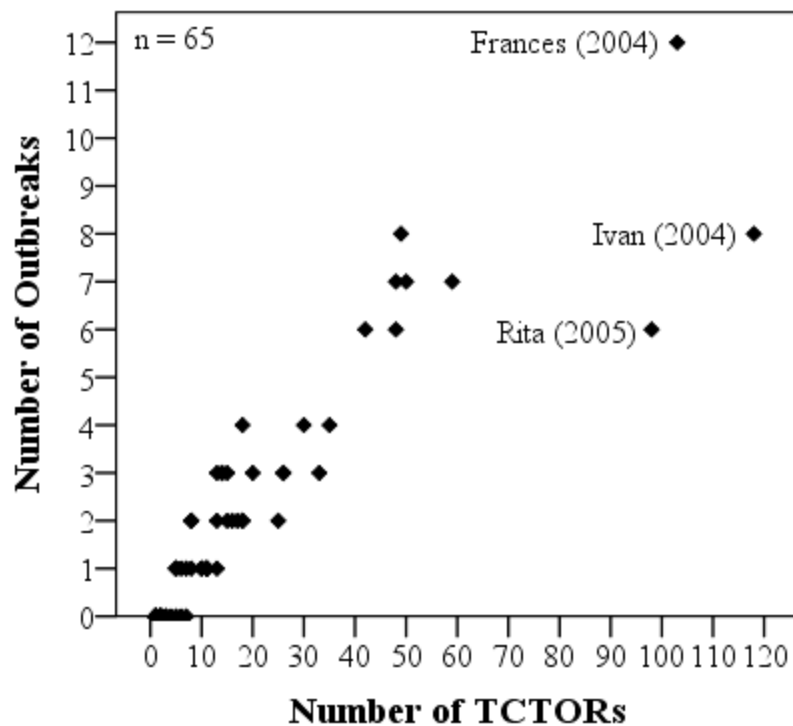


FIGURE 4.2. Scatter plot illustrating the linear association between the total number of TCTORs produced by a TC throughout its life-span and the number of outbreaks that TC produces.

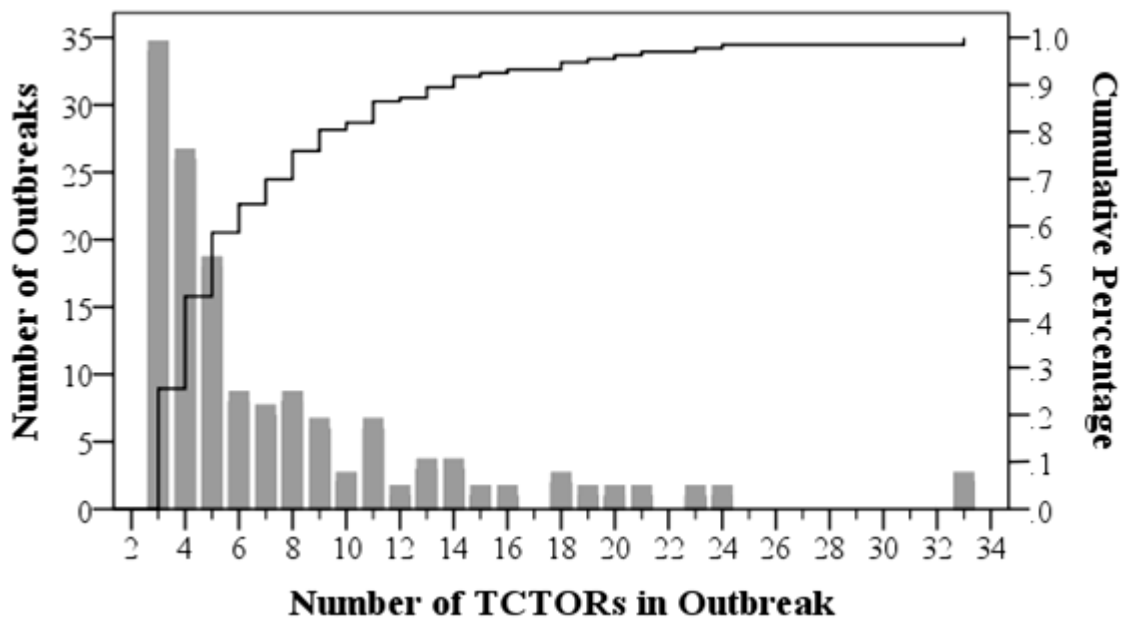


FIGURE 4.3. Bar graph and cumulative percentage graph illustrating the distribution of TCTOR outbreaks, binned by outbreak severity.

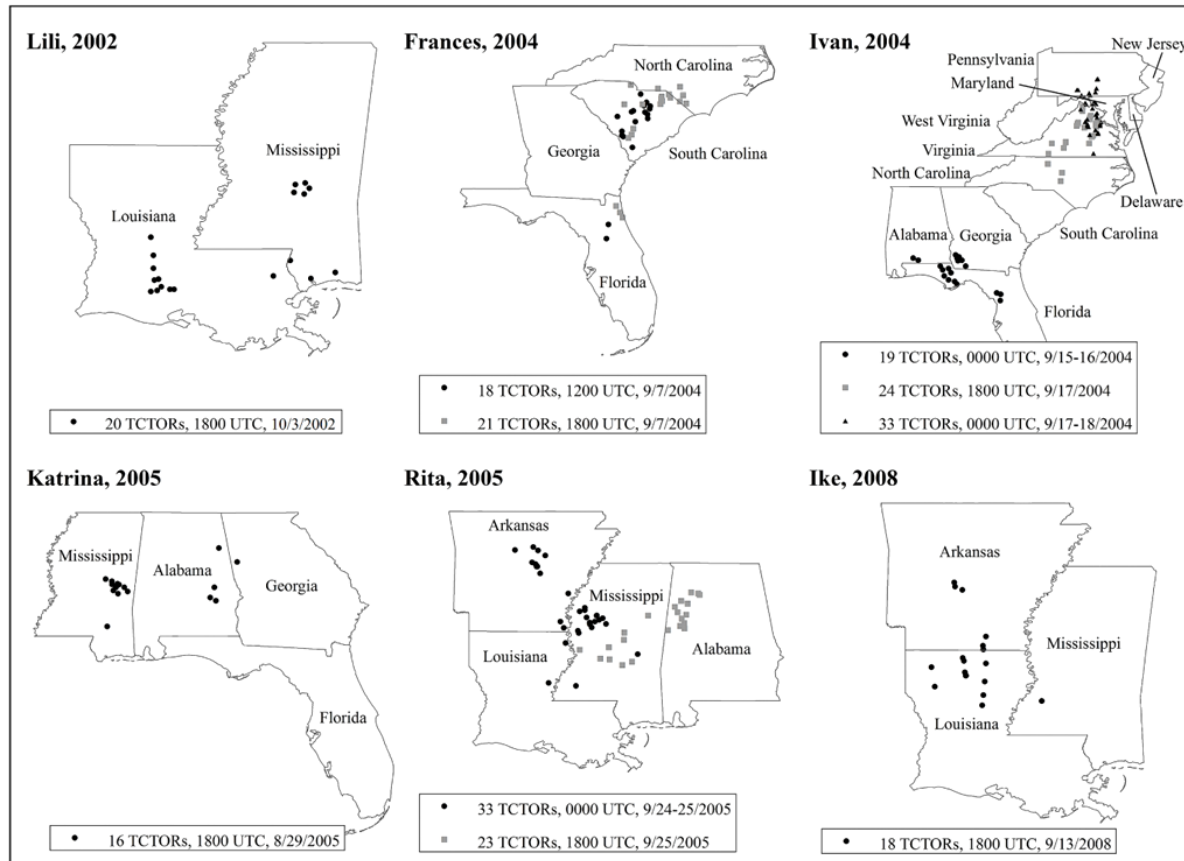


FIGURE 4.4. Ten severest TCTOR outbreaks (1995–2010). Boxed-in text provides the number of TCTORs, the time period over which the outbreak occurred, and the date of the outbreak. The name of the TC that produced the outbreak(s) is provided to the top-left of each map portion.

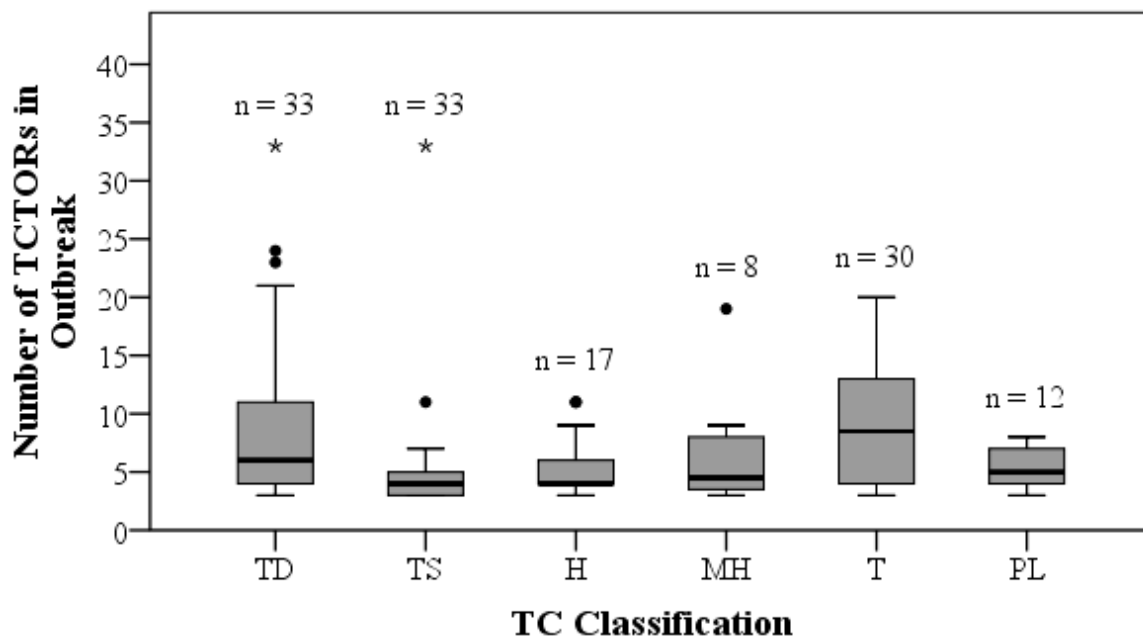


FIGURE 4.5. Boxplots illustrating the distribution of TCTOR outbreak severity, stratified by the classification of their parent TC during the outbreak. [TD=tropical depression, TS=tropical cyclone, H=hurricane, MH=major hurricane, T=transitional, PL=post landfall (extratropical, remnant low, no longer classified)]

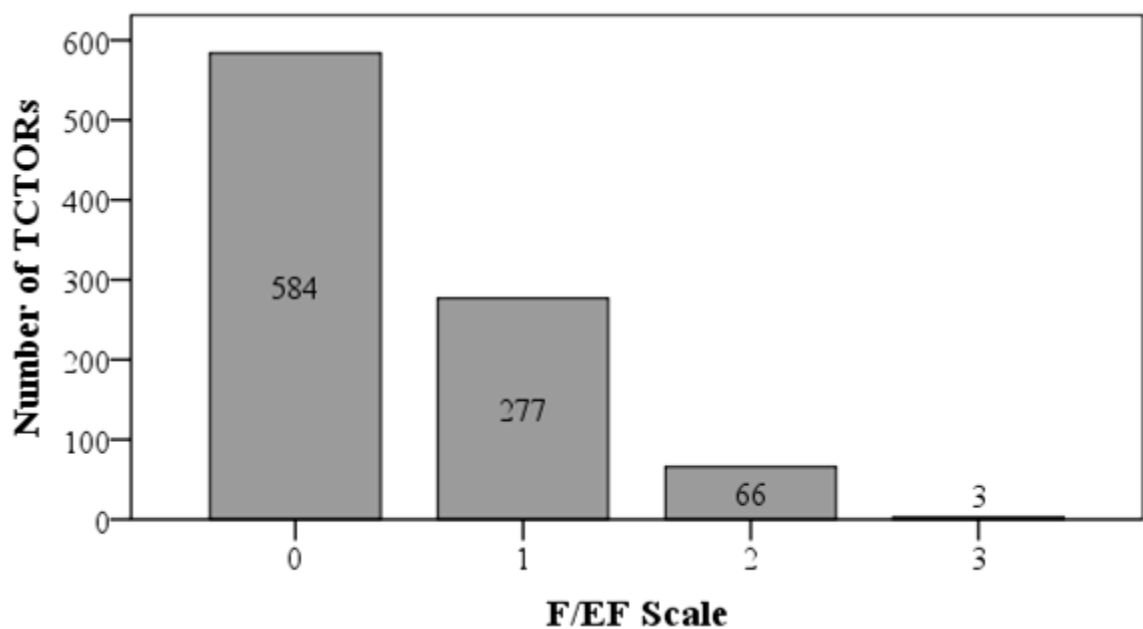


FIGURE 4.6. TCTOR outbreak frequency distribution stratified by F/EF Scale rating.

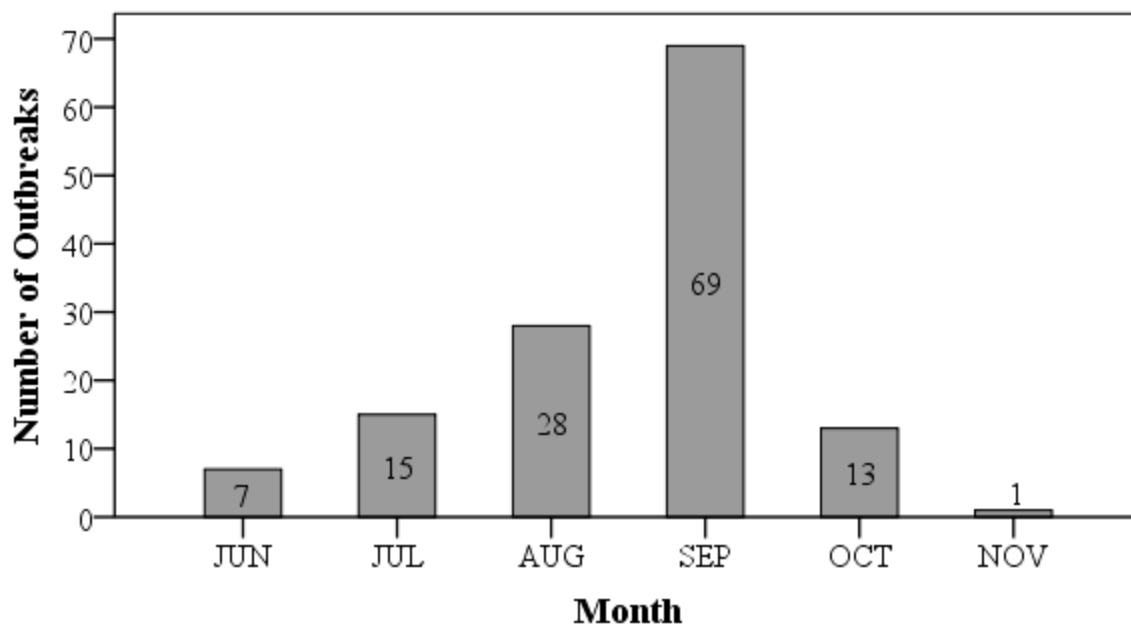


FIGURE 4.7. TCTOR outbreak frequency distribution stratified by month.

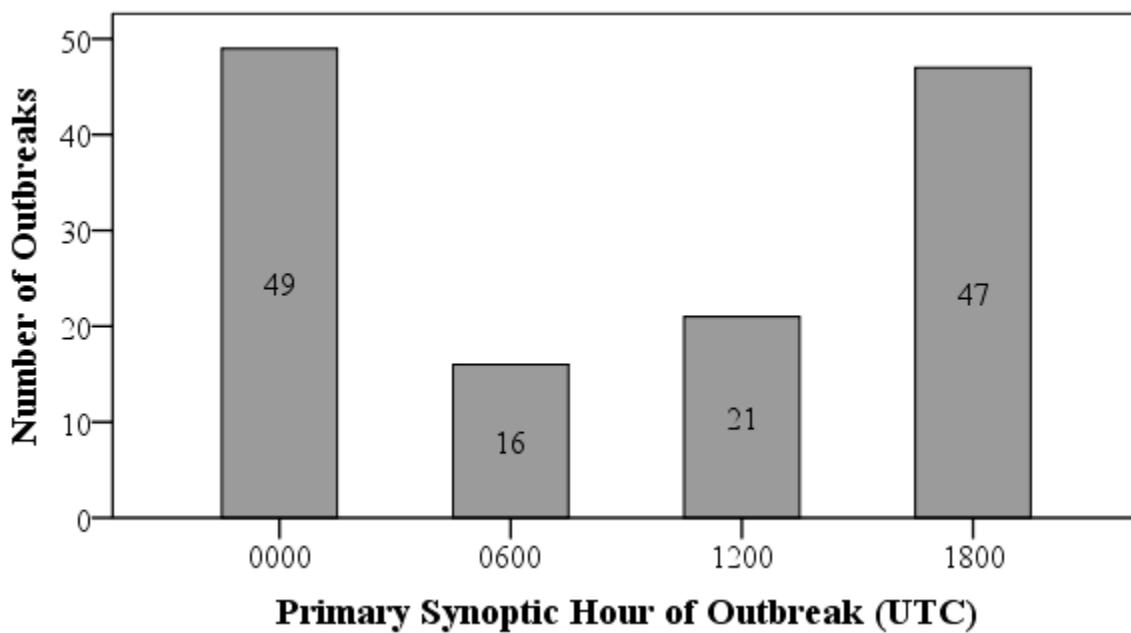


FIGURE 4.8. TCTOR outbreak frequency distribution stratified by synoptic hour.

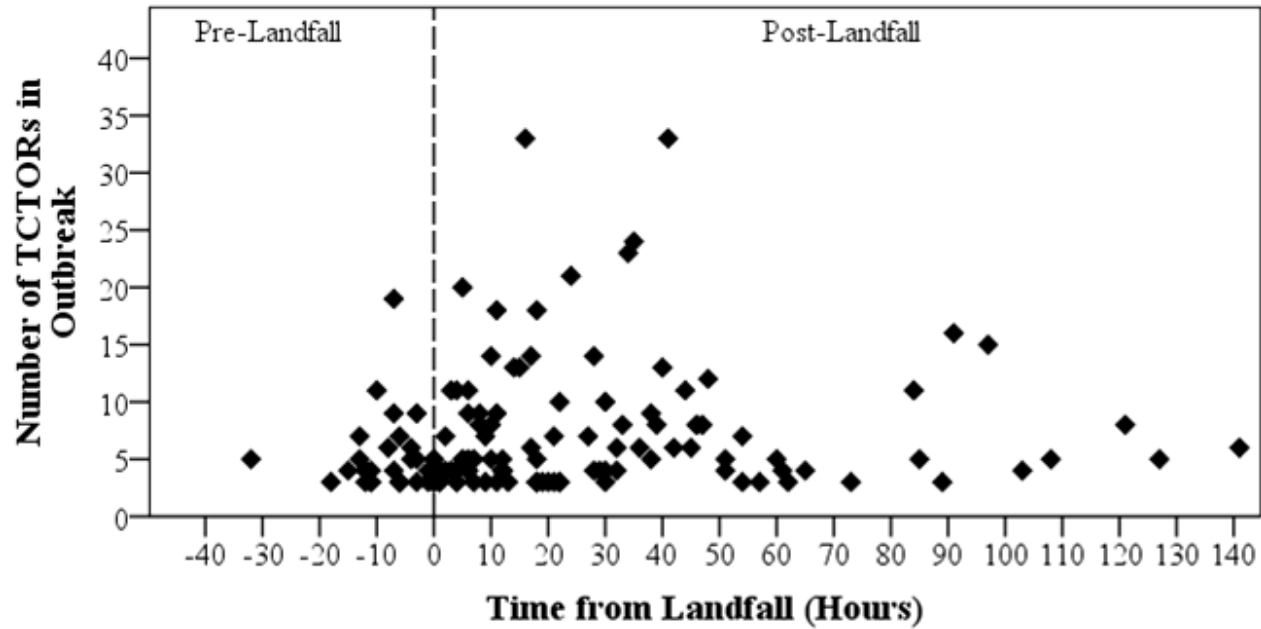


FIGURE 4.9. Scatter plot illustrating the time difference between each TCTOR outbreak synoptic hour and the landfall time of their parent TC, and the number of TCTORs in an outbreak as a function of time from landfall (n = 133).

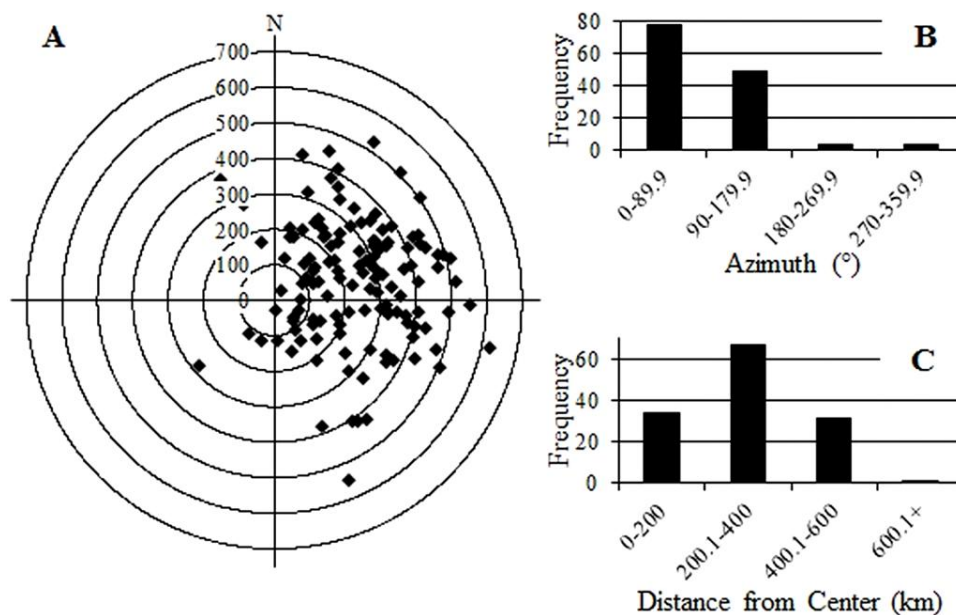


FIGURE 4.10. TCTOR outbreak location within the TC environment. **A.** Location of TCTOR outbreak mean centers (n=133). Azimuth is relative to north and distance rings are in 100 km increments. **B.** Frequency distribution of outbreak mean center location stratified by azimuth location in 90° increments. **C.** Frequency distribution of outbreak mean center location stratified by distance from TC center in 200 km increments.

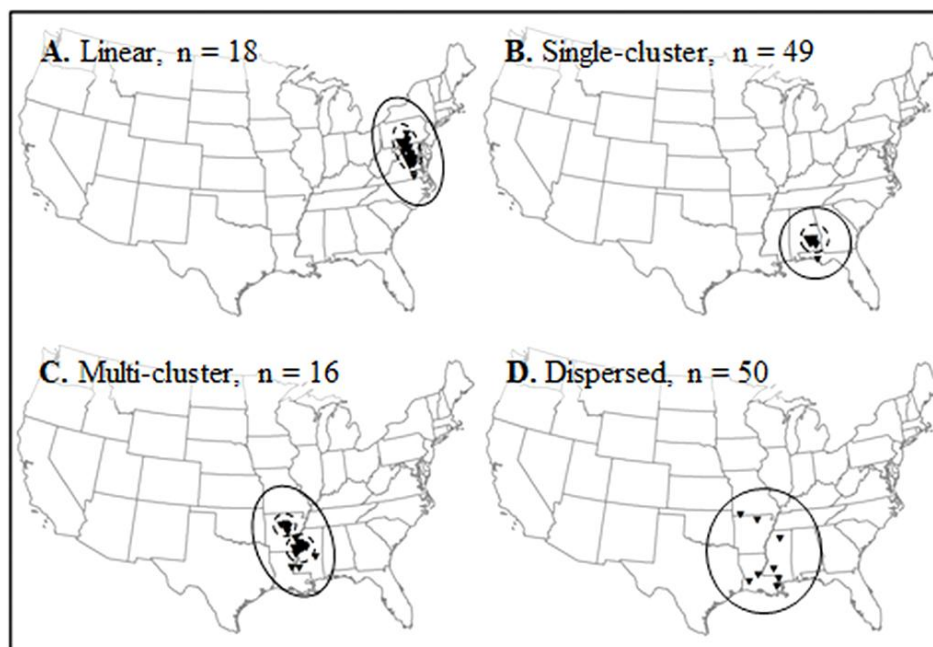


FIGURE 4.11. Illustrative examples of the various spatial configurations in which TCTOR outbreaks occur. **A** illustrates a linear outbreak characterized by three or more linearly aligned TCTORS without a substantial gap. **B** illustrates a single-cluster outbreak characterized by a distinct single cluster of three or more TCTORS. **C** illustrates a multi-cluster outbreak characterized by multiple distinct clusters of three or more TCTORS each. **D** illustrates a dispersed outbreak that does not have any distinct linear or cluster features. Solid line encircles an outbreak region and the dashed lines encircle the dominant linear or cluster feature in the outbreak. [n=the number of outbreaks conforming to each respective configuration]

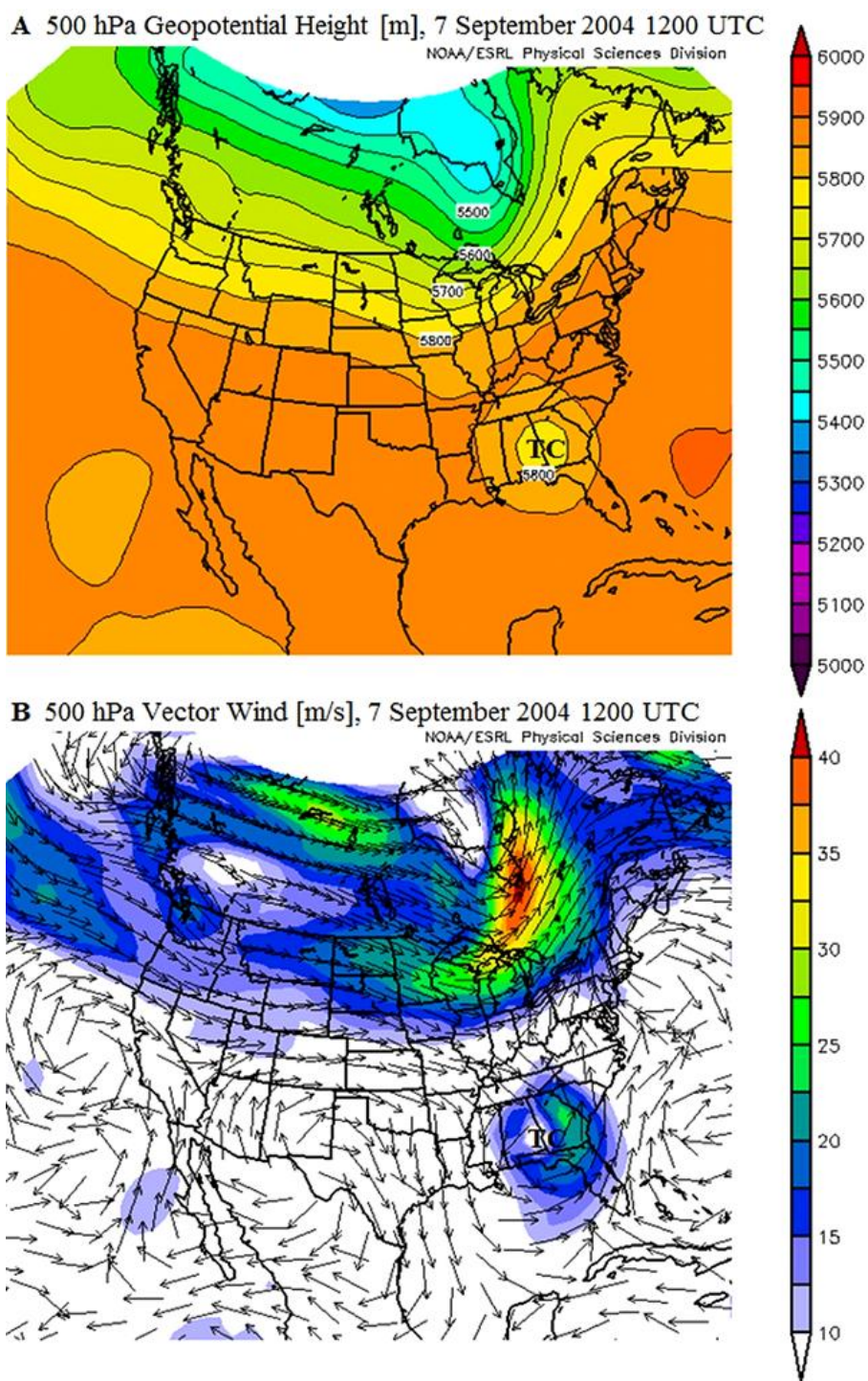


FIGURE 4.12. 500 hPa geopotential height (A) and vector wind (B) plots illustrating a synoptic environment characteristic of Pattern 1 (NCEP-NARR plots obtained from NOAA ESRL's Physical Science Division (NOAA (n. d.)). Note the closed TC circulation just to the south of the midlatitude westerly flow and the southern-most wind vectors of the westerly flow cyclonically enveloping the TC.

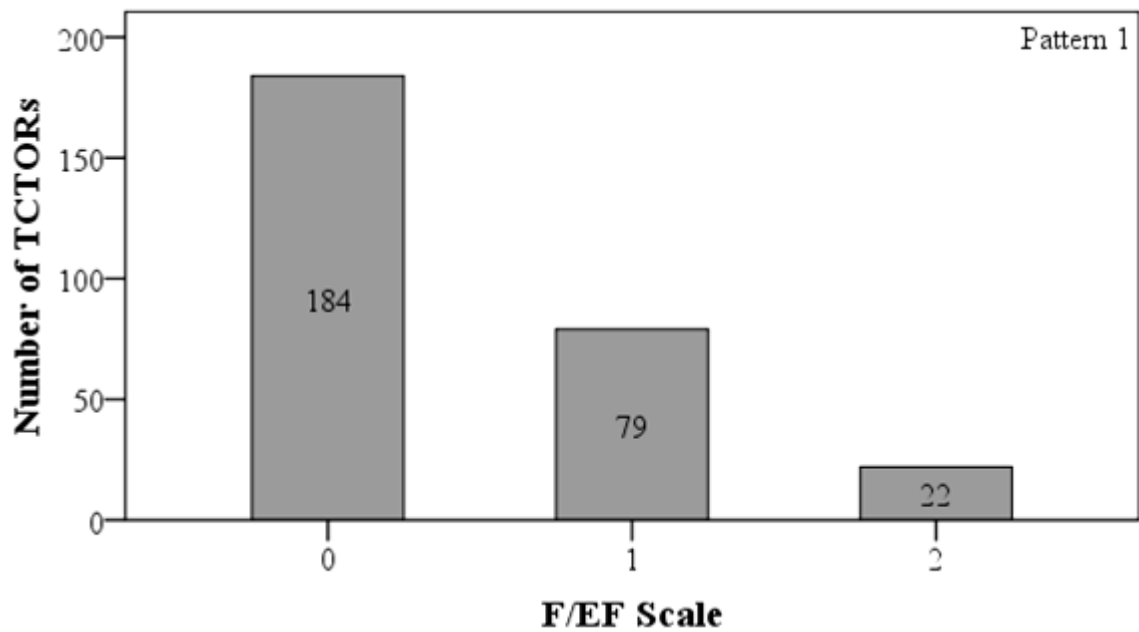


FIGURE 4.13. Pattern 1 TCTOR frequency distribution stratified by F/EF Scale.

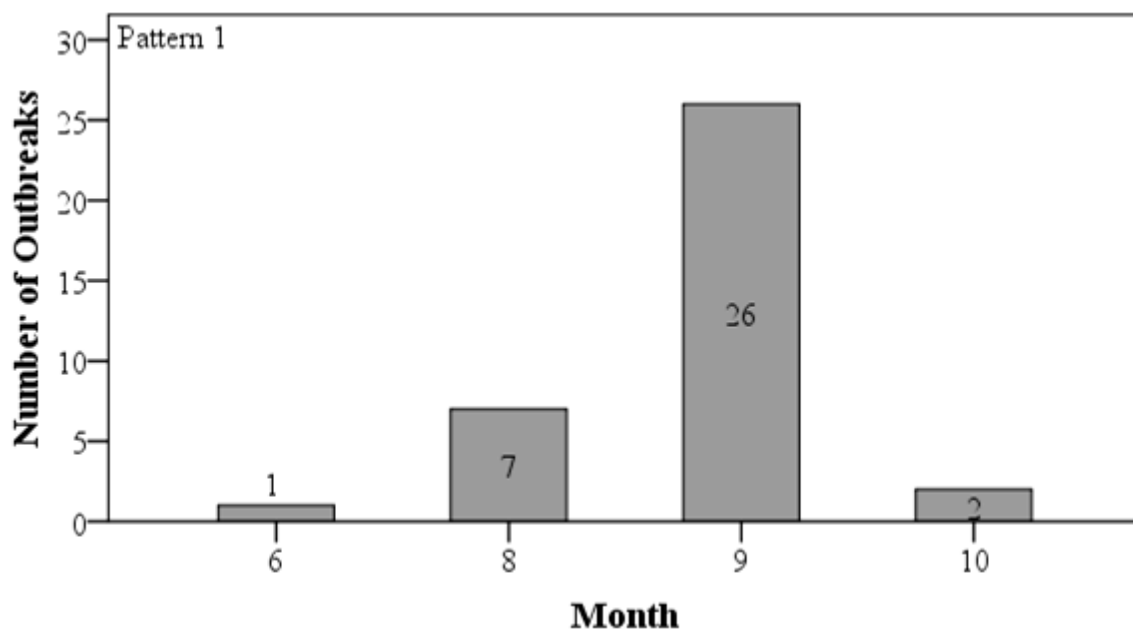


FIGURE 4.14. Pattern 1 TCTOR outbreak frequency distribution stratified by month. No Pattern 1 outbreaks occurred in July.

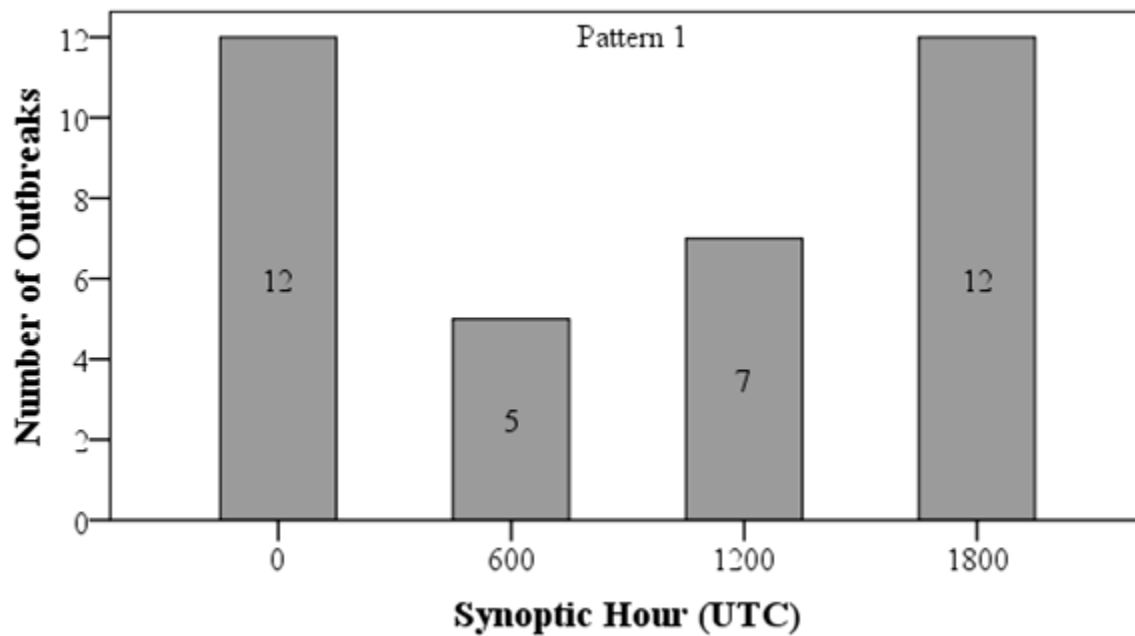


FIGURE 4.15. Pattern 1 TCTOR outbreak frequency distribution stratified by synoptic hour.

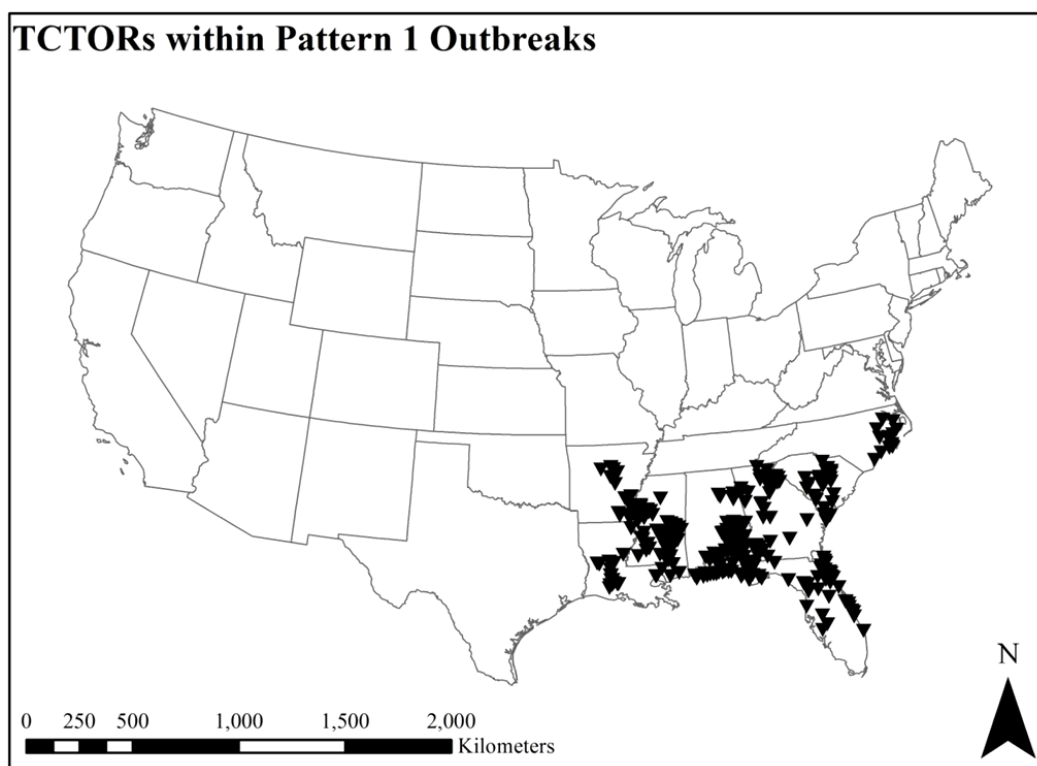


FIGURE 4.16. Spatial distribution of TCTORS within Pattern 1 outbreaks.

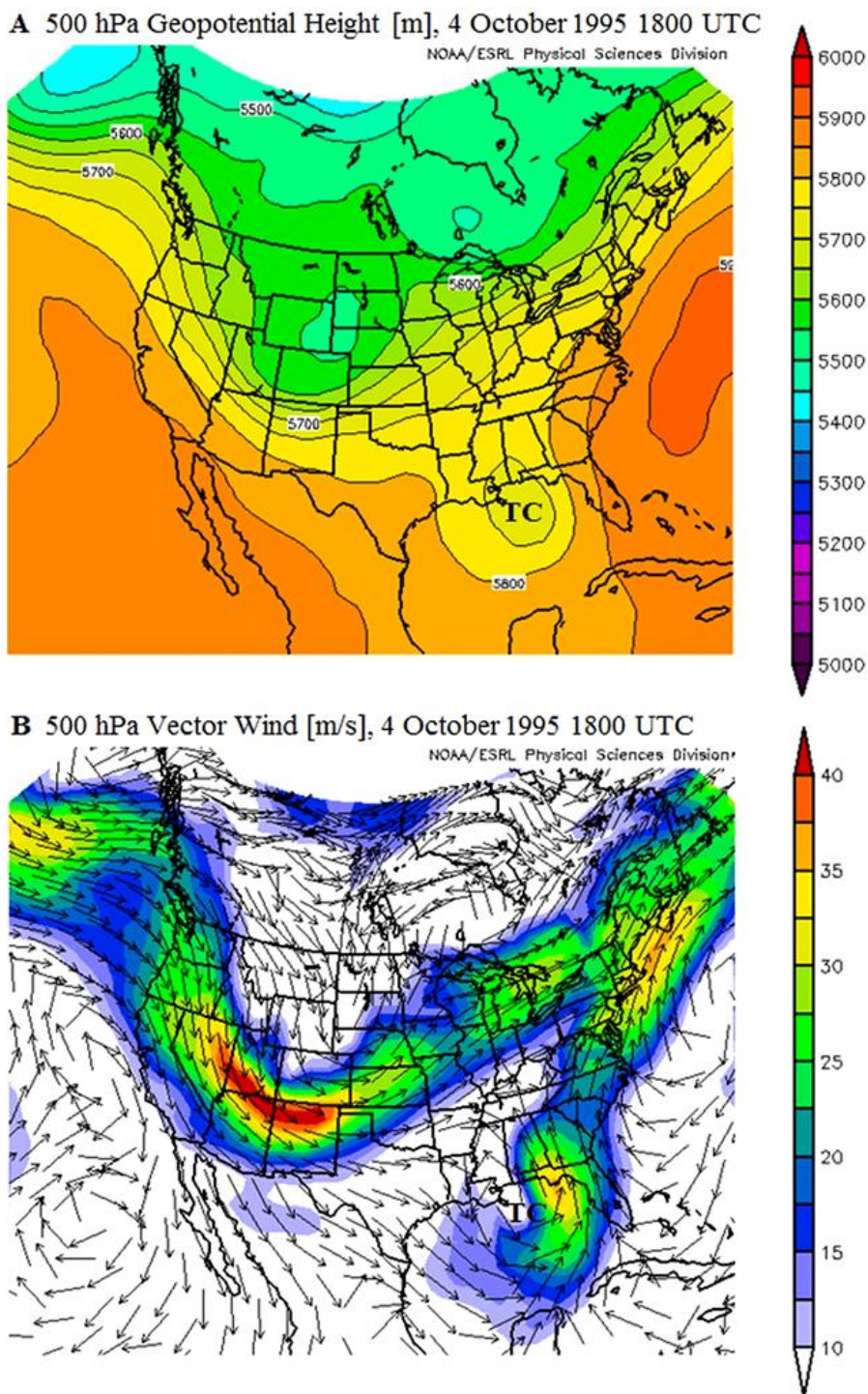


FIGURE 4.17. 500 hPa geopotential height (A) and vector wind (B) plots illustrating a synoptic environment characteristic of Pattern 2 (NCEP-NARR plots obtained from NOAA ESRL's Physical Science Division (NOAA (n. d.)). Note the TC embedded within the midlatitude westerly flow as a closed shortwave trough.

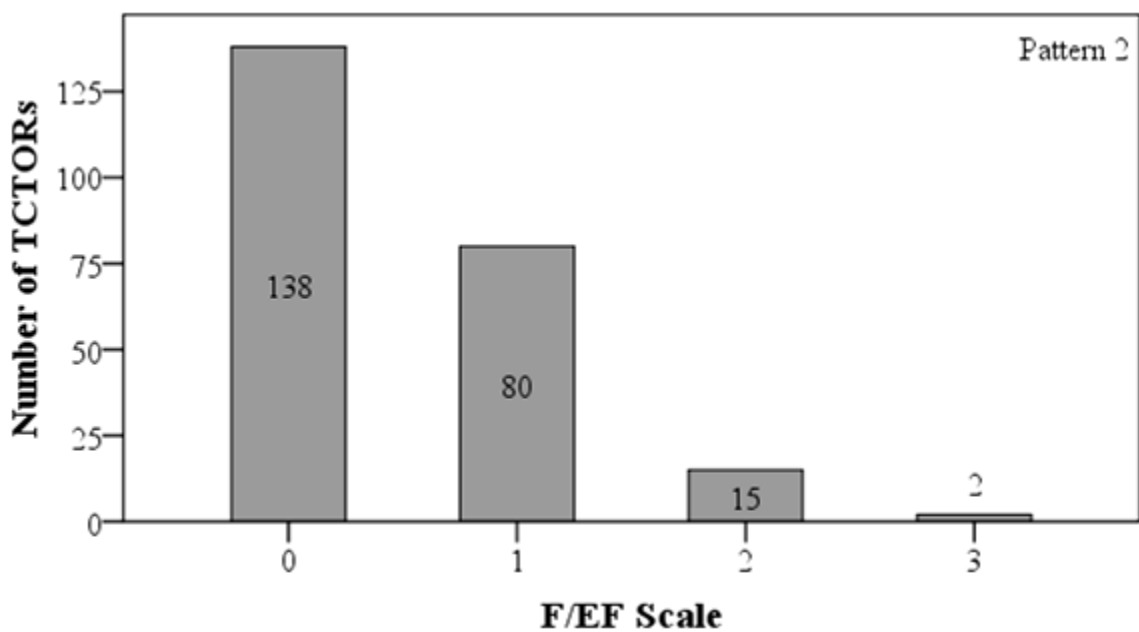


FIGURE 4.18. Pattern 2 TCTOR frequency distribution stratified by F/EF Scale.

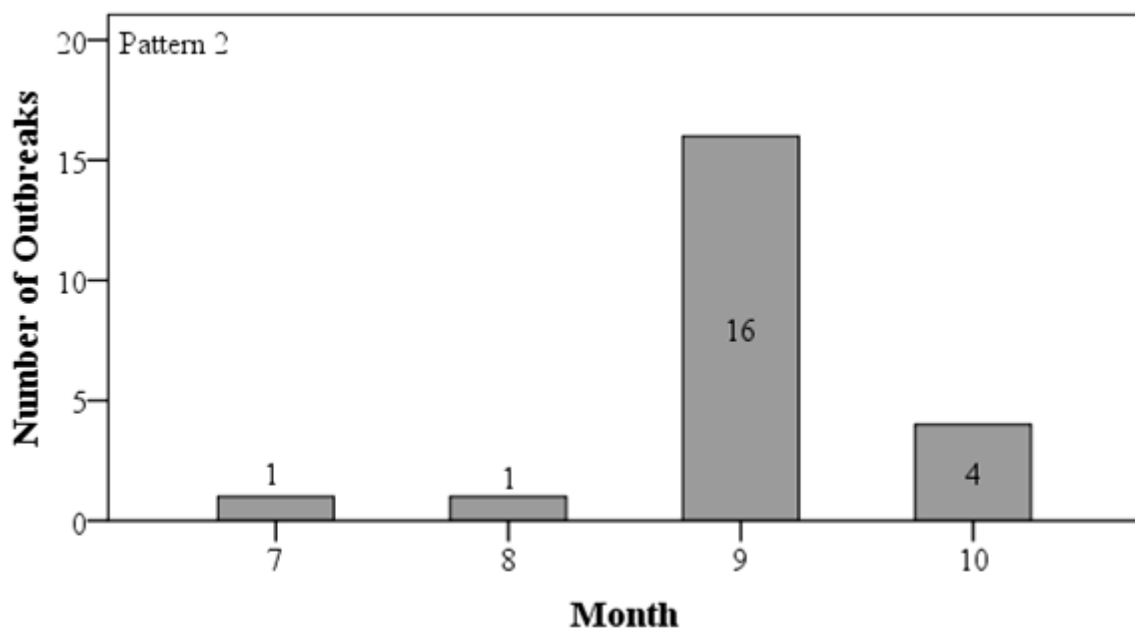


FIGURE 4.19. Pattern 2 TCTOR outbreak frequency distribution stratified by month.

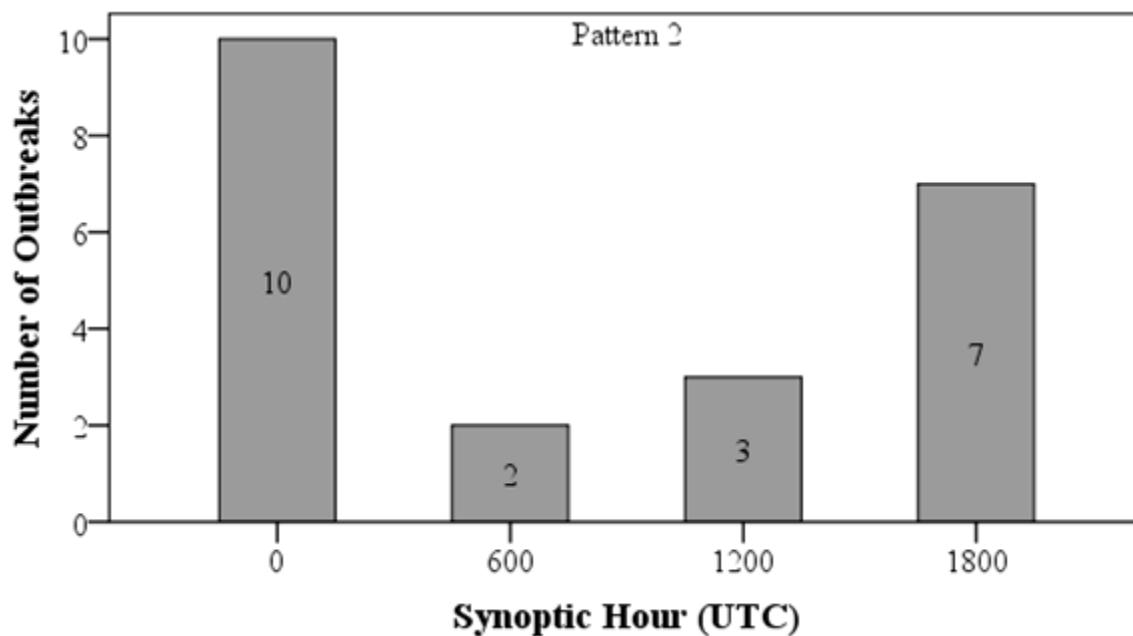


FIGURE 4.20. Pattern 2 TCTOR outbreak frequency distribution stratified by synoptic hour.

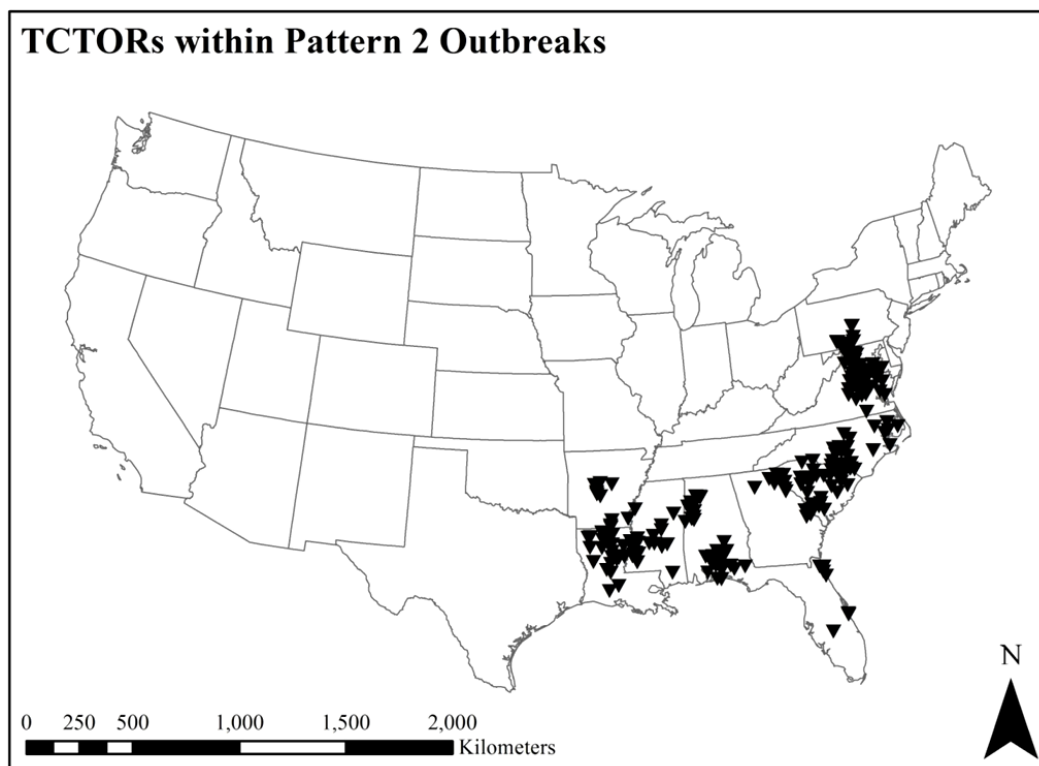


FIGURE 4.21. Spatial distribution of TCTORS within Pattern 2 outbreaks.

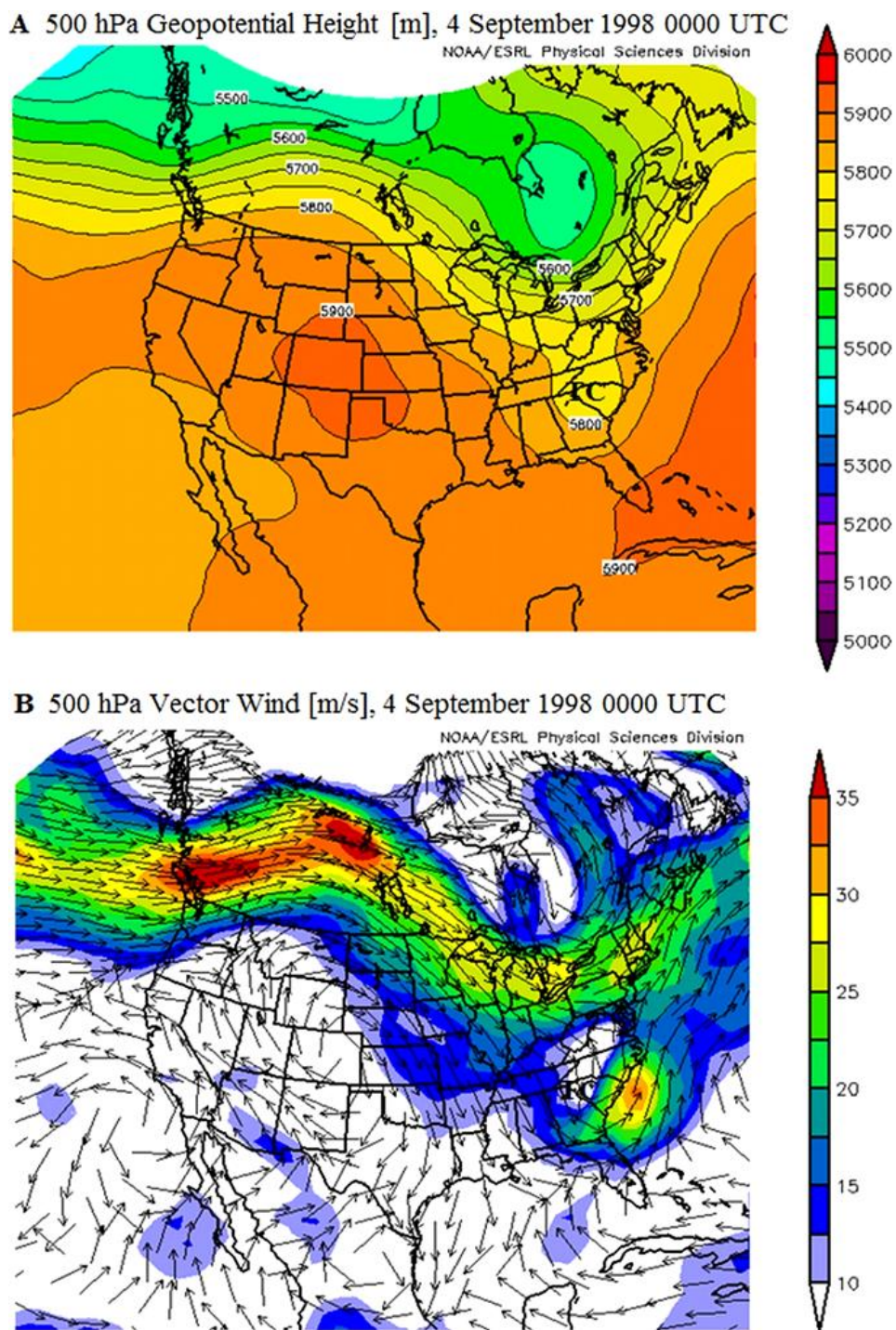


FIGURE 4.22. 500 hPa geopotential height (A) and vector wind (B) plots illustrating a synoptic environment characteristic of Pattern 3 (NCEP-NARR plots obtained from NOAA ESRL's Physical Science Division (NOAA (n. d.)). Note the TC embedded within the midlatitude westerly flow as an open short wave trough.

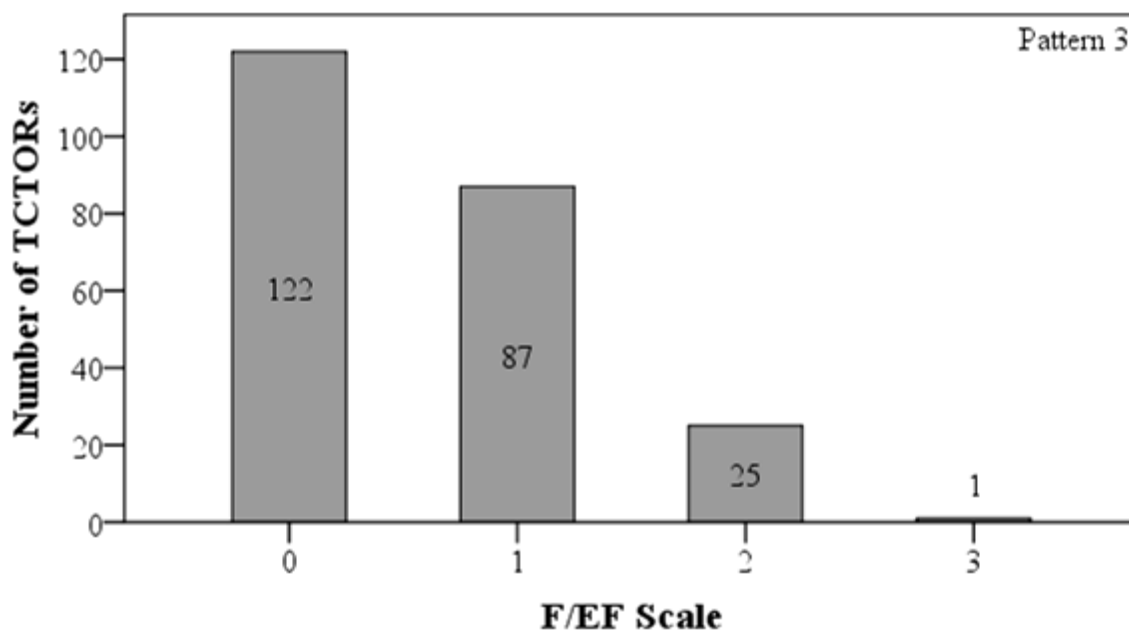


FIGURE 4.23. Pattern 3 TCTOR frequency distribution stratified by F/EF Scale.

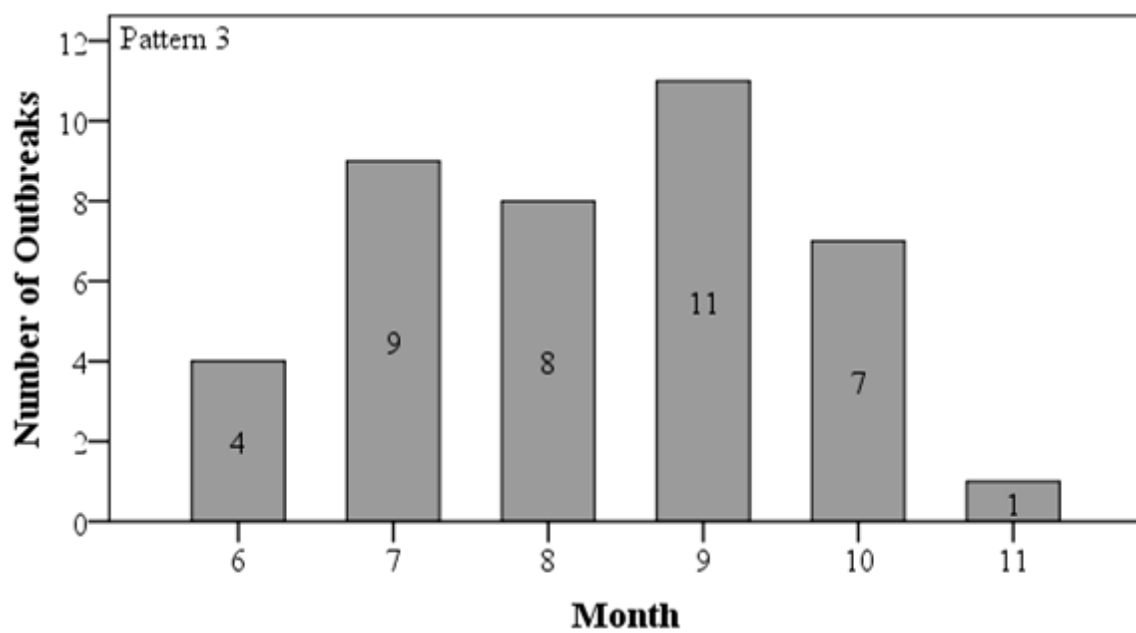


FIGURE 4.24. Pattern 3 TCTOR outbreak frequency distribution stratified by month.

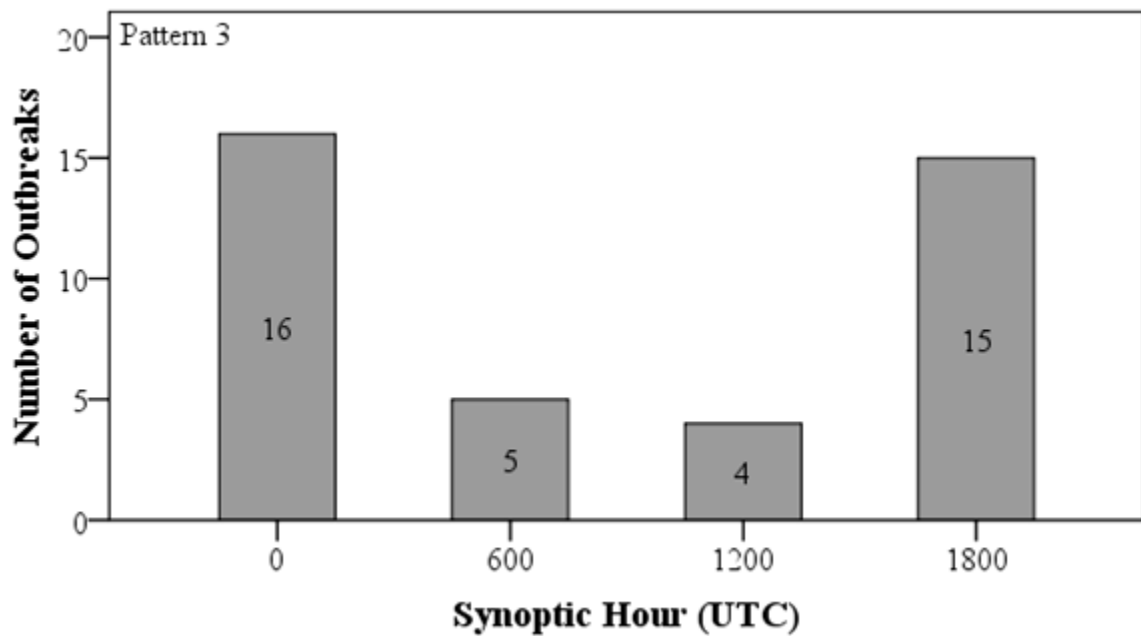


FIGURE 4.25. Pattern 3 TCTOR outbreak frequency distribution stratified by synoptic hour.

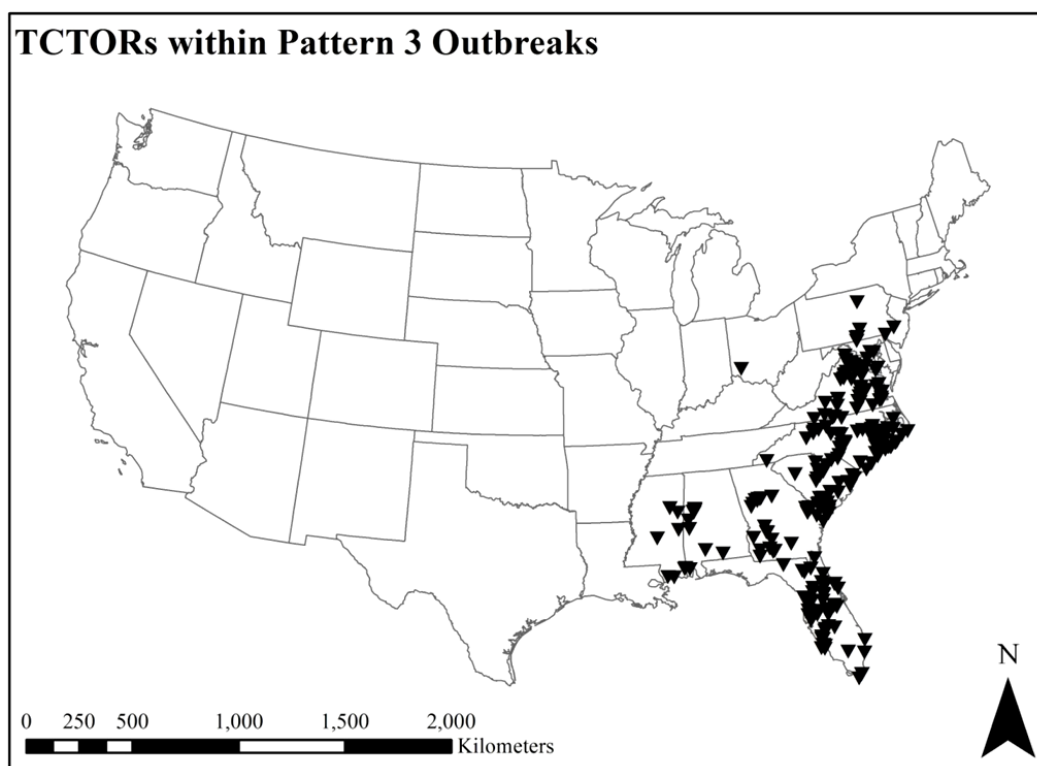


FIGURE 4.26. Spatial distribution of TCTORs within Pattern 3 outbreaks.

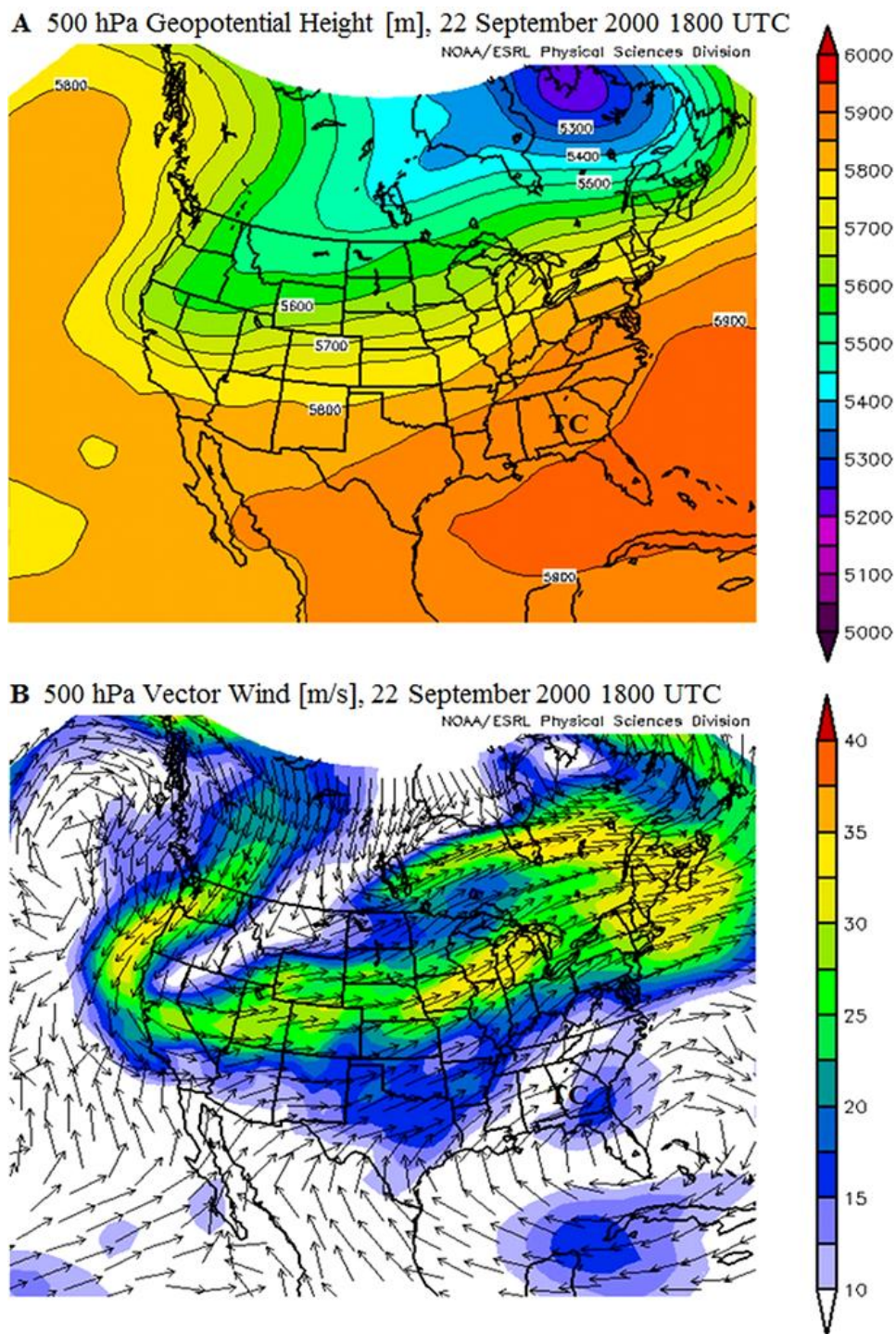


FIGURE 4.27. 500 hPa geopotential height (A) and vector wind (B) plots illustrating a synoptic environment characteristic of Pattern 4 (NCEP-NARR plots obtained from NOAA ESRL's Physical Science Division (NOAA (n. d.)). Note the TC without closed circulation embedded within the southwesterly flow of the subtropical ridge.

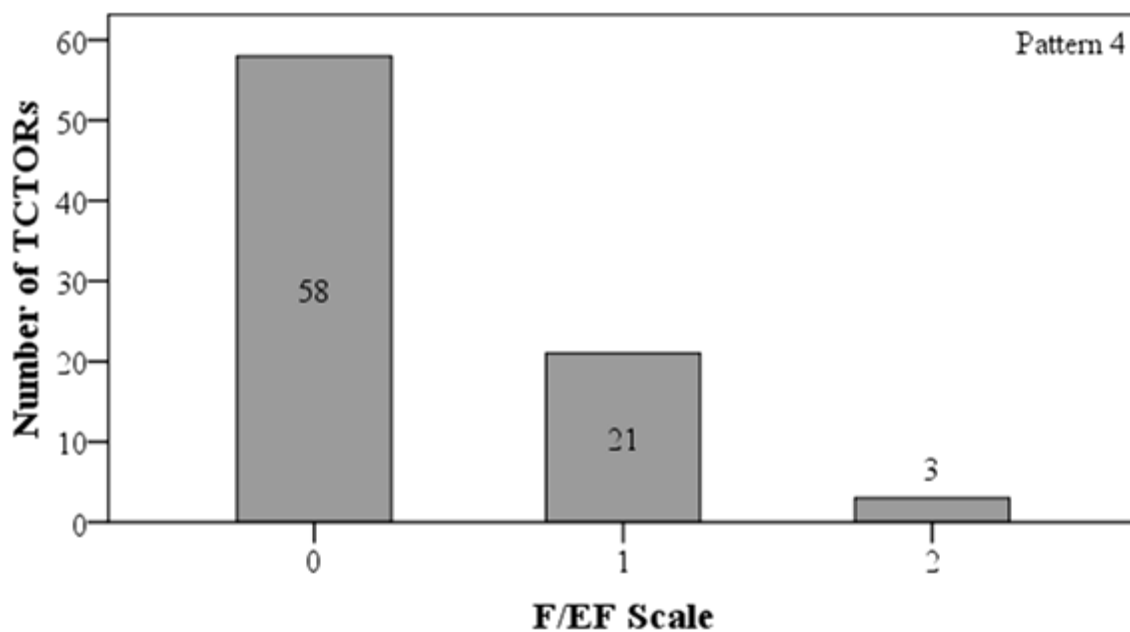


FIGURE 4.28. Pattern 4 TCTOR frequency distribution stratified by F/EF Scale.

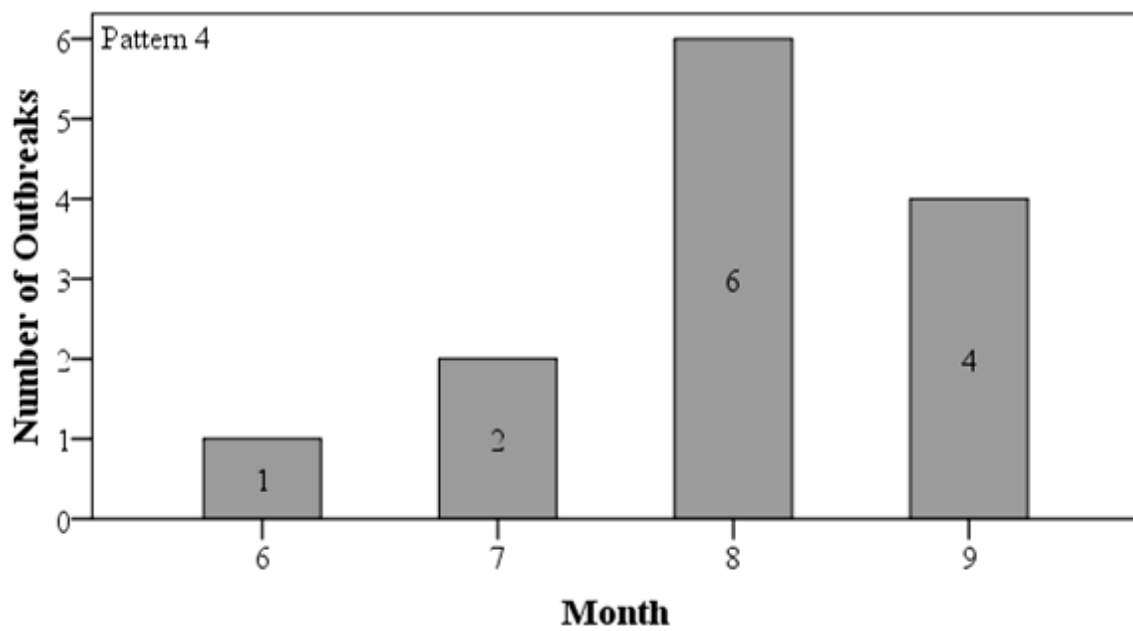


FIGURE 4.29. Pattern 4 TCTOR outbreak frequency distribution stratified by month.

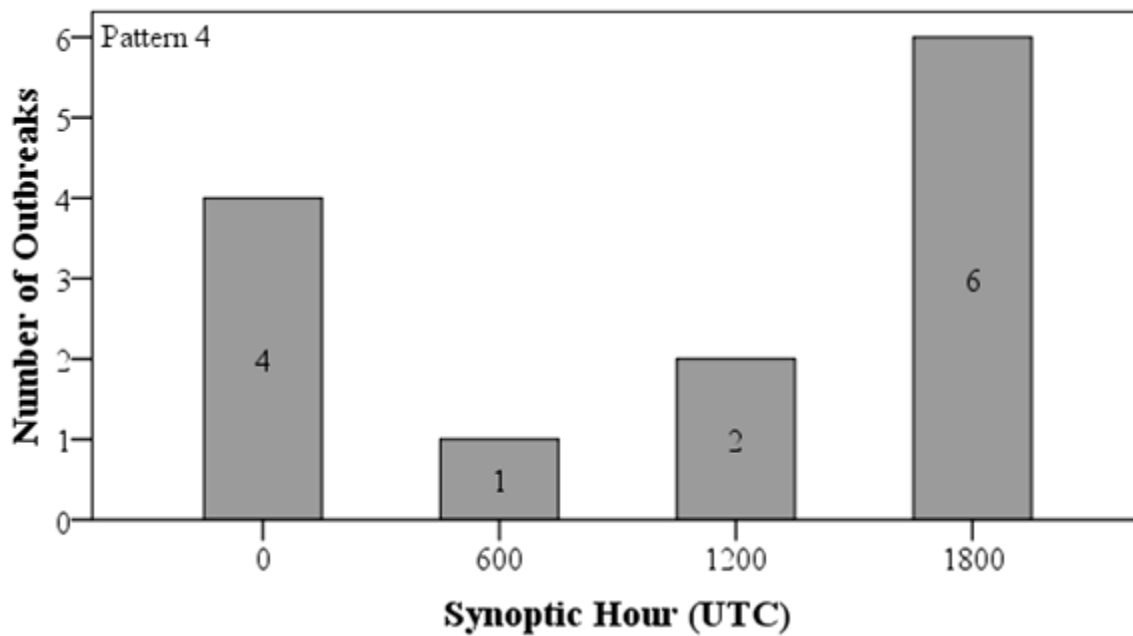


FIGURE 4.30. Pattern 4 TCTOR outbreak frequency distribution stratified by synoptic hour.

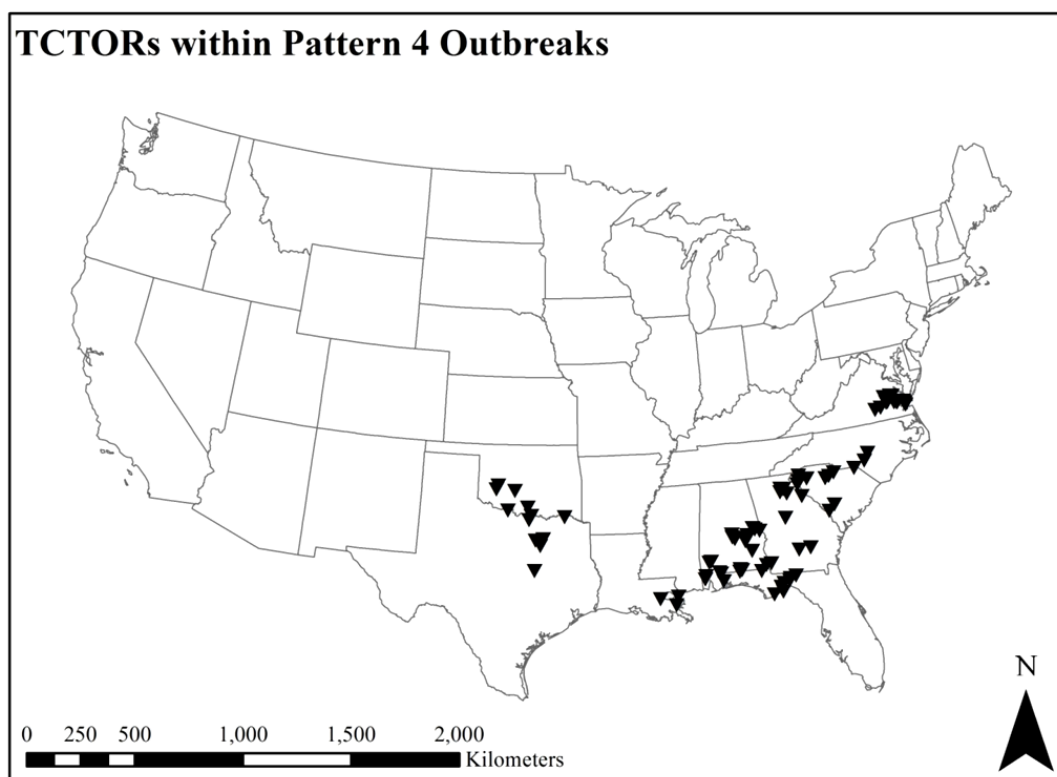


FIGURE 4.31. Spatial distribution of TCTORs within Pattern 4 outbreaks.

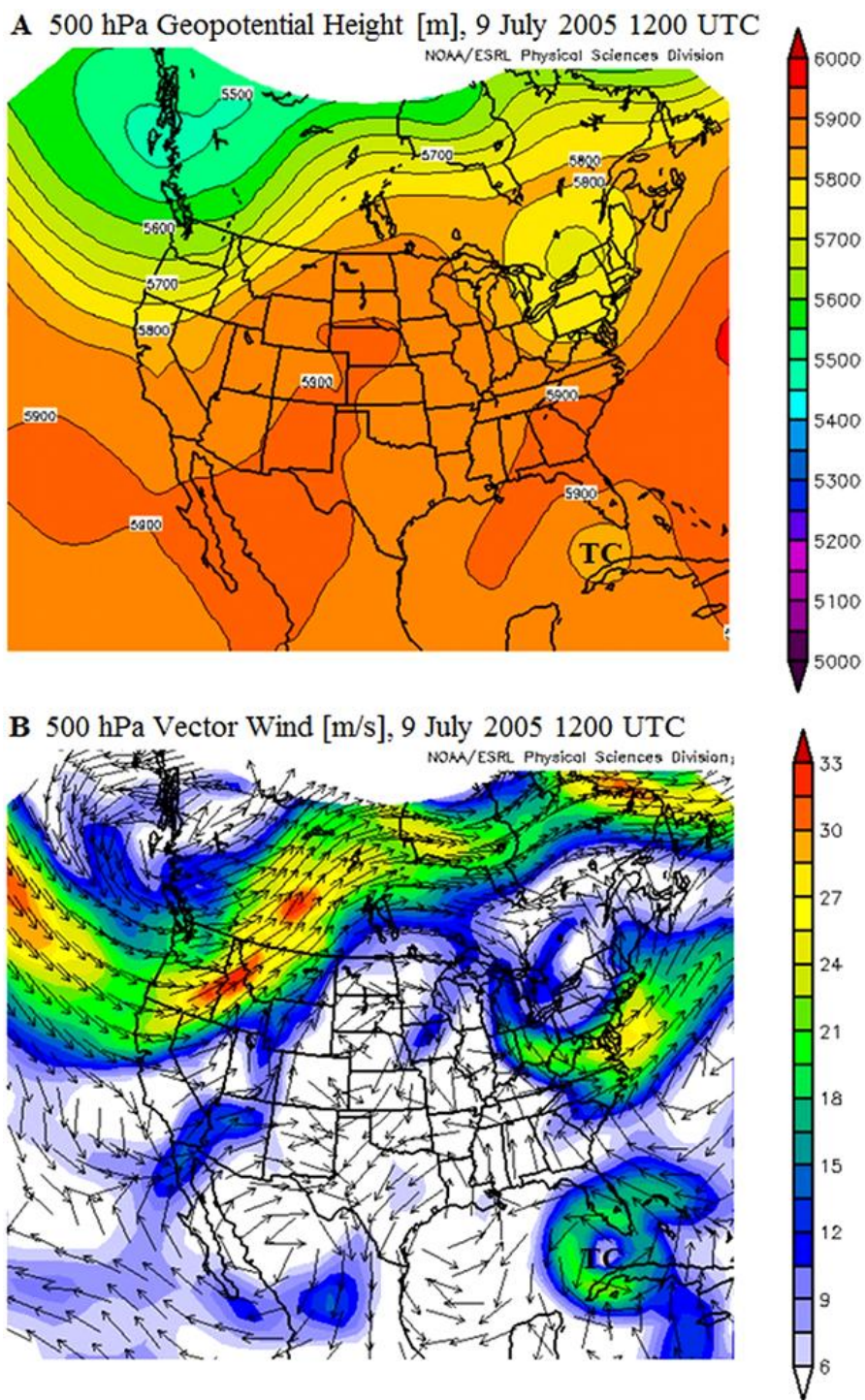


FIGURE 4.32. 500 hPa geopotential height (A) and vector wind (B) plots illustrating a synoptic environment characteristic of Pattern 5 (NCEP-NARR plots obtained from NOAA ESRL's Physical Science Division (NOAA (n. d.)). Note the closed TC circulation cut-off from the midlatitude westerly flow to the north by a region of high pressure.

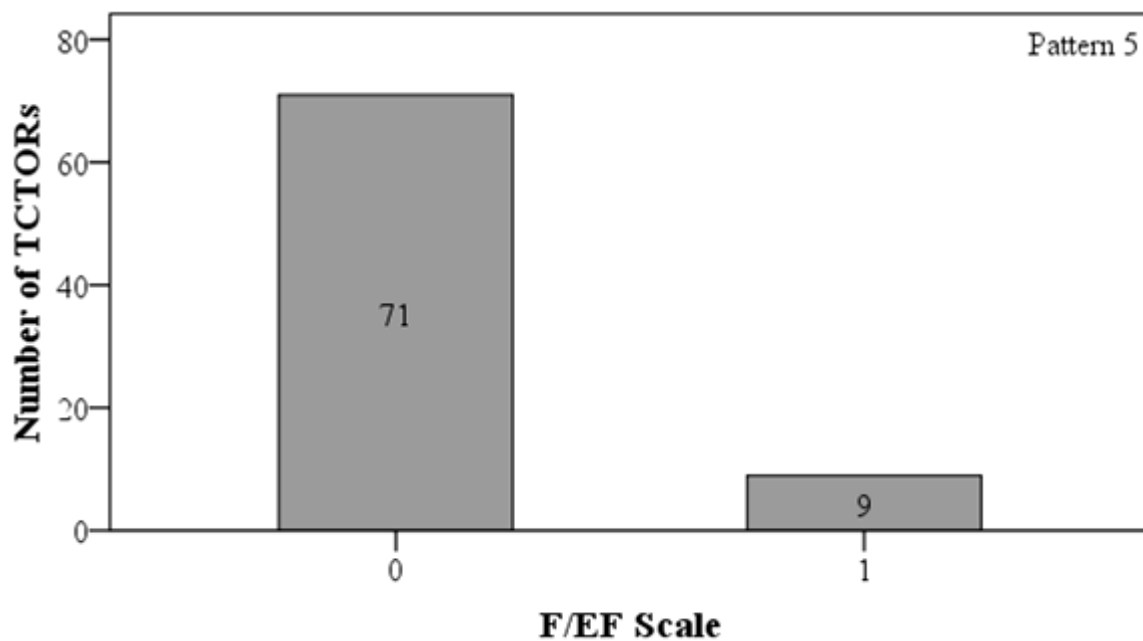


FIGURE 4.33. Pattern 5 TCTOR frequency distribution stratified by F/EF Scale.

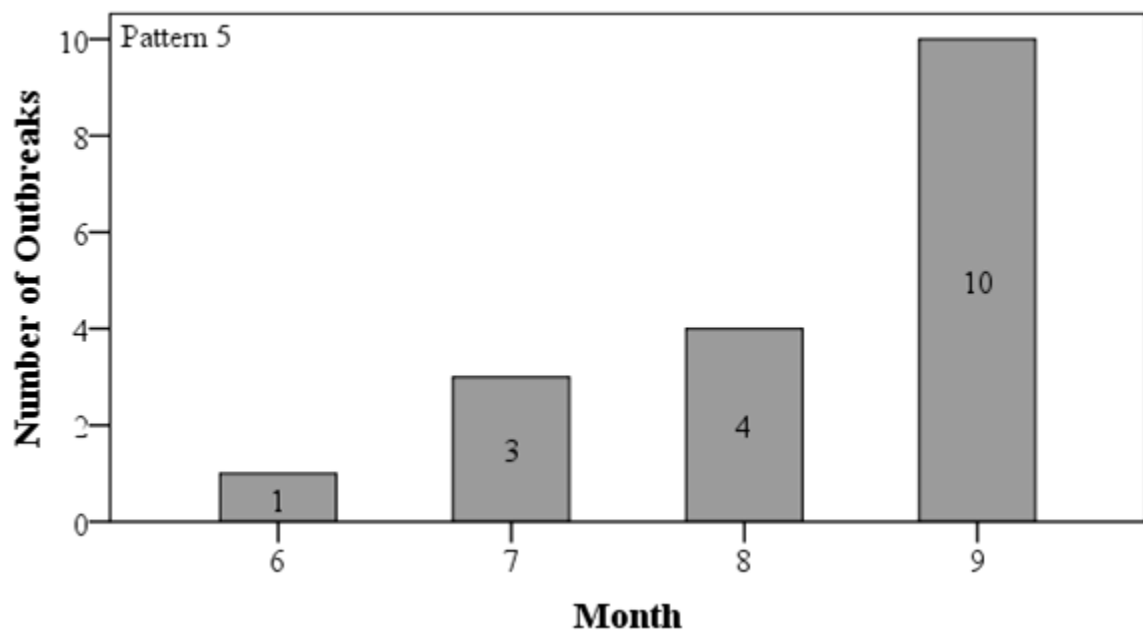


FIGURE 4.34. Pattern 5 TCTOR outbreak frequency distribution stratified by month.

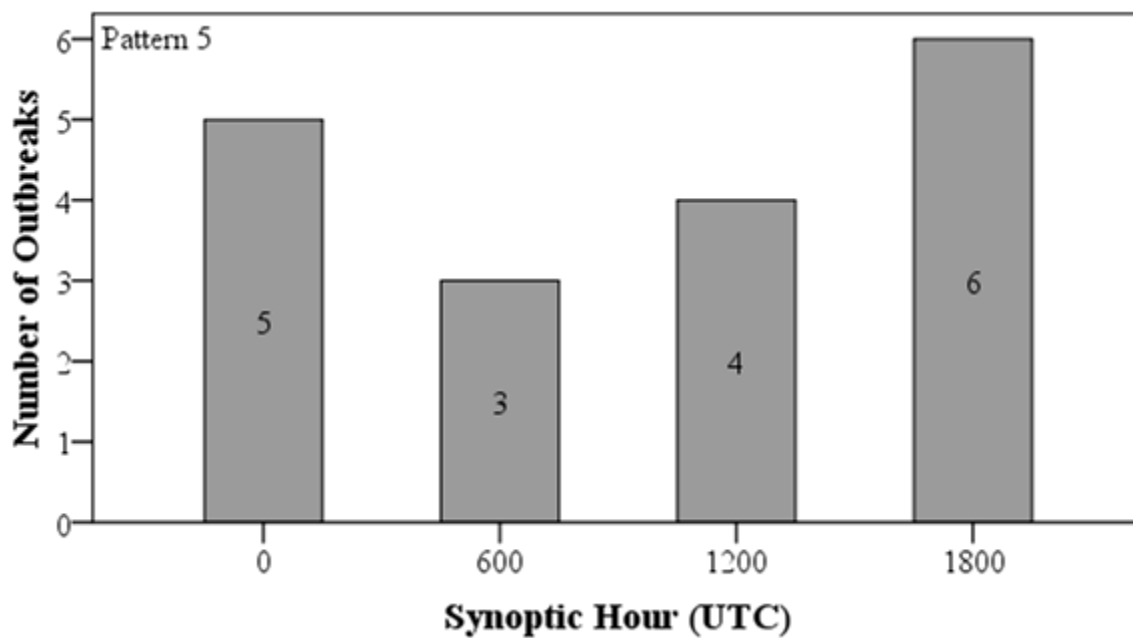


FIGURE 4.35. Pattern 5 TCTOR outbreak frequency distribution stratified by synoptic hour.

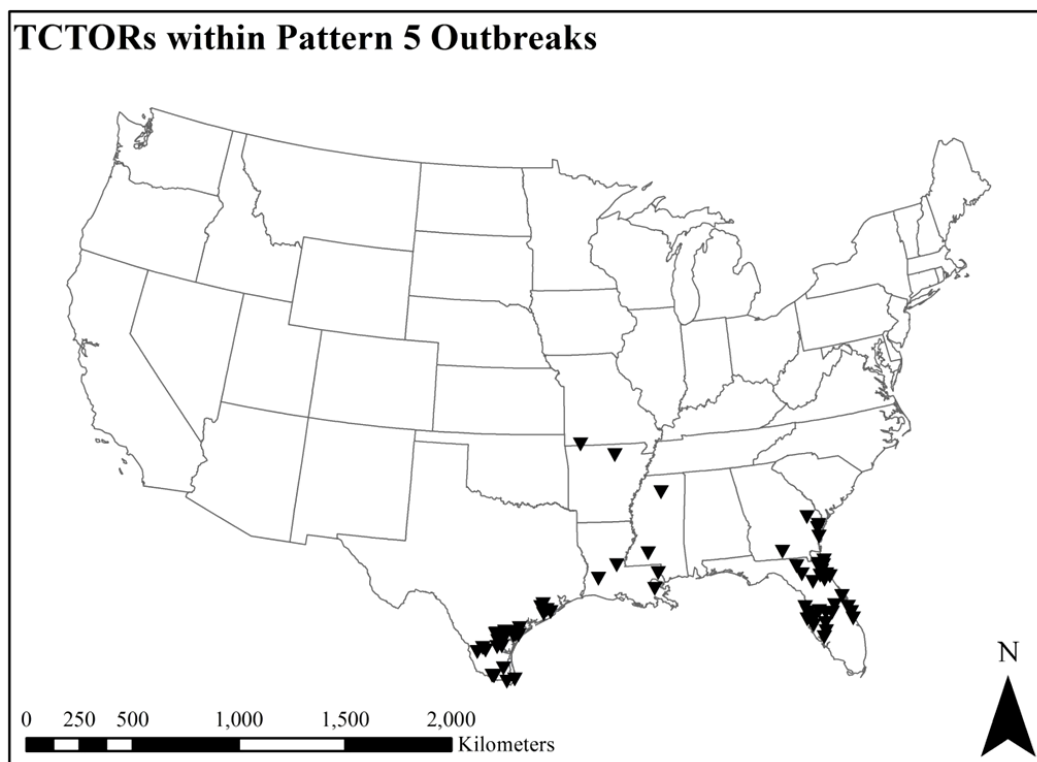


FIGURE 4.36. Spatial distribution of TCTORs within Pattern 5 outbreaks.

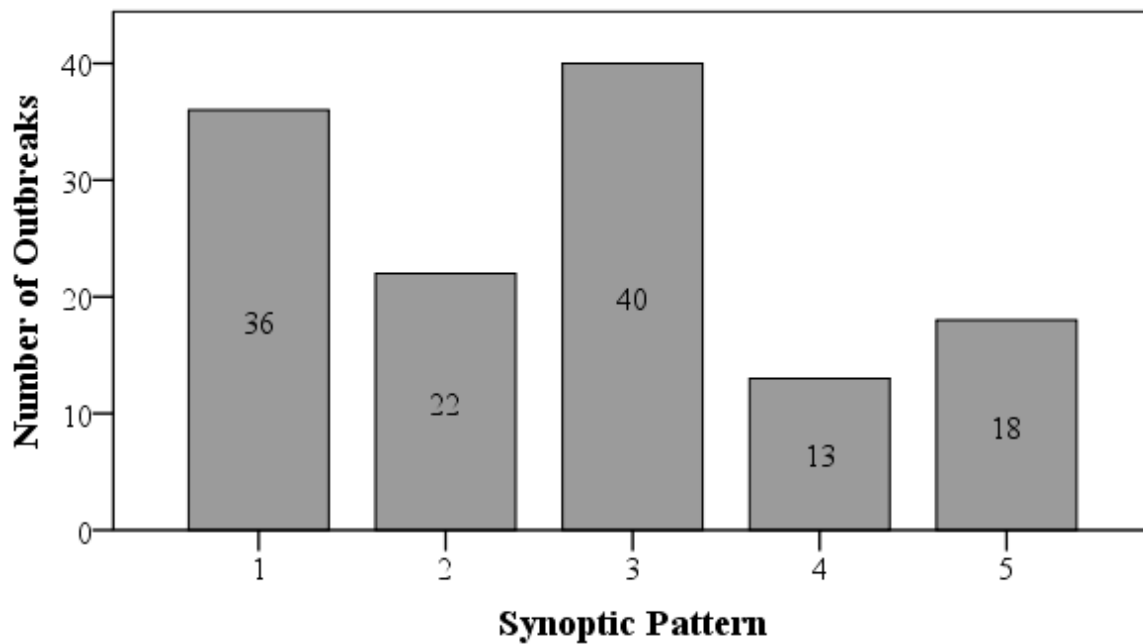


FIGURE 4.37. TCTOR outbreak frequency distribution stratified by synoptic pattern.

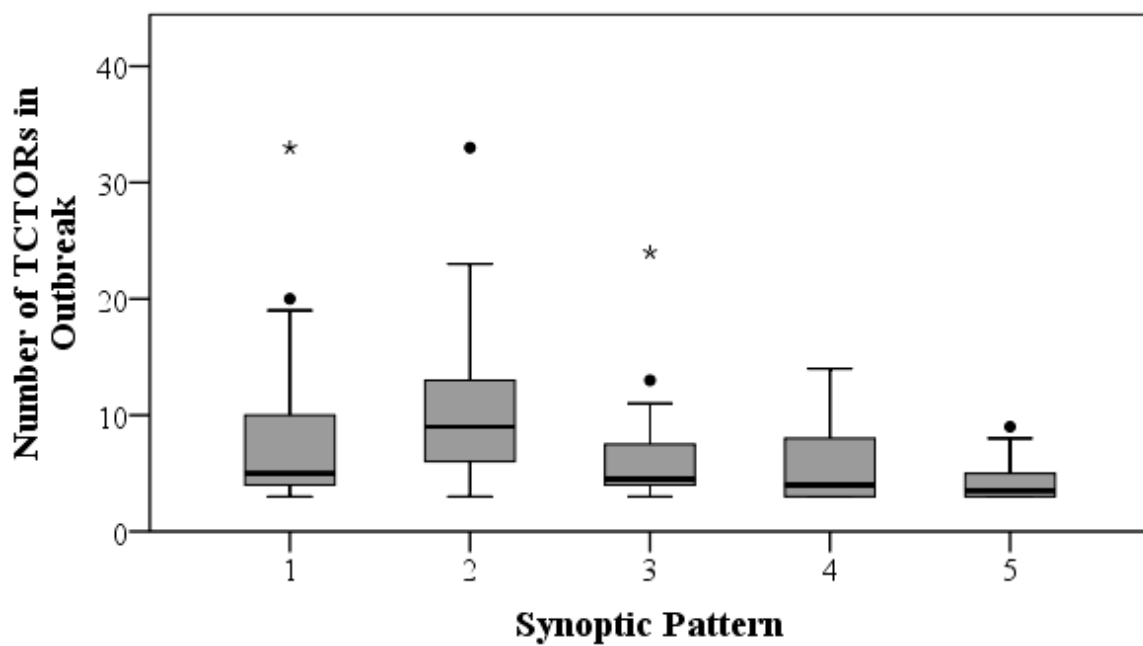


FIGURE 4.38. Boxplots illustrating the distribution of TCTOR outbreak severity, stratified by synoptic pattern.

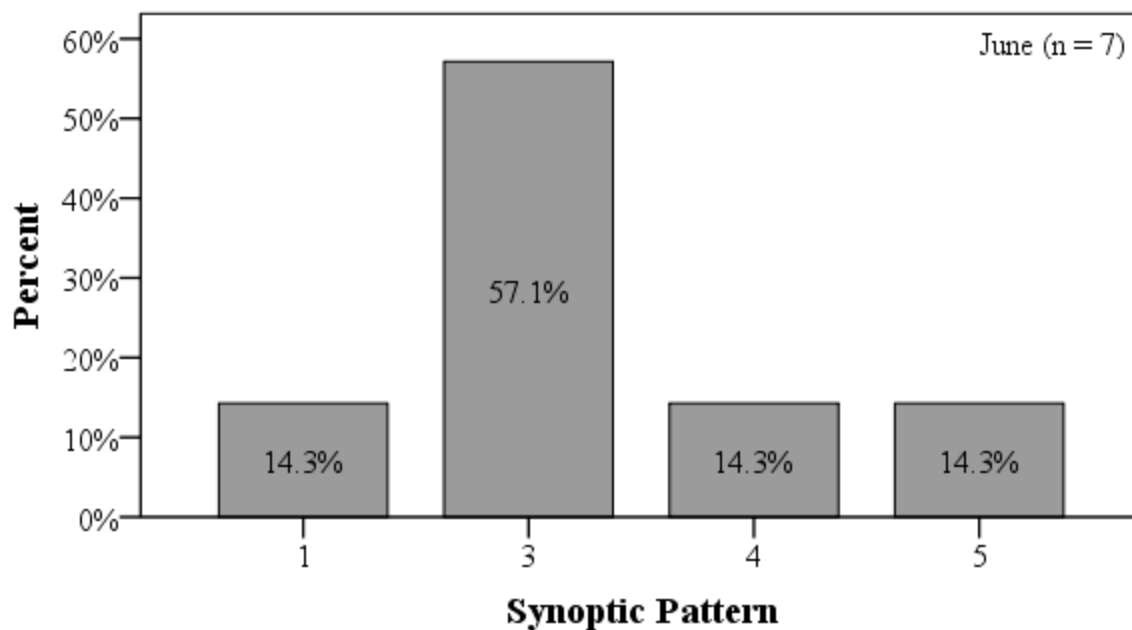


FIGURE 4.39. Relative frequency distribution of June TCTOR outbreaks stratified by synoptic pattern. No Pattern 2 outbreaks occurred in June over the period of record.

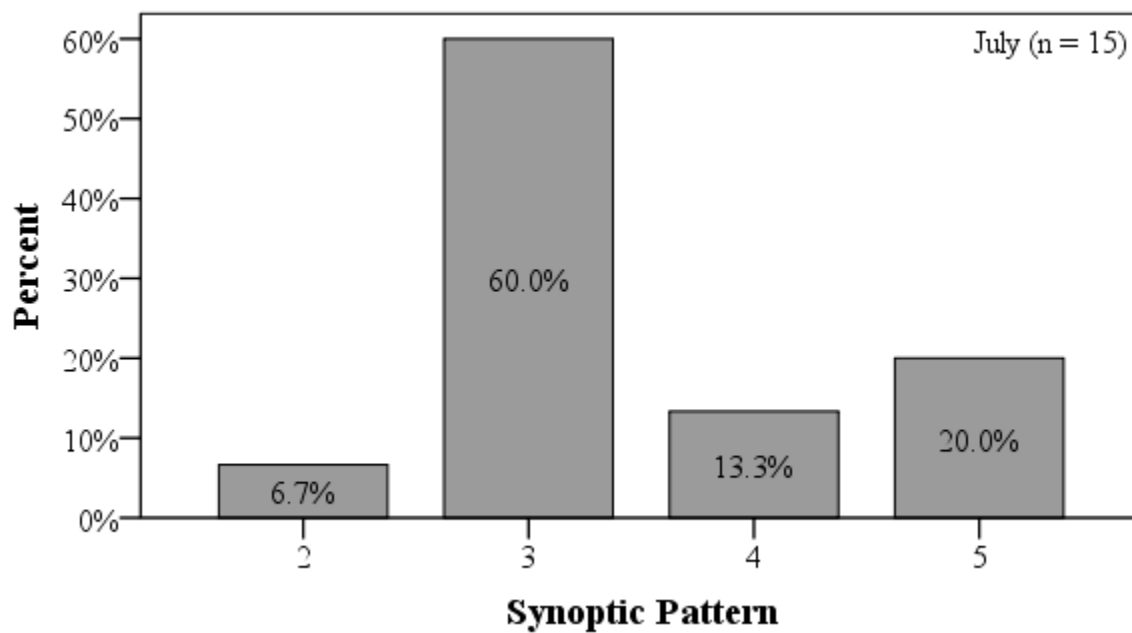


FIGURE 4.40. Relative frequency distribution of July TCTOR outbreaks stratified by synoptic pattern. No Pattern 1 outbreaks occurred in July over the period of record.

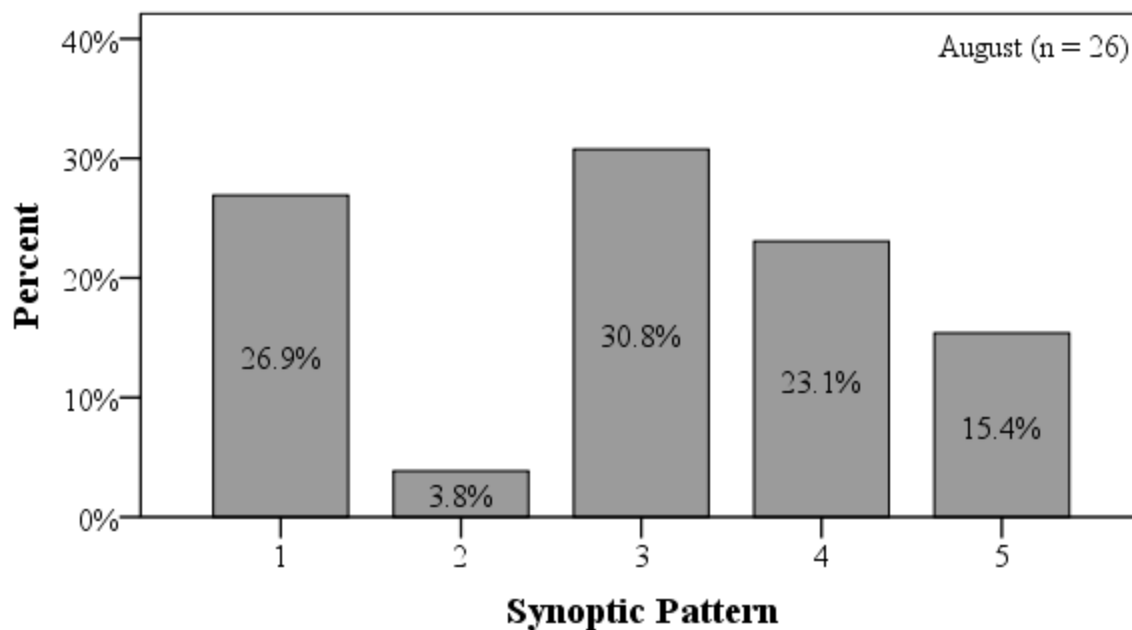


FIGURE 4.41. Relative frequency distribution of August TCTOR outbreaks stratified by synoptic pattern.

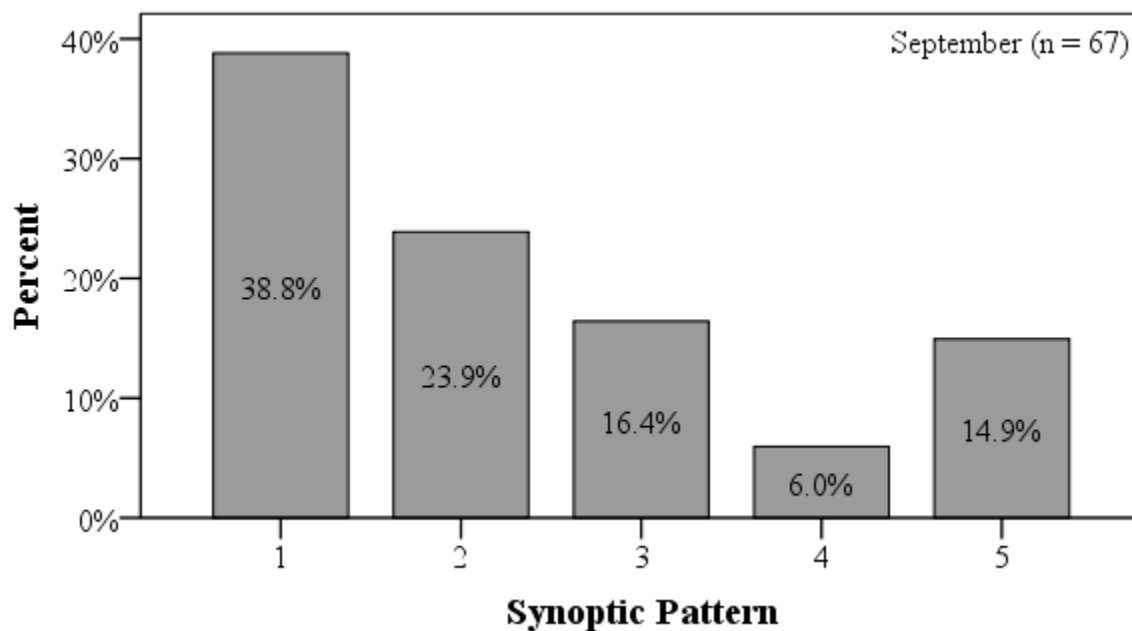


FIGURE 4.42. Relative frequency distribution of September TCTOR outbreaks stratified by synoptic pattern.

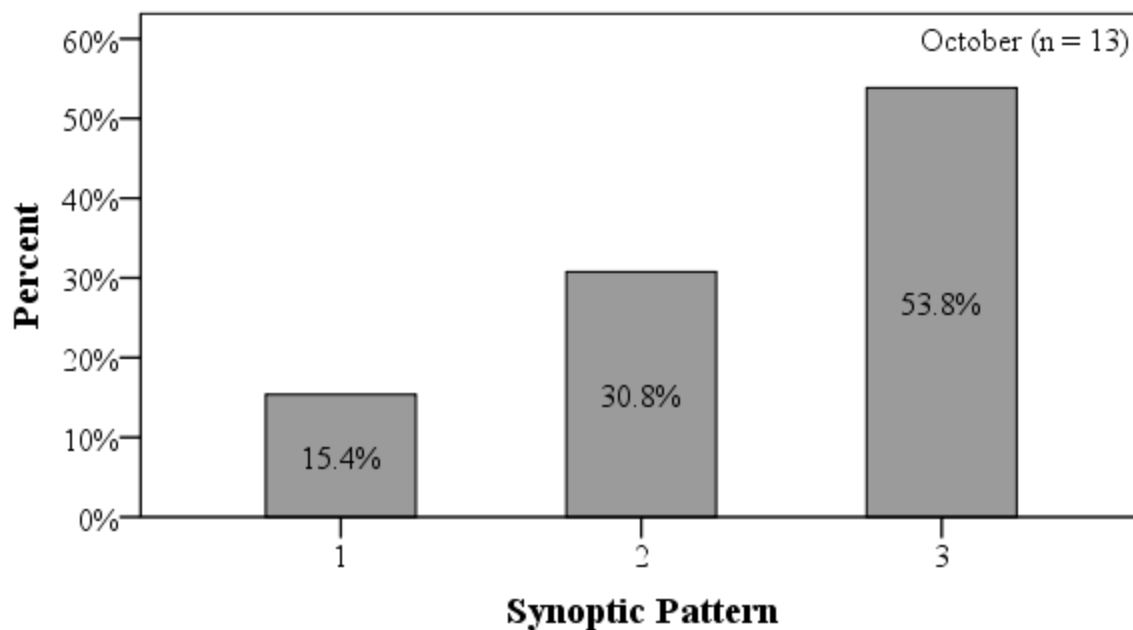


FIGURE 4.43. Relative frequency distribution of October TCTOR outbreaks stratified by synoptic pattern. No Pattern 4 or 5 outbreaks occurred in October over the period of record.

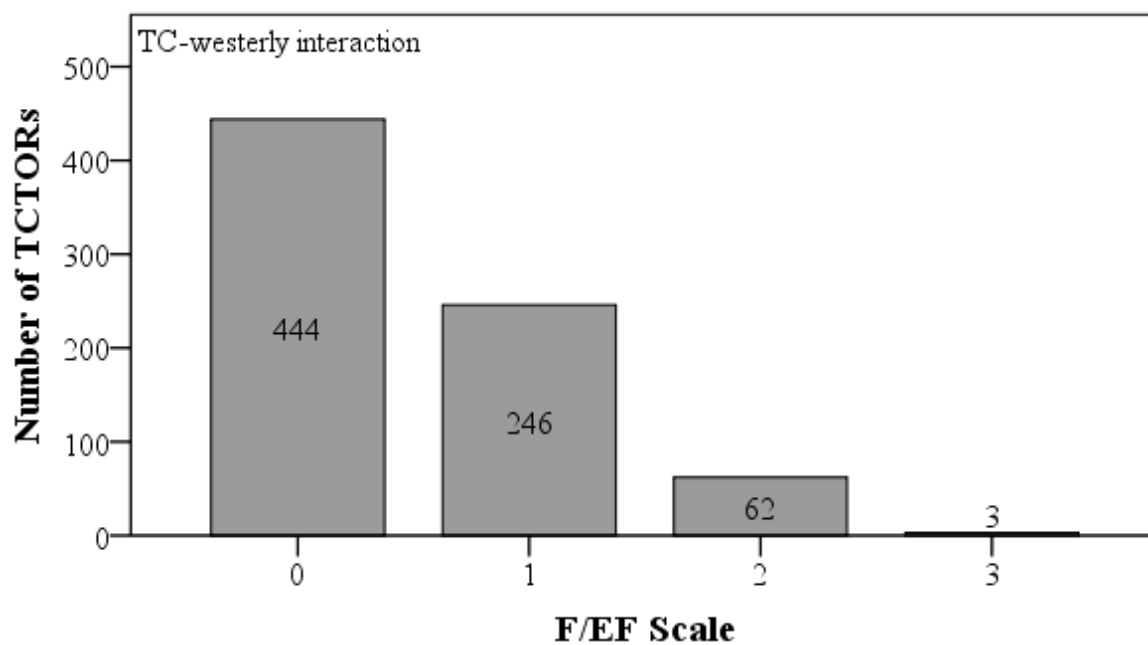


FIGURE 4.44. TCTOR frequency distribution stratified by F/EF Scale for cases exhibiting TC-westerly interaction (Patterns 1, 2, and 3).

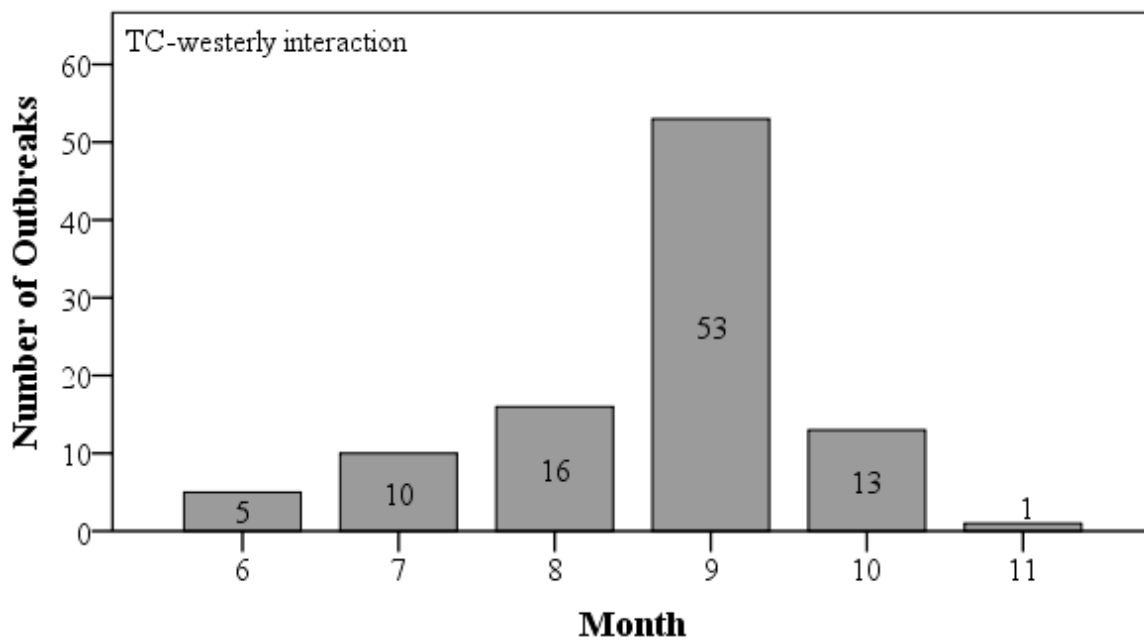


FIGURE 4.45. TCTOR outbreak frequency distribution stratified by month for cases exhibiting TC-westerly interaction (Patterns 1, 2, and 3).

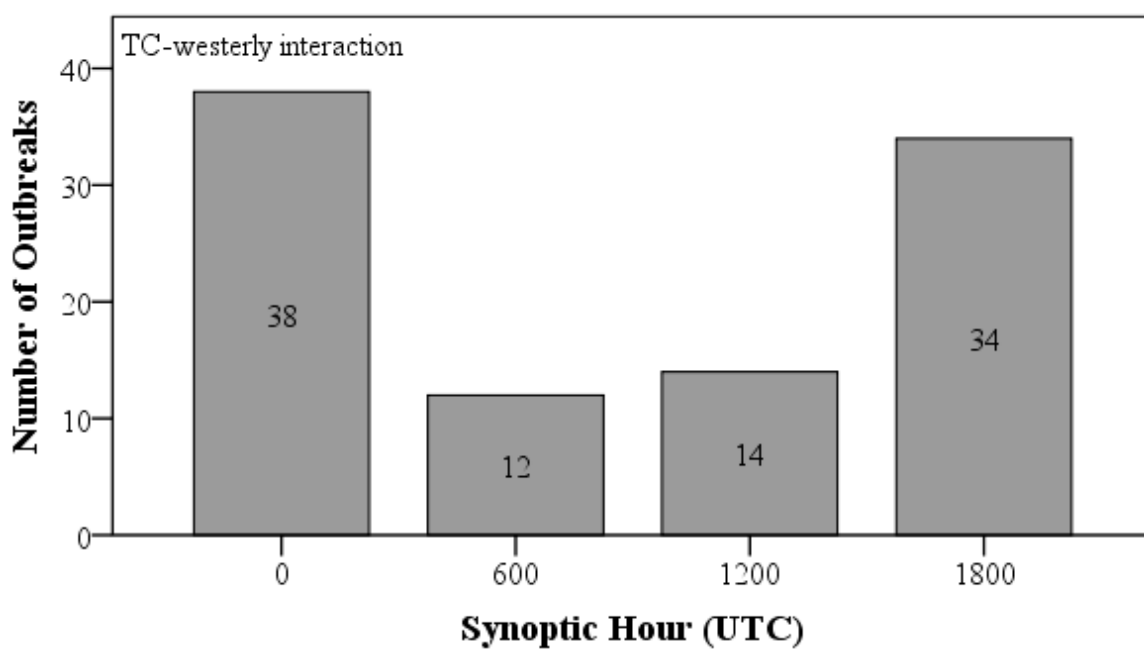


FIGURE 4.46. TCTOR outbreak frequency distribution stratified by synoptic hour for cases exhibiting TC-westerly interaction (Patterns 1, 2, and 3).

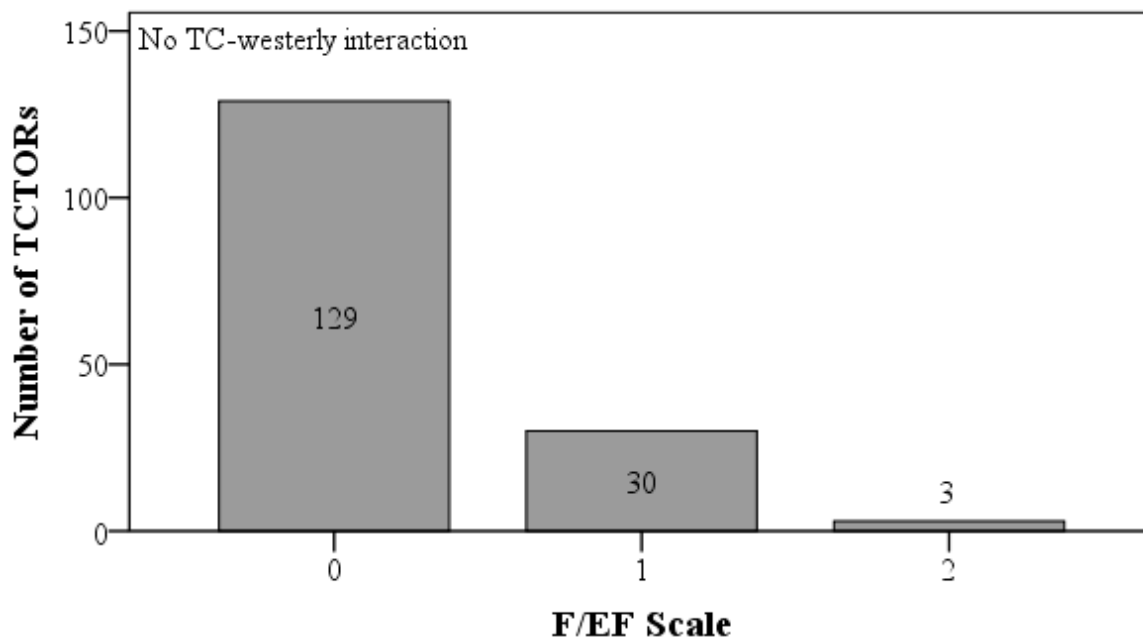


FIGURE 4.47. TCTOR frequency distribution stratified by F/EF Scale for cases exhibiting no TC-westerly interaction (Patterns 4 and 5).

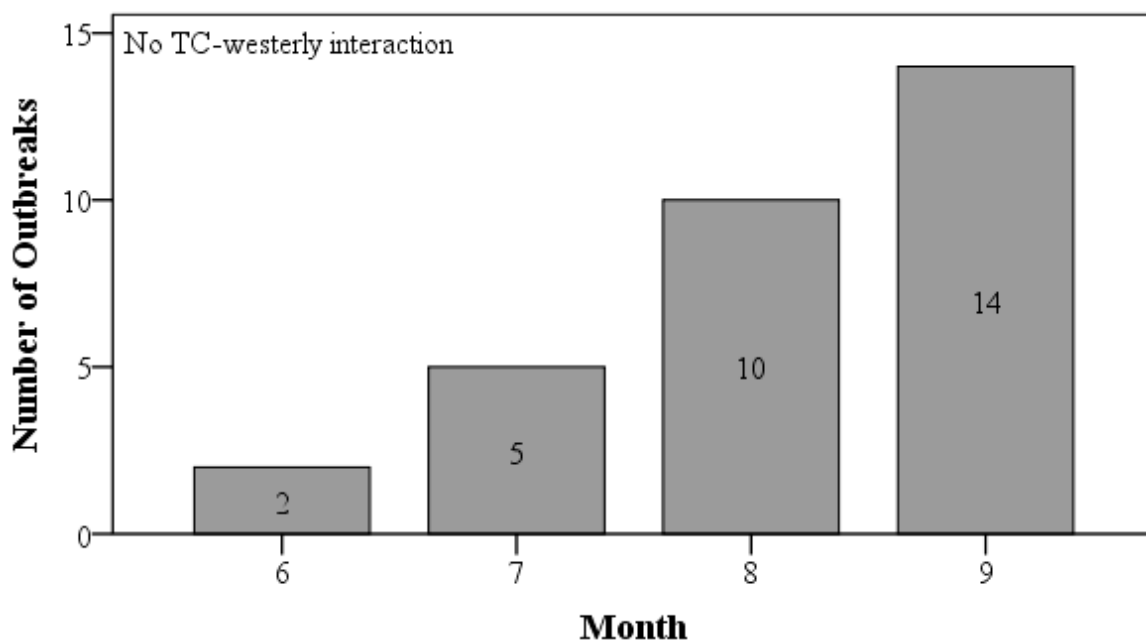


FIGURE 4.48. TCTOR outbreak frequency distribution stratified by month for cases exhibiting no TC-westerly interaction (Patterns 4 and 5).

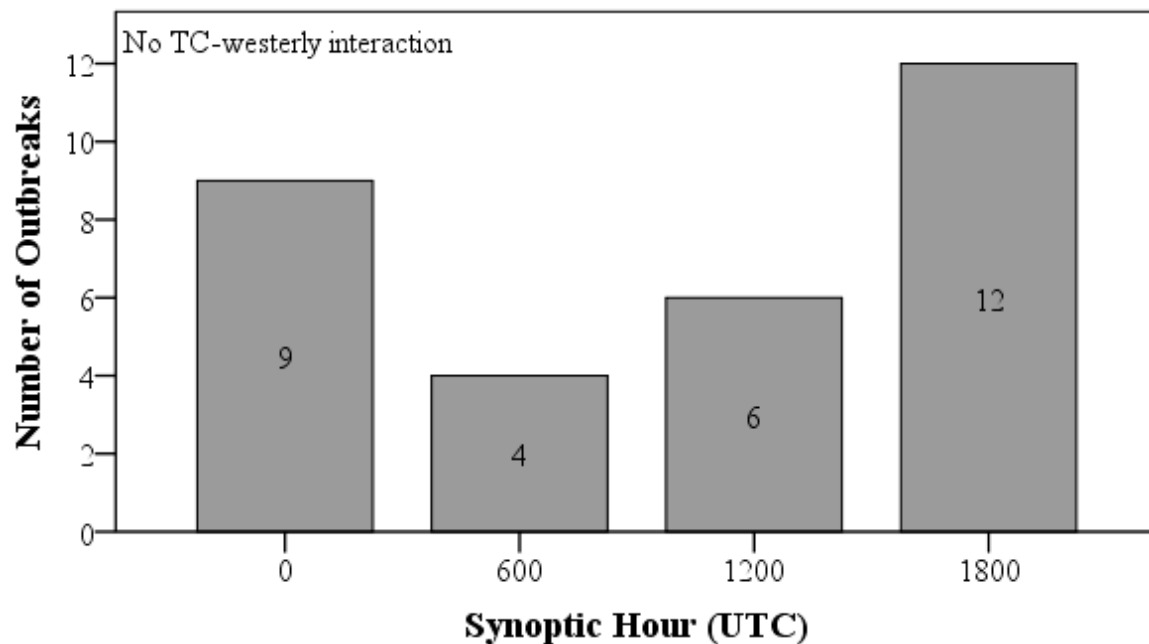


FIGURE 4.49. TCTOR outbreak frequency distribution stratified by synoptic hour for cases exhibiting no TC-westerly interaction (Patterns 4 and 5).

CHAPTER V

DISCUSSION OF RESULTS

5.1 Tropical Cyclone Tornado Outbreaks: Definition Concerns

The results of this study suggest that TCTORs cluster over multiple temporal and spatial scales. This, in turn, suggests that different definitions, utilizing different TCTOR frequency thresholds and temporal and spatial parameters, also could be used to identify and analyze TCTOR outbreaks. Sixty-eight percent of the outbreaks identified in this study, for example, occurred in a six hour window adjacent to another outbreak. Multiple temporal strings of outbreaks occurred, ranging from two to six consecutive outbreaks. All of TC Rita's (2005) six outbreaks occurred in consecutive six hour windows from 24 September 2005 at 1800 UTC to 26 September 2005 at 0000 UTC. Consecutive outbreaks such as these could be considered one longer-lasting outbreak with a longer temporal parameter. The exploration of TCTOR outbreaks using multiple temporal scales, and the development of a TCTOR outbreak classification scheme that accounts for outbreaks with different temporal scales, would be an insightful addition to the current single-definition approach.

In addition to the observed temporal strings, the spatial overlap observed with many TCTOR outbreaks (see Figure 4.1A, B, and C) also suggests that some of the outbreaks identified in this study may be considered to be a segment of a larger outbreak, especially those outbreaks that occurred in consecutive temporal windows. Post hoc

visual examination of the spatial distribution of the outbreaks revealed that they tend to conform to particular spatial configurations. Similar to the aforementioned multi temporal scale approach, spatial dispersion and configuration can be taken into account when developing an outbreak classification scheme that not only considers outbreaks over multiple temporal scales but also over multiple spatial scales and configurations. The development of a posteriori definition based on a data-derived spatio-temporal classification scheme may reduce the bias that accompanies subjective definitions developed a priori.

5.2 Tropical Cyclone Tornado Outbreak Climatology

The results of this study are generally consistent with those of previous TCTOR climatology studies. Previous studies that examined individual TCTORS have reported a climatological peak in September (Smith 1965; Novlan and Gray 1974; Moore and Dixon 2011a). This study, likewise, found that the majority of TCTOR outbreaks occurred in September. Individual TCTORS also have been shown to occur most frequently during afternoon and evening hours of the day (Novlan and Gray 1974; Gentry 1983; McCaul 1991; Schultz and Cecil 2009; Edwards 2010a; Moore and Dixon 2011a). TCTOR outbreaks were similarly shown to be most common during the 1800 UTC and 0000 UTC windows, which span local afternoon, evening, and night hours. TCTOR outbreaks also were shown to be most common after their associated TC landfall, especially in the forty hour period directly after landfall in which the most severe outbreaks tended to cluster (see Figure 4.9), which is in general agreement with the landfall-relative temporal trend reported by McCaul (1991), Schultz and Cecil (2009), and Moore and Dixon (2011a).

The examination of outbreaks rather than individual TCTORs has provided a unique perspective to complement these previous findings. In essence, outbreaks are temporal periods when TCs are producing TCTORs at a relatively high rate, and identifying when outbreaks are most common allows one to ascertain when TCs are most likely to produce a relatively large number of TCTORs. As an example, consider the diurnal distribution of TCTOR outbreaks. An afternoon or evening climatological maximum indicates that TCTORs have occurred most often during these hours, but there also is the possibility that this maximum is induced by a single or a few extreme outbreaks. By examining the frequency distribution of outbreaks, this study has verified that TCs produce TCTORs at a relatively high rate during local afternoon, evening, and night hours. The relatively high frequency of TCTOR outbreaks during afternoon hours supports the previously noted importance of surface heating-induced buoyant forcing (e.g., Schultz and Cecil 2009; Edwards 2010a), especially when combined with mid-level dry air intrusion (McCaul 1991; Curtis 2004). However, a diurnal observation bias cannot be ruled out as a potential contributing factor (McCaul 1991).

The spatial distribution of outbreak mean centers within the TC environment is consistent with that reported by previous climatological studies (e.g., McCaul 1991; Schultz and Cecil 2009; Edwards 2010a). In addition to this corroboration, subjective examination of the spatial distribution of individual outbreaks revealed that TCTOR outbreaks tend to occur in somewhat distinct configurations: linear, single-cluster, multi-clustered, and dispersed. The observed linear, single-cluster, and multi-cluster configurations are particularly noteworthy because they represent TCTOR outbreaks that are clustered, both temporally and spatially. As a result, these outbreaks are particularly

hazardous to life and property. The dispersed configuration represents outbreaks that are temporally clustered but have spatially-isolated TCTORs.

Caveats must be kept in mind when considering the identified spatial configurations, primarily concerning the subjective and descriptive nature of the analysis. One caveat is related to the cartographic scale at which the visual analysis was conducted. This classification is based on plots at a scale of 1:19,500,000. Re-examination and classification at a smaller or larger scale would likely result in a different classification for several outbreaks and perhaps the identification of configurations not identified at the current scale. The linear outbreak in Fig. 4.11A, for instance, appears as a relatively broad linear swath of TCTORs at this scale but examination at a larger scale reveals multiple linear outbreaks, as defined by this study. Several outbreaks also displayed characteristics of multiple configurations. Some dispersed outbreaks displayed linear features with substantial gaps between the TCTORs. Because of the gaps, these outbreaks were classified as dispersed. Several of these outbreaks could be considered linear if gaps were not an exclusionary factor.

Analytical methods, such as spatial cluster analysis for point data in a geographic information system (e.g., average nearest neighbor analysis, Ripley's k-function analysis, directional distribution analysis, and central feature analysis), may provide an easily reproducible and optimized classification scheme with less within-group variability and, overall, less subjectivity. However, because the spatial configuration analysis presented here was based on observations of already-identified outbreaks and is descriptive in nature, the exploration of these analytical methods and the establishment of a quantitative classification scheme are beyond the scope of this study.

5.3 Synoptic Patterns Associated with Tropical Cyclone Tornado Outbreaks:

Forcing Mechanisms

This study identified five synoptic patterns that correspond to TCTOR outbreaks. The next logical question is: Why are these recurring patterns associated with TCTOR outbreaks? Prior to discussing potential synoptic scale forcings associated with the synoptic patterns, it must be acknowledged that other sub-synoptic scale forcings that are favorable to TCTOR genesis, such as convective outflow, baroclinic boundaries, and low-level moisture convergence (Bluestein 1993; Markowski, Rasmussen, and Straka 1998; Rasmussen et al. 2000; Gilmore and Wicker 2002), are also likely to be present within the TC environment.

Water-to-land transition, and the resulting increase in surface friction, also is a likely source of vertical wind shear and lift within the TC environment, both of which are favorable conditions for TCTOR genesis. Orographic elements and their influence on air flow also may produce environments conducive to TCTOR genesis. Varying amounts of low-level speed convergence and forced lift are possible during landfall as a TC's surface winds encounter increasingly high elevations and increased roughness (increased friction). Elevated land surfaces create more opposing friction to surface winds than lower, flat land surfaces.

The coastal plains and Appalachian region along the east coast provide a source of substantial orographic lift (relative to the Gulf Coastal Plains), low-level speed convergence-induced lift, and surface friction-induced wind shear. These topography-related forcings may enhance the TCTOR potential not only for East Coast landfalls but also for Gulf Coast landfalls that track northward through the East Coastal Plains to the

east of the Appalachian Mountains. Figure 5.1 illustrates the spatial distribution of individual TCTORs that occurred in an outbreak over the study period along with the topography of the eastern half of the United States; note the general clustering of TCTORs to the east of the Appalachian Mountains.

The following proposed synoptic scale dynamic processes are thought to act in conjunction with, and perhaps enhance, forcings at different scales and levels of the atmosphere. For instance, synoptic scale dynamic processes downstream of a midlatitude trough (i.e., upper-level divergence and upward vertical motion) may reduce convective inhibition, which makes it easier for an air parcel to reach the level of free convection, ultimately enhancing widespread convection (Bluestein 1993; Doswell and Bosart 2001).

There are several plausible synoptic scale mid-to-upper tropospheric dynamic processes associated with Patterns 1–4 that are favorable for TCTORs. Pattern 1 outbreaks are produced by TCs with closed circulation at 500 hPa, typically with a 500 hPa midlatitude trough to the north or northwest (Figures 3.3 and 4.12). In this synoptic situation, a TC is tracking into an environment of ever-increasing vertical wind shear and varying degrees of cyclonic vorticity advection and upward acceleration. Pattern 2 and 3 outbreaks both are produced by TCs that are embedded within the midlatitude westerlies as shortwave troughs, but differ with respect to whether their associated TC circulation is closed (Figures 3.4, 3.5, 4.17, and 4.22). Thus, similar to Pattern 1 but perhaps more evidently, Pattern 2 and 3 TCs are located within sheared environments with varying degrees of cyclonic vorticity advection and upward acceleration. The ambient wind shear in which Pattern 1–3 outbreaks are located is provided by the midlatitude westerly flow and is especially enhanced when the TC is interacting with a mid-to-upper level

midlatitude trough (Molinari et al. 2006; Ritchie and Elsberry 2007; Molinari and Vollaro 2010a and 2010b). In addition to providing wind shear, troughs also provide ample relative vorticity, especially near their axes where maxima are located, and cyclonic vorticity advection, which induces upward vertical motion over a synoptic scale (Figure 5.2; Bluestein 1993).

Another dynamic synoptic scale forcing perhaps at work, especially in Pattern 2 outbreaks, is mid-to-upper tropospheric diffluent flow. Diffluence is a wind flow pattern in which air spreads laterally outward from a central axis that is oriented parallel to the overall direction of wind flow; and because diffuence aloft is essentially horizontal divergence, it may induce upward acceleration and often is considered to be favorable for severe thunderstorm development (NWS 2009). Varying degrees of diffluent flow are observable in Pattern 2 outbreaks where gradient wind flow fans out downstream and to the north of the closed TC isoheight (Figure 5.3).

Pattern 4 outbreaks, which are produced by TCs located within the western portion of the North Atlantic subtropical anticyclone, are located in a region of synoptic scale upward vertical motion. Because of their asymmetric structure (i.e., the surface high is to the east of the upper-level high), upward vertical motion is typical within the western half of subtropical high pressure cells which, in turn, leads to often unstable and humid conditions (Nieuwolt 1977). In addition, the southwesterly-to-southerly flow within which these TCs are embedded steer them towards the midlatitude westerlies. It is, therefore, plausible that they experience ever-increasing amounts of ambient wind shear, cyclonic vorticity, and upward vertical motion, especially if tracking towards the downstream side of a trough.

No apparent synoptic scale processes are evident with Pattern 5 outbreaks. Given that the spatial distribution of Pattern 5 outbreaks is along the southeast Texas coastline, the east coastlines of Georgia and Florida, and in the Florida peninsula (Figure 4.36), they are likely contingent on topography-related forcings (i.e., friction-induced vertical wind shear and surface convergence-induced lift) along with additional sub-synoptic scale forcing. Verbout et al. (2007), similarly, noted that mesoscale and storm scale processes can produce environments favorable for TCTOR outbreaks in atypical synoptic environments, as might have been the case with TC Beulah (1967).

The presence of synoptic scale forcing mechanisms is likely to increase the chance for relatively severe TCTOR outbreaks. TCTOR outbreaks in Patterns 1–4 occur in environments that are known to support synoptic scale upward acceleration. These patterns also had the four largest mean and median outbreak severity metrics (Table 4.3). Pattern 1–3 outbreaks occur in environments with relatively strong ambient wind shear associated with the midlatitude westerlies in addition to the synoptic scale ascension. The presence of these forcings may have contributed to relatively large mean, median, and maximum outbreak severity metrics found with Patterns 1–3 (Tables 4.3 and 4.9). Pattern 2 outbreaks, in addition to the above mentioned synoptic scale forcings, occur in environments that exhibit diffluent flow at 500 hPa, which would likely enhance the already-present upward acceleration. Pattern 2 outbreaks are, therefore, associated with the most proposed synoptic forcing mechanisms and also have the largest mean and median severity metrics (Table 4.3). Pattern 5 outbreaks, which occur in environments that do not exhibit any clear signs of synoptic forcing like Pattern 1–4 outbreaks, had the smallest mean, median, and maximum outbreak severity metrics (Table 4.3).

5.3.1 Importance of the Midlatitude Westerlies

Pattern 1–3 outbreaks are produced by TCs that are beginning to interact with, or are embedded within, the midlatitude westerlies, often with a midlatitude longer-wave trough to the north or northwest. Previous studies of the ET stage of TCs have reported that trough interaction can lead to a reintensification stage of the TC life cycle (Harr and Elsberry 2000; Hart and Evans 2001; Klein, Harr, and Elsberry 2002; Ritchie and Elsberry 2003 and 2007; Molinari and Vollaro 2010b). An increase in ambient wind shear associated with trough interaction also has been linked to increased low-level convergence and widespread upward vertical motion in the downshear half of the TC environment (Black et al. 2002; Braun, Montgomery, and Pu 2006; Reasor, Eastin, and Gamache 2009). Ambient wind shear has likewise been linked to elevated CAPE, SRH, and local vertical wind shear, in addition to severe convection in the downshear half (especially the downshear left quadrant) of the TC environment (Molinari and Vollaro 2008 and 2010a; Molinari et al. 2012).

The documented changes to the internal structure and dynamics of a TC environment brought upon by interaction with midlatitude wind shear, including TC intensification, low-level convergence, upward vertical motion, enhanced CAPE, SRH, and local vertical wind shear, and severe convective activity, can hypothetically increase TCTOR potential and lead to TCTOR outbreaks. Many of these changes have been shown to occur in preferred locations within the TC environment, much like TCTORs favor the right-front quadrant. The preferred locations where the aforementioned changes tend to occur (i.e., the downshear half and downshear left quadrant) vary depending on the direction of the ambient shear vector (Figure 5.4). Given southwesterly ambient

shear, as might be found with a TC located downstream of a midlatitude trough axis and upstream of the succeeding ridge axis, the downshear half of a TC generally corresponds to the region of greatest TCTOR occurrence. Ambient wind shear from the west-northwest, as might be found near the base of a midlatitude trough or just upstream of its axis, generally aligns the downshear left quadrant with the right-front quadrant of the TC relative to north. The downshear left quadrant and the north-relative right-front quadrant are absolutely aligned with a westerly ambient shear.

The physical cause of the downshear enhancement to these parameters is the focus of active research (e.g. Jones 2000; Reasor et al. 2000; Frank and Ritchie 2001; Molinari et al. 2012). Frank and Ritchie (2001) propose that the enhancements arise to counter vortex tilting caused by westerly shear. They suggest that moderate westerly shear tilts the TC vortex and that internal dynamics of the TC work to balance the tilt with the development of deep convective circulation in the downshear portion of the TC. Essentially, the updrafts of the downshear convective circulation act to force the TC vortex back towards a vertical orientation. They also propose that the updrafts rise in a helical motion. Corbosiero and Molinari (2002) provide a more thorough discussion of Frank and Ritchie's (2001) hypothesis along with alternative hypotheses. These hypotheses have potential application to TCTORs in that they may provide a physical reason for the marked spatial distribution of TCTORs within the TC environment.

Not only may the midlatitude westerlies alter the internal dynamics of a TC, they also may induce a change to the entire TC structure from a tropical to an extratropical system through ET. The various stages of interaction between TCs and the midlatitude westerlies illustrated in Patterns 1–3 are reminiscent of Klein, Harr, and Elsberry's (2000)

conceptual framework for ET, particularly their transformation stage, which begins when the outer circulation of a TC begins to interact with the baroclinic midlatitude environment and ends when a TC is embedded within this environment as an open short wave trough. Pattern 1 outbreaks occur within a synoptic scale environment suggestive of the onset of TC transformation and Pattern 3 outbreaks occur within synoptic scale environments similar to the end of the transformation stage. Pattern 2 outbreaks occur in a synoptic scale environment that likely emerges in the middle of the transformation stage.

Key physical processes occur during the transformation stage identified by Klein, Harr, and Elsberry (2000) that might promote TCTOR-favorable environments. For instance, relatively cold, dry air is entrained into the western half of the TC environment whereas relatively warm, moist air is entrained into the eastern half of the TC environment, which is, coincidentally, where nearly all TCTORS are produced. Another transformation process noted by Klein, Harr, and Elsberry (2000) is downshear tilting of the TC's warm core aloft. This downshear tilt is similar to Frank and Ritchie's (2001) shear-induced vortex tilt hypothesis for the development of severe convection and helicity in the downshear half of the TC environment. It is possible that both correspond to the same physical processes. It also is possible that the downshear enhancement of CAPE, SRH, localized wind shear, and severe convection observed during previous investigations (Corbosiero and Molinari 2002; Black et al. 2002; Braun, Montgomery, and Pu 2006; Molinari and Vollaro 2008 and 2010a; Reasor, Eastin, and Gamache 2009; Molinari et al. 2012) temporally correspond to the transformation stage of ET. Continued research into the transformation stage of ET, and especially into the corresponding

structural changes occurring within the TC environment, may reveal possible internal dynamics associated with ET that are conducive to TCTORs.

5.3.2 Seasonality of the Midlatitude Westerlies

TCTOR outbreaks that occur within the sheared midlatitude westerlies (i.e., Patterns 1, 2, and 3) were shown to become increasingly common as the North Atlantic Basin hurricane season progresses whereas those isolated from this sheared environment were shown to become less common (Table 4.12). This is likely related to the southward expansion and strengthening of the midlatitude westerly wind belt during the northern hemisphere fall and winter (Harmon 1991), which roughly corresponds to the latter half of the North Atlantic Basin hurricane season. A general southward trend is observed by tracing the location of the 5850 m isoheight in monthly composites throughout the North Atlantic Basin hurricane season (Figure 5.5). The southward expansion of the westerlies provides more time over which northward tracking TCs can interact with an ambient environment with ample vertical wind shear. Cyclonic vorticity advection and synoptic scale upward vertical motion likewise extend southward when midlatitude troughs propagate eastward through the extended westerly wind belt.

Assuming that increased ambient wind shear (and the associated enhancements to CAPE, SRH, localized wind shear, and severe convection within the TC environment), cyclonic vorticity advection, and synoptic scale upward vertical motion enhance TCTOR potential, the southward expansion of the westerly wind belt may provide insight into why September and October TCTOR outbreaks are slightly more severe, on average, than those in earlier months and why the most severe outbreaks have occurred primarily in these months (Figure 4.4; Appendix C). Nine of the ten most severe outbreaks over the

period of record occurred in September or October; one of the ten occurred in August. Even though they may have a greater likelihood of being relatively severe when they occur, decreased late season TC activity reduces the likelihood for TCTOR outbreaks of any severity. The westerly wind belt is extended farthest south in November, for example, but there are few opportunities for TCTOR outbreaks because there are so few TCs; there are only three recorded November or later TCs in the TCTOR data set (Mitch 1998, Michelle 2001, and Olga 2007) and only one TCTOR outbreak in November associated with TC Mitch (1998).

5.3.3 Comparison of Results with Previous Findings

Two previous studies (Verbout et al. 2007; Cohen 2010) examined the association between TCTORs and 500 hPa geopotential height patterns. Both of these studies used map compositing techniques to differentiate between outbreak and non-outbreak cases, and their definitions of outbreak differ from that used in this study (see Table 3.5 for their definitions).

Verbout et al. (2007) found a direct association between TC recurvature and TCTOR frequency. As a result, they searched for potential causes of recurvature, and therefore TCTOR outbreaks, with a sample of TC landfalls in Texas. They found that 500 hPa geopotential height composites differentiate between outbreak and non-outbreak TCs, reporting an outbreak composite with a 500 hPa midlatitude trough over the north-central United States whereas a 500 hPa midlatitude ridge is situated over the north-central United States with the jet stream far poleward of the TC feature in the non-outbreak composite. They also reported that all five of the outbreaks used to develop the outbreak composite were associated with a 500 hPa midlatitude trough, verifying the

composite. The general characteristics of Pattern 1 outbreaks identified in this study (i.e., closed circulation TC at 500 hPa with a midlatitude 500 hPa trough to the north or northwest) are consistent with the 500 hPa geopotential height outbreak composite produced by Verbout et al. (2007).

Verbout et al. (2007) also composited seven non-outbreak TCs that recurved over the eastern United States to further assess the role of midlatitude troughs in recurvature, and thus TCTOR outbreaks, and reported that the 500 hPa composite depicts a trough located to the northwest of the TC feature at landfall. From this they concluded that interaction with midlatitude troughs often results in recurvature, but that whereas this interaction appears to promote TCTOR genesis in Texas, it does not promote TCTOR outbreaks in east coast-recurving TCs because their right-front quadrant, which is the quadrant in which the majority of TCTORs occur, often is situated offshore. This may be true for TCs straddling the East Coastline, especially if the TC quadrants are defined relative to TC heading rather than absolute north. Not all TCs, however, straddle the East Coastline as they track north or northeastward. Some of the TCs examined in this study tracked through the East Coastal Plains between the Appalachian Mountains and the East Coastline where they produced many TCTOR outbreaks (Figure 5.5).

Unlike Verbout et al. (2007), Cohen (2010) did not report a direct association between 500 hPa midlatitude troughs and recurvature or TCTOR outbreaks. Cohen (2010) composited five geopotential height plots associated with TCTOR outbreaks in the west Gulf Coast region; he repeated this procedure for the central and eastern Gulf Coast regions as well. He also repeated this procedure for non-outbreak cases. The

outbreak composites for each region depict a 500 hPa midlatitude trough situated generally over the western United States.

Cohen's (2010) 500 hPa outbreak composite for the western Gulf Coast depicts a trough axis just off of the northwest coast of the United States and a TC feature just to the southeast of Texas in the Gulf. No indication of interaction between the TC feature and the trough exists because the TC appears to be located in the southern portion of a well-developed subtropical ridge. This western Gulf Coast outbreak pattern is most similar to the Pattern 5 outbreaks identified in this study.

Cohen's (2010) 500 hPa composite for central Gulf Coast outbreaks depicts a similar trough position to that shown in the western Gulf Coast composite, but the TC feature in the central Gulf Coast composite is located farther north and east and is also within the northern portion of the subtropical ridge. This composite is most similar to the Pattern 1 outbreaks identified in this study but also is reminiscent of a Pattern 2 outbreak.

Cohen's (2010) 500 hPa composite for eastern Gulf Coast outbreaks depicts a midlatitude trough in a position similar to that of the western and central Gulf Coast composites, but also depicts a shorter-wave trough embedded within the longer-wave trough; the shorter-wave trough appears to be transitioning to a cut-off low. The TC feature is located to the south of Louisiana, Mississippi, and Alabama. The general features, and their relative location, of this composite are similar to those of both Pattern 1 and 5 outbreaks identified in this study; the 500 hPa vector wind flow would be assessed to determine whether the TC is interacting with, or isolated from, the westerlies.

Cohen's (2010) 500 hPa non-outbreak composites for the central and eastern Gulf Coast regions are similar to the Pattern 3 outbreaks identified in this study. Both depict a

TC embedded within the midlatitude westerlies as an open shortwave trough located downstream of a longer-wave trough axis. This is interesting, and perplexing, because Pattern 3 had the largest number of outbreaks in this study whereas Cohen (2010) reports composites similar to Pattern 3 to be associated with non-outbreak TCs. It is possible that Cohen's (2010) composites are unrepresentative because they consist of only five outbreaks. Forty TCTOR outbreaks were classified as Pattern 3 in this study (i.e., TCs embedded within the midlatitude westerly flow as open shortwave troughs, often located downstream of a longer-wave trough axis), which is seemingly contrary to Cohen's (2010) central and eastern Gulf Coast non-outbreak composites. It also is possible that the presence or absence of additional variables, which are not accounted for by this study or Cohen (2010), allow similar synoptic patterns to produce TCTOR outbreaks in some cases whereas no outbreaks are produced in others. The disparity also may relate to the design of each respective methodology, including the use of different classification methods and temporal parameters.

Previous studies, such as Verbout et al. (2007) and McCaul (1991), have discussed the potential importance of midlatitude ambient wind shear to TCTOR outbreaks. Verbout et al. (2007) noted that El Niño years are associated with anomalously strong westerly shear located over the western North Atlantic Ocean and Caribbean Sea and found that TCs during these years have a higher chance of producing a TCTOR outbreak, even though the number of TCs during these years is reduced, ironically, by the same enhanced shear that may favor TCTOR production. McCaul (1991) suggested that entrainment into the westerlies and the associated across-TC ambient shear may enhance localized shear and helicity within TCs and, thus, enhance

TCTOR development, typically in their right-front quadrant. The results of this study support these conclusions by showing that TCs that are interacting with, and embedding within, the midlatitude westerlies have produced more, and more severe, TCTOR outbreaks.

In addition to confirming the important of westerly wind shear to TCTOR outbreaks, the results of this study indicate that it is during the early stages of interaction with the westerlies that a TC is most likely to produce an outbreak. The largest outbreaks identified in this study, as indicated by the mean, median, and maximum outbreak severity metrics, were produced in Pattern 1 and 2 environments, which represent TCs that are beginning to interact with the westerlies and those that are embedded in the westerlies as closed shortwave troughs.

Frances (2004) well illustrates the tendency for a TC to produce its most severe outbreaks during the early-to-mid stages of westerly interaction (i.e., Pattern 1 and 2). Frances produced twelve outbreaks, which ranged in severity from three to twenty-one TCTORs (Figure 5.6). The first seven outbreaks, which occur while Frances is isolated from the midlatitude westerlies (the four Pattern 5 outbreaks) and during the earliest westerly-interaction stages (the first three Patterns 1 outbreaks), do not exceed a severity of five TCTORs. However, as Frances' interaction with the sheared westerlies continues, the outbreaks become generally more severe. The two most severe outbreaks occurred during the last Pattern 1 outbreak and the first Pattern 2.

Additional studies not focused on TCTORs have examined the effect of midlatitude westerly shear on TC intensity and internal structure (e.g. Black et al. 2002; Braun, Montgomery, and Pu 2006; Molinari and Vollaro 2008; 2010a, and 2010b;

Reasor, Eastin, and Gamache 2009; Molinari et al. 2012). These studies have provided insight into the spatial distribution of TCTORs within the TC environment by showing that environmental parameters such as CAPE, SRH, local vertical wind shear, and severe convection are enhanced in the same general region of the TC environment where TCTORs occur most frequently. The hypothesis proposed by Frank and Ritchie (2001; see section 5.3 for a synopsis of their hypothesis) to explain enhanced severe convection in the downshear quadrants of a TC may also explain why TCTORs are most common when their associated TC is located in the sheared westerlies and why TCTORs occur predominately in the right half of the TC environment relative to north.

It also must be noted that Pattern1, and especially Patterns 2 and 3, generally resemble the classic tornado outbreak setting (Miller 1972; Johns and Doswell 1992; Doswell, Weiss, and Johns 1993; Mercer et al. 2012) in that the TCs, and the TCTOR outbreaks, are located in the synoptically-favorable region to the east or southeast of a progressive 500 hPa midlatitude trough. Although the general synoptic scale features of TCTOR outbreaks in Patterns 1–3 are similar to those of this classic setting, there is variability in terms of TC circulation (i.e., whether circulation is closed at 500 hPa), TC location relative to the 500 hPa midlatitude trough (all TCs in these patterns were located downstream of the trough axis and upstream of the successive ridge axis, but their precise location varies), wavelength and amplitude of the 500 hPa midlatitude trough, and the tilt, if any, of the 500 hPa midlatitude trough. Within-pattern variability is not unique to these results. Mercer et al. (2012), for instance, reported that the individual events used to develop their 500 hPa composites for tornado outbreaks shared the same general features but varied in terms of wavelength, wave amplitude, and trough tilt.

5.4 Chapter Five Figures

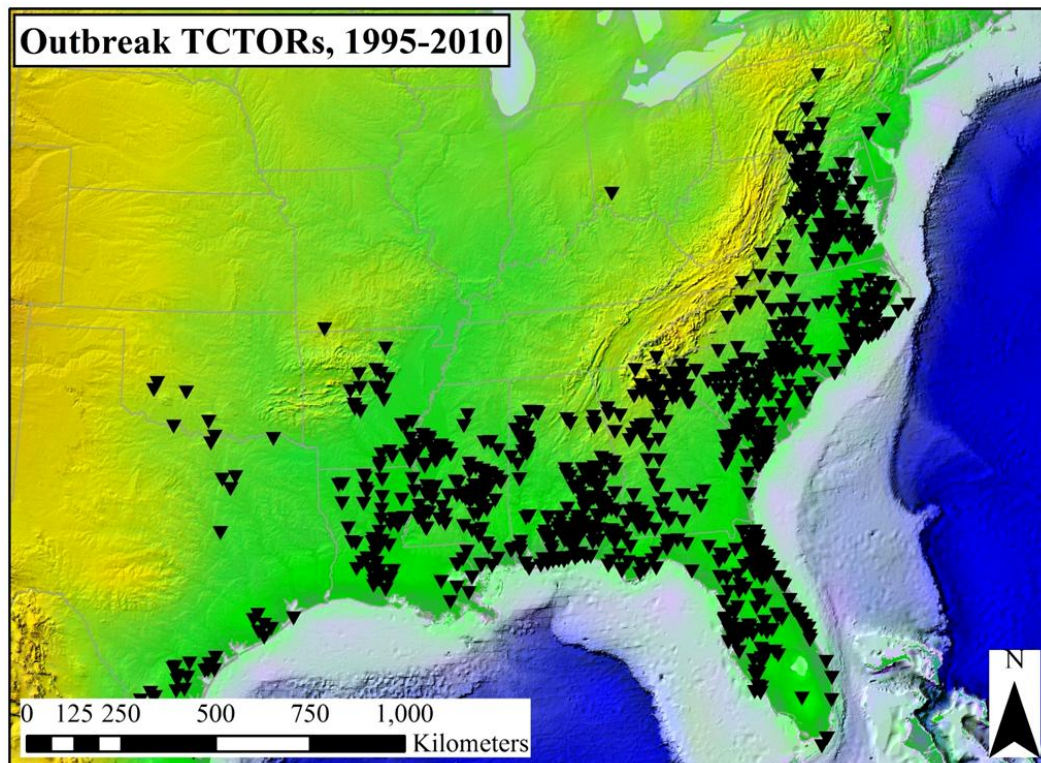


FIGURE 5.1. Map illustrating the distribution of TCTORs that occurred in an outbreak over the period 1995–2010 along with topography and bathymetry. The basemap depicting topography and bathymetry was obtained from ESRI (2008). TCTOR touchdown coordinates were obtained from the TCTOR database (Edwards 2010b).

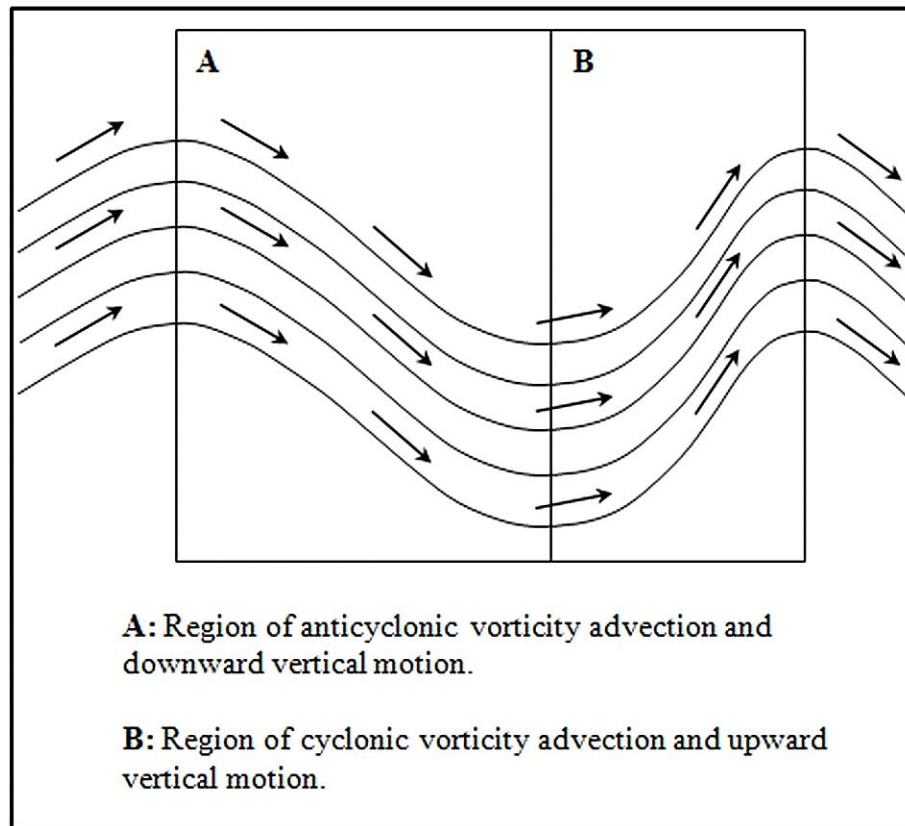


FIGURE 5.2. Schematic of midlatitude westerly meridional flow aloft. Regions of anticyclonic (**A**) and cyclonic (**B**) vorticity advection and the resultant downward (**A**) and upward (**B**) vertical motion are labeled.

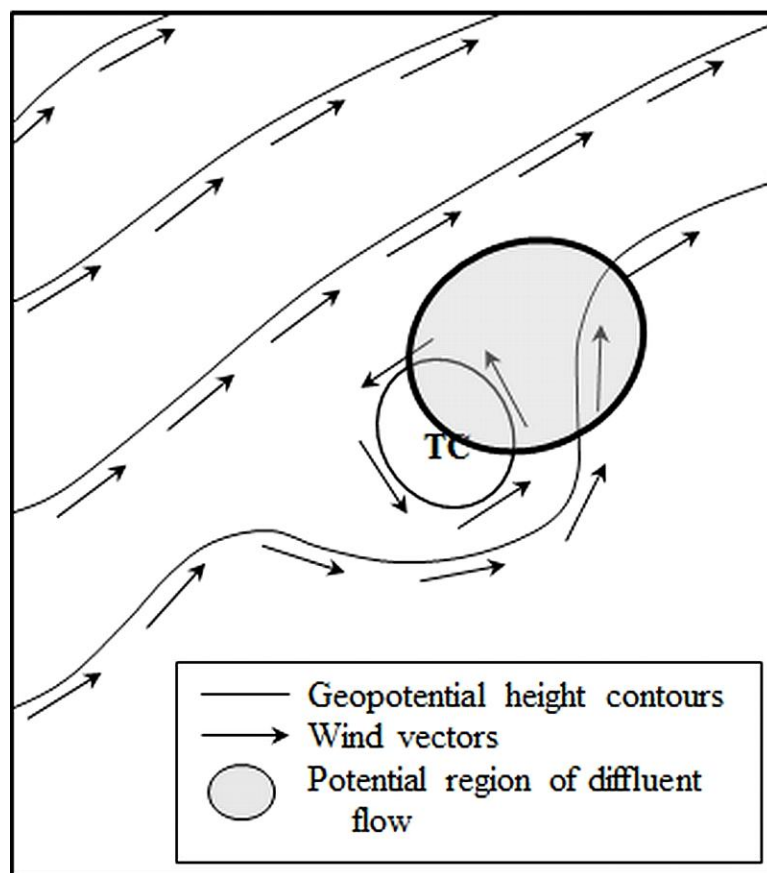


FIGURE 5.3. Schematic of an idealized Pattern 2 outbreak illustrating a potential region of diffluent flow. Note the lateral divergence of the isoheights and wind vectors characteristic of diffluent flow.

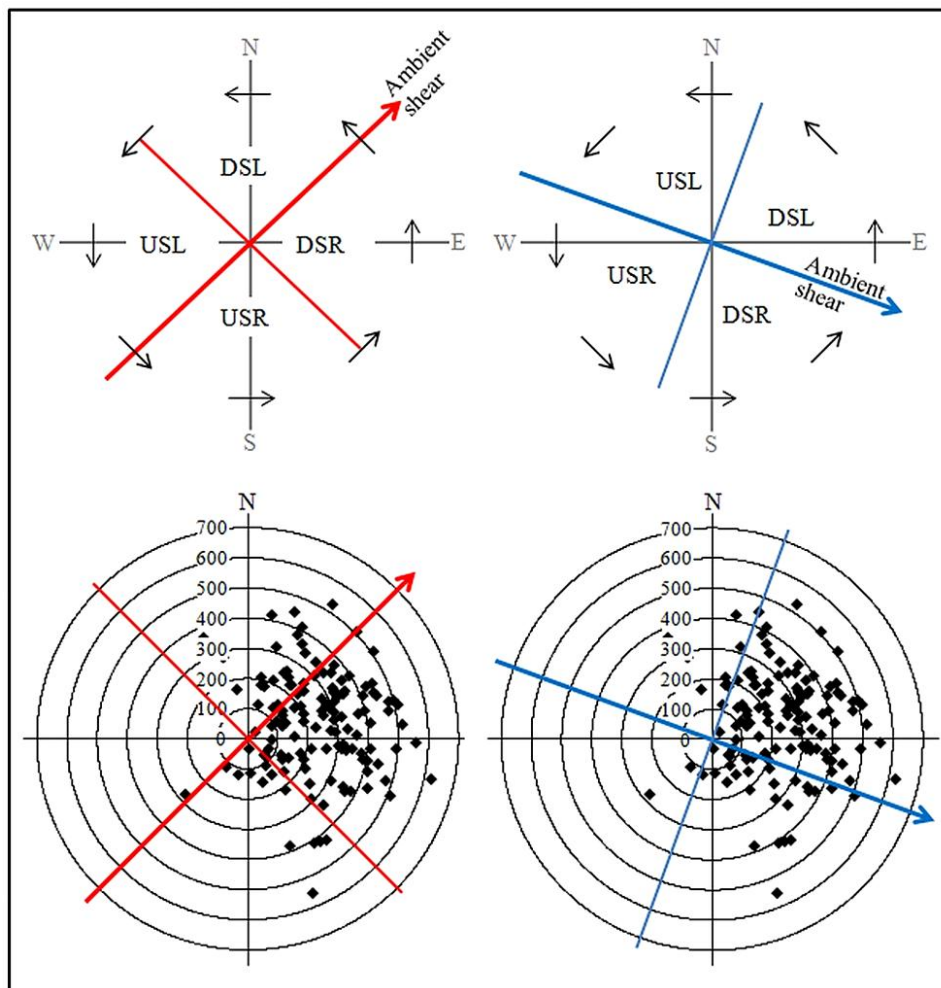


FIGURE 5.4. Conceptual diagram illustrating the geometry between an ambient wind shear vector (bold red and blue arrows) and a hypothetical TC environment. The two figures on the left depict a southwesterly shear vector. The top-left figure conceptualizes the ambient shear-relative quadrants. The bottom-left figure depicts the mean centers of the TCTOR outbreaks identified in this study (black squares) relative to TC center with the ambient shear-relative quadrants overlain. The two figures on the right are the same but for a west-northwesterly ambient shear vector. Range circles in the bottom figures are in kilometers. [USL=upshear left, USR=upshear right, DSL=downshear left, DSR=downshear right]

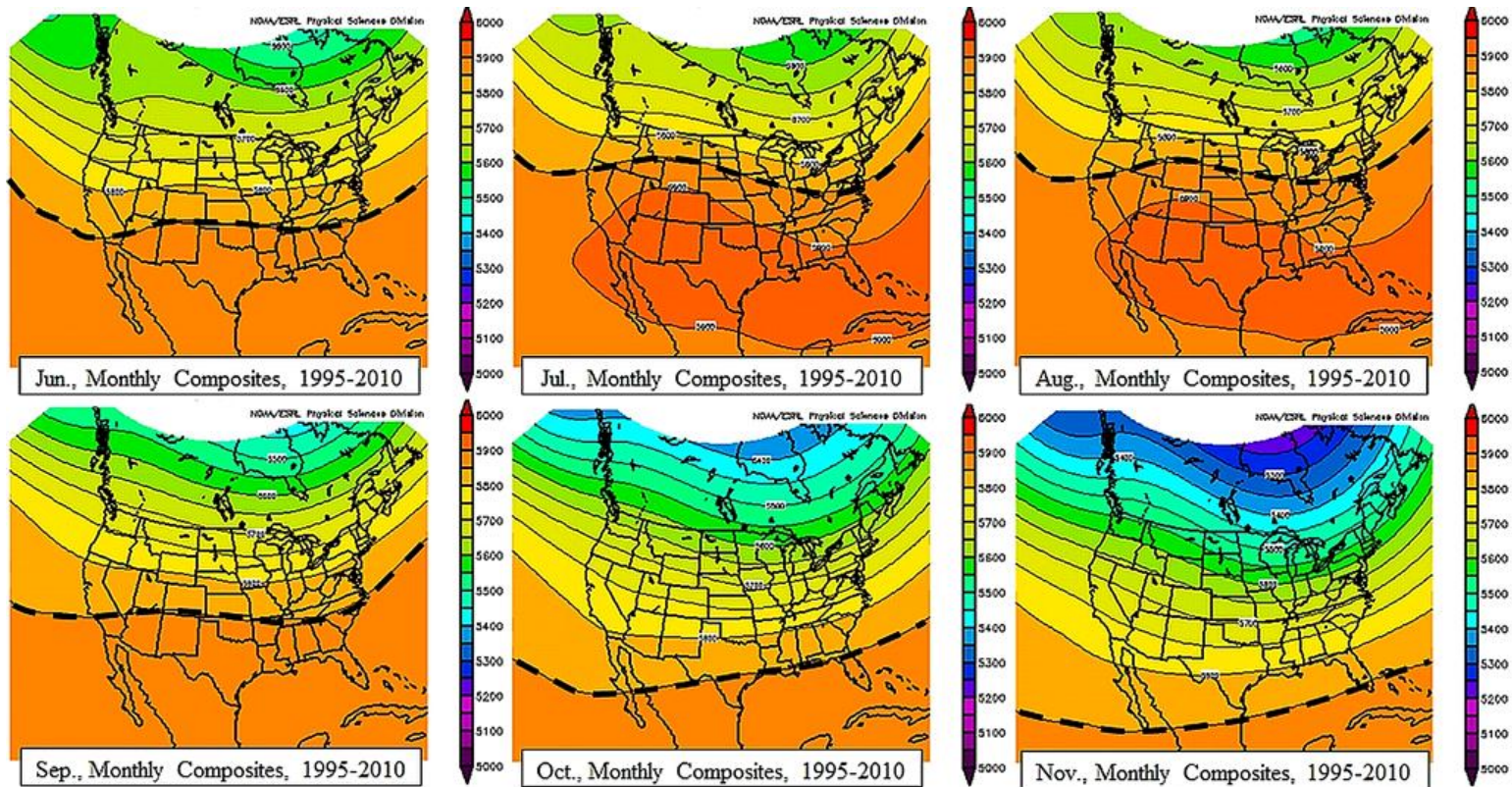


FIGURE 5.5. 500 hPa geopotential height [m] monthly composite plots over the period 1995–2010. Note the general southward progression of the 5850 m isoheight, which is emphasized with the black dashed line in each plot, from early to late hurricane season. The midlatitude westerly flow often extends south of this circumpolar isoheight, as indicated by 500 hPa vector wind plots, but tracing the 5850 m isoheight allows direct comparison of the relative location of the southern-most extent of the westerlies in each monthly composite. NCEP-NARR plots obtained from NOAA ESRL's Physical Science Division (NOAA (n. d.)).

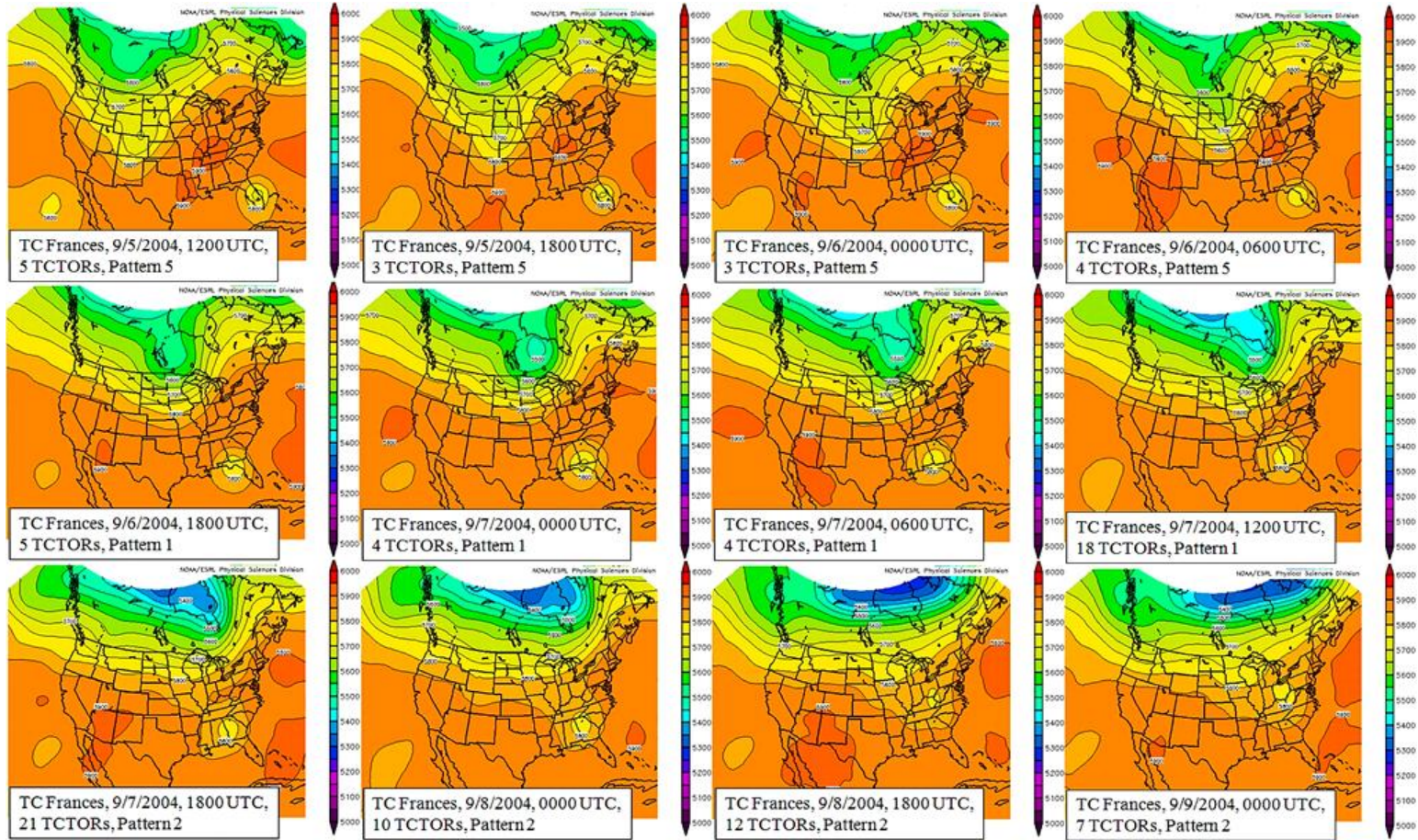


FIGURE 5.6. 500 hPa geopotential height [m] plots corresponding to TC Frances' (2004) TCTOR outbreaks in sequential order from the first (top-left) to the last (bottom-right). The four outbreaks in the top row are all Pattern 5s, the four in the middle row are Pattern 1s, and the four in the bottom row are Pattern 2s. NCEP-NARR plots obtained from NOAA ES&P's Physical Sciences Division (NOAA (n. d.)).

CHAPTER VI

CONCLUSION

6.1 Summary

This study identified and analyzed TCTOR outbreaks and their corresponding synoptic environments. TCTOR outbreaks were defined as three or more TCTORs in a six hour window centered about one of the following synoptic hours: 0000 UTC, 0600 UTC, 1200 UTC, and 1800 UTC. The TCTOR dataset (Edwards 2010b) produced by Roger Edwards of the SPC was used to identify outbreaks.

One hundred and thirty-three TCTOR outbreaks were identified over the period 1995–2010 in association with East and Gulf Coast landfalling TCs. The outbreaks ranged in severity from the minimum frequency threshold of three to an observed maximum of thirty-three. Seventy-five percent of the outbreaks consisted of nine or fewer TCTORs and half of five or fewer. The maximum outbreak severity, however, demonstrates that TCs are capable of producing TCTORs at relatively high rates (i.e., thirty-three TCTORs in six hours).

The temporal and spatial analysis revealed when and where TCs produce the greatest numbers of TCTORs. The temporal distributions show that TCs produce the greatest number of TCTORs during afternoon and night hours (local time), during the middle and latter half of the North Atlantic Basin hurricane season, and near the time of landfall out to approximately forty hours after landfall. The spatial distributions show

that TCTOR outbreaks are most common in the right half of the TC environment relative to north, with modal frequencies observed in the right-front quadrant and between 200 km and 400 km from TC center. Over a larger area, TCTOR outbreaks are most common in the eastern portion of the Gulf Coast Region and along the East Coast between the Appalachian Mountains and the East Coastline. Visual examination of the outbreak's spatial distribution revealed that they conform generally to four spatial configurations: linear, single-cluster, multi-cluster, and dispersed. The linear and single-cluster outbreaks, and to a lesser extent the multi-cluster outbreaks, are clustered both temporally and spatially. The dispersed outbreaks, on the other hand, are temporally clustered but have spatially-isolated TCTORS.

Synoptic plots of 500 hPa geopotential height and wind vectors were obtained from the NCEP-NARR project (Mesinger et al. 2006; NCDC 2011; NOAA n.d.) to analyze the synoptic environments in which TCTOR outbreaks most often occur. The synoptic plots for a given outbreak correspond to that outbreak's central synoptic hour so that all TCTORS in a given outbreak occur within three hours of the synoptic plots. The manual classification of these plots identified five synoptic patterns based on 500 hPa geopotential height and vector wind plots (Table 6.1). One hundred and twenty-nine of the 133 identified outbreaks fit the criteria of one of the five patterns; four outbreaks were classified as other because they did not reasonably fit the criteria of any of the patterns.

Thirty-six outbreaks were classified as Pattern 1. Pattern 1 outbreaks are produced by TCs with closed circulation at 500 hPa that are located in the northern portion of the subtropical ridge and exhibit signs of proto-interaction with the midlatitude westerlies. Twenty-two outbreaks were classified as Pattern 2. These outbreaks are

produced by TCs that are embedded within the midlatitude westerlies as closed shortwave troughs and often are located downstream of a longer-wave trough axis. Forty outbreaks were classified as Pattern 3. The synoptic environment of these outbreaks is similar to that of Pattern 2, except the TCs in Pattern 3 are open rather than closed shortwave troughs. Thirteen outbreaks were classified as Pattern 4. These outbreaks are produced by TCs that do not have closed circulation at 500 hPa that are embedded within the southerly or southwesterly flow of the western portion of the North Atlantic subtropical anticyclone. Eighteen outbreaks were classified as Pattern 5. Pattern 5 outbreaks are produced by TCs with closed circulation at 500 hPa that are cut off from midlatitude westerlies by a region of relatively high geopotential heights and unorganized flow.

The five synoptic patterns can be aggregated into two general groups: (1) outbreaks produced by TCs that are beginning to interact with, or are embedded within, the sheared midlatitude westerlies and (2) outbreaks produced by TCs that are isolated from the sheared midlatitude westerlies. Patterns 1–3 illustrate the various stages a TC may encounter when tracking into the midlatitude westerlies, from 500 hPa closed circulation TCs beginning to interact with the westerlies to TCs fully embedded within the westerlies as 500 hPa open shortwave troughs.

The TCs in Patterns 1–4 are located within synoptic environments that are known to have TCTOR-favorable synoptic scale forcing. Pattern 1–4 outbreaks are located within regions of synoptic scale ascension. In addition to ascension, Pattern 1–3 outbreaks are located in environments with relatively strong ambient wind shear because they are beginning to interact with, or embedded within, the westerlies. Pattern 2

outbreaks also show signs of upper-level diffluent flow, which may further enhance upward vertical motion.

The results of this study allude to a link between the number of synoptic scale forcing mechanisms and the severity of TCTOR outbreaks. Pattern 2 outbreaks occur in an environment exhibiting signs of the most proposed synoptic scale forcing mechanisms (synoptic scale ascension, relatively strong ambient wind shear, and upper-level diffluent flow) and, as a result, had the largest median and mean outbreak severity metrics. Pattern 1 and 3 outbreaks occur in environments with two evident synoptic scale forcing mechanisms (synoptic scale ascension and ambient wind shear) and had the second and third largest median outbreak severity metrics, respectively. Pattern 4 outbreaks occurred in environments with one evident synoptic scale forcing (ascension associated with the western portion of the North Atlantic subtropical anticyclone) and, as a result, this pattern had the fourth largest median outbreak severity. Pattern 5 outbreaks occurred in environments without evident signs of any synoptic scale forcing and had the smallest median and mean outbreak severity.

The three synoptic patterns in which TCs are interacting with, or embedded within, the westerlies (Patterns 1–3) had the greatest outbreak activity in terms of frequency, typical severity, and extremes (Table 6.1). Coincidentally, research on the interaction between TCs and their ambient environment has shown that interaction with, and entrainment into, the sheared westerly flow of the midlatitudes may bring upon internal changes to the TC environment (e.g., Klein, Harr, and Elsberry 2000 and 2002; Frank and Ritchie 2001; Corbosiero and Molinari 2002; Molinari and Vollaro 2010a and 2010b; Molinari et al. 2012). It is proposed here that these changes may promote

TCTOR genesis. In essence, this is an example of synoptic scale TCTOR forcing (i.e., ambient wind shear associated with midlatitude westerly flow) working in conjunction with, or perhaps even inducing, smaller scale TCTOR forcings (severe convective cells, local wind shear, and helical flow).

Moderate to strong ambient wind shear has been linked to high values of CAPE, SRH, localized wind shear, and severe convection in the downshear quadrants of the TC environment (Corbosiero and Molinari 2002; Black et al. 2002; Braun, Montgomery, and Pu 2006; Molinari and Vollaro 2008 and 2010a; Reasor, Eastin, and Gamache 2009; Molinari et al. 2012). The hypotheses proposed to explain the downshear enhancements of these parameters may also provide a physical explanation for the observed spatial distribution of TCTORS within the TC environment. In general, severe convective storms develop in the downshear quadrants of a TC to counter vortex tilting created by westerly wind shear. Given that the ambient shear vector typically has a moderate to strong westerly component while a TC is embedded within the westerlies, the downshear quadrants are in general alignment with the right half, relative to north, of the TC, which is where nearly all TCTORS occur (Figure 5.4). It is possible that the severe convective storms produced in the downshear quadrants to counter vortex tilting are responsible for a large portion of TCTORS.

Expansion and strengthening of the midlatitude westerly wind belt during the Northern Hemisphere fall and winter may be associated with the observed increase in TCTOR activity in the middle and latter half of the North Atlantic Basin hurricane season. In general, TCs encounter the expanded westerly wind belt sooner in their life span, allowing the ambient wind shear associated with the westerlies to impact the TC

environment for a longer period of time. Moreover, the ambient wind shear, in general, strengthens during these seasons as the equator-to-pole temperature gradient increases. Convective updrafts may also strengthen in the downshear quadrants of TCs to counter the amplified vortex tilt caused by the enhanced westerly shear. The expansion and strengthening of westerly wind shear, and the resulting convective enhancements, may be associated with the observed increase in typical outbreak severity observed in September and October.

6.2 Future Research

This study defined a TCTOR outbreak as three or more TCTORs in a six hour period centered about one of the primary synoptic hours: 0000 UTC, 0600 UTC, 1200 UTC, or 1800 UTC. Because this study also analyzed the synoptic environments corresponding to TCTOR outbreaks, the outbreak definition had to ensure that the outbreaks and synoptic plots were temporally synchronized; this is why the outbreak's temporal windows are centered about synoptic hours. Other outbreak definitions could have been used, and some would likely better fit the observed TCTOR clusters, but they would not have facilitated a consistent identification process nor would they have synchronized with the synoptic plots. Research focused on the spatial and temporal clustering of TCTORs could lead to the development of a data-derived, posteriori outbreak definition. Such research would be an insightful addition to the current spatio-temporal understanding of TCTORs.

This study manually classified the synoptic environment corresponding to the identified TCTOR outbreaks. Dayan, Tubi, and Levy (2012) suggest that comparing different synoptic classification methods may lead to additional insight on the interaction

between synoptic scale atmospheric circulation and the surface environment that may be missed when using only one method. It would be insightful to apply other classification methods, such as correlation-, PCA-, and cluster-based classification, to the study of TCTOR outbreaks. These methods may reveal patterns in the synoptic variables included in the initial iteration of this study's classification process but not included in the final synoptic patterns (i.e., 200 hPa vector wind, 600 hPa specific humidity, 900 hPa horizontal convergence, and low-level baroclinic zones). They also might have success in identifying patterns that include some combination of multiple variables rather than the use of only a single variable.

TCTOR outbreaks within the five synoptic patterns identified in this study share common characteristics, but they often vary in terms of TC circulation (i.e., open or closed circulation), location of the TC relative to a midlatitude trough, wavelength of the trough, amplitude of the trough, and tilt of the trough. Within-pattern variability such as this is not unique to this study or to the manual classification method. Mercer et al. (2012), for instance, used a PCA method and reported that the individual events used to develop their 500 hPa composites for tornado outbreaks shared the same general features but varied in terms of wavelength, wave amplitude, and tilt of the trough feature. Relative vorticity and vertical motion are influenced by the wavelength and amplitude of upper tropospheric waves. Shorter wavelengths and higher amplitude waves force the midlatitude westerly flow to follow a more tightly curved path and, as a result, are associated with greater amounts of cyclonic vorticity and upward vertical motion (Harmon 1991). Similarly, negatively tilted midlatitude troughs often are associated with upper-level diffluent flow and synoptic scale ascension downstream of their axis

(Harmon 1991). If these synoptic scale forcings are directly related to TCTOR potential, as proposed here, then this line of investigation would benefit from a classification that accounts for the wavelength, amplitude, and tilt of midlatitude troughs. Further partitioning of the synoptic patterns in this study based on some of the above characteristics would reduce the number of outbreaks in most patterns, and would therefore hinder statistical analysis, but would nonetheless be useful for descriptive analysis and would contribute well and even expand the results of this study. A larger dataset is needed for this additional partitioning if statistical analysis is to be conducted.

It was noted during the first iteration of the classification process that the TCTOR outbreaks identified in this study tend to occur near the left-exit region of a curved jet streak at the 500 hPa level. This tendency was prominent in most outbreaks in all patterns, thus it was not a distinguishing factor between patterns and was not a criteria for any of the patterns. These wind maxima are observable in Figures 4.12B, 4.17B, 4.22B, 4.27B, and 4.32B; especially the first three of these figures. The TCTOR outbreaks corresponding to these 500 hPa vector wind plots are proximate to the left-exit region of the wind maxima within the TC environment. Cohen (2010), likewise, noted that the outbreaks examined in his study were proximate to wind maxima at the 850 hPa level in the northeast portion of the TC environment. Previous studies (e.g., Kloth and Davies-Jones 1980; Harnack and Quinlan 1989; Rose et al. 2004) have empirically linked non-TC tornadoes to select regions of mid- and upper-level jet streaks. Rose et al. (2004) showed that tornadoes occur primarily in the exit regions (primarily the left-exit region) of jet streaks but, also, that they can occur in the entrance regions, although far less often. An examination of jet streaks at multiple levels of the atmosphere, and their association

with TCTORs, would compliment previous non-TC tornado studies and contribute to the previous TCTOR studies.

Previous studies have plotted the location of TCTORs within the TC environment with the azimuth defined relative to north and relative to TC heading. Given the link between the ambient shear vector and TCTOR-favorable parameters such as CAPE, SRH, local vertical wind shear, and severe convection, it would be interesting to examine the location of TCTORs in an ambient shear vector-relative framework. The fact that the downshear quadrants of the TC environments generally align with the quadrants of maximum TCTOR activity warrants additional investigation into possible connections between these bodies of literature.

Lastly, research on the ET of TCs, specifically the transformation stages and the associated internal changes a TC may undergo (Klein, Harr, and Elsberry 2000), may prove applicable to the study of TCTORs. Additional efforts should be dedicated towards understanding the possible connections between ET and TCTOR production. Bridging these bodies of literature may provide further physical insight into the link between the ambient environment in which a TC is located, internal dynamics of a TC, and TCTOR activity.

6.3 Concluding Statement

TCs encounter various ambient environments as they track from the tropics and subtropics to the middle latitudes. Previous research has shown that these environments influence a TC's track and internal structure (e.g., Gray 1998; Klein, Harr, and Elsberry 2000 and 2002; Frank and Ritchie 2001; Arnott, Evans, and Chiaromonte 2004; Wang and Wu 2004; Molinari et al. 2006; Emanuel 2007; Ritchie and Elsberry 2007; Hill and

Lackmann 2009; Hendricks et al. 2010; Matyas 2010; Molinari and Vollaro 2010a and 2010b). Moderate to strong ambient wind shear, for instance, has been shown to enhance severe convection, CAPE, SRH, and localized wind shear in the downshear quadrants of the TC environment (Black et al. 2002; Braun, Montgomery, and Pu 2006; Molinari and Vollaro 2008 and 2010a; Reasor, Eastin, and Gamache 2009; Molinari et al. 2012).

Pattern 1–3 outbreaks are produced by TCs that are beginning to interact with, or embedded within, the sheared midlatitude westerlies. The aforementioned downshear enhancements may, therefore, be occurring during Pattern 1–3 outbreaks. An enhancement to these variables could hypothetically lead to TCTOR-favorable environments, and thus more TCTORS. One might, therefore, postulate that TCs interacting with, or embedded within, the midlatitude westerlies will produce more TCTORS than those isolated from this sheared environment and that these TCTORS will be most common in the downshear quadrants of the TC environment.

Other TCTOR-favorable synoptic scale forcing mechanisms, in addition to ambient wind shear, also are known to be present in environments similar to those represented by Patterns 1–4, including cyclonic vorticity advection, upward vertical motion, and diffluent flow. The presence and magnitude of these forcings are contingent on the circulation patterns of the midlatitude westerly flow. For instance, a relatively short wavelength, high amplitude midlatitude trough with downstream diffluent flow that exceeds the associated speed convergence would be associated with greater cyclonic vorticity advection and upward vertical motion downstream of the trough axis than a long wavelength, low amplitude trough with downstream confluent flow. The presence of these synoptic scale forcings does not guarantee TCTOR genesis, nor is it mandatory.

Additional research is needed to determine how often the synoptic patterns identified in this study emerge when TCTOR outbreaks do not occur. This study shows that TCTOR outbreaks can occur in atypical synoptic settings with few, if any, synoptic scale forcing mechanisms. Sub-synoptic scale and topography-related forcing mechanisms are, perhaps, sole factors responsible for the TCTOR-favorable environments in these outbreaks, whereas synoptic scale forcing mechanisms enhance these factors in the more typical TCTOR-favorable synoptic patterns (i.e., Patterns 1–3).

6.4 Chapter Six Tables

Table 6.1. Summary of the five synoptic patterns, their verbal description, and their descriptive statistics.

Synoptic Pattern	TC-Westerly Interaction	Distinguishing Synoptic Features at 500 hPa	Outbreak Severity Descriptive Statistics				
			N	M	Mdn	SD	CV
1	Yes	Closed circulation TC located in the northern portion of the subtropical high	36	7.9	5.0	6.6	0.8
2	Yes	TC is a closed shortwave trough embedded within the westerlies	22	10.7	9.0	7.4	0.7
3	Yes	TC is an open shortwave trough embedded within the westerlies	40	5.9	4.5	3.9	0.7
4	No	Closed circulation TC located within the southerly or southwesterly flow of the North Atlantic subtropical anticyclone	13	6.3	4.0	4.0	0.6
5	No	TC is an open wave in the southern portion of the subtropical high	18	4.4	3.5	1.9	0.4

APPENDIX A
LIST OF ACRONYMS

- AMS: American Meteorological Society
- ANOVA: ANalysis Of VAriance
- BRN: Bulk Richardson Number
- CAPE: Convective Available Potential Energy
- CFSR: Climate Forecast Reanalysis System
- DOE: Department Of Energy
- ESRL: Earth System Research Laboratory
- ET: Extratropical Transition
- GrADS: Grid Analysis and Display System
- MSL: Mean Sea Level
- NARR: North American Regional Reanalysis
- NCAR: National Center for Atmospheric Research
- NCDC: National Climatic Data Center
- NCEP: National Centers for Environmental Prediction
- NOAA: National Oceanic and Atmospheric Administration
- NOMADS: National Operational Model Archive and Distribution System
- NHC: National Hurricane Center
- NSSFC: National Severe Storms Forecast Center

- NWS: National Weather Service
- SELS: SEvere Local Storms
- SPC: Storm Prediction Center
- SRH: Storm Relative Helicity
- TC: Tropical Cyclone
- TCTOR: Tropical Cyclone TORnado
- UTC: Universal Coordinated Time
- WFO: Weather Forecast Office
- WSR: Weather Surveillance Radar

APPENDIX B

SAFFIR-SIMPSON HURRICANE WIND SCALE AND FUJITA/ENANCED FUJITA TORNAOD DAMAGE SCALE

The Saffir-Simpson Hurricane Wind Scale ranks TCs by their one minute sustained wind speed at a height of ten meters (NHC 2012a). Category one is minimum intensity and Category five is maximum intensity. Category three, four, and five TCs often are referred to as *major* hurricanes.

Saffir-Simpson Category	Sustained Wind Speed
TD	≤ 61 km/h; ≤ 38 mph
TS	62–118 km/h; 39–73 mph
Category 1	119–153 km/h; 74–95 mph
Category 2	154–177 km/h; 96–110 mph
Category 3	178–208 km/h; 111–129 mph
Category 4	209–251 km/h; 130–156 mph
Category 5	252+ km/h; 157+ mph

(source: NHC 2012a and 2012b)

The Fujita Tornado Damage Scale (F-Scale) and the Enhanced Fujita Tornado Damage Scale (EF-Scale) estimate tornado wind speeds using observed damage indicators. The EF-Scale was implemented in the United States on 1 February 2007 (SPC 2011). Category zero is minimum intensity and Category five is maximum intensity for both scales.

F-Scale	Estimated Wind Speed	EF-Scale	Estimated Wind Speed
0	< 117 km/h; < 73 mph	0	< 137 km/h; < 85 mph
1	117–180 km/h; 73–112 mph	1	137–177 km/h; 85–110 mph
2	181–253 km/h; 113–157 mph	2	178–217 km/h; 111–135 mph
3	254–332 km/h; 158–206 mph	3	218–266 km/h; 136–165 mph
4	333–418 km/h; 207–260 mph	4	267–322 km/h; 166–200 mph
5	419+ km/h; 261+ mph	5	323+ km/h; 201+ mph

(source: SPC 2011)

APPENDIX C

TC LANDFALLS AND THEIR TCTORS (1995–2010)

TC Name	Year	Number of TCTORs	Number of outbreaks	Number of TCTORs per outbreak	Percentage of total TCTORs accounted for by outbreaks
Allison	1995	6	0	-	0
Dean	1995	5	0	-	0
Erin	1995	14	3	3, 3, 4	71
Jerry	1995	2	0	-	0
Opal	1995	35	4	4, 5, 9, 13	89
Bertha	1996	15	2	4, 8	80
Dolly	1996	1	0	-	0
Fran	1996	2	0	-	0
Josephine	1996	26	3	5, 8, 11	92
Danny	1997	13	1	6	46
Charley	1998	1	0	-	0
Bonnie	1998	8	1	6	75
Earl	1998	15	3	3, 4, 4	73
Frances	1998	14	3	3, 3, 3	64
Hermine	1998	3	0	-	0
Georges	1998	48	7	3, 4, 4, 5, 6, 7, 11	83
Mitch	1998	5	1	4	80
Bret	1999	5	1	3	60

TC Name	Year	Number of TCTORs	Number of outbreaks	Number of TCTORs per outbreaks	Percentage of total TCTORs accounted for by outbreaks
Bret	1999	5	1	3	60
Dennis	1999	1	0	-	0
Floyd	1999	18	2	5, 9	78
Harvey	1999	2	0	-	0
Irene	1999	7	0	-	0
Gordon	2000	11	1	4	36
Helene	2000	13	3	3, 4, 5	92
Allison	2001	26	3	3, 5, 8	62
Barry	2001	4	0	-	0
Gabrielle	2001	18	4	3, 4, 5, 5	94
Michelle	2001	2	0	-	0
Fay	2002	11	1	5	45
Gustav	2002	1	0	-	0
Hanna	2002	2	0	-	0
Isadore	2002	10	1	7	70
Lili	2002	25	2	3, 20	92
Kyle	2002	8	2	3, 3	75
Bill	2003	30	4	3, 4, 6, 8	70
Claudette	2003	2	0	-	0
Henri	2003	1	0	-	0
Isabel	2003	1	0	-	0
Bonnie	2004	16	2	3, 11	88
Charley	2004	20	3	4, 4, 9	85

TC Name	Year	Number of TCTORs	Number of outbreaks	Number of TCTORs per outbreak	Percentage of total TCTORs accounted for by outbreaks
Gaston	2004	18	2	3, 14	94
Frances	2004	103	12	3, 3, 4, 4, 4, 5, 5, 7, 10, 12, 18, 21	93
Ivan	2004	118	8	4, 5, 7, 9, 14, 19, 24, 33	97
Jeanne	2004	42	6	3, 3, 4, 6, 9, 11	86
Arlene	2005	3	0	-	0
Cindy	2005	48	6	4, 6, 7, 7, 8, 13	94
Dennis	2005	10	1	5	50
Emily	2005	11	1	9	82
Katrina	2005	59	7	3, 4, 5, 5, 8, 15, 16	95
Rita	2005	98	6	4, 10, 13, 14, 23, 33	99
Tammy	2005	1	0	-	0
Wilma	2005	8	2	3, 4	88
Alberto	2006	17	2	3, 3	35
Ernesto	2006	5	1	3	60
Barry	2007	2	0	-	0
Erin	2007	7	1	4	57
Humberto	2007	1	0	-	0
Olga	2007	2	0	-	0
Dolly	2008	6	1	3	50
Fay	2008	50	7	3, 3, 3, 4, 5, 5, 11	68
Gustav	2008	49	8	3, 3, 3, 3, 5, 7, 8, 11	88
Hanna	2008	1	0	-	0

TC Name	Year	Number of TCTORs	Number of outbreaks	Number of TCTORs per outbreak	Percentage of total TCTORs accounted for by outbreaks
Ike	2008	33	3	4, 6, 18	85
Alex	2010	11	1	6	55
Hermine	2010	13	1	8	62
Total		1,163	133	930	80

APPENDIX D

SYNOPTIC PATTERN PERSISTENCE AND VARIABILITY

TC Name	Year	Synoptic patterns in sequence from first outbreak (left) to last outbreak (right)											Persistent pattern pairs	Variable pattern pairs	
Erin	1995	5	5	6										1	1
Opal	1995	2	2	3	3									2	1
Bertha	1996	3	2											0	1
Josephine	1996	3	3	3										2	0
Danny	1997	3												0	0
Bonnie	1998	2												0	0
Earl	1998	3	3	3										2	0
Frances	1998	6	6	6										2	0
Georges	1998	5	1	1	1	1	3	3						4	2
Mitch	1998	3												0	0
Bret	1999	5												0	0
Floyd	1999	1	1											1	0
Gordon	2000	3												0	0
Helene	2000	4	4	4										2	0
Allison	2001	3	3	3										2	0
Gabrielle	2001	3	1	1	1									2	1
Fay	2002	5												0	0
Isadore	2002	1												0	0
Kyle	2002	3	3											1	0
Lili	2002	1	2											0	1
Bill	2003	4	3	3	3									2	1
Bonnie	2004	3	3											1	0
Charley	2004	3	3	3										2	0
Frances	2004	5	5	5	5	1	1	1	1	2	2	2	2	9	2
Gaston	2004	4	4											1	0
Ivan	2004	1	1	1	1	1	2	3	2					4	3
Jeanne	2004	1	1	2	2	2	3							3	2
Cindy	2005	4	4	3	3	3	3							4	1
Dennis	2005	5												0	0

TC Name	Year	Synoptic patterns in sequence from first outbreak (left) to last outbreak (right)	Persistent pattern pairs	Variable pattern pairs
Emily	2005	5	0	0
Katrina	2005	1 1 1 1 1 3 3	5	1
Rita	2005	1 1 2 2 2 3	3	2
Wilma	2005	1 2	0	1
Alberto	2006	1 3	0	1
Ernesto	2006	3	0	0
Erin	2007	4	0	0
Dolly	2008	5	0	0
Fay	2008	5 1 1 4 4 4 3	3	3
Gustav	2008	1 1 1 1 1 5 2 2	5	2
Ike	2008	1 2 2	1	1
Alex	2010	5	0	0
Hermine	2010	4	0	0

REFERENCES

- Abercromby, R. 1883. On Certain Types of British Weather. *Quarterly Journal of the Royal Meteorological Society* 9: 1–25.
- Abercromby, R. 1887. *Weather: A Popular Exposition of the Nature of Weather Changes from Day to Day*. London: Kegan Paul.
- Abler, R., J. S. Adams, and P. Gould. 1971. *Spatial Organization: The Geographer's View of the World*. New Jersey: Prentice Hall, Inc.
- Agee, E. M., C. Church, C. Morris, and J. Snow. 1975. Some Synoptic and Dynamic Features of Vortices Associated with the Tornado Outbreak of 3 April 1974. *Monthly Weather Review* 103 (4): 318–333.
- Agee, E. M., and A. Hendricks. 2011. An Assessment of the Climatology of Florida Hurricane-Induced Tornadoes (HITs): Technology versus Meteorology. *Journal of Climate* 24: 5218–5222.
- Arnott, J. M., J. L. Evans, and F. Chiaromonte. 2004. Characterization of Extratropical Transition Using Cluster Analysis. *Monthly Weather Review* 132: 2916–2937.
- Ashley, W. S. 2007. Spatial and Temporal Analysis of Tornado Fatalities in the United States: 1880–2005. *Weather and Forecasting* 22 (6): 1214–1228.
- Ashley, S. T., and W. S. Ashley. 2008. The Storm Morphology of Deadly Flooding Events in the United States. *International Journal of Climatology* 28: 493–503.

- Baker, A. K., M. D. Parker, and M. D. Eastin. 2009. Environmental Ingredients for Supercells and Tornadoes within Hurricane Ivan. *Weather and Forecasting* 24: 223–243.
- Barbour, G. B. 1924. Waterspouts and Tornado within a Typhoon. *Monthly Weather Review* 52 (2): 106–108.
- Barnes G.M., E. J. Zipser, D. P. Jorgensen, and R. D. Marks Jr. 1983. Mesoscale and Convective Structure of a Hurricane Rainband. *Journal of the Atmospheric Sciences* 40 (9): 2125–2137.
- Barry, R. G. 1980. Synoptic and Dynamic Climatology. *Progress in Physical Geography* 4: 88–96.
- Barry, R. G. 2005. Synoptic Climatology. In *Encyclopedia of World Climatology*, ed. J. E. Oliver, 700–704. Netherlands: Springer.
- Barry, R. G., and A. M. Carleton. 2001. *Synoptic and Dynamic Climatology*. New York: Routledge.
- Barry, R. G., and A. H. Perry. 1973. *Synoptic Climatology: Methods and Applications*. London: Methuen & Co Ltd.
- Bates, F. C. 1962. Tornadoes in the Central United States. *Transactions Kansas Academy of Science* 65: 215–246.
- Beebe, R. G., and F. C. Bates. 1955. A Mechanism for Assisting in the Release of Convective Instability. *Monthly Weather Review* 83 (1): 1–10.
- Belanger, J. I., J. A. Curry, and C. D. Hoyos. 2009. Variability in Tornado Frequency Associated with U.S. Landfalling Tropical Cyclones. *Geophysical Research Letters* 36, L17805, doi:10.1029/2009GL040013.

- Bentley, M. L., T. L. Mote, and S. F. Byrd. 2000. A Synoptic Climatology of Derecho Producing Mesoscale Convective Systems in the North-Central Plains. *International Journal of Climatology* 20 (11): 1329–1349.
- Black, M. L., J. F. Gamache, F. D. Marks Jr., C. E. Samsury, and H. E. Willoughby. 2002. Eastern Pacific Hurricanes Jimena of 1991 and Olivia of 1994: The Effect of Vertical Shear on Structure and Intensity. *Monthly Weather Review* 130 (9): 2291–2312.
- Bluestein, H. B. 1993. *Synoptic-Dynamic Meteorology in Midlatitudes, Volume II: Observations and Theory of Weather Systems*. New York: Oxford University Press.
- Bogner, P. B., G. M. Barnes, and J. L. Franklin. 2000. Conditional Instability and Shear for Six Hurricanes over the Atlantic Ocean. *Weather and Forecasting* 15 (2): 192–207.
- Braun, S. A., M. T. Montgomery, and Z. Pu. 2006. High-Resolution Simulation of Hurricane Bonnie (1998). Part I: The Organization of Eyewall Vertical Motion. *Journal of the Atmospheric Sciences* 63: 19–42.
- Brettschneider, B. 2008. Climatological Hurricane Landfall Probability for the United States. *Journal of Applied Meteorology and Climatology* 47 (2): 704–716.
- Brooks, H. E., and C. A. Doswell III. 2001. Some Aspects of the International Climatology of Tornadoes by Damage Classification. *Atmospheric Research* 56: 191–201.

- Brooks H. E., C. A. Doswell III, and M. P. Kay. 2003. Climatological Estimates of Local Daily Tornado Probability for the United States. *Weather and Forecasting* 18 (4): 626–640.
- Brooks, H. E., J. W. Lee, and J. P. Craven. 2003. The Spatial Distribution of Severe Thunderstorm and Tornado Environments from Global Reanalysis Data. *Atmospheric Research* 67: 73–94.
- Brotzge, J., and S. Erickson. 2009. NWS Tornado Warnings with Zero or Negative Lead Times. *Weather and Forecasting* 24: 140–154.
- Brotzge, J., and S. Erickson. 2010. Tornadoes without NWS Warning. *Weather and Forecasting* 25: 159–172.
- Burt, J. E., G. M. Barber, and D. L. Rigby. 2009. *Elementary Statistics for Geographers* 3rd edition. New York: The Guilford Press.
- Cannon, A. J., P. H. Whitfield, and E. R. Lord. 2002. Synoptic Map-Pattern Classification Using Recursive Partitioning and Principal Component Analysis. *Monthly Weather Review* 130: 1187–1206.
- Cecil, D. J., and L. A. Schultz. 2010. Tropical Cyclone Tornadoes: Synoptic Scale Influences and Forecasting Applications. *29th Conference on Hurricanes and Tropical Meteorology*, Tucson, AZ, American Meteorological Society, 1C.4. http://ams.confex.com/ams/29Hurricanes/techprogram/paper_168674.htm. last accessed 5 August 2011.
- Clark, A. J., C. J. Schaffer, W. A. Gallus Jr., and K. Johnson-O'Mara. 2009. Climatology of Storm Reports Relative to Upper-Level Jet Streaks. *Weather and Forecasting* 24 (4): 1032–1051.

- Cohen, A. E. 2010. Synoptic-Scale Analysis of Tornado-Producing Tropical Cyclones Along the Gulf Coast. *National Weather Digest* 34 (2): 99–115.
- Comrie, A. C. 1994. A Synoptic Climatology of Rural Ozone Pollution at Three Forest Sites in Pennsylvania. *Atmospheric Environment* 28: 1601–1614.
- Comrie, A. C., and B. Yarnal. 1992. Relationships between Synoptic-Scale Atmospheric Circulation and Ozone Concentrations in Metropolitan Pittsburgh, Pennsylvania. *Atmospheric Environment* 26B: 301–312.
- Corbosiero, K. L. and J. Molinari. 2002. The Effects of Vertical Wind Shear on the Distribution of Convection in Tropical Cyclones. *Monthly Weather Review* 130 (8): 2110–2123.
- Corfidi, S., S. Weiss, J. Kain, S. Corfidi, R. Rabin, and J. Levit. 2010. Revisiting the 3–4 April 1974 Super Outbreak of Tornadoes. *Weather and Forecasting* 25 (2): 465–510.
- Court, A. 1957. Climatology: Complex, Dynamic, and Synoptic. *Annals of the Association of American Geographers* 47 (2): 125–136.
- Curtis, L. 2004. Midlevel Dry Intrusion as a Factor in Tornado Outbreaks Associated with Landfalling Tropical Cyclones from the Atlantic and Gulf of Mexico. *Weather and Forecasting* 19 (2): 411–427.
- Czajkowski, J., K. Simmons, and D. Sutter. 2011. An Analysis of Coastal and Inland Fatalities in Landfalling US Hurricanes. *Natural Hazards*: DOI: 10.1007/s11069-011-9849-x.
- Davies-Jones, D., R. J. Trapp, and H. B. Bluestein. 2001. Tornadoes and Tornadic Storms. *Meteorological Monographs* 28 (50): 167–222.

- Davis, R. E., and D. A. Gay. 1993. A Synoptic Climatological Analysis of Air Quality in the Grand Canyon National Park. *Atmospheric Environment* 27A: 713–727.
- Davis, R. E., and R. F. Rogers. 1992. A Synoptic Climatology of Severe Storms in Virginia. *Professional Geographer* 44: 319–332.
- Davis, R. E., T. M. Stanmeyer, G. V. Jones. 1997. A Synoptic Climatology of Tornadoes in Virginia. *Physical Geography* 18: 383–407.
- Dayan, U., A. Tubi, and I. Levy. 2012. On the Importance of Synoptic Classification Methods with Respect to Environmental Phenomena. *International Journal of Climatology* 32: 681–694.
- Dixon P. G., A. E. Mercer, J. Choi, and J. S. Allen. 2011. Tornado Risk Analysis: Is Dixie Alley an Extension of Tornado Alley? *Bulletin of the American Meteorological Society* 92: 433–441.
- Doswell III, C. A. 1987. The Distinction Between Large-Scale and Mesoscale Contribution to Severe Convection: A Case Study Example. *Weather and Forecasting* 2 (1): 3–16.
- Doswell, C. A., S J. Weiss, and R. H. Johns. 1993. Tornado Forecasting: A Review. In *The Tornado: Its Structure, Dynamics, Prediction, and Hazards*, ed. C. Church, D. Burgess, C. Doswell, R. Davies-Jones, 557–551. Washington DC: American Geophysical Union.
- Doswell III, C. A., and L. F. Bosart. 2001. Extratropical Synoptic-Scale Processes and Severe Convection. *Meteorological Monographs* 28 (50): 27–70.

- Doswell III, C. A., and D. M. Schultz. 2006. On the Use of Indices and Parameters in Forecasting Severe Storms. *Electronic Journal of Severe Storms Meteorology* 1 (3): 1–22.
- Eagleman, J. R. 1983. *Severe and Unusual Weather*. New York: Van Nostrand Reinhold Company.
- Edwards, R. 2008. Tropical Cyclone Tornadoes - A Research and Forecasting Overview. Part I: Climatologies, Distribution, and Forecast Concepts. *24th Conference on Severe Local Storms*, Savannah, GA, American Meteorological Society, 7.A.1. http://ams.confex.com/ams/24SLS/techprogram/paper_141721.htm. last accessed 4 August 2011.
- Edwards, R. 2010a. Tropical Cyclone Tornado Records for the Modernized NWS Era. *25th Conference on Severe Local Storms*. Denver, CO. American Meteorological Society, p3.1. http://ams.confex.com/ams/25SLS/techprogram/paper_175269.htm. last accessed 4 August 2011.
- Edwards, R. 2010b. TCTOR Dataset. <http://www.spc.noaa.gov/misc/edwards/TCTOR/tctor.xls> and <http://www.spc.noaa.gov/misc/edwards/TCTOR/readme.txt>. last accessed 2 May 2011.
- Edwards, R. 2012. Tropical Cyclone Tornadoes: A Review of Knowledge in Research and Prediction. *Electronic Journal of Severe Storms Meteorology* 7 (6): 1–33.

- Edwards, R., and A. E. Pietrycha. 2006. Archetypes for Surface Baroclinic Boundaries Influencing Tropical Cyclone Tornado Occurrence. *23rd Conference on Severe Local Storms*, St. Louis, MO, American Meteorological Society, P8.2. http://ams.confex.com/ams/23SLS/techprogram/paper_114992.htm. last accessed 2 June 2012.
- Edwards, R., A. R. Dean, R. L. Thompson, and B. T. Smith. 2010. Objective Environmental Analyses and Convective Modes for U. S. Tropical Cyclone Tornadoes from 2003-2008. *25th Conference on Severe Local Storms*. Denver, CO. American Meteorological Society, p3.2. http://ams.confex.com/ams/25SLS/techprogram/paper_175397.htm. last accessed 4 August 2011.
- Elsner, J. B., and A. B. Kara. 1999. *Hurricanes of the North Atlantic: Climate and Society*. New York: Oxford University Press.
- Emanuel, K. 2007. Environmental Factors Affecting Tropical Cyclone Power Dissipation. *Journal of Climate* 20: 5497–5509.
- ESRI. 2008. Data and Maps Package. Version 9.3. Redlands, CA: Environmental Systems Research Institute.
- ESRI. 2010. ArcGIS Desktop. Version 10. Redlands, CA: Environmental Systems Research Institute.
- Frank, W. M., and E. A. Ritchie. 2001. Effects of Vertical Wind Shear on the Intensity and Structure of Numerically Simulated Hurricanes. *Monthly Weather Review* 128 (9): 2249–2269.
- Freier, G. D. 1992. *The Wonder of Weather*. New York: Gramercy Books.

- French, A. J., and M. D. Parker. 2008. The Initiation and Evolution of Multiple Modes of Convection within a Meso-Alpha-Scale Region. *Weather and Forecasting* 23 (6): 1221–1252.
- Fujita, T., D. L. Bradbury, and C. F. Van Thullenar. 1970. Palm Sunday Tornadoes of April 11, 1965. *Monthly Weather Review* 98 (1): 29–69.
- Galway, J. G. 1975. Relationship of Tornado Deaths to Severe Weather Watch Areas. *Monthly Weather Review* 103: 737–741.
- Galway, J. G. 1977. Some Climatological Aspects of Tornado Outbreaks. *Monthly Weather Review* 105: 477–484.
- Gamble D. W., and V. G. Meentemeyer. 1997. A Synoptic Climatology of Extreme Unseasonable Floods in the Southeastern United States, 1950–1990. *Physical Geography* 18: 496–524.
- Gentry, R. C. 1983. Genesis of Tornadoes Associated with Hurricanes. *Monthly Weather Review* 111 (9): 1793–1805.
- Giles, B. D. 2005. Reanalysis Projects. In *Encyclopedia of World Climatology*, ed. J. E. Oliver, 615–616. London: Springer.
- Gilmore, M. S., and L. J. Wicker. 2002. Influences of the Local Environment on Supercell Cloud-to-Ground Lightning, Radar Characteristics, and Severe Weather on 2 June 1995. *Monthly Weather Review* 130 (10): 2349–2372.
- Glickman, T. S., Ed. 2000. *Glossary of Meteorology* 2nd ed. American Meteorological Society. <http://amsglossary.allenpress.com/glossary>. last accessed 18 February 2012.

- Gold, E. 1920. Aids to Forecasting: Types of Pressure Distribution, With Notes and Tables for the Fourteen Years 1905–1918. *Geophysical Memoirs* 2 (16): 149–174.
- Grams, J. S., R. L. Thompson, D. V. Snively, J. A. Prentice, G. M. Hodges, and L. J. Reames. 2012. A Climatology and Comparison of Parameters for Significant Tornado Events in the United States. *Weather and Forecasting* 27 (1): 106–123.
- Gray, R. W. 1919. A Tornado within a Hurricane Area. *Monthly Weather Review* 47 (9): 639.
- Gray, W. M. 1998. The Formation of Tropical Cyclones. *Meteorology and Atmospheric Physics* 67: 37–69.
- Grazulis, T. P. 2001. *The Tornado: Nature's Ultimate Windstorm*. Norman: University of Oklahoma Press.
- Hare, F. K. 1955. Dynamic and Synoptic Climatology. *Annals of the Association of American Geographers* 45 (2): 152–162.
- Harman, J. R. 1991. *Synoptic Climatology of the Westerlies: Processes and Patterns*. Washington: Association of American Geographers.
- Harman, J. R. and J. A. Winkler. 1991. Synoptic Climatology: Themes, Applications, and Prospects. *Physical Geography* 12: 220–230.
- Harnack, R. P., and J. S. Quinlan, 1989: Association of Jet Streaks and Vorticity Advection Pattern with Severe Thunderstorms in the Northeastern United States. *National Weather Digest* 14 (1): 5–12.
- Harr, P. A., and R. L. Elsberry. 2000. Extratropical Transition of Tropical Cyclones over the Western North Pacific. Part I: Evolution of Structural Characteristics during the Transition Process. *Monthly Weather Review* 128 (8): 26132–633.

- Hart, R. E., and J. L. Evans. 2001. A Climatology of the Extratropical Transition of Atlantic Tropical Cyclones. *Journal of Climate* 14 (4): 546–564.
- Harvey, D. 1969. *Explanation in Geography*. London: Butler and Tanner Ltd.
- Hendricks, E. A., M. S. Peng, B. Fu, and T. Li. 2010. Quantifying Environmental Control on Tropical Cyclone Intensity Change. *Monthly Weather Review* 138: 3243–3271.
- Hill, E. L., W. Malkin, and W. A. Schulz, Jr. 1966. Tornadoes Associated with Cyclones of Tropical Origin-Practical Features. *Journal of Applied Meteorology* 5 (6): 745–763.
- Hill, K. A., and G. M. Lackmann. 2009. Influence of Environmental Humidity on Tropical Cyclone Size. *Monthly Weather Review* 137 (10): 3294–3315.
- Hills, G. B. 1929. The September 28, 1929, Tornado in Fort Lauderdale, FL. *Monthly Weather Review* 57 (10): 420–421.
- Houze, R. A. Jr. 2010. Clouds in Tropical Cyclones. *Monthly Weather Review* 138 (2): 293–344.
- Inwards, R. L. 1950. *Weather Lore*, fourth edition. London: Rider and Co.
- Johns, R. H., and C. A. Doswell III. 1992. Severe Local Storms Forecasting. *Weather and Forecasting* 7(4): 588–612.
- Jones, P. D., M. Hulme, K. R. Briffa. 1993. A Comparison of Lamb Circulation Types with an Objective Classification Scheme. *International Journal of Climatology* 13: 655–663.

- Jones, S. C., P. A. Harr, J. Abraham, L. F. Bosart, P. J. Bowyer, J. L. Evans, D. E. Hanley, B. N. Hanstrum, R. E. Hart, F. Lalaurette, M. R. Sinclair, R. K. Smith, and C. Throncroft. 2003. The Extratropical Transition of Tropical Cyclones: Forecast Challenges, Current Understanding, and Future Directions. *Weather and Forecasting* 18: 1052–1092.
- Jones, S. C. 2000. The Evolution of Vortices in Vertical Shear: III: Baroclinic Vortices. *Quarterly Journal of the Royal Meteorological Society* 126: 3161–3185.
- Kalkstein, L. S. 1979. A Synoptic Climatological Approach for Environmental Analysis. *Proceedings of the Middle States Division Association of American Geographers* 13: 68–75.
- Kalkstein, L. S., and P. Corrigan. 1986. A Synoptic Climatological Approach for Geographical Analysis: Assessment of Sulfur Dioxide Concentrations. *Annals of the Association of American Geographers* 76 (3): 381–395.
- Kalnay, E., M. Kanamitsu, R. Kistler, W. Collins, D. Deaven, L. Gandin, M. Iredell, S. Saha, G. White, J. Woollen, Y. Zhu, A. Leetmaa, R. Reynolds, M. Chelliah, W. Ebisuzaki, W. Higgins, J. Janowiak, K. C. Mo, C. Ropelewski, J. Wang, Roy Jenne, Dennis Joseph. 1996. The NCEP/NCAR 40-Year Reanalysis Project. *Bulletin of the American Meteorological Society* 77 (3): 437–471.
- Kanamitsu, M., W. Ebisuzaki, J. Woollen, S. Yang, J. J. Hnilo, M. Fiorino, G. L. Potter. 2002. NCEP–DOE AMIP-II Reanalysis (R-2). *Bulletin of the American Meteorological Society* 83 (11): 1631–1643.
- Karapiperis, P. P. 1951. The Tower of the Winds. *Weatherwise* 4: 112–113.

- Keim, B. D. 1996. Spatial, Synoptic, and Seasonal Patterns of Heavy Rainfall in the Southeastern United States. *Physical Geography* 17: 313–328.
- Keim, B. D., and G. E. Faiers. 1995. Heavy Rainfall Distributions by Season: Synoptic Interpretations and Quantile Estimates. *Water Resources Bulletin* 32: 117–124.
- Keim, B. D., and R. A. Muller. 1992. Temporal Fluctuations of Heavy Rainfall Magnitudes in New Orleans, Louisiana: 1871-1992. *Water Resources Bulletin* 28: 721–730.
- Keim, B. D., and R. A. Muller. 2009. *Hurricanes of the Gulf of Mexico*. Baton Rouge: Louisiana State University Press.
- Key, J., and R. G. Crane. 1986. A Comparison of Synoptic Classification Schemes Based on "Objective" Procedures. *Journal of Climatology* 6: 375–388.
- Kimball, S. K. and M. S. Mulekar. 2004. A 15-Year Climatology of North Atlantic Tropical Cyclones. Part I: Size Parameters. *Journal of Climate* 17 (18): 3555–3575.
- Klein, P. M., P. A. Harr, and R. L. Elsberry. 2000. Extratropical Transition of Western North Pacific Tropical Cyclones: An Overview and Conceptual Model of the Transformation Stage. *Weather and Forecasting* 15 (4): 373–395.
- Klein, P. M., P. A. Harr, and R. L. Elsberry. 2002. Extratropical Transition of Western North Pacific Tropical Cyclones: Midlatitude and Tropical Cyclone Contributions to Reintensification. *Monthly Weather Review* 130 (9): 2240–2259.
- Kloth, C. M., and R. P. Davies-Jones. 1980. The Relationship of the 300-mb Jet Stream to Tornado Occurrence. NOAA Technical Memo: ERL NSSL-88. Norman: NOAA.

- Konrad, C. E. 1997. Synoptic-Scale Features Associated with Warm Season Heavy Rainfall Over the Interior Southeastern United States. *Weather and Forecasting* 12: 557–571.
- Lamb, H. H. 1972. British Isles Weather Types and A Register of the Daily Sequence of Circulation Patterns, 1861-1971. *Geophysical Memoirs* 116. London: HMSO.
- Leathers, D. J. 1993. A Synoptic Climatology of Northeastern United States Tornadoes. *Physical Geography* 14: 171–190.
- Leathers, D. J., and A. W. Ellis. 1996. Synoptic Mechanisms Associated with Snowfall Increases to the Lee of Lake Erie and Ontario. *International Journal of Climatology* 16: 1117–1135.
- Leighly, J. B. 1949. Climatology Since the Year 1800. *Transactions of the American Geophysical Union* 30: 658–672.
- Lockwood, J. G. 2005. Atmospheric Circulation, Global. In *Encyclopedia of World Climatology*, ed. J. E. Oliver, 126–134. Netherlands: Springer.
- Malkin, W., and J. G. Galway. 1953. Tornadoes Associated with Hurricanes as Illustrated by Franconia, Va., Tornado, September 1, 1952. *Monthly Weather Review* 81 (9): 299–303.
- Markowski, P. M., E. N. Rasmussen, and J. M. Straka. 1998. The Occurrence of Tornadoes in Supercells Interacting with Boundaries during VORTEX-95. *Weather and Forecasting*, 13 (3): 852–859.
- Markowski, P. M., J. M. Straka, E. N. Rasmussen, and D. O. Blanchard. 1998. Variability of Storm-Relative Helicity During VORTEX. *Monthly Weather Review* 126 (11): 2959–2971.

- Matyas, C. J. 2010. Associations between the Size of Hurricane Rain Fields at Landfall and Their Surrounding Environment. *Meteorology and Atmospheric Physics* 106 (3–4): 135–148.
- May, P. T. 1996. The Organization of Convection in the Rainbands of Tropical Cyclone Laurence. *Monthly Weather Review* 124 (5): 807–815.
- McCaul Jr., E. W. 1987. Observations of the Hurricane “Danny” Tornado Outbreak of 16 August 1985. *Monthly Weather Review* 115 (6): 1206–1223.
- McCaul Jr., E. W. 1991. Buoyancy and Shear Characteristics of Hurricane-Tornado Environments. *Monthly Weather Review* 119 (8): 1954–1978.
- McCaul Jr., E. W. 1993. Hurricane Spawned Tornadic Storms. In *The Tornado: Its Structure, Dynamics, Prediction, and Hazards*, ed. C. Church, D. Burgess, C. Doswell, R. Davies-Jones, 119–142. Washington DC: American Geophysical Union.
- McCaul Jr., E. W., and M. L. Weisman. 1996. Simulations of Shallow Supercell Storms in Landfalling Hurricane Environments. *Monthly Weather Review* 124: 408–429.
- McCaul Jr., E. W., D. E. Buechler, S. J. Goodman, and M. Cammarata. 2004. Doppler Radar and Lightning Network Observations of a Severe Outbreak of Tropical Cyclone Tornadoes. *Monthly Weather Review* 132: 1747–1763.
- Mercer, A. E., C. M. Shafer, C. A. Doswell III, L. M. Leslie, and M. B. Richman. 2012. Synoptic Composites of Tornadic and Nontornadic Outbreaks. *Monthly Weather Review* 140 (8): 2590–2608.

- Mesinger, F., G. DiMego, E. Kalnay, K. Mitchell, P. C. Shafran, W. Ebisuzaki, D. Jović, J. Woollen, E. Rogers, E. H. Berbery, M. B. Ek, Y. Fan, R. Grumbine, W. Higgins, H. Li, Y. Lin, G. Manikin, D. Parrish, and W. Shi. 2006. North American Regional Reanalysis. *Bulletin of the American Meteorological Society* 87 (3): 343–360.
- Meyers, L. S., G. Gamst, and A. J. Guarino. 2006. *Applied Multivariate Research: Design and Interpretation*. London: Sage Publications.
- Miller, R. C. 1972. Notes on Analysis and Severe Storms Forecasting Procedures of the Air Force Global Weather Central. *Air Weather Service Technical Report* 200. Scott Air Force Base: Air Weather Service. <http://chubasco.niu.edu/projects/miller/>. last accessed 7 June 2012.
- Molinari, J., P. Dodge, D. Vollaro, K. L. Corbosiero, and F. Marks Jr. 2006. Mesoscale Aspects of the Downshear Reformation of a Tropical Cyclone. *Journal of the Atmospheric Sciences* 63 (1): 341–354.
- Molinari, J., and D. Vollaro. 2008. Extreme Helicity and Intense Convective Towers in Hurricane Bonnie. *Monthly Weather Review* 136 (11): 4355–4372.
- Molinari, J., and D. Vollaro. 2010a. Distribution of Helicity, CAPE, and Shear in Tropical Cyclones. *Journal of the Atmospheric Sciences* 67 (1): 274–284.
- Molinari, J., and D. Vollaro. 2010b. Rapid Intensification of a Sheared Tropical Storm. *Monthly Weather Review* 138 (10): 3869–3885.
- Molinari, J., D. M. Romps, D. Vollaro, and L. Nguyen. 2012. CAPE in Tropical Cyclones. *Journal of the Atmospheric Sciences* 69 (8): 2452–2463.

- Moore, T. W., and R. W. Dixon. 2011a. Climatology of Tornadoes Associated with Gulf Coast-Landfalling Hurricanes. *Geographical Review* 101 (3): 371–395.
- Moore, T. W., and R. W. Dixon. 2011b. Tropical Cyclone Tornado Casualties. *Natural Hazards* 61(2): 621–634.
- Muller, R. A. 1977. A Synoptic Climatology for Environmental Baseline Analysis: New Orleans. *Journal of Applied Meteorology* 16: 20–33.
- NCDC. 2011. North American Regional Reanalysis Daily Dataset. http://nomads.ncdc.noaa.gov/cgi-bin/ncdc-ui/define-collection.pl?model_sys=narr&model_name=narr-a&grid_name=221. last accessed 8 October 2011.
- NCDC. n. d. International Best Track Archive for Climate Stewardship. <http://www.ncdc.noaa.gov/oa/ibtracs/index.php?name=ibtracs-data>. last accessed 6 August 2012.
- NHC. 2012a. Saffir-Simpson Hurricane Wind Scale. <http://www.nhc.noaa.gov/aboutsshws.php>. last accessed 19 August 2012.
- NHC. 2012b. Tropical Cyclone Climatology. <http://www.nhc.noaa.gov/climo/>. last accessed 27 May 2012.
- Nieuwolt, S. 1977. *Tropical Climatology: An Introduction to the Climates of the Low Latitudes*. New York: John Wiley & Sons.
- NOAA. 2007. NOAA Central Library Data Imaging Project. http://docs.lib.noaa.gov/rescue/dwm/data_rescue_daily_weather_maps.html. last accessed 24 May 2012.
- NOAA. n. d. 3-Hourly NCEP North American Regional Reanalysis (NARR) Composites. <http://www.esrl.noaa.gov/psd/cgi-bin/data/narr/plothour.pl>. last accessed 04 July 2012.

- Novlan, D. J., and W. M. Gray. 1974. Hurricane-Spawmed Tornadoes. *Monthly Weather Review* 102 (7): 476–488.
- NWS. 2009. National Weather Service Glossary. <http://www.weather.gov/glossary/>. last accessed 27 July 2011.
- NWS. n. d. Tropical Cyclone Tornado Threat Product. http://www.nws.noaa.gov/os/tropical/hazards/pdfs/TC_TornadoThreat_1pager.pdf. last accessed 29 July 2011.
- Orton, R. 1970. Tornadoes Associated with Hurricane Beulah on September 19-23, 1967. *Monthly Weather Review* 98 (7): 541–547.
- Pattison, W. D. 1964. The Four Traditions of Geography. *Journal of Geography* 64 (5): 211–216.
- Pearson, A. D., and A. F. Sadowski. 1965. Hurricane-Induced Tornadoes and Their Distribution. *Monthly Weather Review* 93 (7): 461–464.
- Perry, A. 1983. Growth Points in Synoptic Climatology. *Progress in Physical Geography* 7: 91–96.
- Pielke, R. A. Jr., and R. A. Pielke Sr. 1997. *Hurricanes: Their Nature and Impact on Society*. New York: Johnson Wiley and Sons.
- Pietrycha, A. E., and C. D. Hannon, 2002: Tornado Distribution Associated with Hurricane Floyd 1999. *21st Conf. on Severe Local Storms*, San Antonio: American Meteorological Society. https://ams.confex.com/ams/SLS_WAF_NWP/techprogram/paper_46937.htm. last accessed 26 June 2012.
- Rappaport, E. N. 2000. Loss of Life in the United States Associated with Recent Atlantic Tropical Cyclones. *Bulletin of the American Meteorological Society* 81 (9): 2065–2073.

- Rasmussen, E. N., S. Richardson, J. M. Straka, and P. M. Markowski. 2000. The Association of Significant Tornadoes with a Baroclinic Boundary on 2 June 1995. *Monthly Weather Review* 128 (1): 174–191.
- Reasor, P. D., M. T. Montgomery, F. D. Marks Jr., and J. F. Gamache. 2000. Low-Wavenumber Structure and Evolution of the Hurricane Inner Core Observed by Airborne Dual-Doppler Radar. *Monthly Weather Review* 128 (6): 1653–1680.
- Reasor, P. D., M. D. Eastin, and J. F. Gamache. 2009. Rapidly Intensifying Hurricane Guillermo (1997). Part I: Low-Wavenumber Structure and Evolution. *Monthly Weather Review* 137 (2): 603–631.
- Rice, J. A. 2007. *Mathematical Statistics and Data Analysis*, 3rd edition. Belmont, CA: Brooks/Cole.
- Richardson, L. F. 1922. *Weather Prediction by Numerical Process*. London: Cambridge University Press.
- Ritchie, E. A., and R. L. Elsberry. 2003. Simulations of the Extratropical Transition of Tropical Cyclones: Contributions by the Midlatitude Upper-Level Trough to Reintensification. *Monthly Weather Review* 131 (9): 2112–2128.
- Ritchie, E. A., and R. L. Elsberry. 2007. Simulations of the Extratropical Transition of Tropical Cyclones: Phasing between the Upper-Level Trough and Tropical Cyclones. *Monthly Weather Review* 135 (3): 862–876.
- Roebber, P., D. Schultz, and R. Romero. 2002. Synoptic Regulation of the 3 May 1999 Tornado Outbreak. *Weather and Forecasting* 17 (3): 399–429.

- Root, B., P. Knight, G. Young, S. Greybush, R. Grumm, R. Holmes, and J. Ross. 2007. A Fingerprinting Technique for Major Weather Events. *Journal of Applied Meteorology and Climatology* 46: 1053–1066.
- Rose, S. F., P. V. Hobbs, J. D. Locatelli, and M. T. Stoelinga. 2004. A 10-yr Climatology Relating the Locations of Reported Tornadoes to the Quadrants of Upper-Level Jet Streaks. *Weather and Forecasting* 19 (2): 301–309.
- Rudd, M. I. 1964. Tornadoes during Hurricane Carla at Galveston. *Monthly Weather Review* 92 (5): 251–254.
- Ryan, T. 2009. A Synoptic Climatology of Texas Winter Storms. *National Weather Digest* 33 (1): 37–56.
- Sadowski, A. F. 1962. Tornadoes associated with Hurricane Carla, 1961. *Monthly Weather Review* 90: 514–516.
- Saha, S., S. Moorthi, H. Pan, X. Wu, J. Wang, S. Nadiga, P. Tripp, R. Kistler, J. Woollen, D. Behringer, H. Liu, D. Stokes, R. Grumbine, G. Gayno, J. Wang, Y. Hou, H. Chuang, H. H. Juang, J. Sela, M. Iredell, R. Treadon, D. Kleist, P. V. Delst, D. Keyser, J. Derber, M. Ek, J. Meng, H. Wei, R. Yang, S. Lord, H. V. D. Dool, A. Kumar, W. Wang, C. Long, M. Chelliah, Y. Xue, B. Huang, J. Schemm, W. Ebisuzaki, R. Lin, P. Xie, M. Chen, S. Zhou, W. Higgins, C. Zou, Q. Liu, Y. Chen, Y. Han, L. Cucurull, R. W. Reynolds, G. Rutledge, M. Goldberg. 2010. The NCEP Climate Forecast System Reanalysis. *Bulletin of the American Meteorological Society* 91 (8): 1015–1057.
- Schneider, D. and S. Sharp. 2007. Radar Signatures of Tropical Cyclone Tornadoes in Central North Carolina. *Weather and Forecasting* 22 (2): 278–286.

- Schultz, L. A. and D. J. Cecil. 2009. Tropical Cyclone Tornadoes, 1950-2007. *Monthly Weather Review* 137 (10): 3471–3484.
- Shafer, C. M., A. E. Mercer, C. A. Doswell III, M. B. Richman, and L. M. Leslie. 2009. Evaluation of WFR Forecasts of Tornadic and Nontornadic Outbreaks when Initialized with Synoptic-Scale Input. *Monthly Weather Review* 137: 1250–1271.
- Sheridan, S. C. and C. L. Cameron. 2010. Synoptic Climatology and the General Circulation Model. *Progress in Physical Geography* 34 (1): 101–109.
- Skaggs, R. H. 2004. Climatology in American Geography. *Annals of the Association of American Geographers* 94 (3): 446–457.
- Smith, J. S. 1965. The Hurricane-Tornado. *Monthly Weather Review* 93 (7): 453–459.
- Snell, W. L. and E. W. McCaul. 1993. Doppler Signatures of Tornadoes Spawned by Hurricane Andrew Near Montgomery, Alabama. *26th Conference on Radar Meteorology*, Norman, American Meteorological Society, 80–82.
- SPC. 2011. The Enhanced Fujita Scale (EF Scale). <http://www.spc.noaa.gov/efscale/>. last accessed 19 August 2012.
- Spratt, Scott M., David W. Sharp, Pat Welsh, Al Sandrik, Frank Alsheimer and Charlie Paxton. 1997. A WSR-88D Assessment of Tropical Cyclone Outer Rainband Tornadoes. *Weather and Forecasting* 12: 479–501.
- SPSS 2009. PASW Statistics 18. Chicago, IL: SPSS Inc.
- Stewart, S. R. 2006. Tropical Cyclone Report-Hurricane Cindy. http://www.nhc.noaa.gov/pdf/TCR-AL032005_Cindy.pdf. last accessed 06 September 2011.

- Stringer, E. T. 1972. *Foundations of Climatology*. San Francisco: W. H. Freeman and Company.
- Suckling, P. W., and J. E. Hay. 1978. On the Use of Synoptic Weather Map Typing to Define Solar Radiation Regimes. *Monthly Weather Review* 106 (11): 1521–1531.
- Suzuki, O., H. Niino, H. Ohno, and H. Nirasawa. 2000. Tornado-Producing Minisupercells Associated with Typhoon 9019. *Monthly Weather Review* 128: 1868–1882.
- Sweeney, J. C., and G. P. O'Hare. 1992. Geographical Variations in Precipitation Yields and Circulation Types in Britain and Ireland. *Transactions-Institute of British Geographers* 17: 448–463.
- Verbout, S. M., D. M. Schulz, L. M. Leslie, H. E. Brooks, D. J. Karoly, and K. L. Elmore. 2007. Tornado Outbreaks Associated with Landfalling Hurricanes in the North Atlantic Basin: 1954-2004. *Meteorology and Atmospheric Physics* 97 (1–4): 255–271.
- Vescio, M. D., S. S. Weiss, and F. P. Ostby. 1996. Tornadoes Associated with Tropical Storm Beryl. *National Weather Association Digest* 1 (21): 2–10.
- Wang, Y., and C. C. Wu. 2004. Current Understanding of Tropical Cyclone Structure and Intensity Changes - A Review. *Meteorology and Atmospheric Physics* 87: 257–278.
- Weiss S.J., 1987: Some Climatological Aspects of Forecasting Tornadoes Associated with Tropical Cyclones. *Preprints, 17th Conference on Hurricanes and Tropical Meteorology*, American Meteorological Society, Miami, 160–163.

Yarnal, B. 1993. *Synoptic Climatology in Environmental Analysis: A Primer*. Florida: Belhaven Press.

Yarnal, B., A. C. Comrie, B. Frakes, and D. P. Brown. 2001. Developments and Prospects in Synoptic Climatology. *International Journal of Climatology* 21: 1923–1950.

VITA

Todd W. Moore was born in Beaumont, Texas, on 14 October 1981, the son of Tommy and Elizabeth Moore and brother of Suzanne Moore. After completing his studies at Monsignor Kelly Catholic High School, Beaumont, Texas, in 2000, he began his studies at Texas State University-San Marcos. In May 2005 he received the degree of Bachelor of Science with a major in Physical Geography from Texas State. Two years later, in 2007, he entered the Graduate College of Texas State and earned the degree of Master of Science with a major in Geography in May 2009. In August 2009, he entered the Graduate College of Texas State seeking the degree of Doctor of Philosophy with a major in Environmental Geography.

Email address: tm1008@txstate.edu

This dissertation was typed by Todd W. Moore.